



January 2023

## Exploring Zinc Amido-Oxazolate Complexes As Catalysts For Ring Opening Polymerization (ROP) And Ring Opening Co-Polymerization (ROCOP)

Muneer Shaik

[How does access to this work benefit you? Let us know!](#)

Follow this and additional works at: <https://commons.und.edu/theses>

---

### Recommended Citation

Shaik, Muneer, "Exploring Zinc Amido-Oxazolate Complexes As Catalysts For Ring Opening Polymerization (ROP) And Ring Opening Co-Polymerization (ROCOP)" (2023). *Theses and Dissertations*. 5338.

<https://commons.und.edu/theses/5338>

This Dissertation is brought to you for free and open access by the Theses, Dissertations, and Senior Projects at UND Scholarly Commons. It has been accepted for inclusion in Theses and Dissertations by an authorized administrator of UND Scholarly Commons. For more information, please contact [und.common@library.und.edu](mailto:und.common@library.und.edu).

EXPLORING ZINC AMIDO-OXAZOLINATE COMPLEXES AS CATALYSTS FOR  
RING OPENING POLYMERIZATION (ROP) AND RING OPENING CO-  
POLYMERIZATION (ROCOP)

By

Muneer Shaik

M.Sc. Organic Chemistry, Osmania University, India, 2011  
Master of Science, University of North Dakota, USA, 2018

A Dissertation

Submitted to the Graduate School

of the

University of North Dakota

in partial fulfillment of the requirements

for the degree of

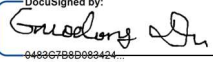
Doctor of Philosophy

Grand Forks, North Dakota

August

**2023**

This document, submitted in partial fulfillment of the requirements for the degree from the University of North Dakota, has been read by the Faculty Advisory Committee under whom the work has been done and is hereby approved.

DocuSigned by:  
  
0483C7B8B083424...  
Dr. Guodong Du


DocuSigned by:  
  
0C80D575B0BF4D4...  
Dr. Qianli Rick Chu

DocuSigned by:  
  
130DD6CE7E0043D...  
Dr. Julia Xiaojun Zhao

DocuSigned by:  
  
1F133492A5A4A3F...  
Dr. Binglin Sui

DocuSigned by:  
  
A9EAB00FF9E4424...  
Dr. Edward Kolodka

This document is being submitted by the appointed advisory committee as having met all the requirements of the School of Graduate Studies at the University of North Dakota and is hereby approved.

DocuSigned by:  
  
2E0AF088C733403...  
Chris Nelson  
Dean of the School of Graduate Studies  
Date: 07 /20/2023

## PERMISSION

Title	Exploring Zinc Amido-Oxazolate Complexes as Catalysts for Ring Opening Polymerization (ROP) and Ring Opening Co-Polymerization (ROCOP)
Department	Chemistry
Degree	Doctor of Philosophy

In presenting this dissertation in partial fulfillment of the requirements for a graduate degree from the University of North Dakota, I agree that the library of this University shall make it freely available for inspection. I further agree that permission for extensive copying for scholarly purposes may be granted by the professor who supervised my dissertation work or, in his absence, by the chairperson of the department or the dean of the Graduate School. It is understood that any copying or publication or other use of this dissertation or part thereof for financial gain shall not be allowed without my written permission. It is also understood that due recognition shall be given to me and to the University of North Dakota in any scholarly use which may be made of any material in my dissertation.

*Muneer Shaik*

---

Signature

August 2023

---

Date



## Table of Contents

LIST OF FIGURES .....	viii
LIST OF TABLES .....	x
LIST OF SCHEMES .....	xi
ABBREVIATIONS .....	xii
ABSTRACT .....	xv
CHAPTER I .....	1
I.1 GENERAL INTRODUCTION .....	1
I.2.1 Cationic ring-opening polymerization .....	6
I.2.2 Anionic ring opening polymerization. ....	8
I.2.3 Coordination-Insertion Ring Opening Polymerization. ....	9
I.2.4 Metal complexes used to catalyze ROP of cyclic esters. ....	10
I.2.5 Macrocyclic Polymers via Ring Opening Polymerization. ....	12
I.3 Ring Opening Copolymerization of Epoxides and Cyclic Anhydrides .....	15
I.4. REFERENCES .....	21
CHAPTER II .....	42

AMIDO-OXAZOLINATO ZINC COMPLEXES CATALYZED RING OPENING COPOLYMERIZATION AND TERPOLYMERIZATION OF CYCLIC ANHYDRIDES AND EPOXIDES.....	42
II.1 INTRODUCTION.....	42
II.2 RESULTS AND DISCUSSION .....	44
II.2.1 Optimizing Reactions with MA/CHO .....	44
II.2.2 Comparison of Epoxides in ROCOP with MA.....	47
II.2.3. Effect of Catalysts and Anhydrides in ROCOP .....	50
II.2.4 Terpolymerization of MA and Two Epoxides .....	52
II.2.5 Thermal Properties of Copolymers and Terpolymers.....	55
II.3 CONCLUSIONS .....	57
II.4 EXPERIMENTAL SECTION .....	58
II.5 REFERENCES.....	61
CHAPTER III .....	74
HIGH GLASS TRANSITION TEMPERATURE POLYESTERS VIA RING-OPENING COPOLYMERIZATION OF EPOXIDES WITH NOVEL CYCLOBUTANE ANHYDRIDES.....	74

III.1 INTRODUCTION .....	74
III.2 RESULTS AND DISSCUSSION.....	77
III.2.1 Polymer synthesis and characterization.....	77
III.2.2 Mechanistic Hypotheses .....	82
III.2.3 Thermal Properties .....	84
III.3 CONCLUSION.....	86
III.4 EXPERIMENTAL SECTION .....	87
III.5 REFERENCES .....	89
CHAPTER IV .....	98
MACROCYCLIC POLYESTERS FROM RING OPENING POLYMERIZATION OF LACTONES USING ZINC AMIDO-OXAZOLINATE CATALYSTS.....	98
IV .1 INTRODUCTION .....	98
IV.2 RESULTS AND DISCUSSION.....	100
IV.2.1 ROP of Lactones .....	100
IV.2.2 Microstructure of Cyclic and Linear PVL and PCL.....	102
IV.2.3 Differentiation between Linear and Cyclic Polyesters by Crystallization Kinetics .....	103

IV.2.4 Synthesis of Statistical or Random Copolymers .....	106
IV.2.5 Synthesis of Gradient Copolymers.....	108
IV.2.6 Synthesis of Block Copolymers .....	110
IV.2.7 Thermal Properties of Homopolymer and Copolymers .....	112
IV.3 CONCLUSION.....	116
IV.4 EXPERIMENTAL SECTION.....	117
IV.5 REFERENCES .....	127
APPENDIX I .....	139
APPENDIX II .....	158
APPENDIX III.....	164

## LIST OF FIGURES

1. Production of plastics worldwide from 1950 to 2018.....	1
2. Routes for the synthesis of polyesters.....	3
3. Different pathways for the synthesis of polyesters.....	4
4. List of the metal complexes used for ROP of lactide.....	11
5. Structures of NHC-Tethered Titanium (IV), Yttrium (III), Magnesium (II), and Zinc (II) Bifunctional Complexes Employed for the ROP of Lactide.....	13
6. NHC–Zn(C <sub>6</sub> F <sub>5</sub> ) <sub>2</sub> and NHC–Metal Chloride Adducts Employed for the ROP of Cyclic Esters.....	14
7. Structures of NHOs in combination with simple metal halides Such as LiCl, MgI <sub>2</sub> , MgCl <sub>2</sub> , YCl <sub>3</sub> , ZnI <sub>2</sub> , AlCl <sub>3</sub> as the LA to achieve controlled homo-and copolymerization of various cyclic esters.....	15
8. General reaction mechanism of the ROCOP.....	16
9. Porphyrin and corrole catalysts.....	17
10. List of Salcyl, Salph, and Salen complexes used for ROCOP.....	18
11. C <sub>1</sub> -Symmetric Zn-Complexes used for ROCOP of epoxides and CO <sub>2</sub> .....	20
12. Amido-oxazolate zinc complexes for ROCOP of CHO with anhydride.....	44
13. <sup>1</sup> H and <sup>13</sup> C NMR of polyester from PGE & MA with catalyst <b>1</b> .....	49
14. <sup>1</sup> H NMR spectrum of terpolymer poly(CHO-PGE-MA).....	54

15.	TGA profiles of the copolymers and terpolymers .....	57
16.	Cyclic anhydride and epoxide comonomers investigated in this work.....	78
17.	<sup>1</sup> H-NMR of CHO-CBAN-1 Co-polyester.....	79
18.	<sup>13</sup> C-NMR of CHO-CBAN-1 Co-polyester.....	80
19.	Hypothesized chain propagation step.....	83
20.	DSC and TGA graphs of polyesters with <b>1a</b> anhydride as comonomer.....	86
21.	<sup>1</sup> H NMR of polycaprolactones.....	103
22.	Relative crystallinity ( $\chi_c$ ) as a function of time for cyclic and linear PCL during isothermal crystallization at 45 °C.....	105
23.	Hoffman-Weeks plots of (a) Linear PCL and (b) Cyclic PCL.....	106
24.	<sup>13</sup> C and DOSY- NMR of PCL- <i>s</i> -PVL from $\delta$ -VL and $\epsilon$ -CL .....	108
25.	<sup>13</sup> C- NMR and DOSY-NMR spectra of PCL- <i>g</i> -PBL.....	109
26.	<sup>13</sup> C- NMR and DOSY-NMR of PBL- <i>b</i> -PVL (Two-step reaction).....	111
27.	TGA and DSC profiles of a block polyester PCL- <i>b</i> -PBL.....	115

## LIST OF TABLES

1. Standard thermodynamics parameters of cyclic esters polymerization.....	6
2. Optimization of reaction conditions between MA and CHO.....	46
3. ROCOP of MA with different Epoxides.....	48
4. ROCOP of CHO with different cyclic anhydrides.....	54
5. Terpolymerization of MA with two different epoxides.....	56
6. Thermal properties of co- and terpolymers.....	57
7. Copolymerization of 1a-1c with different epoxides.....	81
8. Thermal properties of copolymers.....	85
9. ROP of $\delta$ -Valerolactone and $\epsilon$ -Caprolactone with Zn Catalyst ( <b>1a</b> ).....	101
10. Copolyesters with Achiral Zn Catalyst ( <b>1b</b> ).....	107
11. Thermal Studies of PCL and PVL with achiral catalyst <b>1b</b> .....	113
12. Thermal properties of cyclic copolymers.....	115

## LIST OF SCHEMES

1. Schematic representation of ROP of cyclic ester. $R = (CH_2)_{0-3}$ and /or $(CHR'')$ .....	5
2. Generalized Mechanisms (ACEM and AMM) Involved in the LA-Mediated Cationic ROP.....	8
3. Various Types of Chain Initiation and Propagation Pathways That Have Been Proposed to Be Involved in the ROP of Lactones by LBs for Polymer Chain Formation.....	9
4. The proposed reaction pathway for the coordination-insertion-mediated ring-opening polymerization of a cyclic ester.....	10
5. Chain propagation step explaining the reactivity of epoxides.....	50
6. ROCOP of epoxides and CBAN using zinc amido-oxazolate complex as catalyst.....	77
7. ROP of $\epsilon$ -CL and $\delta$ -VL with Zn catalysts.....	101



## ABBREVIATIONS

BDI	$\beta$ -diketiminat
<i>rac</i> -BBL	<i>racemic</i> $\beta$ -Butyrolactone
BnOH	Benzyl alcohol
CaH <sub>2</sub>	Calcium Hydride
CBAN	Cyclobutane Anhydride
CDCl <sub>3</sub>	Deuterated Chloroform
CHO	Cyclohexane Oxide
CTA	Chain Transfer Agent
DOSY	Diffusion Ordered Spectroscopy
DSC	Differential Scanning Calorimetry
$\bar{D}$	Polydispersity Index
ECH	Epichlorohydrin
ESI	Electrospray Ionization
GPC	Gel Permeation Chromatography

HDPE	High Density Polyethylene
LDPE	Low Density Polyethylene
MA	Maleic Anhydride
$M_n$	Number-average molecular weight
$M_w$	Weight average molecular weight
MW	Molecular Weight
NMR	Nuclear Magnetic Resonance Spectroscopy
PA	Phthalic Anhydride
P3HB/PHB	Poly-3-(hydroxybutyrate)
PCL	Polycaprolactone
PV	Polyvalerolactone
PE	Polyethylene
PET	Polyethylene Terephthalate
PGE	Phenyl Glycidyl Ether
PHA	Polyhydroxyalkanoates

PLA	Poly lactide/ Polylactic acid
PP	Polypropylene
PS	Polystyrene
PVOH	Polyvinyl Alcohol
ROP	Ring-Opening Polymerization
SA	Succinic Anhydride
SO	Styrene Oxide
THF	Tetrahydrofuran
$T_m$	Melting Temperature
TMS	Tetramethylsilane
TOF	Turnover frequency
TON	Turnover number
TGA	Thermogravimetric Analysis
$T_g$	Glass Transition Temperature
Zn	Zinc-metal

## ABSTRACT

This research aims to explore the potential of zinc amido-oxazolate complexes as catalysts for ring opening polymerization (ROP) and ring opening copolymerization (ROCOP). ROP is a method for synthesizing polymers by opening cyclic monomers, while ROCOP involves using two different monomers to create a copolymer. The ROP of lactones is a well-established method for the synthesis of polyesters, whereas the ROCOP of epoxides and cyclic anhydrides is a more recent development. Zinc amido-oxazolate complexes are a promising class of catalysts due to their tunable electronic properties and high reactivity. The catalytic activity of these complexes can be tuned by modifying the structure of the ligands and the reaction conditions, such as temperature, solvent, and concentration. One of the advantages of using zinc amido-oxazolate complexes as catalysts for ROP and ROCOP is their ability to control the molecular weight and polydispersity of the resulting polymers. This control allows for the production of polymers with specific properties, such as high molecular weight and narrow molecular weight distribution, which are important for various applications.

Through the use of a series of highly active chiral and achiral bidentate N-N amido-oxazolate zinc complexes, we were able to catalyze the ring-opening copolymerization (ROCOP) of epoxides with various anhydrides, resulting in polyesters with tunable glass transition temperatures ranging from 60 °C to 165 °C, and the ring-opening polymerization

(ROP) of lactones, yielding cyclic polyesters with high molecular weights. Cyclic statistical, gradient, and diblock copolymers are formed using ROP of  $\epsilon$ -CL,  $\delta$ -VL, and  $\beta$ -BBL by altering the reaction conditions or taking advantage of the different reactivity of the various monomers.  $^1\text{H}$ -NMR,  $^{13}\text{C}$ -NMR, DOSY, ESI mass spectrometry, GPC, TGA, and DSC techniques were used to analyze the structure of cyclic copolymers.

## CHAPTER I

### I.1 GENERAL INTRODUCTION

Polymers have become an integral part of modern society because of their many potential applications.<sup>1,2,3,4</sup> Their popularity has skyrocketed due to their affordability, lightweight nature, and impressive durability since 1950s. Their versatility makes them useful for a variety of purposes, ranging from packaging to aerospace technology. This has resulted in the production of over 380 million tons of plastic globally each year (Fig. 1).<sup>4,5,6</sup> However, this has come at a cost to the environment, as the chemicals used to produce these synthetic polymers are largely derived from petroleum, and the polymers can become contaminants in the natural environment and oceans. The demand for polymers has only increased with time, leading to a greater dependence on fossil fuels and contributing to the problem of non-biodegradable waste that can take centuries to decompose.<sup>7</sup>

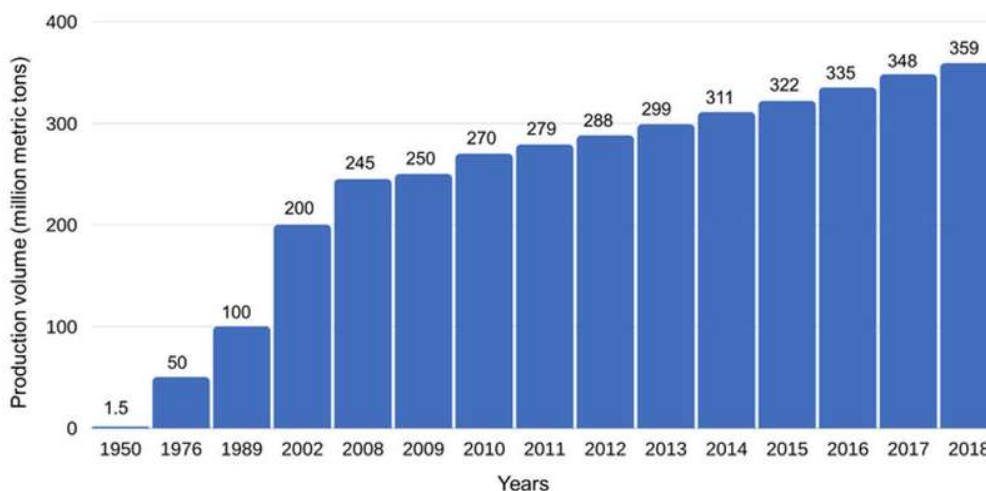


Figure 1: Production of plastics worldwide from 1950 to 2018 (in million metric tons)

With the growing concern for the environment and the need to reduce the amount of nondegradable polymers in landfills and oceans, there has been a significant increase in interest and reliance on methods such as green synthesis of sustainable polymers, chemical upcycling and chemical recycling to avoid or to reduce the depletion of fossil fuels. One of the main focuses is on synthesis of polymers from biomass feedstocks. However, in order to manufacture such polymers, there are three major challenges that must be addressed: (i) the development of high-performance sustainable polymers, elastomers, and thermosets, (ii) advancements in sustainable polymer degradation, chemical recycling, and compatibilization, and (iii) the conversion of biomass feedstocks into common monomers like styrene, methacrylate, and isoprene, which can be integrated into existing polymer industries to create biodegradable and biocompatible polymers with enhanced properties. Significant efforts have been made to tackle these obstacles and create sustainable polymers that are more environmentally friendly.

Among the known biodegradable polymers, aliphatic polyesters have a significant place, since hydrolytic and/or enzymatic chain breakage results in hydroxy acids, which, in most instances, are eventually metabolized.<sup>8,9</sup> Polyesters are one of the most prevalent and adaptable synthetic polymers, which have a specific role in sectors including textiles, plastics, and coatings. Two major approaches are known to produce polyesters: step-growth polymerization (SGP) and chain-growth polymerization (CGP) (Figure 2). SGP includes polycondensation of diacids or diesters

with diols that demands severe conditions and extended reaction times, and generally result in low molecular weights polyesters and multiple side products.<sup>7,10</sup>

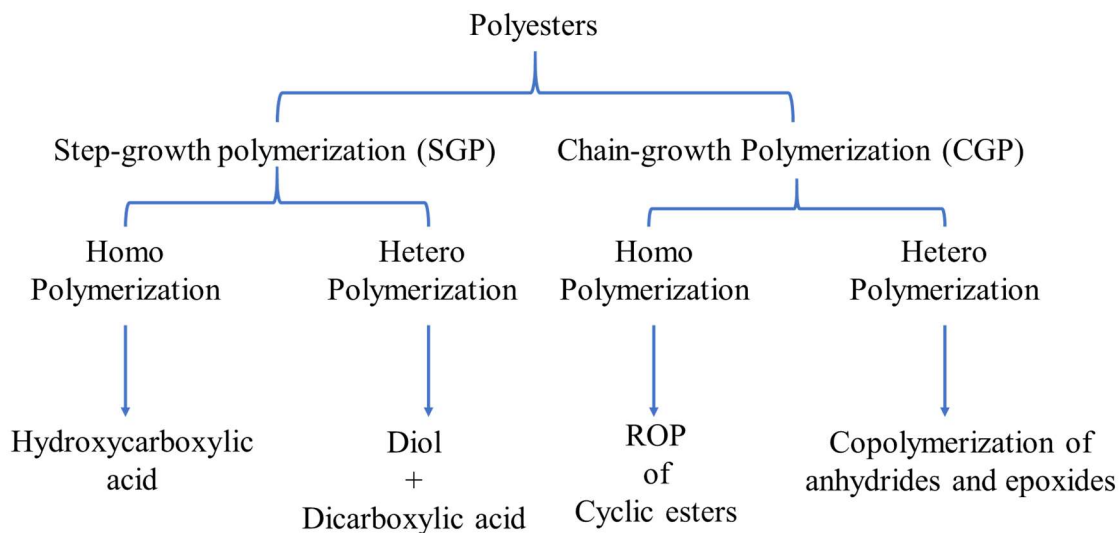


Figure 2. Routes for the synthesis of polyesters

In recent years, chain-growth polymerization (CGP) techniques for the production of polyesters, such as ring-opening polymerization (ROP) and ring-opening copolymerization (ROCOP), have received considerable attention (Fig. 3). Step-growth polymerization requires more energy than chain-growth polymerization; as a result, moderate conditions are sufficient for the CGP reactions to occur. In step-growth polymerization, water or alcohol is produced as a byproduct (which must be eliminated to enhance the polymerization reaction rate and increase the conversion), whereas chain-growth polymerization produces no byproduct (100% atom economy). In terms of the



variety of polymers that can be produced, a diverse number of monomers can be used with SGP to produce polyesters for specific applications, whereas a more restricted number of monomers are generally available for CGP. SGP lacks control over polymer microstructure and molecular weight, in contrast to CGP, whose microstructure and molecular weight can be more easily manipulated by the action of catalysts.<sup>11</sup>

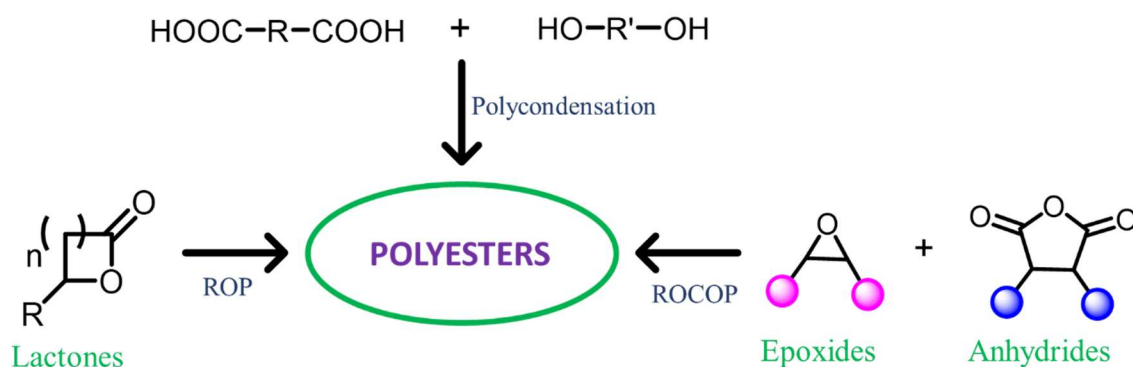
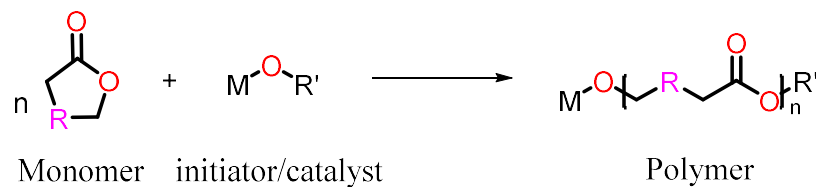


Figure 3. Different pathways for the synthesis of polyesters

## I.2 Ring opening polymerization (ROP) of cyclic esters

ROP of cyclic compounds for the formation of polymers has been thoroughly investigated during the past 40 years, due to versatility to produce variety of biomedical polymers in a controlled manner. Although the majority of these polyesters have a linear structure, it is feasible to create star-shaped, grafted, cross-linked, and hyperbranched structures by selecting the suitable catalysts and initiators via ROP (Scheme 1). The

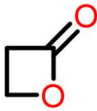
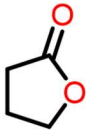
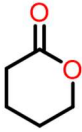
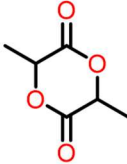
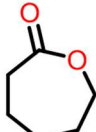
physical, mechanical, and degradation properties of these various macromolecules are studied to determine the structure-to-property relationships.<sup>12</sup>



Scheme 1: Schematic representation of ROP of cyclic ester. R= (CH<sub>2</sub>)<sub>0-7</sub> and /or (CHR'')

While the kinetics and selectivity of the ring-opening process are significantly influenced by the nature of the reactive chain ends, catalysts, and monomers, the thermodynamics of ROP is driven by the enthalpy of ring-opening for strained cyclic monomers or by the entropy of ring-opening for strainless large or macrocyclic monomers (Table 1). Depending on the initiator, polymerization follows one of three main reaction mechanisms: cationic, anionic, or "coordination-insertion" mechanisms. Initiation via radicals, zwitterionic or active hydrogen is also feasible, although these techniques are not widely employed.<sup>13,14</sup>

Table 1. Standard thermodynamics parameters of cyclic esters polymerization.

Monomer					
Ring size	4	5	6	6	7
$\Delta H/KJmol^{-1}$	-82.3	5.1	-27.4	-22.9	-28.8
$\Delta S/Jmol^{-1}K^{-1}$	-74	-29.9	65.0	-25.0	-53.9

### I.2.1 Cationic ring-opening polymerization

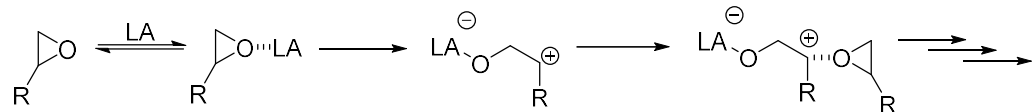
Lewis's acids (LAs) and Lewis bases (LBs) may mediate or catalyze the ROP, which is succinctly stated as follows.<sup>15</sup> The ROP supported by LAs is closely connected to the cationic ROP method, which uses positively charged active centers to transform heterocyclic monomers into bigger cycles and/or acyclic polymers.<sup>16,17,18</sup>

This form of polymerization uses catalysts which are acidic and have active sites that can accept two electrons. As these kinds of electrophiles, such as cyclic ethers, thioethers, amines, lactones, thiolactones, lactides, lactams, carbonates, siloxanes, phosphazenes, and others, may activate electron-rich sites, cyclic monomers that are capable of polymerization often include such sites.<sup>19,20,21</sup> There are two widely recognized mechanisms: the activated chain end mechanism (ACEM) and the activated

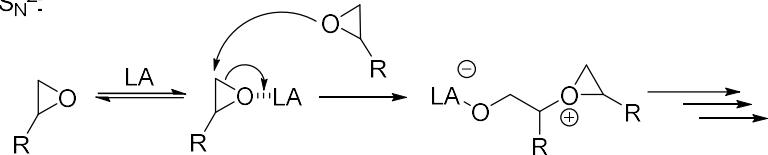
monomer mechanism (AMM), Scheme 2. The ability of these mechanisms to function may be influenced by a number of variables, including the type of catalysts used, the monomer being used, the use of a (co)initiator, and the polymerization conditions. The first mechanism (ACEM), which uses the ROP of oxiranes as an example, includes a propagating chain end of an electron-deficient site that joins to an incoming monomer through an  $S_N1$  or  $S_N2$  route. Before another monomer attacks in the  $S_N1$  pathway, the coordinated monomer opens its rings. In the  $S_N2$  route, the entering monomer is attacked before the ring is opened (Scheme 2). This is known as the activated chain end mechanism (ACEM) because the active site always remains at the chain end of the developing polymer. In the second mechanism, the monomer is repeatedly attacked by a nucleophile, usually an additional initiator or its polymeric counterparts, after being activated by the catalyst. It is known as the activated monomer mechanism (AMM) because the cationic charge is present on the activated monomer but not at the end of the polymer chain.<sup>10,11</sup>

**Activated Chain End Mechanism:**

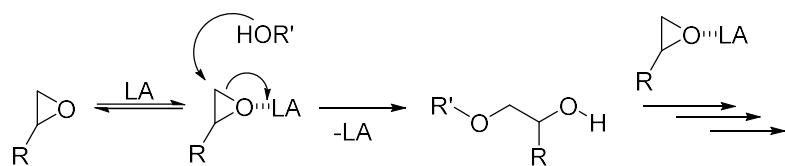
$S_N^1$ :



$S_N^2$ :



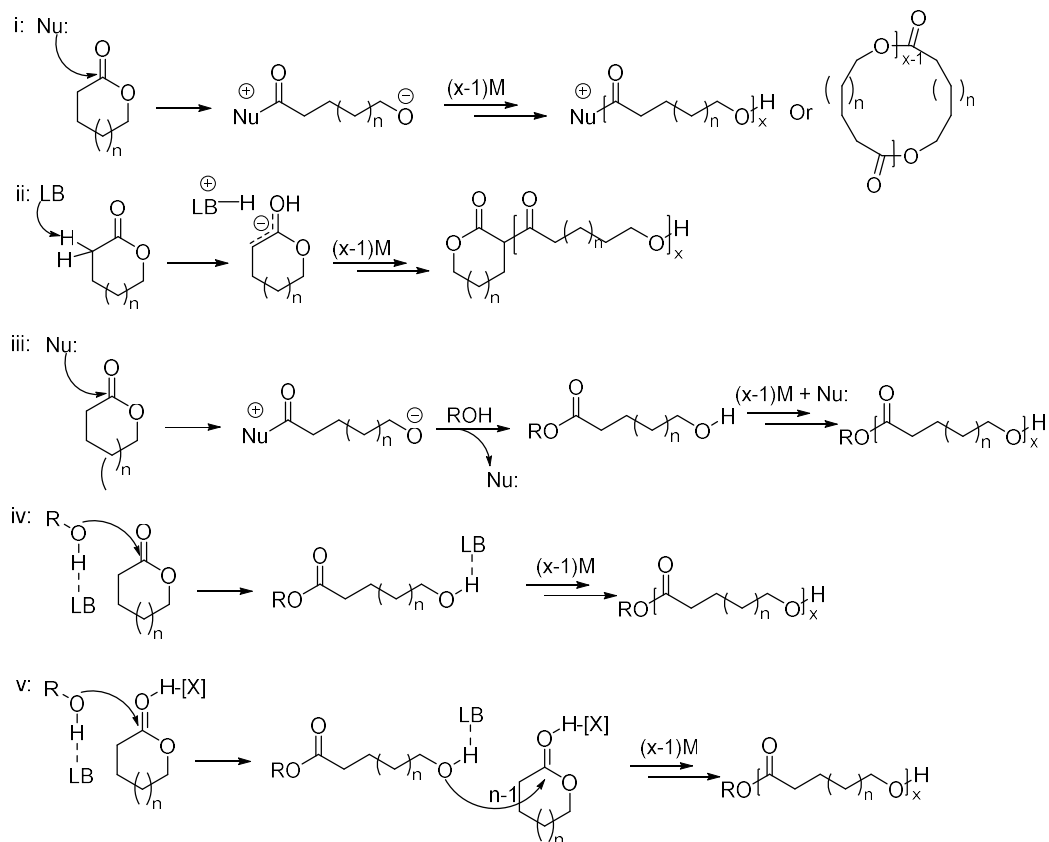
**Activated Monomer Mechanism:**



**Scheme 2:** Generalized Mechanisms Involved in the LA-Mediated Cationic ROP

**I.2.2 Anionic ring opening polymerization.**

The Lewis basicity, steric hindrance, and other important LB features, as well as the use of an alcohol initiator, are what determine the precise mechanism of the LB-mediated ROP. As an example, the nucleophilic assault of the LB on the monomer to produce a zwitterionic species for subsequent chain propagation was suggested for the LB-mediated ROP of lactones in the absence of an alcohol initiator (Scheme 3, i). It has been shown that this zwitterionic ROP is useful for synthesizing cyclic macromolecules with comparatively high MWs.<sup>22,23</sup>

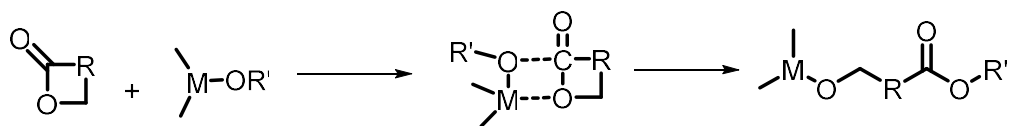


**Scheme 3:** Various Types of Chain Initiation and Propagation Pathways That Have Been Proposed to Be Involved in the ROP of Lactones by LBs for Polymer Chain Formation

### I.2.3 Coordination-Insertion Ring Opening Polymerization.

The pseudo-anionic ring-opening polymerization is frequently referred to as "coordination-insertion" ROP, as the propagation is believed to involve coordination of the monomer to the active species, followed by insertion of the monomer into the metal-oxygen bond via reorganization of the electrons. The coordination-insertion mechanism is

depicted in a schematic format in Scheme 4.<sup>24</sup> During propagation, the growing chain remains attached to the metal via an alkoxide bond. The reaction is terminated by the formation of a hydroxyl end group via hydrolysis. With the functional alkoxy-substituted initiators, macromolecules with active end groups for post-polymerization reactions are produced. Since coordination-insertion polymerization can produce well-defined polyesters via living polymerization, it has been extensively studied.<sup>25</sup> Using two monomers with similar reactivity, block copolymers can be formed by sequential addition to a "living" system.<sup>26</sup>



**Scheme 4:** The proposed reaction pathway for the coordination-insertion-mediated ring-opening polymerization of a cyclic ester.

#### I.2.4 Metal complexes used to catalyze ROP of cyclic esters.

Many metal-based catalysts have been intensively investigated for ROP (mostly Sn, but other Lewis acids such as Al, Zn, Ti, and different lanthanides have also been widely investigated).<sup>27,28,29,30,31</sup> The study of ligand variation (Fig. 4) has improved the understanding of how catalyst structure impacts polymer microstructure and overall polymerization performance. Simple metal alkoxides and carboxylates, such as tin octoate,

are inexpensive and convenient ROP catalysts that are employed in the production of PLA. However, those well-defined single-site metal catalysts with auxiliary ligands outperform in terms of selectivity, particularly stereoselectivity.

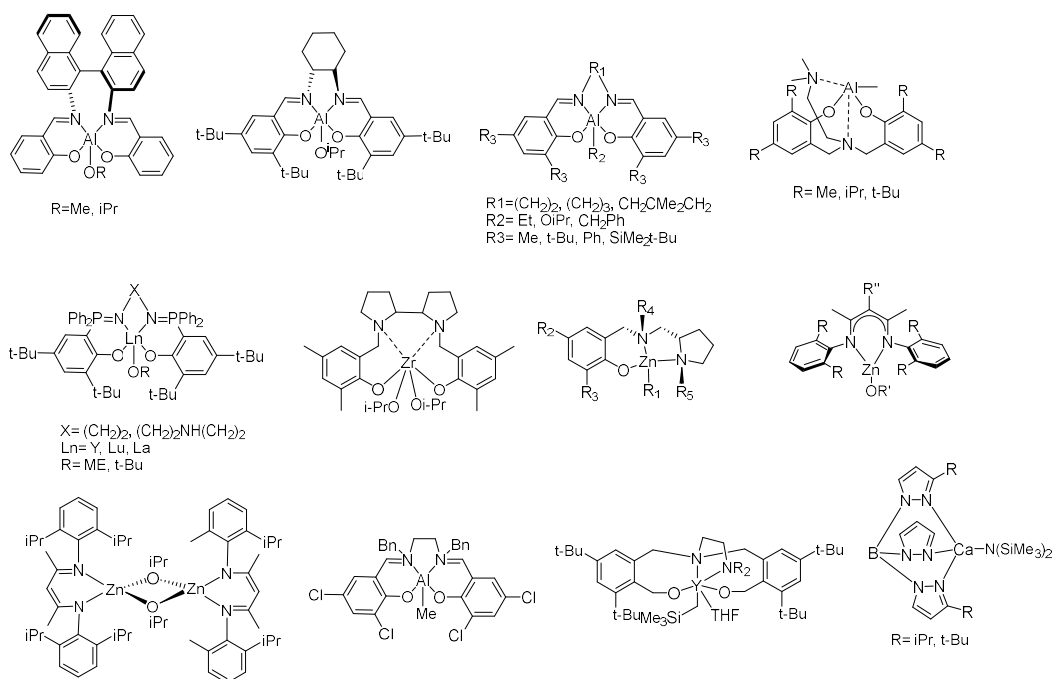


Figure 4: Examples of metal complexes used for ROP of lactide.

The auxiliary ligands have shown to be a key component in ROP catalysis for fine-tuning the electronic and steric characteristics of the metal center and controlling polymerization selectivity. Many review papers on the synthesis and catalytic performance of various types of metal catalysts have been published in the last decade, with Al, Zn, group 3, group 4 metals supported by N or O-type multidendate ligands gaining the most attention (Fig. 4)



<sup>32,33,34,35,36,37,38,39</sup> Some of these catalysts exhibit not only extraordinarily high reactivity (TOF>1000h<sup>-1</sup>), but also high regio-/stereoselectivity for asymmetric monomer ROP. For example, zinc catalyst with a  $\beta$ -diiminate amido ligand (BDIiPr)Zn[N(SiMe<sub>3</sub>)<sub>2</sub>] demonstrates good reactivity and selectivity for the ROP of a range of lactones and cyclic carbonates. Poly(trimethylenecarbonate) with  $M_n$  as high as 237 kDa with dispersity of 1.68 may be produced in quantifiable yield in 2 hours using just 20 ppm of the Zn catalyst.<sup>40</sup> There was no discernible ether bond in the resultant polymers, suggesting the lack of a decarboxylation process. Furthermore, this catalyst demonstrated outstanding regioselectivity (1% regio-defects) for the ROP of methyl-substituted cyclic carbonates.<sup>41</sup>

#### I.2.5 Macrocyclic Polymers via Ring Opening Polymerization.

Macrocyclic polyesters have attracted considerable interest due to their appealing physical properties that differ from their linear counterparts, such as glass transition temperature ( $T_g$ ), melting temperature ( $T_m$ ), morphologies, melt viscosities, thermal stability, compatibility, hydrodynamic volume, and intrinsic viscosity. In addition to its distinctive physical features, the cyclic topology imparts unique biophysical capabilities, which may provide significant benefits for a variety of biological applications as drug delivery vectors. While the synthesis of high purity cyclic polymers is difficult, a number of methods have been reported, including the statistical cyclization of linear polyesters during ester condensation polymerizations, the ring opening polymerization of lactone

monomers with metal catalysts, the N-heterocyclic carbenes-catalyzed cyclopolymerization of lactides, and the cyclization of,  $\alpha$ -functionalized linear polymer under high dilution. Each of these processes has benefits and drawbacks when it comes to the production of pure cyclic polyesters.<sup>42,43,44</sup> The monomer that was investigated the most for the base-mediated ROP is probably lactide for the production of different forms of PLA materials.<sup>45,46,47,48,49</sup> Hedrick and Waymouth et al. demonstrated for the first time that lactide ROP may be mediated by IMes to create cyclic PLA with  $M_n$  up to 30 kg/mol and  $\text{PDI} = 1.14\text{--}1.31$  (Scheme 2i).<sup>13, 50</sup>  $\epsilon$ -CL and  $\delta$ -VL may be polymerized by Lewis acid-base pairs with more nucleophilic NHCs (Figure 5&6) like  $\text{LiPr(Me)}$  and  $\text{IMe(Me)}$ .<sup>51,52,53,54</sup> Other monomers, such as cyclic siloxanes,<sup>55,56,57,58</sup> cyclic phosphates,<sup>59,60</sup> and N-carboxyanhydrides,<sup>61,62,63,64,65</sup> were also found to produce cyclic polymers by NHC-initiated ROP.

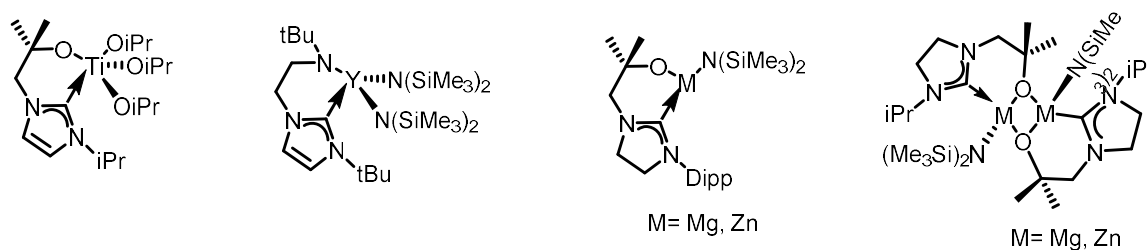


Figure 5: Structures of NHC-Tethered Titanium (IV), Yttrium (III), Magnesium (II), and Zinc (II) Bifunctional Complexes Employed for the ROP of Lactide

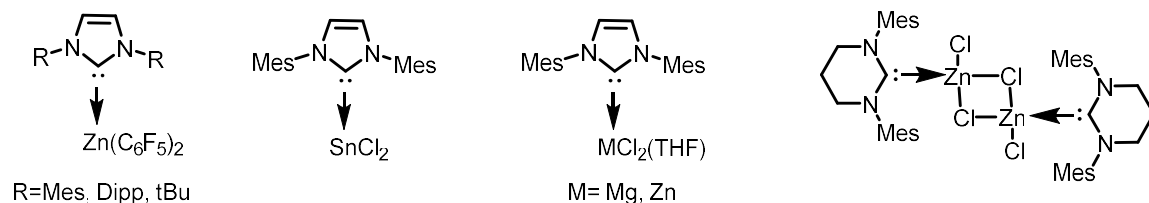


Figure 6: NHC–Zn(C<sub>6</sub>F<sub>5</sub>)<sub>2</sub> and NHC–Metal Chloride Adducts Employed for the ROP of Cyclic Esters

Strongly polarized N-heterocyclic olefins (NHOs) (Figure 7) were also reported to be efficient for the uncontrolled organo-polymerization of lactide, lactones, trimethylene carbonate, and non-strained butyrolactone ( $\gamma$ -BL),<sup>66,67,68</sup> yielding polymers with a linear topology or a combination of cyclic and linear topologies.<sup>69</sup> By analogy with the NHC-mediated ROP, other organic LBs, such as DBU, TBD, and 2-(tert-butylimino)-2-(diethylamino)-1,3-dimethylperhydro-1,3,2-diazaphosphorine (BEMP) can bring about the polymerization of lactide,<sup>70,71,72</sup> a glucose-based cyclic carbonate monomer (methyl 4,6-Obenzylidene-2,3-O-carbonyl- $\alpha$ -D-glucopyranoside), as well as homopolymerization and copolymerization of  $\beta$ -butyrolactone ( $\beta$ -BL) and benzyl  $\beta$ -malolactone.<sup>73,74,75</sup> Waymouth et al. discovered that isothioureas were more selective than DBU initiators for creating cyclic PLAs with no detectable linear impurities.<sup>76</sup> (+)-Sparteine was also used as a direct initiator for the ROP of Lactide, which acted as a dinucleophile, generating the zwitterionic and bisphenolic species (zwitterion).<sup>77</sup> Baceiredo, Mignani, and colleagues used phosphorus ylides as strong nonionic bases for anionic ROP of cyclic siloxanes.<sup>78</sup>

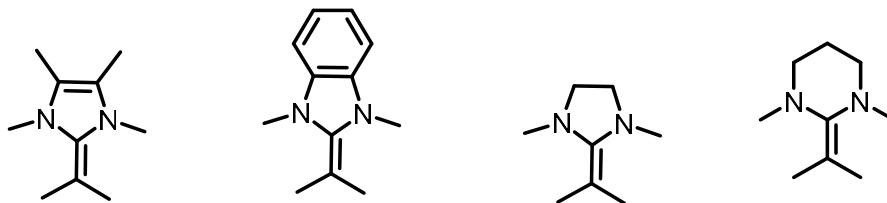


Figure 7: Structures of NHOs in combination with simple metal halides Such as  $\text{LiCl}$ ,  $\text{MgI}_2$ ,  $\text{MgCl}_2$ ,  $\text{YCl}_3$ ,  $\text{ZnI}_2$ ,  $\text{AlCl}_3$  as the LA to achieve controlled homo-and copolymerization of various cyclic esters.

### I.3 Ring Opening Copolymerization of Epoxides and Cyclic Anhydrides

ROCOP of epoxides and cyclic anhydrides is an appealing way toward sustainable polyesters, because of the myriads of available biobased monomers. A Lewis acid catalyst in combination with a nucleophilic or cationic cocatalyst commonly catalyzes ROCOP reactions. The ROCOP propagation cycle consists of three basic steps: (i) epoxide activation by Lewis-acidic metal center binding, (ii) epoxide ring opening via nucleophilic assault on a carboxylate chain end to generate a metal-alkoxide, and (iii) interaction of the metal-alkoxide with cyclic anhydride to form a new ester linkage, enchainning one more repeating unit. The developing polymer chain sequence continues to build an alternating polymer chain (Figure 8).<sup>79,80,81,82,83</sup>

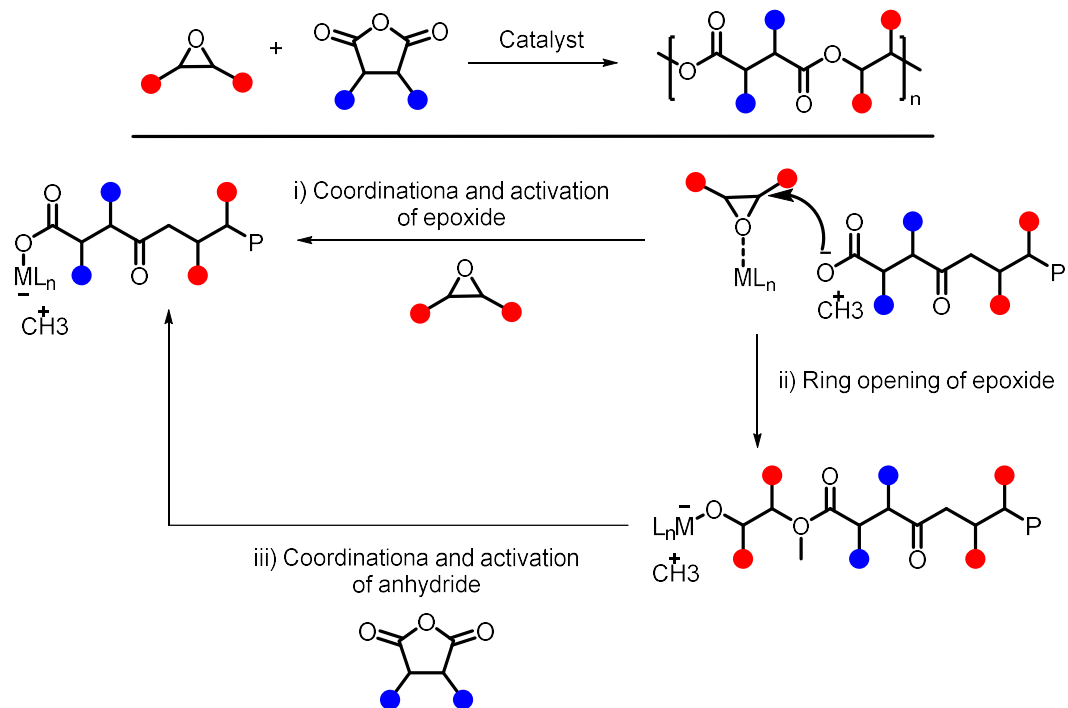


Figure 8: General reaction mechanism of the ROCOP

The earliest reports on the ROCOP of epoxides and anhydrides utilizing tertiary amines were published in the 1960s yielding low molecular weight polymers with broad dispersities and contamination of polyether.<sup>84</sup> Many studies on zinc and aluminum initiators have been published since Fischer and colleagues' original work.<sup>85,86,87,88,89</sup> Aluminum-porphyrin complexes in conjunction with phosphonium or ammonium salts were reported in 1985 as excellent catalysts for the copolymerization of styrene oxide (SO), propylene oxide (PO), and phthalic anhydride (PA), resulting in perfectly-alternating copolymers with TOF of  $5 \text{ h}^{-1}$  (Figure 9).<sup>69,71,90,91,92</sup>

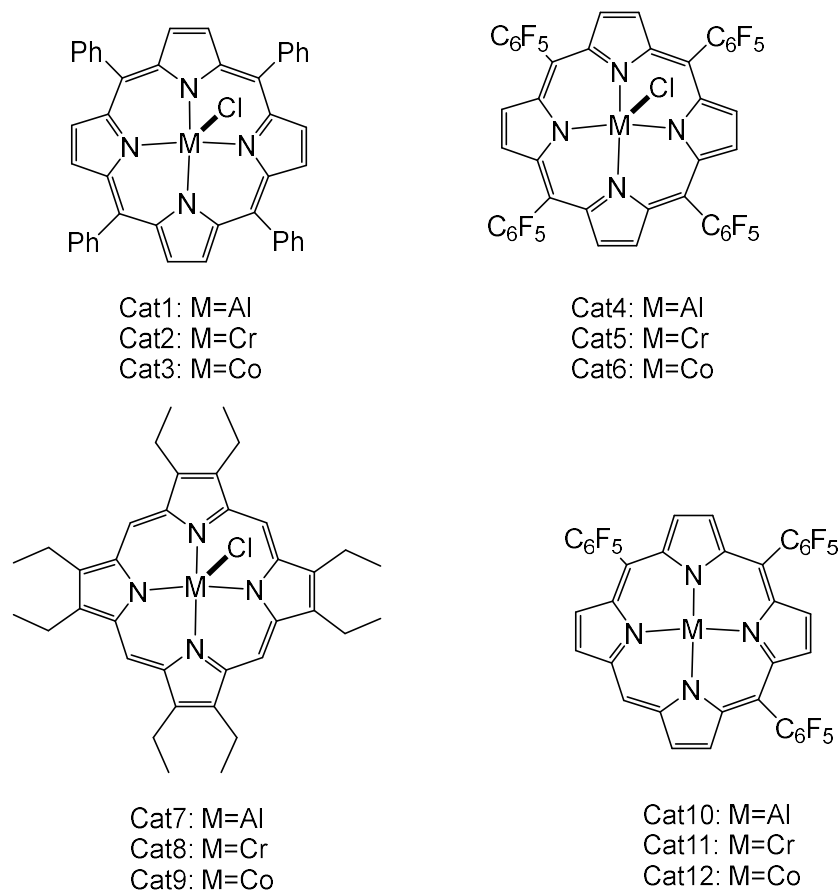


Figure 9: Porphyrin and corrole catalysts

Duchateau and colleagues described the use of a similar porphyrin complex with chromium as a metal center for copolymerizing SO or cyclohexene oxide (CHO) with PA or succinic anhydride (SA). The resulting polymers have high TOFs and molecular weights ranging from 1000 to 20,000 g/mol. Cobalt complexes with the same ligand combination generated polymer with a low TOF of 40 h<sup>-1</sup>.<sup>69,93</sup> Co and Cr complexes have been used to

copolymerize methyl succinic anhydride (MSA), maleic anhydride (MA), SA, or PA with PO (Figure 10).<sup>80</sup>

Coates and colleagues also reported a chromium salen complex for the ROCOP of PO, phenyl glycidyl ether, epichlorohydrin, or allyl glycidyl ether with MA, with a  $M_n$  of 2133 kg/mol (Figure 10). Many aluminum, cobalt, manganese, iron, and chromium complexes of salcy,<sup>70,94,95,96,97,98,99,100,101,102</sup> salph,<sup>81,103,104,105,106</sup> salan,<sup>107</sup> and salen<sup>69</sup> complexes were described by Duchateau and colleagues (Figure 10).

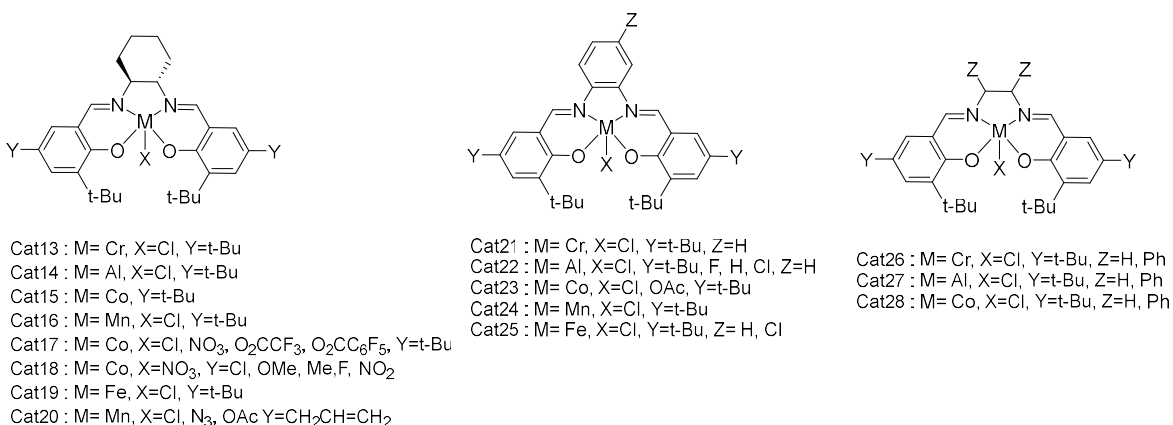


Figure 10: List of Salcyl, Salph, and Salen complexes used for ROCOP.

These complexes were employed, along with a cocatalyst DMAP, to catalyze the ROCOP of CHO with PA, SA, and CPrA, yielding poly(esters) with  $M_n$  of 2-15 kg/mol. The use of chromium-salalen complexes resulted in a high TOF of 150 h<sup>-1</sup>. They also observed that copolymerization of limonene oxide (LO) and PA with  $M_n$  of 4-7 kg/mol resulting from

enhanced activity of Al and Cr salen complexes (Figure 10). Copolymerization of epoxides with CO<sub>2</sub> is another critical event in the development of chemically degradable polycarbonate thermoplastics such isotactic poly(cyclohexene carbonate) (iPCHC).<sup>108</sup> Ellis et al. created a novel family of Zn catalysts for the alternating copolymerization of CO<sub>2</sub> and *meso*-CHO to produce highly isotactic polycarbonates.<sup>109</sup> The opening of a stereoselective S<sub>N</sub>2-type epoxide ring causes desymmetrization during polymerization, resulting in an isotactic polymer. Coates and colleagues identified different  $\beta$ -diiminate zinc complexes that were effective catalysts for ROP of epoxides and ROCOP of epoxide and CO<sub>2</sub> (Figure 11).<sup>110,111</sup> The same catalysts were used for ROCOP with diglycolic anhydride of LO, PO, isobutene oxide, or vinyl cyclohexene oxide.<sup>112,113,114,115,116</sup> Based on existing mechanistic information, the researchers identified a novel class of hybrid C<sub>1</sub>-symmetric ligands with a single stereocenter that, when coordinated to Zn, provided a variety of reactive and stereoselective catalysts.<sup>117,118</sup> Notably, the steric characteristics of ligand substituents successfully influenced the tacticity of the polymer. A preliminary screening of catalysts demonstrated that the presence of steric bulk at the stereocenter increases both activity and stereoselectivity. The researchers consequently constructed the second-generation catalysts which demonstrated strong TOF, enantioselectivity, and narrow molar mass distribution in polymerizations done at 0 °C.<sup>119</sup> Moore et al. were able to produce block copolymers by successive feeding of multiple alicyclic epoxides due to



more complicated polymer structures.<sup>120,121</sup>

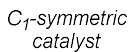


Figure 11: C<sub>1</sub>-Symmetric Zn-Complexes used for ROCOP of epoxides and CO<sub>2</sub>

#### I.4. REFERENCES

- 
1. Fahlman, B.D. (2023). What is “Materials Chemistry”? *Materials Chemistry*. Springer, Cham. **2023** [https://doi.org/10.1007/978-3-031-18784-1\\_1](https://doi.org/10.1007/978-3-031-18784-1_1)
  2. Namazi, H. Polymers in our daily life *BioImpacts*, **2017**, 7, 73-74 doi: 10.15171/bi.2017.09
  3. Kamarudin, S. H.; Rayung, M.; Abu, F.; Ahmad, S.; Fadil, F.; Karim, A. A.; Norizan, M. N.; Sarifuddin, N.; Mat Desa, M. S. Z.; Mohd Basri, M. S.; Samsudin, H.; Abdullah, L. C. A Review on Antimicrobial Packaging from Biodegradable Polymer Composites. *Polymers* **2022**, 14, 174.
  4. Mangaraj, S., Yadav, A., Bal, L. M. et al. Application of Biodegradable Polymers in Food Packaging Industry: A Comprehensive Review. *J. Package. Technol. Res.* **2019**, 3, 77–96.
  5. Annual production of plastics worldwide from 1950 to 2021., <https://www.statista.com/statistics/282732/global-production-of-plastics-since-1950/>  
Accessed on 05/03/2023
  6. Chemical and Material Polymers Market  
<https://www.precedenceresearch.com/polymers-market> Accessed on 05/08/2023

- 
7. Samir, A., Ashour, F.H., Hakim, A.A.A.; Bassyouni, M. Recent advances in biodegradable polymers for sustainable applications. *npj Mater Degrad.* **2022**, *6*, 68.
  8. Bher, A., Cho, Y., Auras, R., Boosting Degradation of Biodegradable Polymers. *Macromol. Rapid Commun.* **2023**, *44*, 2200769
  9. La Fuente, CIA, Maniglia, BC, Tadini, CC. Biodegradable polymers: A review about biodegradation and its implications and applications. *Packag Technol Sci.* **2023**, *36*, 81- 95.
  - 10 Nomura, K.; Awand, B. W.; Synthesis of Bio-Based Aliphatic Polyesters from Plant Oils by Efficient Molecular Catalysis: A Selected Survey from Recent Reports *ACS Sustainable Chem. Eng.* **2021**, *9*, 5486–5505.
  11. Zhang, X.; Fevre, M.; Jones, G. O.; Waymouth, R. M. Catalysis as an Enabling Science for Sustainable Polymers *Chem. Rev.* **2018**, *118*, 839–885.
  12. Pesenti, T.; Nicolas, J. 100th Anniversary of Macromolecular Science Viewpoint: Degradable Polymers from Radical Ring-Opening Polymerization: Latest Advances, New Directions, and Ongoing Challenges *ACS Macro Lett.* **2020**, *9*, 1812–1835.
  13. Olsén, P.; Odelius, K.; Albertsson, A. Thermodynamic Presynthetic Considerations for Ring-Opening Polymerization *Biomacromolecules* **2016**, *17*, 699–709.

- 
14. Duda, A., Kowalski, A., Libiszowski, J. and Penczek, S. (2005), Thermodynamic and Kinetic Polymerizability of Cyclic Esters. *Macromol. Symp.* **2005**, 224, 71-84.
15. Chen, E.Y.X. Polymerization by Classical and Frustrated Lewis Pairs. In Frustrated Lewis Pairs II: Expanding the Scope; Stephan, D. W., Erker, G., Eds.; Springer-Verlag: Berlin, Heidelberg, **2013**, 334, 239–260.
16. Matyjaszewski, K. In *Cationic Polymerizations: Mechanisms, Synthesis & Applications*; Matyjaszewski, K., Ed.; Marcel Dekker, Inc.: New York, 1996.
17. Odian, G. *Principles of Polymerization*; Wiley: Hoboken, NJ, 2004
18. Xia, Y., Yuan, P., Zhang, Y., Sun, Y., Hong, M. Converting Non-strained  $\gamma$ -Valerolactone and Derivatives into Sustainable Polythioesters via Isomerization-driven Cationic Ring-Opening Polymerization of Thionolactone Intermediate *Angew. Chem.* **2023**, 135, e202217812
19. Nuyken, O.; Pask, S. D. Ring-Opening Polymerization-An Introductory Review. *Polymers* **2013**, 5, 361–403.
20. Penczek, S. Cationic Ring-Opening Polymerization (CROP) Major Mechanistic Phenomena. *J. Polym. Sci., PartA: Polym. Chem.* **2000**, 38, 1919–1933
21. Kubisa, P.; Penczek, S. Cationic Activated Monomer Polymerization of Heterocyclic Monomers. *Prog. Polym. Sci.* **1999**, 24, 1409–1437.

- 
22. Culkin, D. A.; Jeong, W. H.; Csihony, S.; Gomez, E. D.; Balsara, N. R.; Hedrick, J. L.; Waymouth, R. M. Zwitterionic Polymerization of Lactide to Cyclic Poly(lactide) by using N Heterocyclic Carbene Organocatalysts. *Angew. Chem., Int. Ed.* **2007**, *46*, 2627–2630.
23. Jadrich, C. N.; Pane, V. E.; Lin, B.; Jones, G. O.; Hedrick, J. L.; Park, N. H.; Waymouth, R. M. A Cation-Dependent Dual Activation Motif for Anionic Ring-Opening Polymerization of Cyclic Esters *J. Am. Chem. Soc.* **2022**, *144*, 8439–8443.
24. Rao, W., Cai, C., Tang, J., Wei, Y., Gao, C., Yu, L. and Ding, J. Coordination Insertion Mechanism of Ring-Opening Polymerization of Lactide Catalyzed by Stannous Octoate. *Chin. J. Chem.*, **2001**, *39* 1965-1974.
25. Mecerreyes D.; Jérôme R.; Dubois Ph. Novel macromolecular architectures based in aliphatic polysters: Relevance of the “coordination-insertion” ring-opening polymerization, *Adv. Polym. Sci.*, **1999**, *147*, 1
26. Löfgren A.; Albertsson A.-C.; Dubois Ph.; Jérôme R.; Teyssié Ph., Synthesis and characterization of biodegradable homopolymers and block copolymers based on 1,5dioxepan-2-one *Macromolecules*, **1994**, *27*, 5556–5562.
27. Duda, A.; Penczek, S.; Kowalski, A.; Libiszowski, J. Polymerizations of  $\epsilon$ -caprolactone and L, L-dilactide initiated with stannous octoate and stannous butoxide-a comparison. *Macromol. Symp.* **2000**, *153*, 41–53.

- 
28. Fan, L.; Xiong, Y. B.; Tu, K. H.; Shen, Z. Q. Ring-opening polymerization of D, L-lactide by lanthanide tris(2,4,6-trimethylphenolate): characteristics and kinetics. *Chin. J. Chem.* **2005**, *23*, 613–616.
29. Kowalski, A.; Libiszowski, J.; Majerska, K.; Duda, A.; Penczek, S. Kinetics and mechanism of 3-caprolactone and L, L-lactide polymerization co-initiated with zinc octoate or aluminum acetylacetonate: The next proofs for the general alkoxide mechanism. *Polymer* 2007, **48**, 3952– 3960.
30. Duan, R. L.; Qu, Z.; Pang, X.; Zhang, Y.; Sun, Z. Q.; Zhang, H.; Bian, X. C.; Chen, X. S. Ring-Opening Polymerization of Lactide Catalyzed by Bimetallic Salen-Type Titanium Complexes. *Chin. J. Chem.* **2017**, *35*, 640– 644.
31. Dubois, Ph.; Jacobs, C.; Jerome, R.; Teyssie, Ph. Macromolecular engineering of polylactones and polylactides. 4. Mechanism and kinetics of lactide homopolymerization by aluminum isopropoxide. *Macromolecules* 1991, **24**, 2266– 2270.
32. Dechy, C. O.; Martin, V. B.; Bourissou, D. Controlled ring-opening polymerization of lactide and glycolide. *Chem. Rev.* **2004**, *104*, 6147–6176.
33. Sarazin, Y.; Carpentier, J. F. Discrete Cationic Complexes for Ring-Opening Polymerization Catalysis of Cyclic Esters and Epoxides. *Chem. Rev.* **2015**, *115*, 3564–3614.

- 
34. Amgoune, A.; Thomas, C. M.; Carpentier, J.-F. Controlled ring-opening polymerization of lactide by group 3 metal complexes. *Pure Appl. Chem.* **2007**, *79*, 2013–2030.
35. Sauer, A.; Kapelski, A.; Fliedel, C.; Dagorne, S.; Kol, M.; Okuda, J. Structurally well-defined group 4 metal complexes as initiators for the ring-opening polymerization of lactide monomers. *Dalton Trans.* **2013**, *42*, 9007–9023.
36. Carpentier, J. F. Rare-Earth Complexes Supported by Tripodal Tetradentate Bis(phenolate) Ligands: A Privileged Class of Catalysts for Ring-Opening Polymerization of Cyclic Esters. *Organometallics*. **2015**, *34*, 4175–4189.
37. Dijkstra, P. J.; Du, H. Z.; Feijen, J. Single site catalysts for stereoselective ring-opening polymerization of lactides. *Polym. Chem.* **2011**, *2*, 520–527.
38. Labet, M.; Thielemans, W. Synthesis of polycaprolactone: a review. *Chem. Soc. Rev.* **2009**, *38*, 3484–3504.
39. Ajellal, N.; Carpentier, J. F.; Guillaume, C.; Guillaume, S. M.; Helou, M.; Poirier, V.; Sarazin, Y.; Trifonov, A. Metal-catalyzed immortal ring-opening polymerization of lactones, lactides and cyclic carbonates. *Dalton Trans.* **2010**, *39*, 8363–8376

- 
40. Helou, M.; Miserque, O.; Brusson, J.-M.; Carpentier, J.-F.; Guillaume, S. M. Ultra-productive, Zinc-Mediated, Immortal Ring Opening Polymerization of Trimethylene Carbonate. *Chem. Eur. J.* **2008**, *14*, 8772–8775.
41. Brignou, P.; Carpentier, J.-F.; Guillaume, S. M. Metal-and Organo-Catalyzed Ring-Opening Polymerization of  $\alpha$ -Methyl-Trimethylene Carbonate: Insights in to the Microstructure of the Polycarbonate. *Macromolecules* **2011**, *44*, 5127–5135.
42. Hoskin, J. N.; Grayson, S. M. Cyclic polyesters: synthetic approaches and potential applications *Polym. Chem.*, **2011**, *2*, 289-299.
43. Yang, P. B.; Davidson, M. G.; Edler, K.J.; Brown, S. Synthesis, properties, and applications of bio-based cyclic aliphatic polyesters. *Biomacromolecules*. **2021**, *22*, 3649–3667.
44. Weng, C. and Tang, X. (2023), Circular Polymers from Ring-Opening Polymerization of Five-Membered (Thio)lactones and Derivatives. *Chin. J. Chem.* **2023**, <https://doi.org/10.1002/cjoc.202200841>
45. Auras, R., Poly(lactic acid). In *Encyclopedia of Polymer Science and Technology*; Mark, H. F., Ed.; Wiley: Hoboken, NJ, 2014; Vol. 10, pp 165–175.
46. Thomas, C. M. Stereocontrolled Ring-Opening Polymerization of Cyclic Esters: Synthesis of New Polyester Microstructures. *Chem. Soc.Rev.* **2010**, *39*, 165–173.



- 
47. Stanford, M. J.; Dove, A. P. Stereocontrolled Ring-Opening Polymerization of Lactide. *Chem. Soc. Rev.* **2010**, *39*, 486–494.
48. Platel, R. H.; Hodgson, L. M.; Williams, C. K. Biocompatible Initiators for Lactide Polymerization. *Polym. Rev.* **2008**, *48*, 11–63.
49. Dechy-Cabaret, O.; Martin-Vaca, B.; Bourissou, D. Controlled Ring-Opening Polymerization of Lactide and Glycolide. *Chem. Rev.* **2004**, *104*, 6147–6176.
50. Brown, H. A.; Waymouth, R. M. Zwitterionic Ring-Opening Polymerization for the Synthesis of High Molecular Weight Cyclic Polymers. *Acc. Chem. Res.* **2013**, *46*, 2585–2596.
51. Brown, H. A.; Xiong, S. L.; Medvedev, G. A.; Chang, Y. A.; Abu-Omar, M. M.; Caruthers, J. M.; Waymouth, R. M. Zwitterionic Ring-Opening Polymerization: Models for Kinetics of Cyclic Poly(caprolactone) Synthesis. *Macromolecules* **2014**, *47*, 2955–2963.
52. Acharya, A. K.; Chang, Y. A.; Jones, G. O.; Rice, J. E.; Hedrick, J. L.; Horn, H. W.; Waymouth, R. M. Experimental and Computational Studies on the Mechanism of Zwitterionic Ring-Opening Polymerization of  $\delta$ -Valerolactone with N-Heterocyclic Carbenes. *J. Phys. Chem. B* **2014**, *118*, 6553–6560.

- 
53. Pan, Z.; Gao, D.; Zhang, C.; Guo, L.; Li, J.; Cui, C. Synthesis and Reactivity of N-heterocyclic Carbene Stabilized Lanthanide (II) Bis(amido) Complexes. *Organometallics* **2021**, *40*, 1728–1734.
54. Hong, M.; Chen, J.; Chen, E. Y.-X. Polymerization of Polar Monomers Mediated by Main-Group Lewis Acid–Base Pairs. *Chem. Rev.* **2018**, *118*, 10551–10616.
55. Brown, H. A.; Chang, Y. A.; Waymouth, R. M. Zwitterionic Polymerization to Generate High Molecular Weight Cyclic Poly(Carbosiloxane)s. *J. Am. Chem. Soc.* **2013**, *135*, 18738–18741.
56. Rodriguez, M.; Marrot, S.; Kato, T.; Sterin, S.; Fleury, E.; Baceiredo, A. Catalytic Activity of N-Heterocyclic Carbenes in Ring Opening Polymerization of Cyclic Siloxanes. *J. Organomet. Chem.* **2007**, *692*, 705–708.
57. Bezlepina, K.A.; Milenin, S.A.; Vasilenko, N.G.; Muzafarov, A.M. Ring-Opening Polymerization (ROP) and Catalytic Rearrangement as a Way to Obtain Siloxane Mono- and Telechelics, as Well as Well-Organized Branching Centers: History and Prospects. *Polymers* **2022**, *14*, 2408.
58. Shi, J.; Liu, Z.; Zhao, N.; Liu, Z.; Li, Z. Controlled Ring-Opening Polymerization of Hexamethylcyclotrisiloxane Catalyzed by Trisphosphazene Organobase to Well-Defined Poly(dimethylsiloxane)s *Macromolecules* **2022**, *55*, 2844–2853.

- 
59. Stukenbroeker, T. S.; Solis-Ibarra, D.; Waymouth, R. M. Synthesis and Topological Trapping of Cyclic Poly(alkylene phosphates). *Macromolecules* **2014**, *47*, 8224–8230.
60. Morodo, R.; Riva, R.; van den Akker, N. M. S.; Molin, D. G. M.; Jérôme, C.; Monbaliu, J. C. M. Accelerating the end-to-end production of cyclic phosphate monomers with modular flow chemistry *Chem. Sci.*, **2022**, *13*, 10699-10706.
61. Guo, L.; Zhang, D. H. Cyclic Poly( $\alpha$ -peptoid)s and Their Block Copolymers from N-Heterocyclic Carbene-Mediated Ring Opening Polymerizations of N-Substituted N-Carboxyanhydrides. *J. Am. Chem. Soc.* **2009**, *131*, 18072–18074.
62. Guo, L.; Lahasky, S. H.; Ghale, K.; Zhang, D. H. N-Heterocyclic Carbene-Mediated Zwitterionic Polymerization of N-Substituted N-Carboxyanhydrides toward Poly( $\alpha$ -peptoid)s: Kinetic, Mechanism, and Architectural Control. *J. Am. Chem. Soc.* **2012**, *134*, 9163–9171.
63. Zhang, D. H.; Lahasky, S. H.; Guo, L.; Lee, C. U.; Lavan, M. Polypeptoid Materials: Current Status and Future Perspectives. *Macromolecules* **2012**, *45*, 5833–5841.
64. Jiang, J.; Zhang, X.; Fan, Z.; Du, J. Ring-Opening Polymerization of N-Carboxyanhydride-Induced Self-Assembly for Fabricating Biodegradable Polymer Vesicles *ACS Macro Lett.* **2019**, *8*, 1216–1221.

- 
65. Wang, S.; Lu, H. Ring-Opening Polymerization of Amino Acid N-Carboxyanhydrides with Unprotected/Reactive Side Groups. I. d-Penicillamine N-Carboxyanhydride *ACS Macro Lett.* **2023**, *12*, XXX, 555–562
66. Naumann, S.; Thomas, A. W.; Dove, A. P. Highly Polarized Alkenes as Organo catalysts for the Polymerization of Lactones and TrimethyleneCarbonate. *ACS Macro Lett.* **2016**, *5*, 134–138.
67. Walther, P.; Frey, W.; Naumann, S. Polarized Olefins as Enabling (Co)catalysts for the Polymerization of  $\gamma$ -Butyrolactone. *Polym. Chem.* **2018**, *9*, 3674–3683.
- 68 Song, Q.; Zhao, J.; Zhang, G.; Peruch, F.; Carlotti, S. Ring-opening (co)polymerization of  $\gamma$ -butyrolactone: a review. *Polym. J.* **2020**, *52*, 3–11.
69. Hong, M.; Chen, E. Y.-X. Completely Recyclable Biopolymers with Linear and Cyclic Topologies via Ring-Opening Polymerization of  $\gamma$ -Butyrolactone. *Nat. Chem.* **2016**, *8*, 42–49
70. Brown, H. A.; DeCrisci, A. G.; Hedrick, J. L.; Waymouth, R. M. Amidine-Mediated Zwitterionic Polymerization of Lactide. *ACS MacroLett.* **2012**, *1*, 1113–1115.
71. Azechi, M.; Matsumoto, K.; Endo, T. Anionic Ring-Opening Polymerization of a Five-Membered Cyclic Carbonate Having a Glucopyrano side Structure. *J. Polym.Sci., PartA: Polym.Chem.* **2013**, *51*, 1651–1655.

- 
72. Haba, O.; Tomizuka, H.; Endo, T. Anionic Ring-Opening Polymerization of Methyl 4,6-O-benzylidene-2,3-O-carbonyl- $\alpha$ -D-glucopyranoside: A First Example of Anionic Ring-Opening Polymerization of Five-Membered Cyclic Carbonate without Elimination of CO<sub>2</sub>. *Macromolecules* **2005**, *38*, 3562–3563.
73. Jaffredo, C. G.; Carpentier, J. F.; Guillaume, S. M. Controlled ROP of  $\beta$ -Butyrolactone Simply Mediated by Amidine, Guanidine, and Phosphazene Organocatalysts. *Macromol. Rapid Commun.* **2012**, *33*, 1938–1944.
74. Jaffredo, C. G.; Carpentier, J. F.; Guillaume, S. M. Poly(hydroxyalkanoate) Block or Random Copolymers of  $\beta$ -Butyrolactone and Benzyl  $\beta$ -Malolactone: A Matter of Catalytic Tuning. *Macromolecules* **2013**, *46*, 6765–6776.
75. Jaffredo, C. G.; Carpentier, J. F.; Guillaume, S. M. Organocatalyzed Controlled ROP of  $\beta$ -Lactones towards Poly(hydroxyalkanoate)s: from  $\beta$ -Butyrolactone to Benzyl  $\beta$ -Malolactone Polymers. *Polym. Chem.* **2013**, *4*, 3837–3850.
76. Zhang, X. Y.; Waymouth, R. M. Zwitterionic Ring Opening Polymerization with Isothioureas. *ACS MacroLett.* **2014**, *3*, 1024–1028.
77. Coulembier, O.; DeWinter, J.; Josse, T.; Mespouille, L.; Gerbaux, P.; Dubois, P. One-Step Synthesis of Polylactide Macrocycles from Sparteine-Initiated ROP. *Polym. Chem.* **2014**, *5*, 2103–2108.

- 
78. Bessmertnykh, A.; Ben, F.; Baceiredo, A.; Mignani, G. Anionic Ring-Opening Polymerization of Cyclic Organosiloxanes Using Phosphorus Ylides as Strong Non-Ionic Bases. *J. Organomet. Chem.* **2003**, *686*, 281–285.
79. Longo, J. M.; Sanford, M. J.; Coates, G. W. Ring-opening Copolymerization of Epoxides and Cyclic Anhydrides with Discrete Metal Complexes: Structure-Property Relationships. *Chem. Rev.* **2016**, *116*, 15167–15197.
80. Childers, M. I.; Longo, J. M.; VanZee, N. J.; LaPointe, A. M.; Coates, G. W. Stereoselective Epoxide Polymerization and Copolymerization. *Chem. Rev.* **2014**, *114*, 8129–8152.
81. Huijser, S.; Hosseini Nejad, E.; Sablong, R.; deJong, C.; Koning, C. E.; Duchateau, R. Ring-Opening Co- and Terpolymerization of an Alicyclic Oxirane with Carboxylic Acid Anhydrides and CO<sub>2</sub> in the Presence of Chromium Porphyrinato and Salen Catalysts. *Macromolecules.* **2011**, *44*, 1132–1139.
82. Darensbourg, D. J.; Poland, R. R.; Escobedo, C. Kinetic Studies of the Alternating Copolymerization of Cyclic Acid Anhydrides and Epoxides, and the Terpolymerization of Cyclic Acid Anhydrides, Epoxides, and CO<sub>2</sub> Catalyzed by (Salen)Cr<sup>III</sup>Cl. *Macromolecules.* **2012**, *45*, 2242–2248.

- 
83. Harrold, N. D.; Li, Y.; Chisholm, M. H. Studies of Ring Opening Reactions of Styrene Oxide by Chromium Tetraphenylporphyrin Initiators. Mechanistic and Stereochemical Considerations. *Macromolecules*. **2013**, *46*, 692–698.
84. Fischer, R.F. Polyesters from epoxides and anhydrides. *J. Polym. Sci.* **1960**, *44*, 155-172.
85. Luston, J.; Manasek, Z. Copolymerization of Epoxides with Cyclic Anhydrides Catalyzed by Tertiary Amines in the Presence of Proton Donating Compounds. *J. Macromol. Sci., Chem.* **1979**, *13*, 853–867.
86. Luston, J.; Vass, F. Anionic Copolymerization of Cyclic Ethers with Cyclic Anhydrides. *Adv. Polym. Sci.* **1984**, *56*, 91–133.
87. Masters, J. E. Epoxide-Anhydride-Hydroxy Polymer Compositions and Method of Making Same. U. S. Patent US2908663, October 13, 1959.
88. Nagata, N.; Taniguchi, S. Copolymers of epoxy resins, unsaturated carboxylic acids or anhydrides, and other copolymerizable monomers for use as coatings and sizing agents. Patent GB 1081295 19670831, 1967.
89. Sakai, S.; Ito, H.; Ishii, Y. Reactivity and Polymerizability of Cyclic Compounds. IX. Copolymerization of Epoxides with Succinic Anhydride Catalyzed by Organotin Compounds. *Kogyo Kagaku Zasshi* **1968**, *71*, 186–187.

- 
90. Aida, T.; Sanuki, K.; Inoue, S. Well-controlled polymerization by metalloporphyrin. Synthesis of copolymer with alternating sequence and regulated molecular weight from cyclic acid anhydride and epoxide catalyzed by the system of aluminum porphyrin coupled with quaternary organic salt *Macromolecules*. **1985**, *18*, 1049–1055.
91. Aida, T.; Inoue, S. Catalytic reaction on both sides of a metalloporphyrin plane. Alternating copolymerization of phthalic anhydride and epoxyp propane with an aluminum porphyrin-quaternary salt system *J. Am. Chem. Soc.* **1985**, *107*, 1358–1364
92. Bernard, A.; Chatterjee, C.; Chisholm, M. H. The Influence of the Metal (Al, Cr and Co) and the Substituents of the Porphyrin in Controlling the Reactions Involved in the Copolymerization of Propylene Oxide and Cyclic Anhydrides by Porphyrin Metal (III) Complexes. *Polymer* **2013**, *54*, 2639–2646.
93. Hosseini Nejad, E.; Paoniasari, A.; Koning, C. E.; Duchateau, R. Semi-aromatic polyesters by alternating ring-opening copolymerisation of styrene oxide and anhydrides *Polym. Chem.* **2012**, *3*, 1308–1313.
- 94 Robert, C.; deMontigny, F.; Thomas, C. M. Tandem Synthesis of Alternating Polyesters from Renewable Resources. *Nat. Commun.* **2011**, *2*, 586.



- 
95. Hosseini Nejad, E.; vanMelis, C. G. W.; Vermeer, T. J.; Koning, C. E.; Duchateau, R. Alternating Ring-Opening Polymerization of Cyclohexene Oxide and Anhydrides: Effect of Catalyst, Cocatalyst, and Anhydride Structure. *Macromolecules* **2012**, *45*, 1770–1776.
96. Biermann, U.; Sehlinger, A.; Meier, M. A. R.; Metzger, J. O. Catalytic Copolymerization of Methyl-9,10-Epoxyoctadecanoate and Cyclic Anhydride under Neat Conditions. *Eur. J. LipidSci. Technol.* **2016**, *118*, 104–110.
97. DiCiccio, A. M.; Coates, G. W. Ring-Opening Copolymerization of Maleic Anhydride with Epoxides: A Chain-Growth Approach to Unsaturated Polyesters. *J. Am. Chem. Soc.* **2011**, *133*, 10724–10727.
98. Longo, J. M.; DiCiccio, A. M.; Coates, G. W. Poly(propylenesuccinate): A New Polymer Stereocomplex. *J. Am. Chem. Soc.* **2014**, *136*, 15897–15900.
99. Liu, D.; Zhang, Z.; Zhang, X.; Lu, X. Alternating Ring-Opening Copolymerization of Cyclohexene Oxide and Maleic Anhydride with Diallyl-Modified Manganese (III)–Salen Catalysts. *Aust. J. Chem.* **2015**, *69*, 47–55.
100. Mundil, R.; Host'alek, Z.; Sedenkova, I.; Merna, J. Alternating Ring-Opening Copolymerization of Cyclohexene Oxide with Phthalic Anhydride Catalyzed by Iron(III)Salen Complexes. *Macromol. Res.* **2015**, *23*, 161–166.

- 
101. Duan, Z.; Wang, X.; Gao, Q.; Zhang, L.; Liu, B.; Kim, I. Highly Active Bifunctional Cobalt-Salen Complexes for the Synthesis of Poly(Ester-Block-Carbonate) Copolymer Via Terpolymerization of Carbon Dioxide, Propylene Oxide, and Norbornene Anhydride Isomer: Roles of Anhydride Conformation Consideration. *J. Polym. Sci., PartA: Polym. Chem.* **2014**, *52*, 789–795.
102. Jeon, J. Y.; Eo, S. C.; Varghese, J. K.; Lee, B. Y. Copolymerization and Terpolymerization of Carbon Dioxide/Propylene Oxide/Phthalic Anhydride Using a (Salen)Co(III) Complex Tethering Four Quaternary Ammonium Salts. *Beilstein J. Org. Chem.* **2014**, *10*, 1787–1795.
103. Nejad, E. H.; Paoniasari, A.; vanMelis, C. G. W.; Koning, C. E.; Duchateau, R. Catalytic Ring-Opening Copolymerization of Limonene Oxide and Phthalic Anhydride: Toward Partially Renewable Polyesters. *Macromolecules* **2013**, *46*, 631–637.
104. Sanford, M. J.; Pena Carrodegua, L.; VanZee, N. J.; Kleij, A. W.; Coates, G. W. Alternating Copolymerization of Propylene Oxide and Cyclohexene Oxide with Tricyclic Anhydrides: Access to Partially Renewable Aliphatic Polyesters with High Glass Transition Temperatures. *Macromolecules* **2016**, *49*, 6394–6400.
105. VanZee, N. J.; Coates, G. W. Alternating Copolymerization of Propylene Oxide with Biorenewable Terpene-Based Cyclic Anhydrides: A Sustainable Route to Aliphatic

---

Polyesters with High Glass Transition Temperatures. *Angew. Chem., Int. Ed.* **2015**, *54*, 2665–2668

106. VanZee, N. J.; Sanford, M. J.; Coates, G. W. Electronic Effects of Aluminum Complexes in the Copolymerization of Propylene Oxide with Tricyclic Anhydrides: Access to Well-Defined, Functionalizable Aliphatic Polyesters. *J. Am. Chem. Soc.* **2016**, *138*, 2755–2761.

107. Liu, J.; Bao, Y. -Y.; Liu, Y.; Ren, W. -M.; Lu, X. -B. Binuclear Chromium-Salan Complex Catalyzed Alternating Copolymerization of Epoxides and Cyclic Anhydrides. *Polym. Chem.* **2013**, *4*, 1439–1444.

108. Liu, Y.; Zhou, H.; Guo, J. Z.; Ren, W. M.; Lu, X. B. Completely Recyclable Monomers and Polycarbonate: Approach to Sustainable Polymers. *Angew. Chem., Int. Ed.* **2017**, *56*, 4862–4866.

109. Ellis, W. C.; Jung, Y.; Mulzer, M.; DiGirolamo, R.; Lobkovsky, E. B.; Coates, G. W. Copolymerization of CO<sub>2</sub> and Meso Epoxides Using Enantioselective  $\beta$ -Diiminate Catalysts: A Route to Highly Isotactic Polycarbonates. *Chem. Sci.* **2014**, *5*, 4004–4011.

110. Jeske, R. C.; DiCiccio, A. M.; Coates, G. W. Alternating Copolymerization of Epoxides and Cyclic Anhydrides: An Improved Route to Aliphatic Polyesters. *J. Am. Chem. Soc.* **2007**, *129*, 11330–11331.

- 
111. Cheng, M.; Moore, D. R.; Reczek, J. J.; Chamberlain, B. M.; Lobkovsky, E. B.; Coates, G. W. Single-Site  $\beta$ -Diiminate Zinc Catalysts for the Alternating Copolymerization of CO<sub>2</sub> and Epoxides: Catalyst Synthesis and Unprecedented Polymerization Activity. *J. Am. Chem. Soc.* **2001**, *123*, 8738–8749.
112. Nozaki, K.; Nakano, K.; Hiyama, T. Optically Active Polycarbonates: Asymmetric Alternating Copolymerization of Cyclohexene Oxide and Carbon Dioxide. *J. Am. Chem. Soc.* **1999**, *121*, 11008–11009.
113. Cheng, M.; Darling, N. A.; Lobkovsky, E. B.; Coates, G. W. Enantiomerically-Enriched Organic Reagents via Polymer Synthesis: Enantioselective Copolymerization of Cycloalkene Oxides and CO<sub>2</sub> Using Homogeneous, Zinc-Based Catalysts. *Chem. Commun.* **2000**, 2007–2008.
114. Nakano, K.; Nozaki, K.; Hiyama, T. A symmetric Alternating Copolymerization of Cyclohexene Oxide and CO<sub>2</sub> with Dimeric Zinc Complexes. *J. Am. Chem. Soc.* **2003**, *125*, 5501–5510.
115. Xiao, Y.; Wang, Z.; Ding, K. Copolymerization of Cyclohexene Oxide with CO<sub>2</sub> by Using Intramolecular Dinuclear Zinc Catalysts. *Chem. Eur. J.* **2005**, *11*, 3668–3678.

- 
116. Abbina, S.; Du, G. Chiral Amido-Oxazolinato Zinc Complexes for Asymmetric Alternating Copolymerization of CO<sub>2</sub> and Cyclohexene Oxide. *Organometallics*. **2012**, *31*, 7394–7403.
117. Cheng, M.; Lobkovsky, E. B.; Coates, G. W. Catalytic Reactions Involving C1 Feedstocks: New High-Activity Zn(II)-Based Catalysts for the Alternating Copolymerization of Carbon Dioxide and Epoxides. *J. Am. Chem. Soc.* **1998**, *120*, 11018–11019.
118. Kim, J. G.; Cowman, C. D.; LaPointe, A. M.; Wiesner, U.; Coates, G. W. Tailored Living Block Copolymerization: Multiblock Poly(cyclohexenecarbonate)s with Sequence Control. *Macromolecules* **2011**, *44*, 1110–1113.
119. Moore, D. R.; Cheng, M.; Lobkovsky, E. B.; Coates, G. W. Electronic and Steric Effects on Catalysts for CO<sub>2</sub>/Epoxide Polymerization: Subtle Modifications Resulting in Superior Activities. *Angew. Chem., Int. Ed.* **2002**, *41*, 2599–2602.
120. Moore, D. R.; Cheng, M.; Lobkovsky, E. B.; Coates, G. W. Mechanism of the Alternating Copolymerization of Epoxides and CO<sub>2</sub> using  $\beta$ -Diiminate Zinc Catalysts: Evidence for A Bimetallic Epoxide Enchainment. *J. Am. Chem. Soc.* **2003**, *125*, 11911–11924.

---

121. Shao, H.; Reddi, Y.; Cramer, C. J. Modeling the Mechanism of CO<sub>2</sub>/Cyclohexene Oxide Copolymerization Catalyzed by Chiral Zinc  $\beta$ -diiminates: Factors Affecting Reactivity and Isotacticity. *ACS Catal.* **2020**, *10*, 8870–8879.

## CHAPTER II

### AMIDO-OXAZOLINATO ZINC COMPLEXES CATALYZED RING OPENING COPOLYMERIZATION AND TERPOLYMERIZATION OF CYCLIC ANHYDRIDES AND EPOXIDES

#### II.1 INTRODUCTION

Polyesters are an important class of biodegradable and biocompatible polymers that possess various applications in drug delivery, orthopedic implants, artificial tissues, and commodity materials.<sup>(1-4)</sup> Typical synthetic methods of polyesters involve step growth polycondensation or ring-opening polymerization (ROP).<sup>5-6</sup> The step-growth polymerization of diols and diacids/diesters usually requires high temperatures and long reaction times, and can lead to side reactions and low molecular weight polymers.<sup>7-10</sup> ROP of cyclic esters effectively produces polyesters with controlled structure and molecular weight, but the availability of cyclic monomers may be limited. Catalytic ring-opening copolymerization (ROCOP) of epoxides and cyclic anhydrides is another technique to produce polyesters that has gained increased attention in recent years.<sup>11,12</sup> This approach could possibly circumvent the limitations posed by the aforementioned methods while taking advantage of both. Specifically, a wide selection of diverse epoxides and cyclic anhydrides offers the structural flexibility and tunability of the step growth polymerization. The milder reaction conditions and potential controllability of the chain growth polymerization may lead to more economical production and well-defined polymer

structures.<sup>13</sup> Additionally, ROCOP with two or more different epoxides or cyclic anhydrides provides endless possibilities in modifying the polymer backbone structure and thermomechanical properties. The increasing availability of bio-derived epoxides and cyclic anhydrides further enhances the attractiveness of the approach.<sup>14-16</sup>

Generally, ROCOP of epoxides and cyclic anhydrides is believed to proceed through alternating insertion of the two monomers into the growing chain of alkoxide and carboxylate, a mechanistic scenario very similar to ROCOP of epoxides and CO<sub>2</sub> that generates polycarbonates.<sup>17,18</sup> While the polycarbonate synthesis *via* ROCOP has been well-studied and various catalysts have been reported,<sup>19,20</sup> ROCOP of epoxides and cyclic anhydrides for polyesters has seen a rapid growth only in the last decade, notably since the advance made by Coates and co-workers that zinc  $\beta$ -diketiminate catalyzed ROCOP afforded polyesters with high molecular weight and narrow dispersity.<sup>21</sup> Most of the catalysts are based on Lewis acidic metals supported by various ligands, such as Cr,<sup>22-30</sup> Co,<sup>31-36</sup> Zn,<sup>37-44</sup> Al,<sup>45-53</sup> and Mg,<sup>54,55</sup> and metal-free organocatalysts are also being developed more recently.<sup>56-62</sup> These progresses have led to highly active and selective catalysts,<sup>63</sup> well-controlled polymer structure and molecular weight, and adjustable polymer sequences.<sup>64</sup> A series of amido oxazolinato zinc complexes, analogous to the widely studied  $\beta$ -diketiminato zinc catalysts, have been shown to be effective in the synthesis of biodegradable polymers including polycarbonates, polylactides and polyesters via catalytic ring opening polymerization and copolymerization.<sup>65-67</sup> Herein we describe the applications of zinc catalysts (Scheme 1) in ROCOP of cyclic anhydrides and various



epoxides and investigate their application in the terpolymerization. The focus is on maleic anhydride (MA) because the ROCOP with MA leads to formation of unsaturated polyesters, which have been widely used in a variety of applications based on the post-polymerization modification of C=C double bonds.<sup>68-70</sup>

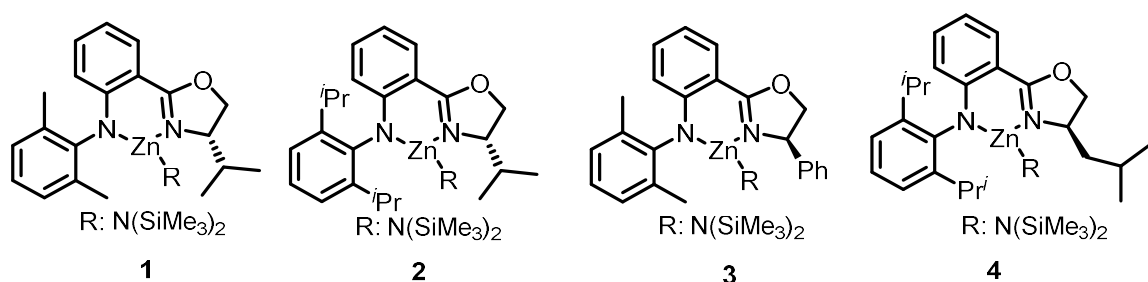


Figure 1. Amido-oxazolinato zinc complexes for ROCOP of CHO with anhydrides.

## II.2 RESULTS AND DISCUSSION

### II.2.1 Optimizing Reactions with MA/CHO

Previously we have investigated the zinc (complexes **1-4**) catalyzed ROCOP using styrene oxide (SO) as a representative electron withdrawing epoxide for preparation of semi-aromatic polyesters with different cyclic anhydrides.<sup>39</sup> Among them, the maleic anhydride (MA) showed the highest selectivity towards polyester formation. Hence, we focused here on MA and cyclohexene oxide (CHO), an aliphatic epoxide. Because CHO could easily undergo homopolymerization at elevated temperatures in the presence of a catalyst, the initial reaction conditions were varied in an attempt to minimize the formation of ether linkages in the ROCOP of CHO and MA. Following the standard conditions

identified earlier with SO, the reaction was carried out with CHO:MA:**1** ratio of 100:100:1 in toluene at 100 °C. Complete conversion of CHO was achieved in 16 h with 53% poly(ester) linkage with  $M_n$  of 5900 g/mol and dispersity ( $\bar{D}$ ) of 1.29. Despite of the moderate molecular weight, 47% poly(ether) was formed under this condition (Table 1, entry 2). To lower the concentration of CHO, a solution of CHO in toluene was slowly added to a solution of MA and cat-**1** in toluene over a period of 30 min. The reaction reached 100% conversion of CHO in 24 h and afforded polymer with 73% poly(ester) linkages and lower molecular weight ( $M_n$  2700 g/mol), presumably due to the dilution of reaction mixture. Using CHO:MA:cat-**1** ratio of 200:200:1, reaction afforded polymer with 61% ester linkages in 9 h with  $M_n$  of 2300 g/mol and  $\bar{D}$  of 1.20 (Table 1, entry 4). To see the effect of dilution, the same reaction was repeated with 10 mL toluene instead of the previously used 2 mL. As expected, reaction took longer time and  $M_n$  was decreased to 1200 g/mol without much change in the selectivity towards poly(ester) (Table 1, entry 5). Under bulk conditions without solvent, homopolymerization of CHO was predominant, leading to 76% poly(ether) content (Table 1, entry 6). The conversion reached a plateau due to the viscous nature of the reaction mixture that limited the reactivity between two co-monomers in the reaction. Using excess MA in the reaction afforded low molecular weight polymers (Table 1, entry 7). The trace amount of maleic acid present in MA even after multiple sublimations may have acted as chain transfer agents that leads to low molecular weight polymers. The similar result was observed in the last run, where excess co-monomers resulted in low molecular weight polymers (Table 1, entry 8). Without catalyst,

the reaction of CHO and MA afforded no poly(ester) or poly(ether) at 100 °C and extended reaction time. (Table 1, entry 1). Considering both reactivity and selectivity, epoxide:anhydride:catalyst ratio of 200:200:1 at 100 °C was employed in the later runs.

**Table 1.** Optimization of reaction conditions between MA and CHO.<sup>a</sup>

Entry	[cat]:[CHO]:[MA]	Time (h)	Conv <sub>n</sub> (%) <sup>b</sup>	Ester% <sup>b</sup>	<i>M<sub>n</sub></i> (kg/mol) <sup>c</sup>	<i>Đ</i> <sup>c</sup>
1	0:100:100	24	0	-	-	-
3	1:100:100	16	100	53	5.9	1.29
2 <sup>d</sup>	1:100:100	24	100	73	2.7	1.43
4	1:200:200	9	100	61	2.3	1.20
5 <sup>e</sup>	1:200:200	16	96	65	1.2	1.19
6 <sup>f</sup>	1:200:200	0.92	88	14	3.8	1.82
7	1:200:400	1	100	46	0.78	1.12
8	1:1000:1000	1.5	100	34	1.2	1.28

<sup>a</sup>All reactions were performed using cat-1 in toluene (2 mL) at 100 °C. <sup>b</sup>The conversion of CHO and the ester% were determined by measuring the intensities of peaks by <sup>1</sup>H NMR spectroscopy. <sup>c</sup>Determined by GPC using THF as solvent with a flow rate of 1 mL/min. <sup>d</sup>CHO in toluene was added slowly to a solution of catalyst and maleic anhydride. <sup>e</sup>5 times the normal volume of toluene was used. <sup>f</sup>Bulk reaction without toluene.

## II.2.2 Comparison of Epoxides in ROCOP with MA

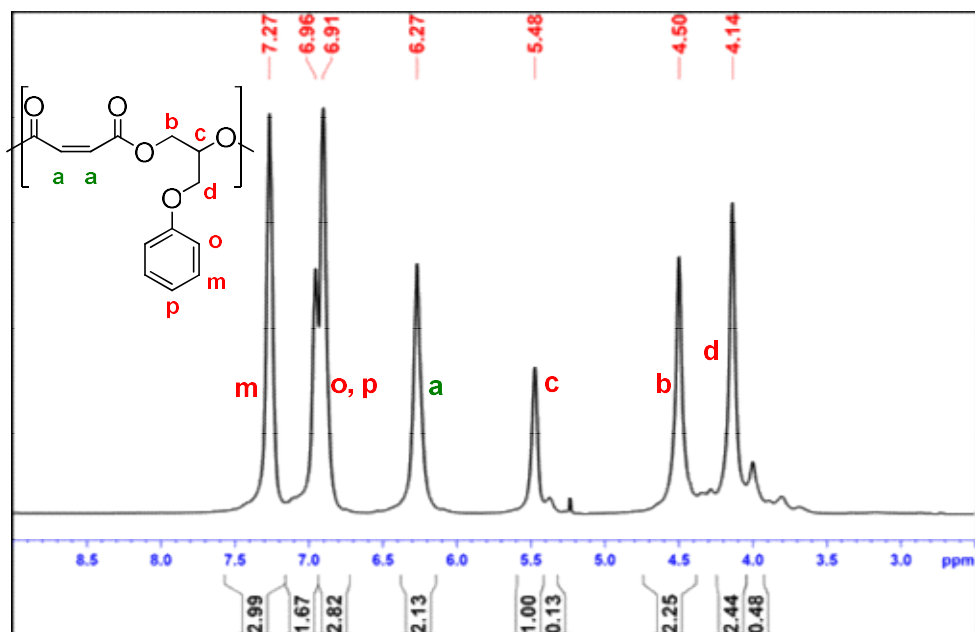
Given the difference observed between CHO and SO, we were interested in further comparing the reactivity of different epoxides by including a third epoxide, phenyl glycidyl ether (PGE) in the copolymerization with MA catalyzed by cat-1. The results are summarized in Table 2. Clearly, the reactivity of PGE in ROCOP with MA was much lower compared to SO and CHO, requiring longer time (48 h) for a complete conversion of PGE. Conversely, the selectivity towards ester linkages was high, reaching up to 95% under the employed reaction conditions. The molecular weight was also higher with a broad dispersity. The  $^1\text{H}$  and  $^{13}\text{C}$  NMR of the purified polyester are shown in Figure 1. The olefinic proton peaks are observed at 6.27 ppm, and the ester bridge signals are observed at 5.5 (methine) and 4.5 (methylene) ppm. The assignments are confirmed by 2D NMR techniques (see Figures A.I-5 and A.I-6 in the Appendix A.I). These results showed minimal amount of ether signals from the homopolymerization of PGE and are in support of the alternating nature of the polyester structure.

**Table 2.** ROCOP of MA with different Epoxides.<sup>a</sup>

Entry	Epoxides	Time/h	Conv <sub>n</sub> %	Ester%	$M_n/\text{kg mol}^{-1}$	$\bar{D}$
1	SO	0.33	100	76	2.6	1.13
2	CHO	9	100	61	2.3	1.29

3            PGE            48            100            95            4.8            2.05

<sup>a</sup>All reactions were performed using catalyst **1** in toluene (2 mL) at 100 °C with [Cat]:[MA]:[Epoxide] = 1:200:200. The conversion of epoxides and the ester% were determined by <sup>1</sup>H NMR spectroscopy.



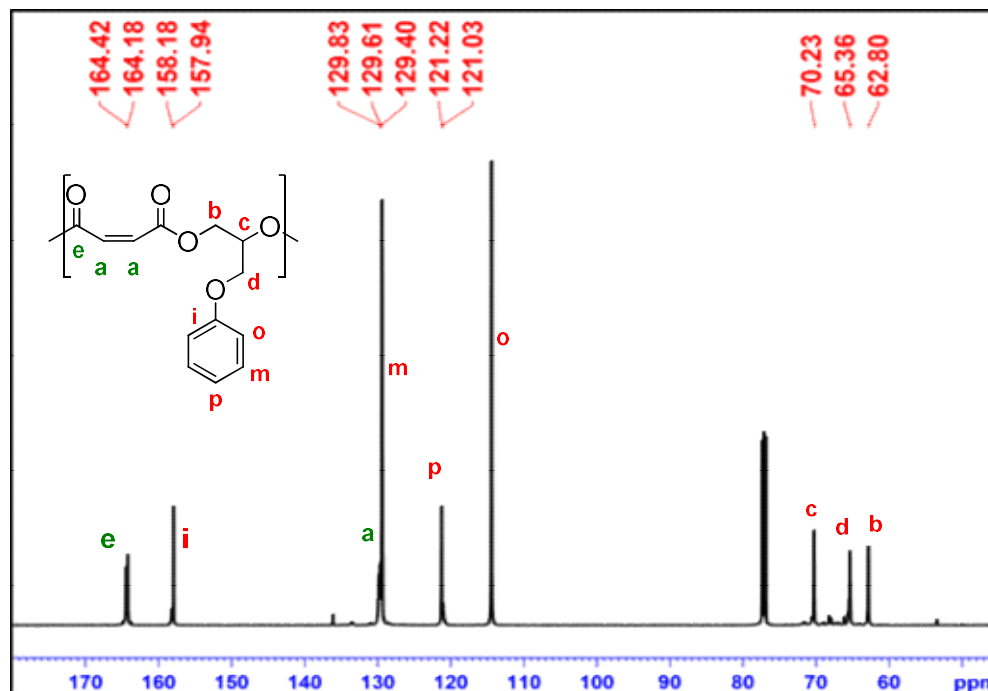
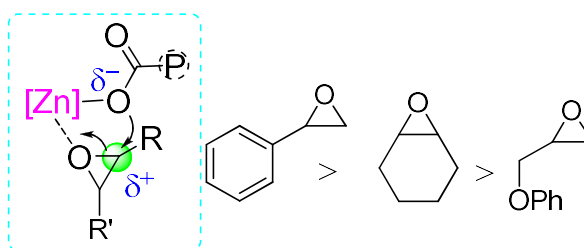


**Figure 2.**  $^1\text{H}$  (top) and  $^{13}\text{C}$  NMR (bottom) of polyester from PGE & MA with catalyst **1**

The observed relative reactivity of epoxides,  $\text{SO} > \text{CHO} > \text{PGE}$ , can be explained approximately based on their electronic factors. Generally, zinc catalyzed ROCOP involves the nucleophilic attack of chain ends on epoxide and anhydride monomers alternatingly in the chain propagation. The ring opening reaction at the epoxide is electronically controlled, i.e., the attack at the electron-deficient site is favored (Scheme 2). SO features an electron withdrawing phenyl substituent that facilitates the nucleophilic attack of propagating carboxylates on the epoxide ring, leading to a comparably fast reaction. In comparison, the electron donating nature of substituents in PGE and CHO renders them less active for the epoxide ring-opening event. The electronic dependence on the epoxide monomer resembles the effect of catalysts and selectivity in ROCOP of SO

and MA.<sup>39</sup> The fact that both SO with an electron withdrawing group and PGE with an electron donating group give higher selectivity toward ester linkages suggests that the propensity of CHO toward homopolymerization (to polyether) is mostly due to the ring strains in CHO.



**Scheme 1:** Chain propagation step explaining the reactivity of epoxides.

### II.2.3. Effect of Catalysts and Anhydrides in ROCOP

With CHO as a representative aliphatic epoxide, we further investigated the effect of different catalysts and anhydrides. As seen in Table 3, complexes **2-4** showed comparable activity, resulting in complete conversion of CHO in 2-4 h and comparable molecular weight of polymers. However, the selectivity towards ester linkages was decreased (37-44% polyester). In these cases, MA was not completely consumed in the reaction. We further explored the effect of cyclic anhydrides on ROCOP. High conversion of CHO was observed within 3-6 h with phthalic anhydride (PA) (entries 5-8), though the selectivity towards polyester and the molecular weights were low (34-43% polyester). ROCOP with succinic anhydride (SA) (entries 9-12) generally afforded polymers with higher selectivity (50-66% polyester) and higher molecular weights but required longer

reaction times (6-11 h). Cat-**2** bearing isopropyl substituent on the anilino moiety as well as on the oxazoline ring afforded 58% selectivity and  $M_n$  of 4200 g/mol, however, 100% conversion was not achieved in this case (entry 10). Overall, the relative activity of the three cyclic anhydrides in the reaction could be attributed to the ring strain in the cyclic anhydrides: PA>MA>SA, while the structural features of catalysts **1-4** seemed to exert no clear trend in their reactivity. This latter observation is in contrast with the ROCOP of SO and cyclic anhydrides, where both electronic and steric features of catalysts play a noticeable role.<sup>39</sup>

**Table 3.** ROCOP of CHO with different cyclic anhydrides.<sup>a</sup>

Entry	Catalyst	Anhydride	Time (h)	Conv (%) <sup>b</sup>	Ester% <sup>b</sup>	$M_n$ (kg/mol) <sup>c</sup>	$\bar{D}$ <sup>c</sup>
1	<b>1</b>	MA	9	100	61	2.3	1.29
2	<b>2</b>	MA	3.5	100	44	2.6	1.30
3	<b>3</b>	MA	2	100	37	5.3	1.30
4	<b>4</b>	MA	2	100	40	2.9	1.34
5	<b>1</b>	PA	3	93	37	1.5	1.17
6	<b>2</b>	PA	5.5	97	40	1.8	1.24
7	<b>3</b>	PA	3	100	41	1.9	1.15
8	<b>4</b>	PA	4.5	97	44	1.8	1.20
9	<b>1</b>	SA	9	98	60	3.7	1.24



10	<b>2</b>	SA	5.5	78	74	4.2	1.30
11	<b>3</b>	SA	9	91	55	4.2	1.15
12	<b>4</b>	SA	11	98	67	3.3	1.14

---

<sup>a</sup>All reactions were performed with [CHO]:[anhydride]:[cat]=200:200:1 in toluene (2 mL) at 100 °C.

<sup>b</sup>Determined by measuring the intensities of peaks on <sup>1</sup>H NMR spectroscopy. <sup>c</sup>Determined by GPC using THF as solvent with a flow rate of 1 mL/min.

## II.2.4 Terpolymerization of MA and Two Epoxides

One common strategy for tuning the polymer properties such as glass transition temperature ( $T_g$ ) is to incorporate additional monomers to form block or random copolymers.<sup>71-75</sup> Given the versatility of the current zinc catalysts for various epoxides and anhydrides, we were interested to see if terpolymerization could be achieved and how it could affect the properties of the resulting terpolymers. For this purpose, we selected the three epoxides (SO, CHO, and PGE) differing in their rates of reactions with maleic anhydride (MA) to synthesize terpolymers from MA and two epoxides catalyzed by cat-1. Selected results are summarized in Table 4.

To take advantage of the reactivity difference of epoxides, we first carried out the terpolymerization of 2 equiv of MA with one equiv of CHO and one equiv of PGE in one pot, in an attempt to obtain diblock polyesters in a single step.<sup>76-78</sup> Monitoring the reaction by <sup>1</sup>H NMR spectroscopy showed that SO was consumed within a few hours while the complete conversion of the second epoxide PGE was much slower, as expected from the

activity difference of SO and PGE. However, the molecular weight of the resulting polymer was only 4.3 kg/mol, much less than the theoretical value estimated from the catalyst loading and conversion (Table 4, entry 4). Running the reaction in one pot but two steps by sequential addition of CHO and PGE gave similar results; particularly, the molecular weights obtained after the complete consumption of first addition of CHO showed little increase during the second step when PGE was added (Table 4, entry 1). Reversing the order of the two steps, i.e, adding PGE first followed by CHO, led to somewhat higher molecular weight but still lower than the theoretical value (Table 4, entry 2). A representative  $^1\text{H}$  NMR spectrum of the terpolymer p(CHO-PGE-MA) is shown in Figure 2. The ratio of the PGE-derived ester to the CHO-derived ester is about 1.7:1. The relatively low CHO component as ester may be a result of CHO homopolymerization. Different combinations of two epoxides afforded similar results in terms of molecular weights and compositions (entries 5, 6). Thus, it appeared that the diblock polyesters were not obtained under these conditions. Instead, they were mostly likely random polymers. We ascribed this to the presence of chain transfer agents and transesterification reaction that led to the scrambling of the ester linkages and shorter chains.

**Table 4.** Terpolymerization of MA with two different epoxides<sup>a</sup>

Run	Step 1	Step 2	Ester ratio <sup>b</sup>	$M_n$ <sup>c</sup> /kg mol <sup>-1</sup>	$\bar{D}$ <sup>c</sup>
1	CHO/MA	PGE/MA	CHO:PGE = 1.0:2.3	4.8	2.21

2	PGE/MA	CHO/MA	CHO:PGE = 1.0:2.7	10.3	1.88
3	SO/MA	CHO/MA	SO:CHO = 1.0: 0.26	3.9	1.41
4	CHO/PGE/MA		CHO:PGE = 1.0:1.7	4.3	1.88
5	CHO/SO/MA		SO:CHO = 1.0:0.94	2.0	1.34
6	SO/PGE/MA		SO:PGE = 1.0:1.0	1.9	1.40

<sup>a</sup>All reactions were performed using cat-1 in toluene (2 mL) at 100 °C. The first three were run in two steps while the last three were run in a single step with both epoxides present from the start. <sup>b</sup>The ester ratios were determined from the intensities of the corresponding ester peaks in the polymers by <sup>1</sup>H NMR spectroscopy. <sup>c</sup>Determined by GPC using THF as eluent.

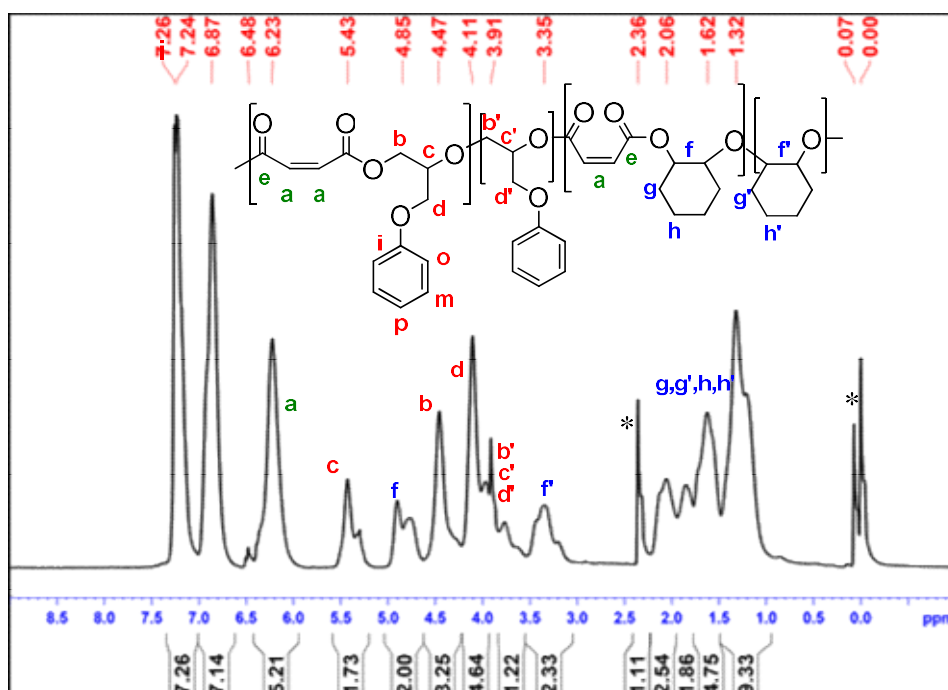


**Figure 3.** <sup>1</sup>H NMR spectrum of terpolymer poly(CHO-PGE-MA) (Table 4, entry 4)

### II.2.5 Thermal Properties of Copolymers and Terpolymers

The thermal properties of the terpolymers were next studied with DSC and TGA techniques. For comparison, we first investigated the behaviors of copolyesters, poly(CHO-*alt*-MA), poly(SO-*alt*-MA) and poly(PGE-*alt*-MA) synthesized in the present study, the results of which are summarized in Table 5. As expected, the glass-transition temperatures ( $T_g$ ) of the polymers are dependent on the structure of the epoxide monomers. poly(CHO-*alt*-MA) has the highest  $T_g$  at 63 °C among the three, which can be attributed to the presence of rigid cyclohexane ring structure in the polymer main chain. poly(SO-*alt*-MA) has a  $T_g$  of 39 °C, and poly(PGE-*alt*-MA) has a lowest  $T_g$  of 30 °C, which can be rationalized on the basis of the steric bulk of the substituents. For the terpolymer poly(CHO/PGE-*alt*-MA), a single glass transition temperature was observed at 41-44 °C, which falls between the  $T_g$  of poly(CHO-*alt*-MA) and poly(PGE-*alt*-MA). The other terpolymers also displayed a single glass transition that mostly fall between the corresponding copolymers. These results suggested that the terpolymers were mostly random polymers, in agreement with the assignments from NMR and GPC studies earlier.

The thermal stability of these polyesters were examined by TGA, and the results are summarized in Figure 3 and Table 5. All the polymers have thermal degradation temperature above 200 °C, typical of polyester behavior. Generally, the terpolymers showed a single stage thermal decomposition profile and the  $T_{50\%}$  values of the terpolymers fall in between the  $T_{50\%}$  of the corresponding copolymers. In some cases, a poorly resolved second peak could be observed in the differential thermal analysis (DTA)

plot (Figure A.I-19), and both peaks were somewhat shifted towards the middle. The observations suggested that the resulting polymers are likely random terpolymers, but perhaps with enriched segments of copolyesters.

**Table 5:** Thermal properties of co- and terpolymers<sup>a,b</sup>

Entry	Polymer	$T_g$	$T_{-5\%}$	$T_{-50\%}$
Table 2, entry 1	p(SO-MA)	39	256	314
Table 2, entry 2	p(CHO-MA)	63	211	349
Table 2, entry 3	p(PGE-MA)	30	244	387
Table 4, entry 1	p(CHO-PGE-MA)	41	213	375
Table 4, entry 2	p(CHO-PGE-MA)	44	281	370
Table 4, entry 3	p(SO-CHO-MA)	61	219	352
Table 4, entry 4	p(CHO-PGE-MA)	43	208	366
Table 4, entry 5	p(CHO-SO-MA)	59	156	316
Table 4, entry 6	p(SO-PGE-MA)	24	199	350

<sup>a</sup>Temperatures in °C. <sup>b</sup> $T_g$  values were determined from the second heating cycle in DSC.  $T_{-5\%}$  and  $T_{-50\%}$ , refer to the temperatures at which 5%, and 50% weight losses were observed in TGA, respectively.

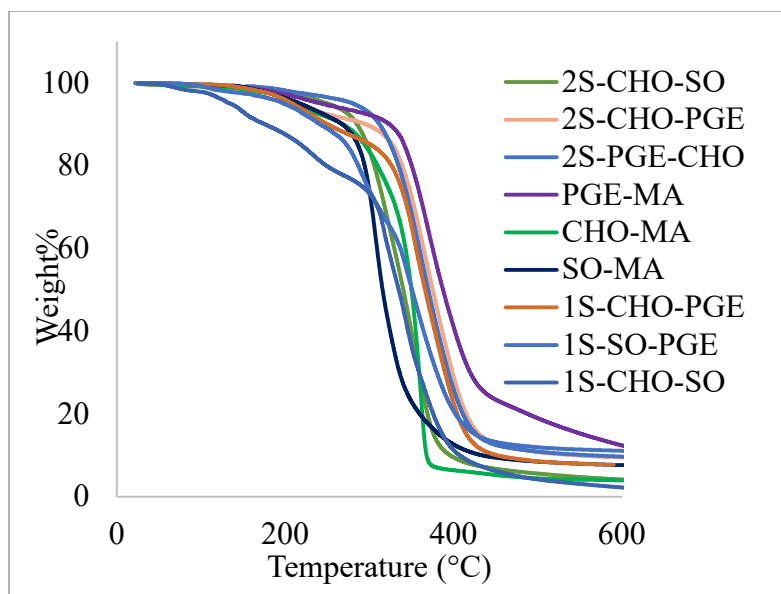


**Figure 4.** TGA profiles of the copolymers and terpolymers (1S for one-step and 2S for two-step reactions)

### II.3 CONCLUSIONS

In summary, we have demonstrated that the amido-oxazolate zinc complexes **1–4** are effective catalysts for the ROCOP of maleic anhydride with various epoxides, leading to the synthesis of unsaturated polyesters with easily modifiable backbones. The relative activity of epoxides (SO > CHO > PGE) in these reactions can be correlated with the electronic and steric features of the substrates, along with considerations of the chain propagation steps. The reactivity of the zinc catalysts is further exploited to prepare terpolymers from one anhydride and two epoxides, providing additional structural possibilities for the polyesters. Future studies will focus on the synthesis of copolymers with controlled segments and their potential applications.

## II.4 EXPERIMENTAL SECTION

### **General Considerations.**

### **Materials and Methods.**

Solvents used in polymerization reaction and ligand syntheses including toluene and hexanes were distilled under nitrogen over Na/benzophenone. Deuterated solvents purchased from Cambridge Isotope Laboratories and distilled over  $\text{CaH}_2$  and degassed prior to use and stored in a glovebox. Analytical grade THF was purchased from Fisher Scientific and used as received. Cyclohexene oxide, styrene oxide and phenyl glycidyl ether were stirred over ground  $\text{CaH}_2$  overnight, vacuum transferred to a dry Schlenk flask, degassed by three freeze-pump-thaw cycles, and stored in a glovebox with 4 Å molecular sieves. Maleic anhydride, phthalic anhydride, and succinic anhydride were purified by sublimation under nitrogen. Zinc bis(trimethylsilyl)amide<sup>1</sup> and the amido-oxazolate zinc complexes were synthesized following the literature procedures.

All reactions with air- and/or moisture sensitive compounds were carried out under dry nitrogen atmosphere using standard glovebox or Schlenk line techniques. 1D and 2D NMR experiments were recorded with a Bruker AVANCE-500 NMR spectrometer and the spectra were referenced to the residual peaks in  $\text{CDCl}_3$  ( $^1\text{H}$ , and  $^{13}\text{C}$ ). The microstructures of polyesters samples were characterized by  $^{13}\text{C}$  NMR spectra recorded at room temperature in  $\text{CDCl}_3$  with concentrations in the range 1 to 1.5 mg/mL. Gel permeation chromatography (GPC) analysis was performed with a Varian Prostar equipped with auto

sampler model 400, a PLgel 5 mm mixed-D column, a Prostar 355 RI detector, and THF as eluent at a flow rate of 1 mL min<sup>-1</sup> (20 °C). Polystyrene standards purchased from Agilent technologies were used for calibration. Galaxie software was used to operate the instrument and Cirrus software for data processing. Differential scanning calorimetry (DSC) measurements were obtained on a Perkin Elmer Jade differential scanning calorimeter and the instrument was calibrated using zinc and indium standards. Samples were prepared in aluminum pans. All polyesters were analyzed using the following heating program: -30 °C to 200 °C at 20 °C/min. The glass transition temperature ( $T_g$ ) of the polymer samples were determined from the second heating cycles with a heating/cooling rate of 5 °C/min under nitrogen atmosphere (20 mL/min). DSC data were analyzed using Pyris V9.0.2 software. The reported  $T_g$  values are the average of three runs; all the individual runs were from the second heating cycles of fresh polyesters samples.

### **General Procedure for ROCOP of Cyclic anhydrides and Epoxides**

A flame dried Schlenk flask was charged with a mixture of catalyst (0.5 mol%), maleic anhydride and epoxide in toluene (4 mL) in a glovebox under nitrogen. The flask was maintained at desired temperature using an oil bath controlled with a thermocouple. Small aliquots of the reaction mixture were collected at different time intervals to monitor the reaction with <sup>1</sup>H NMR spectroscopy. The stirring was continued until nearly complete conversion of epoxide was observed. At the end of the reaction, the reaction mixture was concentrated in *vacuo*. The resulting polymers were purified by dissolving the crude



reaction mixture in methylenechloride (1–3 mL), followed by addition of methanol (4-5 mL), aided by cooling with liquid nitrogen. The solid polymer products were collected and dried in *vacuo* until constant weight was obtained. Purified polymers were characterized by various NMR and GPC techniques.

#### **A Specific Example of Maleic Anhydride and Cyclohexene Oxide using Catalyst 1a.**

A flame dried Schlenk flask was loaded with a mixture of catalyst **1a** (10.0 mg, 0.0187 mmol, 0.5 mol%), maleic anhydride (3.75 mmol) and cyclohexene oxide (3.75 mmol) in toluene (4 mL) in a glovebox. The flask was heated to 100 °C and stirred for 2-9 hrs. The conversion of cyclohexene oxide was confirmed by <sup>1</sup>H NMR spectroscopy and the reaction mixture was then concentrated in *vacuo*. The polymer was precipitated from addition of DCM (1–3 mL) and methanol (4-5 mL). After filtration, the polymer was dried in *vacuo* until constant weight was noted.

#### **Examples of Terpolymerization using Catalyst 1a**

For the one-step terpolymerization, a flame dried Schlenk flask was loaded with a mixture of catalyst **1a** (10.0 mg, 0.0187 mmol, 0.5 mol%), maleic anhydride (7.5 mmol), cyclohexene oxide (3.75 mmol), styrene oxide (3.75 mmol) in toluene (4 mL) in a glovebox. The flask was heated to 100 °C and stirred for 2-9 hrs. After the complete conversion of epoxides was confirmed by <sup>1</sup>H NMR spectroscopy, the reaction mixture were concentrated in *vacuo*. The polymer was precipitated from addition of DCM (1–3 mL) and methanol (4-5 mL). After filtration, the polymer was dried in *vacuo* until constant weight.

For the two-step terpolymerization using catalyst **1a**, a flame dried Schlenk flask was loaded with a mixture of catalyst **1a** (10.0 mg, 0.0187 mmol, 0.5 mol%), maleic anhydride (3.75 mmol) and cyclohexene oxide (3.75 mmol) in toluene (4 mL) in a glovebox. The flask was heated to 100 °C and stirred for 2-9 hrs, until the complete conversion of CHO was confirmed by <sup>1</sup>H NMR spectroscopy. In the second step, to the same flask styrene oxide (3.75 mmol), and maleic anhydride (3.75 mmol) was added in a glovebox. The flask was again heated to 100 °C and stirred for 0.5-1 hrs. The conversion of SO was confirmed by <sup>1</sup>H NMR spectroscopy and the reaction mixture were concentrated in *vacuo*. The polymer was precipitated from addition of DCM (1–3 mL) and methanol (4–5 mL). After filtration, the polymer was dried in *vacuo* until constant weight.

## II.5 REFERENCES

1. Okada, M. Chemical syntheses of biodegradable polymers. *Prog. Polym. Sci.* **2002**, *27*, 87–133
2. Manavitehrani, I.; Fathi, A.; Badr, H.; Daly, S.; Shirazi, N. A.; Dehghani, F. Biomedical applications of biodegradable polyesters. *Polymers* **2016**, *8*, 20.
3. Dadsetan, M.; Liu, M.; Pumbeger, M.; Giraldo, C. V.; Ruesink, T.; Lu, L.; Yaszemski, M. J.; A stimuli-responsive hydrogel for doxorubicin delivery. *Biomaterials* **2010**, *31*, 8051–8062.
4. Lee, J. W.; Kang, K. S.; Lee, S. H.; Kim, J. Y.; Lee, B. K.; Cho, D. W. Bone regeneration using a produced customized poly(propylene fumarate)/diethylfumarate photopolymer 3D

- scaffold incorporating BMP-2 loaded PLGA microspheres. *Biomaterials* **2011**, *32*, 744–752.
5. Becker, G.; Wurm, F. R. Functional biodegradable polymers via ring-opening polymerization of monomers without protective groups. *Chem. Soc. Rev.* **2018**, *47*, 7739–7782.
  6. Lutson, J.; Vass, F. Anionic copolymerization of cyclic ethers with cyclic anhydrides. *Adv. Polym. Sci.* **1984**, *56*, 91–133.
  7. Thomas, C. M. Stereocontrolled ring-opening polymerization of cyclic esters: synthesis of new polyester microstructures. *Chem. Soc. Rev.* **2010**, *39*, 165–173.
  8. Robert, C.; de Montigny, F.; Thomas, C. T. Tandem synthesis of alternating polyesters from renewable resources. *Nat. Commun.* **2011**, *2*, 586.
  9. Kricheldorf, H. R. Syntheses of biodegradable and biocompatible polymers by means of bismuth catalysts *Chem. Rev.* **2009**, *109*, 5579–5594.
  10. Yoneyama, M.; Kakimoto, M.; Imai, Y. Novel synthesis of polyesters by palladium-catalyzed polycondensation of aromatic dibromides, bisphenols, or aliphatic diols with carbon monoxide. *Macromolecules* **1989**, *22*, 2593–2596.
  11. Childers, M. I.; Longo, J. M.; Van Zee, N. J.; LaPointe, A. M.; Coates, G. W. Stereoselective epoxide polymerization and copolymerization. *Chem. Rev.* **2014**, *114*, 8129–8152.
  12. Sarazin, Y.; Carpentier, J. F.; Discrete cationic complexes for ring-opening polymerization catalysis of cyclic esters and epoxides. *Chem. Rev.* **2015**, *115*, 3564–3614.

13. Tschan, M. J.-L.; Brulé, E.; Haquette, P.; Thomas, C. M. Synthesis of biodegradable polymers from renewable resources. *Polym. Chem.* **2012**, *3*, 836–851.
14. Sanford, M. J.; Carrodegua, L. P.; Van Zee, N. J.; Kleij, A. W.; Coates, G. W. Alternating Copolymerization of Propylene Oxide and Cyclohexene Oxide with Tricyclic Anhydrides: Access to Partially Renewable Aliphatic Polyesters with High Glass Transition Temperatures. *Macromolecules* **2016**, *49*, 6394-6400.
15. Carrodegua, L. P.; Martín, C.; Kleij, A. W. Semiaromatic polyesters derived from renewable terpene oxides with high glass transitions. *Macromolecules* **2017**, *50*, 5337-5345.
16. Zhu, Y.; Romain, C.; Williams, C. K. Sustainable polymers from renewable resources. *Nature* **2016**, *540*, 354-362.
17. Paul, S.; Zhu, Y.; Romain, C.; Brooks, R.; Sainia, P. K.; Williams, C. K. Ring-opening copolymerization (ROCOP): synthesis and properties of polyesters and polycarbonates *Chem. Commun.* **2015**, *51*, 6459-6479
18. Coates, G. W.; Moore, D. R. Discrete Metal-Based Catalysts for the Copolymerization of CO<sub>2</sub> and Epoxides: Discovery, Reactivity, Optimization, and Mechanism. *Angew. Chem. Int. Ed.* **2004**, *43*, 6618-6639.
19. Wang, Y.; Darensbourg, D. J. Carbon dioxide-based functional polycarbonates: Metal catalyzed copolymerization of CO<sub>2</sub> and epoxides. *Coord. Chem. Rev.* **2018**, *372*, 85-100
20. Kozak, C. M.; Ambrose, K.; Anderson, T. S. Copolymerization of carbon dioxide and epoxides by metal coordination complexes. *Coord. Chem. Rev.* **2018**, *376*, 565-587.

21. Jeske, R. C.; DiCiccio, A. M.; Coates, G. W. Alternating copolymerization of epoxides and cyclic anhydrides: an improved route to aliphatic polyesters. *J. Am. Chem. Soc.* **2007**, *129*, 11330–11331.
22. Liu, Y. Guo, J.-Z.; Lu, H.-W.; Wang, H.-B.; Lu, X.-B. Copolymerization of carbon dioxide and epoxides by metal coordination complexes. *Macromolecules* **2018**, *51*, 771–778.
23. Han, B.; Zhang, L.; Yang, M.; Liu, B. Dong, X.; Theato, P. Highly Cis/Trans-Stereoselective (ONSO)CrCl-Catalyzed Ring-Opening Copolymerization of Norbornene Anhydrides and Epoxides. *Macromolecules* **2016**, *49*, 6232-6239.
24. Huijser, S.; Nejad, E. H.; Sablong, R.; Jong, C. D.; Koning, C. E.; Duchateau, R. Ring-Opening Co- and Terpolymerization of an Alicyclic Oxirane with Carboxylic Acid Anhydrides and CO<sub>2</sub> in the Presence of Chromium Porphyrinato and Salen Catalysts. *Macromolecules* **2011**, *44*, 1132–1139.
25. Nejad, E. H.; Paoniasari, A.; Koning, C. E.; Duchateau, R. Semi-aromatic polyesters by alternating ring-opening copolymerisation of styrene oxide and anhydrides. *Polym. Chem.* **2012**, *3*, 1308-1313.
26. DiCiccio, A. M.; Coates, G. W. Ring-opening copolymerization of maleic anhydride with epoxides: A chain-growth approach to unsaturated polyesters. *J. Am. Chem. Soc.* **2011**, *133*, 10724-10727.
27. Darensbourg, D. J.; Poland, R. P.; Escobedo, C. Kinetic Studies of the Alternating Copolymerization of Cyclic Acid Anhydrides and Epoxides, and the Terpolymerization of

- Cyclic Acid Anhydrides, Epoxides, and CO<sub>2</sub> Catalyzed by (salen)Cr<sup>III</sup>Cl. *Macromolecules* **2012**, *45*, 2242–2248.
28. Liu, J.; Bao, Y.-Y.; Liu, Y.; Ren, W.-M.; Lu, X.-B. Binuclear chromium–salan complex catalyzed alternating copolymerization of epoxides and cyclic anhydrides. *Polym. Chem.* **2013**, *4*, 1439-1444.
29. Baumgartner, R.; Song, Z.; Zhang, Y.; Cheng, J. Functional polyesters derived from alternating copolymerization of norbornene anhydride and epoxides. *Polym. Chem.* **2015**, *6*, 3586-3590
30. Si, G.; Zhang, L.; Han, B.; Duan, Z.; Li, B.; Dong, J.; Li, X.; Liu, B. Novel chromium complexes with a [OSSO]-type bis(phenolato) dianionic ligand mediate the alternating ring-opening copolymerization of epoxides and phthalic anhydride. *Polym. Chem.* **2015**, *6*, 6372-6377.
31. Longo, J. M.; DiCiccio, A. M.; Coates, G. W. Poly (propylene succinate): a new polymer stereocomplex. *J. Am. Chem. Soc.* **2014**, *136*, 15897-15900.
32. Duan, Z.; Wang, X.; Gao, Q.; Zhang, L.; Liu, B.; Kim, I. J. Highly active bifunctional cobalt-salen complexes for the synthesis of poly(ester-block -carbonate) copolymer via terpolymerization of carbon dioxide, propylene oxide, and norbornene anhydride isomer: Roles of anhydride conformation consideration. *Polym. Sci. Part A: Polym. Chem.* **2014**, *52*, 789-795
33. DiCiccio, A. M.; Longo, J. M.; Rodríguez-Calero, G. G.; Coates, G. W. Development of highly active and regioselective catalysts for the copolymerization of epoxides with cyclic

- anhydrides: an unanticipated effect of electronic variation. *J. Am. Chem. Soc.* **2016**, *138*, 7107-7113
34. Kamphuis, A. J.; Piccioni, F.; Pescarmona, P. P. CO<sub>2</sub>-fixation into cyclic and polymeric carbonates: principles and applications *Green Chem.* **2019**, *21*, 406-448.
35. Nejad, E. H.; van Melis, C. G. W.; Vermeer, T. J.; Koning, C. E.; Duchateau, R. Alternating ring-opening polymerization of cyclohexene oxide and anhydrides: Effect of catalyst, cocatalyst, and anhydride structure *Macromolecules* **2012**, *45*, 1770-1776
36. Nejad, E. H.; Paoniasari, A.; van Melis, C. G. W.; Koning, C. E.; Duchateau, R. Catalytic ring-opening copolymerization of limonene oxide and phthalic anhydride: Toward partially renewable polyesters *Macromolecules* **2013**, *46*, 631-637.
37. Winkler, M.; Romain, C.; Meier, M. A. R.; Williams, C. K.; Renewable polycarbonates and polyesters from 1,4-cyclohexadiene *Green Chem.* **2015**, *17*, 300-306
38. Zhu, Y.; Romain, C.; Williams, C. K. Selective polymerization catalysis: controlling the metal chain end group to prepare block copolyesters *J. Am. Chem. Soc.* **2015**, *137*, 12179-12182.
39. Abbina, S.; Chidara, V.; Du, G. Ring-Opening Copolymerization of Styrene Oxide and Cyclic Anhydrides by using Highly Effective Zinc Amido-Oxazolate Catalysts *ChemCatChem* **2017**, *9*, 1343-1348
40. Ellis, W. C.; Jung, Y.; Mulzer, M.; Di Girolamo, R.; Lobkovsky, E. B.; Coates, G. W. Copolymerization of CO<sub>2</sub> and meso epoxides using enantioselective  $\beta$ -diiminate catalysts: a route to highly isotactic polycarbonates *Chem. Sci.* **2014**, *5*, 4004-4011

41. Zhu, L.; Liu, D.; Wu, L.; Feng, W.; Zhang, X. Wu, J.; Fan, D.; Lü, X.; Lu, R.; Shi, Q. A trinuclear  $[\text{Zn}_3(\text{L})_2(\text{OAc})_2]$  complex based on the asymmetrical bis-Schiff-base ligand H2L for ring-opening copolymerization of CHO and MA *Inorg. Chem. Commun.* **2013**, 37, 182-185
42. Liu, D.-F.; Wu, L.-Y.; Feng, W.-X.; Zhang, X.-M.; Wu, J.; Zhu, L.-Q.; Fan, D.-D.; Lu, X.-Q. Shi, Q. Ring-opening copolymerization of CHO and MA catalyzed by mononuclear  $[\text{Zn}(\text{L}_2)(\text{H}_2\text{O})]$  or trinuclear  $[\text{Zn}_3(\text{L}_2)_2(\text{OAc})_2]$  complex based on the asymmetrical bis-Schiff-base ligand precursor *J. Mol. Catal. A: Chem.* **2014**, 382, 136-145
43. Liu, Y.; Xiao, M.; Wang, S.; Xia, L.; Hang, D.; Cui, G.; Meng, Y. Mechanism studies of terpolymerization of phthalic anhydride, propylene epoxide, and carbon dioxide catalyzed by ZnGA *RSC Adv.* **2014**, 4, 9503-9508
44. Sun, X.-K.; Zhang, X.-H.; Chen, S.; Du, B.-Y.; Wang, Q.; Fan, Z.-Q.; Qi, G.-R. One-pot terpolymerization of  $\text{CO}_2$ , cyclohexene oxide and maleic anhydride using a highly active heterogeneous double metal cyanide complex catalyst *Polymer* **2010**, 51, 5719-5725.
45. Fieser, M. E.; Sanford, M. J.; Mitchell, L. A.; Dunbar, C. R.; Mandal, M.; Van Zee, N. J.; Urness, D. M.; Cramer, C. J.; Coates, G. W.; Tolman, W. B. Mechanistic insights into the alternating copolymerization of epoxides and cyclic anhydrides using a (Salph)AlCl and iminium salt catalytic system *J. Am. Chem. Soc.* **2017**, 139, 15222-15231
46. Van Zee, N. J.; Sanford, M. J.; Coates, G. W. Electronic Effects of Aluminum Complexes in the Copolymerization of Propylene Oxide with Tricyclic Anhydrides: Access to Well-Defined, Functionalizable Aliphatic Polyesters *J. Am. Chem. Soc.* **2016**, 138, 2755-2761



47. Van Zee, N. J.; Coates, G. W.; Alternating Copolymerization of Propylene Oxide with Biorenewable Terpene-Based Cyclic Anhydrides: A Sustainable Route to Aliphatic Polyesters with High Glass Transition Temperatures *Angew. Chem. Int. Ed.* **2015**, *54*, 2665-2668
48. Bernard, A.; Chatterjee, C.; Chisholm, M. H. The influence of the metal (Al, Cr and Co) and the substituents of the porphyrin in controlling the reactions involved in the copolymerization of propylene oxide and cyclic anhydrides by porphyrin metal(III) complexes *Polymer* **2013**, *54*, 2639-2646
49. De Sarasa Buchaca, M. M.; De la Cruz-Martínez, F.; Martínez, J.; Alonso-Moreno, C.; Fernández-Baeza, J.; Tejeda, J.; Niza, E.; Castro-Osma, J. A.; Otero, A.; Lara-Sánchez, A. Alternating copolymerization of epoxides and anhydrides catalyzed by aluminum complexes *ACS Omega* **2018**, *3*, 17581–17589
50. Yu, X.; Jia, J.; Xu, S.; Lao, K. U.; Sanford, M. J.; Ramakrishnan, R. K.; Nazarenko, S. I.; Hoye, T. R.; Coates, G. W.; DiStasio Jr., R. A. Unraveling substituent effects on the glass transition temperatures of biorenewable polyesters *Nat. Commun.* **2018**, *9*, 2880–2888
51. Sanford, M. J.; Van Zee, N. J.; Coates, G. W. Reversible-deactivation anionic alternating ring-opening copolymerization of epoxides and cyclic anhydrides: access to orthogonally functionalizable multiblock aliphatic polyesters *Chem. Sci.* **2018**, *9*, 134-142
52. Isnard, F.; Santulli, F.; Cozzolino, M.; Lamberti, M.; Pellicchia, C.; Mazzeo, M. Tetracoordinate aluminum complexes bearing phenoxy-based ligands as catalysts for

- epoxide/anhydride copolymerization: some mechanistic insights *Catal. Sci. Technol.* **2019**, *9*, 3090-3098.
53. Brooks, B. A.; Lidston, C. A.; Coates, G. W. Mechanism-inspired design of bifunctional catalysts for the alternating ring-opening copolymerization of epoxides and cyclic anhydrides *J. Am. Chem. Soc.* **2019**, *141*, 12760-12769.
54. Takenouchi, S.; Takasu, A.; Inai, Y.; Hirabayashi, T. Effects of Geometrical Difference of Unsaturated Aliphatic Polyesters on Their Biodegradability II. Isomerization of Poly(maleic anhydride-co-propylene oxide) in the Presence of Morpholine *Polym. J.* **2002**, *34*, 36–42.
55. Saini, P. K.; Romain, C.; Zhu, Y.; Williams, C. K. Di-magnesium and zinc catalysts for the copolymerization of phthalic anhydride and cyclohexene oxide *Polym. Chem.* **2014**, *5*, 6068-6075.
56. Li, H.; Luo, H.; Zhao, J.; Zhang, G. Well-defined and structurally diverse aromatic alternating polyesters synthesized by simple phosphazene catalysis *Macromolecules* **2018**, *51*, 2247-2257
57. Li, H.; Zhao, J.; Zhang, G. Self-buffering organocatalysis tailoring alternating polyester *ACS Macro Lett.* **2017**, *6*, 1094–1098
58. Hošťálek, Z.; Trhlíková, O.; Walterová, Z.; Martinez, T.; Peruch, F.; Cramail, H.; Merna, J. Alternating copolymerization of epoxides with anhydrides initiated by organic bases *Eur. Polym. J.* **2017**, *88*, 433–447

59. Han, B.; Zhang, L.; Liu, B.; Dong, X.; Kim, I.; Duan, Z.; Theato, P. Controllable synthesis of stereoregular polyesters by organocatalytic alternating copolymerizations of cyclohexene oxide and norbornene anhydrides *Macromolecules* **2015**, *48*, 3431–3437
60. Hu, L.-F.; Zhang, C.-J.; Wu, H.-L.; Yang, J.-L.; Liu, B.; Duan, H.-Y.; Zhang, X.-H. Highly active organic lewis pairs for the copolymerization of epoxides with cyclic anhydrides: Metal-free access to well-defined aliphatic polyesters *Macromolecules* **2018**, *51*, 3126-3134
61. Ji, H.-Y.; Chen, X.-L.; Wang, B.; Pan, L.; Li, Y.-S. Metal-free, Regioselective and Stereoregular Alternating Copolymerization of Monosubstituted Epoxides and Tricyclic Anhydrides. *Green Chem.* **2018**, *20*, 3963-3973.
62. Kummari, A.; Pappuru, S.; Gupta, P. K.; Chakraborty, D.; Verma, R. S. Metal-free Lewis pair Catalyst Synergy for Fully Alternating Copolymerization of Norbornene Anhydride and Epoxides: Biocompatible Tests for Derived Polymers. *Mater. Today Commun.* **2019**, *19*, 306-314.
63. Li, J.; Liu, Y.; Ren, W.-M.; Lu, X.-B.; Asymmetric Alternating Copolymerization of meso-Epoxides and Cyclic anhydrides: Efficient Access to Enantiopure Polyesters. *J. Am. Chem. Soc.* **2016**, *138*, 11493-11496.
64. Longo, J. M.; Sanford, M. J.; Coates, G. W. Ring-opening Copolymerization of Epoxides and Cyclic Anhydrides with Discrete Metal Complexes: Structure–property Relationships. *Chem. Rev.* **2016**, *116*, 15167–15197.

65. Abbina, S.; Du, G. Zinc-Catalyzed Highly Isolelective Ring Opening Polymerization of rac-Lactide. *ACS Macro Lett.* **2014**, *3*, 689-692
66. Abbina, S.; Chidara, V. K.; Bian, S.; Ugrinov, A. Du, G. Synthesis of Chiral C2-Symmetric Bimetallic Zinc Complexes of Amido-Oxazolinates and Their Application in Copolymerization of CO<sub>2</sub> and Cyclohexene Oxide *ChemistrySelect* **2016**, *1*, 3175-3183
67. Shaik, M.; Peterson, J.; Du, G. Cyclic and Linear Polyhydroxylbutyrates from Ring-opening Polymerization of  $\beta$ -butyrolactone with Amido-oxazolate Zinc Catalysts. *Macromolecules* **2019**, *52*, 157-166.
68. Farmer, T. J.; Castle, R. L.; Clark, J. H.; Macquarrie, D. J. Synthesis of Unsaturated Polyester Resins from Various Bio-derived Platform Molecules. *Int. J. Mol. Sci.* **2015**, *16*, 14912-14932.
69. Kim, M. S.; Kim, J. H.; Min, B. H.; Chun, H. J.; Han, D. K.; Lee, H. B. Polymeric Scaffolds for Regenerative Medicine. *Polym. Rev.* **2011**, *51*, 23-52.
70. Malik, M.; Choudhary, V.; Varma, I. K. J. Current status of Unsaturated Polyester Resins. *Macromol. Sci., Rev. Macromol. Chem. Phys.* **2000**, *40*, 139-165.
71. Luo, M.; Zhang, X.-H.; Darensbourg, D. J. An Examination of the Steric and Electronic Effects in the Copolymerization of Carbonyl sulfide and Styrene oxide. *Macromolecules* **2015**, *48*, 6057-6062.
72. Isnard, F.; Carratù, M.; Lamberti, M.; Venditto, V.; Mazzeo, M. Copolymerization of Cyclic Esters, Epoxides, and Anhydrides: Evidence of the Dual Role of the Monomers in the Reaction Mixture. *Catal. Sci. Technol.* **2018**, *8*, 5034-5043.

73. Kernbichl, S.; Reiter, M.; Adams, F.; Vagin, S.; Rieger, B. CO<sub>2</sub>-Controlled One-Pot Synthesis of AB, ABA Block, and Statistical Terpolymers from  $\beta$ -Butyrolactone, Epoxides, and CO<sub>2</sub>. *J. Am. Chem. Soc.* **2017**, *139*, 6787-6790.
74. Li, Y.; Zhang, Y.-Y.; Hu, L.-F.; Zhang, X.-H.; Du, B.-Y.; Xu, J.-T. Carbon dioxide-based copolymers with various architectures. *Prog. Polym. Sci.* **2018**, *82*, 120-157.
75. Li, H.; Luo, H.; Zhao, J.; Zhang, G. Sequence-Selective Terpolymerization from Monomer Mixtures Using a Simple Organocatalyst. *ACS Macro Lett.* **2018**, *7*, 1420–1425.
76. Jeske, R. C.; Rowley, J.; Coates, G. W. Pre-Rate-Determining Selectivity in the Terpolymerization of Epoxides, Cyclic Anhydrides, and CO<sub>2</sub>: A One-Step Route to Diblock Copolymers. *Angew. Chem., Int. Ed.* **2008**, *47*, 6041–6044.
77. Zhou, Y.; Hu, C.; Zhang, T.; Xu, X.; Duan, R.; Luo, Y.; Sun, Z.; Pang, X.; Chen, X. One-pot Synthesis of Diblock Polyesters by Catalytic Terpolymerization of Lactide, Epoxides, and Anhydrides. *Macromolecules* **2019**, *52*, 3462-3470.
78. Kernbichl, S.; Reiter, M.; Mock, J.; Rieger, B. Terpolymerization of  $\beta$ -Butyrolactone, Epoxides, and CO<sub>2</sub>: Chemoselective CO<sub>2</sub>-Switch and Its Impact on Kinetics and Material Properties. *Macromolecules* **2019**, *52*, 8476-8483.
79. Abbina, S.; Du, G.; Chiral Amido-Oxazolinat Zinc Complexes for Asymmetric Alternating Copolymerization of CO<sub>2</sub> and Cyclohexene Oxide. *Organometallics* **2012**, *31*, 7394-7403.

80. Binda, P. I.; Abbina, S.; Du, G. Modular Synthesis of Chiral  $\beta$ -diketiminato-type Ligands Containing 2-oxazoline Moiety via Palladium-catalyzed Amination. *Synthesis* **2011**, 2609-2618.

CHAPTER III

HIGH GLASS TRANSITION TEMPERATURE POLYESTERS VIA RING-OPENING  
COPOLYMERIZATION OF EPOXIDES WITH NOVEL CYCLOBUTANE  
ANHYDRIDES

III.1 INTRODUCTION

The ring-opening polymerization (ROP) of lactones and lactides is the most prevalent method for producing aliphatic polyesters.<sup>1,2</sup> Organocatalysts, metal alkoxides, and different metal complexes have all been utilized as initiators for lactones polymerization.<sup>3,4</sup> Nevertheless, unfavorable side reactions like transesterification might restrict the ROP of lactones, particularly at high conversion. Because of the restricted functional variety of the substrate scope and the absence of post-polymerization functionalization on the resultant polyesters, the resulting polymers have a limited range of characteristics. Since commercially available poly(lactic acid) (PLA)<sup>5</sup> has a relatively low  $T_g$  (about 60 °C), there has been interest in generating higher  $T_g$  aliphatic polyesters. Attempts to enhance the  $T_g$  of aliphatic polyesters have mostly centered on the utilization of diols produced from polysaccharides<sup>6,7</sup> and lactide<sup>8</sup> or mannitol<sup>9</sup> derivatives. Nevertheless, the resultant polymers either perform marginally better than PLA ( $T_g$  up to 68 °C) or need extensive reaction periods at low temperatures (20 °C) to achieve moderate conversion. For decades, synthetic strategies for creating polyesters with exceptional thermal properties have been significantly developed. In the midst of all this, ROCOP of epoxides and anhydrides has

attracted the attention of many researchers, which provides an access to aliphatic polyesters from a myriad of non-flexible biobased monomers.<sup>10,11</sup> Varying the monomer sets allows us to tailor the polymer characteristics, and many of the subsequent polyesters are readily functionalized by postpolymerization modification. There is a diverse array of metal complexes reported to catalyze the copolymerization, including zinc,<sup>12</sup> magnesium,<sup>13</sup> chromium,<sup>14</sup> cobalt,<sup>15</sup> manganese,<sup>16</sup> and aluminum complexes.<sup>17</sup> A wide range of salen- and porphyrin-type complexes generally show markedly improved activity with the addition of a nucleophilic cocatalyst such as bis(triphenylphosphine)iminium chloride ([Ph<sub>3</sub>P=N=PPh<sub>3</sub>]Cl or [PPN]Cl).<sup>18</sup>

To achieve high glass transition ( $T_g$ ) temperatures, polyesters are often found to have rigid backbones, which impede rotational flexibility in these polymer chains.<sup>19,20</sup> As a result, one of the efficient strategies to improve chain stiffness is to introduce non-flexible ring structures into the polymer backbone, therefore reducing rotational flexibility. Aromatic and aliphatic rings moieties are often found as components of high- $T_g$  polymers such as aromatic polycarbonates,<sup>21</sup> polynorbornenes,<sup>22</sup> and polyimides<sup>23</sup>. Another typical method of increasing  $T_g$  is to include substituents along or near the polymer backbone to inhibit main-chain rotations through steric interactions. Prominent examples of such polymers are poly( $\alpha$ -methylstyrene), poly(2-methylstyrene), and poly(2,6-dimethylstyrene), all of which have  $T_g$  values that are much greater than their less substituted analogs.



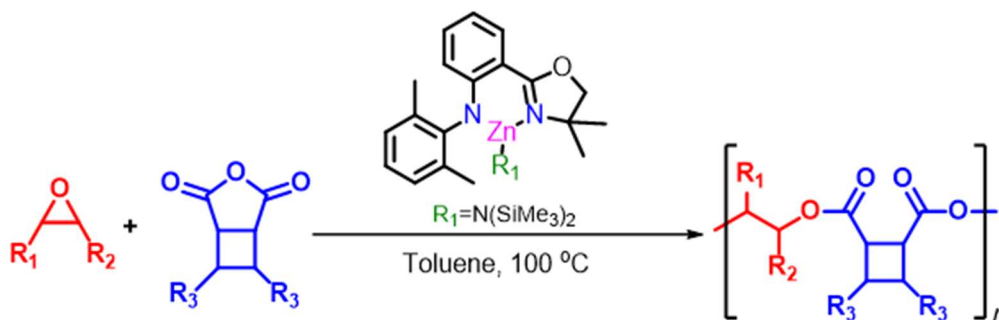
Duchateaus and co-workers has studied on ROCOP of epoxides with alicyclic anhydride containing different ring strains (succinic anhydride, maleic anhydride, citraconic anhydride, cyclopropane-1,2-dicarboxylic acid (CPrA) anhydride, cyclopentane-1,2-dicarboxylic acid anhydride (CPA) and phthalic anhydride), which was performed applying metal salen and porphyrin complexes where for (salen)MX, M = Cr, X = Cl, M = Al, X = Cl, M = Mn, X = Cl, M = Co, X = OAc and salen = *N,N*-bis(3,5-di-*tert*-butylsalicylidene)-diimine and for porphyrin complex, M = Cr, X = Cl, M = Mn, X = Cl, M = Co, X = OAc.<sup>14-a,d,e,i</sup> In 2012, the Darensbourg group reported that polyesters obtained via alternating copolymerization of a series of cyclic acid anhydrides with various epoxides using (salen)CrCl/onium salt catalysts had high molecular weights and narrow molecular weight distributions, and that ROCOP of CHO and cyclohexene anhydride (CHE) results in high  $T_g$  up to 95 °C.<sup>14c</sup> The Coates group has concentrated on alternating copolymerization of epoxides and tricyclic anhydrides using aluminum salen complexes. Tricyclic anhydrides are attractive monomers that may be readily produced via the Diels-Alder process. The abundance of commercially accessible, low-cost biosourced dienes and dienophiles provides several options for employing renewable feedstocks. Moreover, the rigidity of the resultant polymers results in materials with high glass transition temperatures ( $T_g$ ) which range from 66 to 184 °C.<sup>19,24</sup>

To our knowledge, most polymer backbone chains contain 1-, 3-, 5-, and 6-member aliphatic rings attached to alicyclic anhydrides, and very little research has been performed

on the copolymerization of epoxides with cyclobutane-containing anhydrides, and the influence of cyclobutane-containing polyesters on polymer characteristics has not been investigated. Herein we are reporting several aliphatic polyesters with cyclobutane anhydrides, which are readily synthesized from cinnamic acid derivatives using zinc amido-oxazolate complexas catalyst. Introduction of this semi-rigid, cyclobutane-containing anhydrides leads to aliphatic polyesters with perfectly alternating structures in the backbone, and adding substituents to the aromatic group in the anhydrides results in polyesters with high  $T_g$  values that can be obtained with rigid epoxides.

## III.2 RESULTS AND DISSCUSSION

### III.2.1 Polymer synthesis and characterization



Scheme 1. ROCOP of epoxides and CBAN using zinc amido-oxazolate complexas catalyst

We thoroughly investigated the copolymerization of three cyclobutane anhydrides (**1a**, **1b**, and **1c**) using epichlorohydrin (ECH), styrene oxide (SO), phenyl glycidyl ether (PGE), and cyclohexene oxide (CHO) in the presence of zinc amido-oxazolinato complexes as

shown in Figure 1. The copolymerization of the anhydrides with different epoxides has been broadly reported in this work. With reasonable proportions of monomer to the catalyst, 12 polyesters (Table 1) were prepared with narrow dispersity.

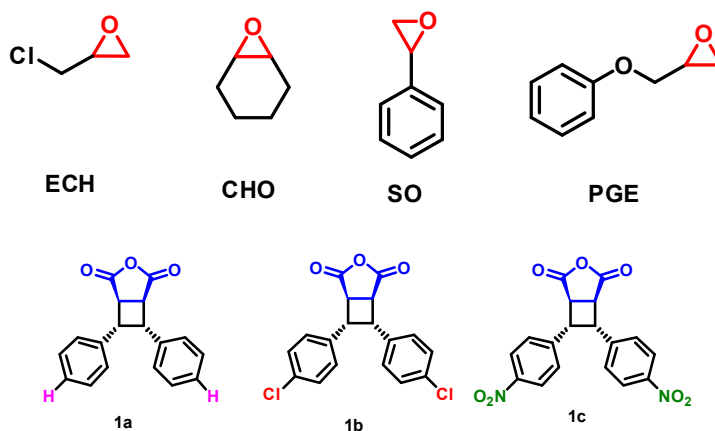


**Figure 1:** Cyclic anhydride and epoxide comonomers investigated in this work

We first studied the polymerization of **1a** with cyclohexene oxide with a feed ratio of [epoxide]:[anhydride]:[cat] = 100:100:1. The reaction was completed in 32 h as determined by analyzing the reaction samples with  $^1\text{H}$ -NMR spectroscopy periodically, producing a poly (CHO-*alt*-**1a**) with a molecular weight of 3.81 kDa (Table 1, entry 1) and narrow dispersity ( $\mathcal{D} = 1.26$ ). The molecular weight of the resultant polyesters was low compared to the calculated theoretical molecular weights. This could be attributed to the presence of a chain transfer agent, most likely from the hydrolysis of anhydride to carboxylic acid. The microstructures of the copolymer poly(CHO-*alt*-**1a**) were characterized by various NMR techniques. In the  $^1\text{H}$  NMR spectrum (Figure 2), the 4.91 ppm peak was ascribed to the two ester methine protons (**a**) of the cyclohexyl ring, and the peaks at 1.30-2.07 ppm were

assigned to the eight methylene protons (**b** and **c**) of the cyclohexyl ring. The cyclobutane moiety was identified by the peak at 4.29 ppm, assigned to two methine protons (**d**) adjacent to C=O, and the peak at 3.79 ppm, assigned to two methine protons (**e**) adjacent to the phenyl ring.

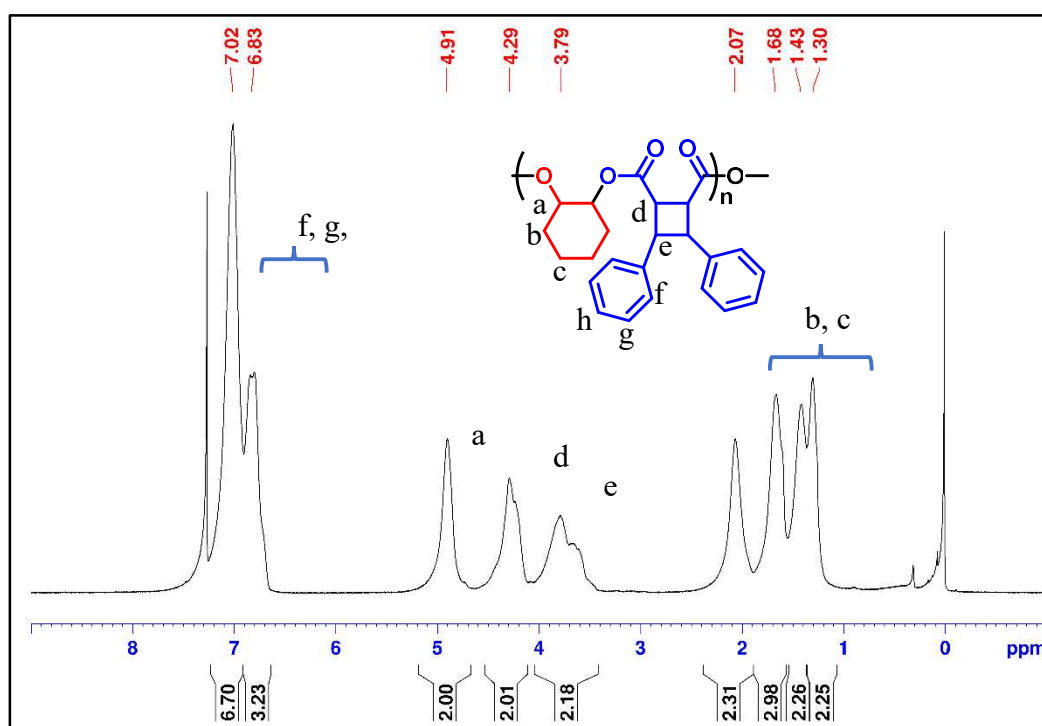


**Figure 2.** <sup>1</sup>H-NMR of CHO-CBAN-1 Co-polyester

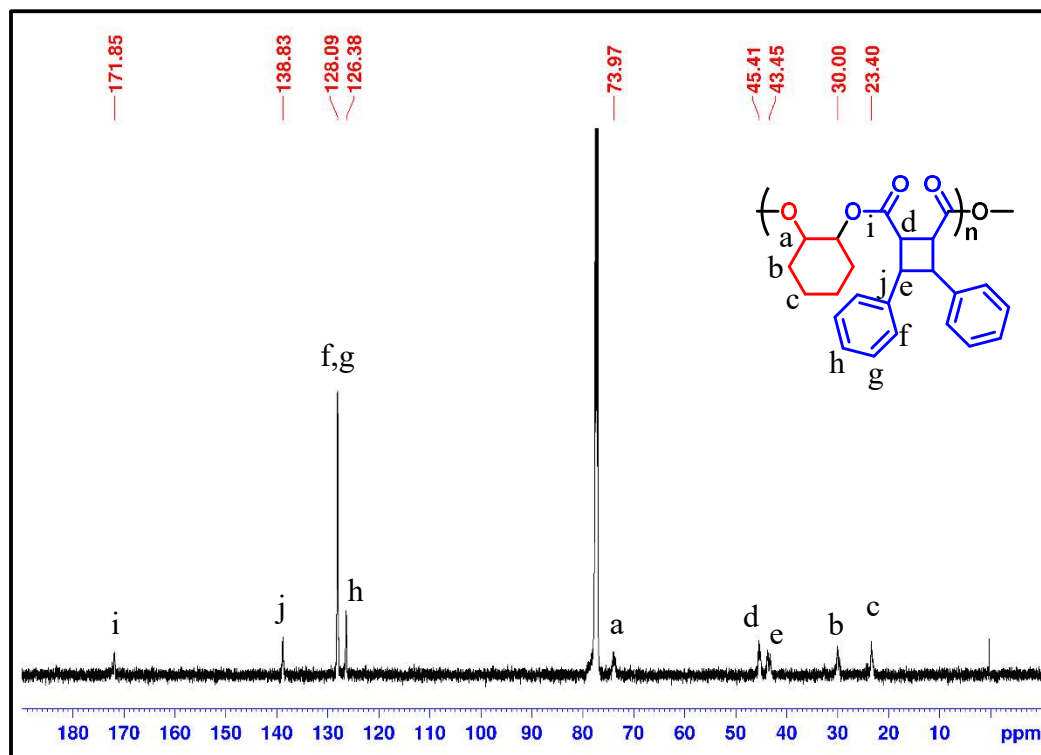


**Figure 3.**  $^{13}\text{C}$ -NMR of CHO-CBAN-1 Co-polyester

In the  $^{13}\text{C}$ -NMR spectrum (Figure 3), the peaks at 23.40 and 30.00 ppm were assigned to 2°-carbons (**b** and **c**) of the cyclohexyl moiety, and the peak at 73.97 ppm was assigned to the 3°-carbons (**a**) of the ester bond. In both  $^1\text{H}$  and  $^{13}\text{C}$ -NMR, no peaks were observed that could be attributed to ether linkages, suggesting that the resultant polyester has a perfectly alternating arrangement of two monomers with >99% of ester bonds in the polymer chain.

**Table1.** Copolymerization of 1a-1c with different epoxides

<i>Entry</i>	<i>Anhydride</i>	<i>Epoxide</i>	<i>T<sub>rxn</sub></i> ( <i>h</i> )	<i>Calc.</i> <i>M<sub>n</sub></i>	<i>M<sub>n</sub><sup>f</sup></i> ( <i>kDa</i> )	<i>Đ<sup>f</sup></i>	<i>Yield</i>	<i>T<sub>g</sub></i>
<b>1</b>	<b>1a</b>	CHO	32	37.6	3.81	1.26	56	131
<b>2</b>	<b>1a</b>	SO	6	39.8	3.18	1.35	41	95
<b>3</b>	<b>1a</b>	PGE	72	42.8	3.10	1.09	27	64
<b>4</b>	<b>1a</b>	ECH	18	37.0	3.85	1.90	38	95
<b>5</b>	<b>1c</b>	CHO	48	46.6	2.60	1.99	72	165
<b>6</b>	<b>1c</b>	SO	8	48.8	5.34	2.16	44	138
<b>7</b>	<b>1c</b>	PGE		51.8	n.d	n.d	n.d	n.d
<b>8</b>	<b>1c</b>	ECH	24	46.1	5.13	1.57	68	n.d

<sup>d</sup>Unless otherwise stated all reactions were carried out with [Cat]:[Epo]:[Anh] = 1:100:100 at 100 °C in Toluene. <sup>e</sup>Monomer conversion was determined by <sup>1</sup>H NMR. <sup>f</sup>Absolute molecular weight, and molecular weight distribution determined by GPC in THF

Next, we investigated the copolymerization reaction with a few representative epoxides including SO, ECH and PGE (see Figure 1). The reaction with ECH took 18 h to achieve >99% conversion and with SO it took 8 h to complete the reaction. The resultant polyesters poly(ECH-*alt*-**1a**) and poly(SO-*alt*-**1a**) had a molecular weight of  $M_n = 3.85$ , & 3.18 KDa and dispersity of 2.50, & 1.35 respectively (Table 1, entry 4,& 2). The polymerization rate for SO is faster than that of CHO and ECH. However, it is slower when compared with maleic anhydride, which took ~0.5 h under comparable conditions. With epoxide PGE, the polymerization was significantly slower, taking 72 h for the conversion of >99%. The relative reactivities of these epoxides in copolymerization with **1a** follow the order SO > ECH > CHO > PGE, which can be approximately explained by the electron withdrawing capability of the substituents that leads to enhanced reactivity towards nucleophilic attack on the epoxides. It should be noted that during the reaction with SO, it was observed that the anhydride **1a** was not completely consumed, and the formation of phenylacetaldehyde

from the isomerization of SO was observed by the  $^1\text{H}$ -NMR analysis of the reaction mixture, which is commonly observed in such reactions.

One of the advantages of epoxide/anhydride copolymerization is that polymer properties can be tuned not only through epoxide but also through anhydride. We further screened the epoxides with anhydride **1c**, a series of polymerization were performed. Analysis of the NMR spectra revealed that the copolymerization of epoxides with anhydride resulted in an exclusive (>99%) alternating pattern in all cases.  $^1\text{H}$  and  $^{13}\text{C}$ -NMR spectra of all the polyester synthesized in this report may be found in Appendix A.I.

### III.2.2 Mechanistic Hypotheses

Based on the relative reactive rates of the epoxides over anhydride **1a**, we hypothesized that the reaction pathways for the formation of alternating copolymers are shown in Figure 5. The reaction is initiated by the coordination of epoxide with the zinc catalyst, followed by the ring-opening to yield an alkoxide species as an intermediate (**A**). This intermediate (**A**) reacts with an anhydride to yield a carboxylate (**B**), which in turn reacts with an epoxide to propagate the polymer chain. In general, the rate of the alkoxide anion reacting with an anhydride monomer ( $k_2$ ) is faster than a carboxylate anion ring-opening an epoxide ( $k_3$ ), hence the latter process is rate determining<sup>28,29</sup>. The reaction rates for the copolymerization of anhydride **1a** observed under similar conditions provided relative reactivities of  $\text{SO} > \text{ECH} > \text{CHO} > \text{PGE}$ .

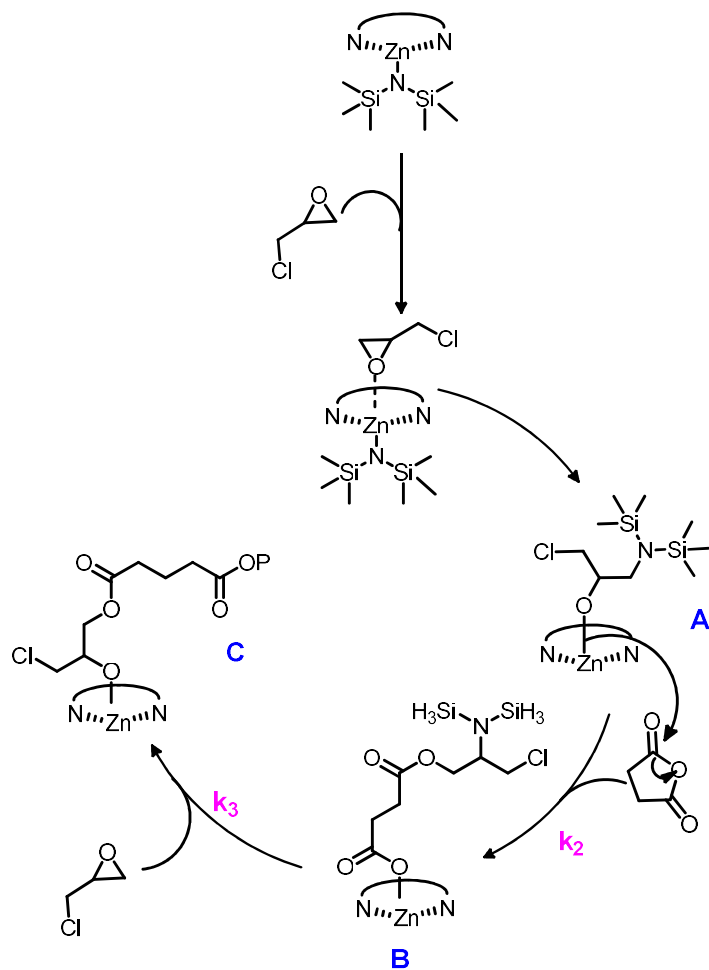


**Figure 5.** Hypothesized chain propagation step<sup>29</sup>



### III.2.3 Thermal Properties

The thermal properties of the various polyesters synthesized from the monomers listed in figure 1 were determined by differential scanning calorimetry (DSC) and thermal gravimetric analysis (TGA). As anticipated, the bulkiness of the pendant groups and rigidity of the monomer structure have a direct effect on the glass transition temperature ( $T_g$ ) of the resultant polyesters, and the  $T_g$  values ranged from 64-165 °C. Poly(PGE-*alt*-**1a**) showed a relatively low  $T_g$  of only 64 °C (Table 2, entry 3), while poly(SO-*alt*-**1a**) and poly(ECH-*alt*-**1a**) showed similar  $T_g$ 's close to 95 °C. The most noteworthy  $T_g$  for the series was observed when a rigid epoxide, CHO, was incorporated, which resulted in poly(CHO-*alt*-**1a**) with a high  $T_g$  of 131 °C.

With the epoxide/anhydride copolymerization, the properties of the polymers can be tuned through anhydrides. We observed that polyesters containing nitro substituents show a significant increase in  $T_g$  compared to the corresponding polymers synthesized with unsubstituted anhydride **1a**. Thus, the polymers produced with anhydrides **1c** show enhanced properties (Table 2). The resultant polyesters have  $T_g$  values ranging from 138 to 165 °C. Poly (SO-*alt*-**1c**) (Appendix A.II-) shows a large increase in  $T_g$  of about 43 °C compared to its corresponding polymer with unsubstituted anhydride. Poly(CHO-*alt*-**1c**) bearing both cyclohexane and cyclobutene rings in the main chain had the highest  $T_g$  of 165 °C.

These observations of  $T_g$  can be correlated with the polymer backbone structure and pendent groups. The CHO-based polyesters have substantially higher  $T_g$  values relative to ECH, SO, and PGE-based analogs due to the decreased chain flexibility imposed by the rigid cyclohexyl ring. The pendent phenoxyl group in PGE is long and flexible, which leads to the lowest  $T_g$  in the corresponding polymers. Overall, the  $T_g$  values increased with epoxides in the order CHO>SO>ECH>PGE. The introduction of the nitro group on the cyclobutene substituents has a large impact on the  $T_g$ , though its action is not easily understood.

Table2. Thermal properties of copolymers

<i>Entry</i>	<i>Monomer</i>	<i>Monomer</i>	$T_g$	$T_{5\%}$	$T_{50\%}$	$T_{max}$
<b>1</b>	ECH	1a	94.4	273	354	351
<b>2</b>	CHO	1a	130.8	308	345	352
<b>3</b>	SO	1a	95	279	344	348
<b>4</b>	PGE	1a	64	302	364	370
<b>5</b>	ECH	1c	n.d	301	492	333, 570
<b>6</b>	CHO	1c	165	283	536	329
<b>7</b>	SO	1c	138	278	567	331, 585
<b>8</b>	PGE	1c				

<sup>h</sup>Temperature in °C. <sup>i</sup> $T_m$  values were determined from the second heating cycle in DSC. <sup>j</sup> $T_{d,5}$ ,  $T_{50\%}$ , and  $T_{max}$  refer to the temperature at which 5%, 50% 99%, and maximum weight losses were observed in TGA respectively

Poly(CHO-*alt*-**1a**) exhibits a high decomposition temperature ( $T_{5\%}$ , defined by the temperature at 5% weight loss) of 308 °C and a maximum decomposition temperature ( $T_{max}$ ) of 352 °C, as measured by thermogravimetric analysis (TGA) (Figure 4). Notably,

polyesters with nitro substituents showed slightly lower  $T_{5\%}$  than their corresponding unsubstituted analogues. Surprisingly, only 50% of the polymer degradation occurred up to 600 °C, and the rest of the decomposition products was char.

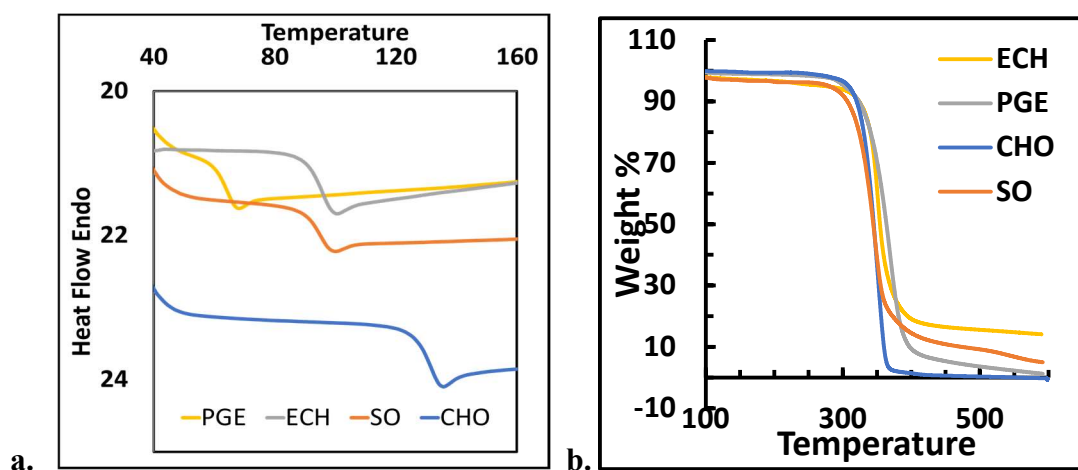


**Figure 4.** a) DSC graph of polyesters with **1a** anhydride as comonomer. b) TGA graph of polyesters with **1a** anhydride as comonomer

### III.3 CONCLUSION

Copolymerization of epoxide and cyclic anhydride catalyzed by Zn complexes produces highly alternating polyesters with high glass transition temperatures and low polydispersity.  $^1\text{H}$  and  $^{13}\text{C}$  NMR analyses showed that Zn complex was highly selective toward polyester formation over polyether formation. The properties of the polyesters can be tuned not only by epoxides but also by anhydrides. For a given anhydride, the relative reactivity of epoxide decreased in the order  $\text{SO} > \text{ECH} > \text{CHO} > \text{PGE}$ . By varying both the

epoxide and anhydride, we were able to tune the  $T_g$  of the resulting polymers over a 100 °C range from 64 °C to an exceptionally high 165 °C. These variable high  $T_g$  values of these materials give them the potential for use in a variety of high-temperature applications. In addition, we are currently investigating the mechanistic details that can account for the high selectivity towards the perfectly alternating copolymers.

### III.4 EXPERIMENTAL SECTION

#### **General Methods and Material**

##### **Materials**

All reactions with air- and/or moisture-sensitive compounds were performed under dry nitrogen using standard glovebox (VAC atmosphere controller) and/or Schlenk line techniques. Deuterated solvents were purchased from Cambridge Isotope Laboratories. Analytical grade THF was purchased from Fisher Scientific and used as received. Other chemicals were purchased from Sigma-Aldrich. Epoxides were distilled over  $\text{CaH}_2$  following three freeze-pump-thaw cycles and stored in 4 Å molecular sieves. Anhydrides were dried under vacuum for 3-4 days.  $\text{CDCl}_3$  was distilled over  $\text{CaH}_2$  and degassed before use. DMSO,  $\text{CD}_2\text{Cl}_2$  were used for the pure polymer due to the poor solubility in  $\text{CDCl}_3$ . Toluene was distilled under nitrogen from Na/benzophenone. The synthesis of zinc complex was conducted according to the literature methods<sup>16</sup>.

##### **Methods and Instrumentation**

NMR experiments (1D, and 2D) were recorded on a Bruker AVANCE 500 NMR spectrometer, and the spectra were referenced to the residual peaks in  $\text{CDCl}_3$ . The microstructures of polymers were characterized by examining the carbon atoms peaks in the  $^{13}\text{C}$  NMR spectra recorded at room temperature in  $\text{CDCl}_3$  with concentrations in the range of 1 to 1.5 mg/mL. Gel permeation chromatography (GPC) analysis was performed on an Agilent Infinity, using a PLgel 5 mm Mixed-D column, a UV detector, and THF as eluent at a flow rate of  $1\text{ mL min}^{-1}$  ( $20\text{ }^\circ\text{C}$ ). Polystyrene standards from Agilent technologies were used for calibration. Agilent software was used to operate the instrument for data processing. A 6210 TOF MS with ESI detection (Agilent Technologies, Santa Clara, CA, USA) was used for mass spectra. The analyte-containing solution was introduced into the instrument by direct infusion using a syringe drive ( $5\text{ mL min}^{-1}$ ). The electrospray ionization (e.g., capillary) and collision-induced dissociation (e.g., fragmentor) potentials were set to 3500 V, and 150 V. Acetic acid was used as an electrolyte at  $25\text{ mmol L}^{-1}$ . Mass Hunter Qualitative Analysis software was used for data processing. Differential scanning calorimetry (DSC) was recorded with Perkin Elmer Jade DSC with a ramping rate of  $20\text{ }^\circ\text{C/min}$  under nitrogen protection. Heat flow was recorded from both the first heating and cooling curve. Thermogravimetric analysis (TGA) was carried out with a Hi-Res TGA Q500 from TA Instruments using alumina pans at a heating rate of  $20\text{ }^\circ\text{C/min}$  under nitrogen with a sample weight of about 10 mg.

### **Copolymerization procedure**

In a glove box, an oven-dried 10 mL Schlenk flask equipped with a magnetic stir bar was charged with Zn-catalyst (0.0187 mmol, 1 equiv.) in toluene (4.0 mL). The mixture was stirred at rt for 5 min. Cyclic anhydride (1.87 mmol, 100 equiv.) was added, followed by the addition of a predetermined amount of epoxide. The flask was capped, and the reaction mixture was stirred at 100 °C. The reaction was monitored by  $^1\text{H}$  NMR spectroscopy until the complete conversion of cyclic anhydride or epoxide (>99%). After removing the solvent in a vacuum, the residue was dissolved in DCM (1–3 mL), followed by the addition of hexane (4–5 mL). The precipitation of the polymeric products was facilitated by immersing the flask in liquid nitrogen. The supernatant was decanted, and the residues were washed and dried under a vacuum. Various NMR techniques, ESI-MS, GPC, TGA, and DSC, were then used to characterize the purified polymers.

### III.5 REFERENCES

1. Paul, S.; Zhu, Y.; Romain, C.; Brooks, R.; Saini, P. K.; Williams, C. K. Ring-opening copolymerization (ROCOP): synthesis and properties of polyesters and polycarbonates. *Chem. Commun.* **2015**, *51*, 6459–6479
2. Auras, R., Poly(lactic acid). In *Encyclopedia of Polymer Science and Technology*; Mark, H. F., Ed.; Wiley: Hoboken, NJ, 2014; Vol. 10, pp 165–175.
3. Lecomte, P.; Jerome, C. In *Synthetic Biodegradable Polymers*; Rieger, B., Kunkel, A., Coates, W. G., Reichardt, R., Dinjus, E., Zevaco, A. T., Eds.; Springer: Berlin, 2012; pp 173–217.

4. Tian, G.; Wang, H.; Song, Y.; Xiang, J.; Ying, Y.; Han, X.; Wang, S.; Zhang, L.; Zhang, J.; Tang, N. Study on zinc oxide-creatinine hybrid catalyst for efficient lactide synthesis with low racemization; *J. Appl. Polym. Sci.* **2023**, e53762. <https://doi.org/10.1002/app.53762>
5. Ikada, Y.; Hideto, T. Biodegradable polyesters for medical and ecological applications *Macromol. Rapid Commun.* **2000**, *21*, 117 – 132.
6. Fenouillot, F.; Rousseau, A.; Colomines, G.; Saint-Loup, R.; Pascault, J. P. Polymers from renewable 1,4:3,6-dianhydrohexitols (isosorbide, isomannide and isoidide): A review. *Prog. Polym. Sci.* **2010**, *35*, 578–622.
7. Storbeck, R.; Ballauff, M. Synthesis and properties of polyesters based on 2,5-furandicarboxylic acid and 1,4:3,6-dianhydrohexitols. *Polymer* **1993**, *34*, 5003–5006.
8. Fiore, G. L.; Jing, F.; Young, V. G., Jr.; Cramer, C. J.; Hillmyer, M. A. High  $T_g$  aliphatic polyesters by the polymerization of spirolactide derivatives. *Polym. Chem.* **2010**, *1*, 870–877.
9. Lavilla, C.; Alla, A.; Martínez de Ilarduya, A.; Munoz-Guerra, S. High  $T_g$  Bio-Based Aliphatic Polyesters from Bicyclic d-Mannitol. *Biomacromolecules* **2013**, *14*, 781–793.
10. Paul, S.; Zhu, Y.; Romain, C.; Brooks, R.; Saini, P. K.; Williams, C. K. Ring-opening copolymerization (ROCOP): synthesis and properties of polyesters and polycarbonates. *Chem. Commun.* **2015**, *51*, 6459–6479.

11. (a) Longo, J. M.; Sanford, M. J.; Coates, G. W. Ring-Opening Copolymerization of Epoxides and Cyclic Anhydrides with Discrete Metal Complexes: Structure–Property Relationships; *Chem. Rev.* **2016**, *116* (24), 15167–15197. (b) Chen, C. M.; Xu, X.; Ji, H. Y.; Wang, B.; Pan, L.; Luo, Y.; Li, Y. S. Alkali Metal Carboxylates: Simple and Versatile Initiators for Ring-Opening Alternating Copolymerization of Cyclic Anhydrides/Epoxides *Macromolecules* **2021** *54*, 713–724 (c) Zhang, J.; Wang, L.; Liu, S.; Kang, X.; Li, Z. A Lewis Pair as Organocatalyst for One-Pot Synthesis of Block Copolymers from a Mixture of Epoxide, Anhydride, and CO<sub>2</sub> *Macromolecules* **2021** *54*, 763–772. (d) Hu, L.; Zhang, X.; Cao, X.; Chen, D. Sun, Y.; Zhang, C.; Zhang, X. Alternating Copolymerization of Isobutylene Oxide and Cyclic Anhydrides: A New Route to Semicrystalline Polyesters *Macromolecules* **2021** *54*, 6182–6190. (e) Abel, B. A.; Lidston, C. A. L.; Coates, G. W. Mechanism-Inspired Design of Bifunctional Catalysts for the Alternating Ring-Opening Copolymerization of Epoxides and Cyclic Anhydrides *J. Am. Chem. Soc.* **2019** *141*, 12760–12769 (f) Chidara, V. K.; Boopathi, S. K.; Hadjichristidis, N.; Gnanou, Y.; Feng, X. Triethylborane-Assisted Synthesis of Random and Block Poly(ester-carbonate)s through One-Pot Terpolymerization of Epoxides, CO<sub>2</sub>, and Cyclic Anhydrides *Macromolecules* **2021** *54*, 2711–2719. (g) Lidston, C. A. L. Abel, B. A. Coates, G. W. Bifunctional Catalysis Prevents Inhibition in Reversible-Deactivation Ring-Opening Copolymerizations of Epoxides and Cyclic Anhydrides *J. Am. Chem. Soc.* **2020** *142*, 20161–20169.



12. Zhu, L.; Liu, D.; Wu, L.; Feng, W.; Zhang, X.; Wu, J.; Fan, D.; Lu, X.; Lu, R.; Shi, Q. A trinuclear  $[\text{Zn}_3(\text{L})_2(\text{OAc})_2]$  complex based on the asymmetrical bis-Schiff-base ligand  $\text{H}_2\text{L}$  for ring-opening copolymerization of CHO and MA. *Inorg. Chem. Commun.* **2013**, *37*, 182–185. (b) Liu, D.-F.; Wu, L.-Y.; Feng, W.-X.; Zhang, X.-M.; Wu, J.; Zhu, L.-Q.; Fan, D.-D.; Lu, X.-Q.; Shi, Q. Ring-opening copolymerization of CHO and MA catalyzed by mononuclear  $[\text{Zn}(\text{L}_2)(\text{H}_2\text{O})]$  or trinuclear  $[\text{Zn}_3(\text{L}_2)_2(\text{OAc})_2]$  complex based on the asymmetrical bis-Schiff-base ligand precursor. *J. Mol. Catal. A: Chem.* **2014**, *382*, 136–145. (c) Liu, Y.; Xiao, M.; Wang, S.; Xia, L.; Hang, D.; Cui, G.; Meng, Y. Mechanism studies of terpolymerization of phthalic anhydride, propylene epoxide, and carbon dioxide catalyzed by ZnGA. *RSC Adv.* **2014**, *4*, 9503–9508. (d) Saini, P. K.; Romain, C.; Zhu, Y.; Williams, C. K. Di-magnesium and zinc catalysts for the copolymerization of phthalic anhydride and cyclohexene oxide. *Polym. Chem.* **2014**, *5*, 6068–6075. (e) Wu, L.-y.; Fan, D.-d.; Lu, X.-q.; Lu, R. Ringopening copolymerization of cyclohexene oxide and maleic anhydride catalyzed by mononuclear  $[\text{Zn}(\text{L})(\text{H}_2\text{O})]$  or binuclear  $[\text{Zn}_2(\text{L})(\text{OAc})_2(\text{H}_2\text{O})]$  complex based on the Salen-type Schiff-base ligand. *Chin. J. Polym. Sci.* **2014**, *32*, 768–777. (f) Winkler, M.; Romain, C.; Meier, M. A. R.; Williams, C. K. Renewable polycarbonates and polyesters from 1,4-cyclohexadiene. *Green Chem.* **2015**, *17*, 300–306. (g) Zhu, Y.; Romain, C.; Williams, C. K. Selective Polymerization Catalysis: Controlling the Metal Chain End Group to Prepare Block Copolyesters. *J. Am. Chem. Soc.* **2015**, *137*,

- 12179–12182. (h) Thevenon, A.; Garden, J. A.; White, A. J. P.; Williams, C. K. Dinuclear Zinc Salen Catalysts for the Ring Opening Copolymerization of Epoxides and Carbon Dioxide or Anhydrides. *Inorg. Chem.* **2015**, *54*, 11906–11915. (i) Garden, J. A.; Saini, P. K.; Williams, C. K. Greater than the Sum of Its Parts: A Heterodinuclear Polymerization Catalyst. *J. Am. Chem. Soc.* **2015**, *137*, 15078–15081. (j) Abbina, S.; Chidara, V. K.; Bian, S.; Ugrinov, A.; Du, G. Synthesis of Chiral  $C_2$ -Symmetric Bimetallic Zinc Complexes of Amido-Oxazolinates and Their Application in Copolymerization of  $CO_2$  and Cyclohexene Oxide *ChemistrySelect* **2016**, *1*, 3175 (k) Abbina, S.; Chidara, V. K.; Du, G. Ring-Opening Copolymerization of Styrene Oxide and Cyclic Anhydrides by using Highly Effective Zinc Amido–Oxazolate Catalysts *ChemCatChem* **2017**, *9*, 1343. (l) Shaik, M.; Chidara, V. K.; Abbina, S.; Du, G. Zinc Amido-Oxazolate Catalyzed Ring-Opening Copolymerization and Terpolymerization of Maleic Anhydride and Epoxides. *Molecules* **2020**, *25*, 4044
13. Takasu, A.; Ito, M.; Inai, Y.; Hirabayashi, T.; Nishimura, Y. Synthesis of Biodegradable Polyesters by Ring-Opening Copolymerization of Cyclic Anhydrides Containing a Double Bond with 1,2-Epoxybutane and One-Pot Preparation of the Itaconic Acid-Based Polymeric Network. *Polym. J.* **1999**, *31*, 961–969.
14. (a) Huijser, S.; HosseiniNejad, E.; Sablong, R.; de Jong, C.; Koning, C. E.; Duchateau, R. Ring-Opening Co- and Terpolymerization of an Alicyclic Oxirane

with Carboxylic Acid Anhydrides and CO<sub>2</sub> in the Presence of Chromium Porphyrinato and Salen Catalysts. *Macromolecules* **2011**, *44*, 1132–1139. (b) Robert, C.; de Montigny, F.; Thomas, C. M. Tandem synthesis of alternating polyesters from renewable resources. *Nat. Commun.* **2011**, *2*, 586. (c) Darensbourg, D. J.; Poland, R. R.; Escobedo, C. Kinetic Studies of the Alternating Copolymerization of Cyclic Acid Anhydrides and Epoxides, and the Terpolymerization of Cyclic Acid Anhydrides, Epoxides, and CO<sub>2</sub> Catalyzed by (salen)Cr<sup>III</sup>Cl. *Macromolecules* **2012**, *45*, 2242–2248. (d) Hosseini Nejad, E.; Paoniasari, A.; Koning, C. E.; Duchateau, R. Semi-aromatic polyesters by alternating ring-opening copolymerisation of styrene oxide and anhydrides. *Polym. Chem.* **2012**, *3*, 1308–1313. (e) Hosseini Nejad, E.; van Melis, C. G. W.; Vermeer, T. J.; Koning, C. E.; Duchateau, R. Alternating Ring-Opening Polymerization of Cyclohexene Oxide and Anhydrides: Effect of Catalyst, Cocatalyst, and Anhydride Structure. *Macromolecules* **2012**, *45*, 1770–1776. (f) Bernard, A.; Chatterjee, C.; Chisholm, M. H. The influence of the metal (Al, Cr and Co) and the substituents of the porphyrin in controlling the reactions involved in the copolymerization of propylene oxide and cyclic anhydrides by porphyrin metal(III) complexes. *Polymer* **2013**, *54*, 2639–2646. (g) Harrold, N. D.; Li, Y.; Chisholm, M. H. Studies of Ring-Opening Reactions of Styrene Oxide by Chromium Tetraphenylporphyrin Initiators. Mechanistic and Stereochemical Considerations. *Macromolecules* **2013**, *46*, 692–698. (h) Liu, J.; Bao, Y.-Y.; Liu, Y.; Ren, W.-M.; Lu, X.-B. Binuclear

- chromium-salan complex catalyzed alternating copolymerization of epoxides and cyclic anhydrides. *Polym. Chem.* **2013**, *4*, 1439–1444. (i) Nejad, E. H.; Paoniasari, A.; van Melis, C. G. W.; Koning, C. E.; Duchateau, R. Catalytic Ring-Opening Copolymerization of Limonene Oxide and Phthalic Anhydride: Toward Partially Renewable Polyesters. *Macromolecules* **2013**, *46*, 631–637. (j) Biermann, U.; Sehlinger, A.; Meier, M. A. R.; Metzger, J. O. Catalytic copolymerization of methyl 9,10-epoxystearate and cyclic anhydrides under neat conditions. *Eur. J. Lipid Sci. Technol.* **2016**, *118*, 104–110. (k) DiCiccio, A. M.; Coates, G. W. Ring-Opening Copolymerization of Maleic Anhydride with Epoxides: A Chain-Growth Approach to Unsaturated Polyesters. *J. Am. Chem. Soc.* **2011**, *133*, 10724–10727.
15. Longo, J. M.; DiCiccio, A. M.; Coates, G. W. Poly(propylene succinate): A New Polymer Stereocomplex. *J. Am. Chem. Soc.* **2014**, *136*, 15897–15900.
16. (a) Robert, C.; Ohkawara, T.; Nozaki, K. Manganese-Corrole Complexes as Versatile Catalysts for the Ring-Opening Homo- and Co-Polymerization of Epoxide. *Chem.-Eur. J.* **2014**, *20*, 4789–4795. (b) Liu, D.-F.; Zhu, L.-Q.; Wu, J.; Wu, L.-Y.; Lu, X.-Q. Ring-opening copolymerization of epoxides and anhydrides using manganese(III) asymmetrical Schiff base complexes as catalysts. *RSC Adv.* **2015**, *5*, 3854–3859. (c) Liu, D.; Zhang, Z.; Zhang, X.; Lu, X. Alternating Ring-Opening Copolymerization of Cyclohexene Oxide and Maleic Anhydride with Diallyl-Modified Manganese(III)–Salen Catalysts. *Aust. J. Chem.* **2016**, *69*, 47–55.

17. (a) Aida, T.; Inoue, S. Catalytic reaction on both sides of a metalloporphyrin plane. Alternating copolymerization of phthalic anhydride and epoxyp propane with an aluminum porphyrin-quaternary salt system. *J. Am. Chem. Soc.* **1985**, *107*, 1358–1364. (b) Aida, T.; Sanuki, K.; Inoue, S. Well-controlled polymerization by metalloporphyrin. Synthesis of copolymer with alternating sequence and regulated molecular weight from cyclic acid anhydride and epoxide catalyzed by the system of aluminum porphyrin coupled with quaternary organic salt. *Macromolecules* **1985**, *18*, 1049–1055. (c) Van Zee, N. J.; Coates, G. W. Alternating Copolymerization of Propylene Oxide with Biorenewable Terpene-Based Cyclic Anhydrides: A Sustainable Route to Aliphatic Polyesters with High Glass Transition Temperatures. *Angew. Chem., Int. Ed.* **2015**, *54*, 2665–2668. (d) Van Zee, N. J.; Sanford, M. J.; Coates, G. W. Electronic Effects of Aluminum Complexes in the Copolymerization of Propylene Oxide with Tricyclic Anhydrides: Access to Well-Defined, Functionalizable Aliphatic Polyesters. *J. Am. Chem. Soc.* **2016**, *138*, 2755–2761.
18. Driscoll, O. J.; Stewart, J. A.; McKeown, P.; Jones, M. D. Ring-Opening Copolymerization Using Simple Fe (III) Complexes and Metal- and Halide-Free Organic Catalysts *Macromolecules* **2021** *54*, 8443–8452.
19. Sanford, M. J.; Pena Carrodegua, L.; Van Zee, N. J.; Kleij, A. W.; Coates, G. W. Alternating Copolymerization of Propylene Oxide and Cyclohexene Oxide with

- Tricyclic Anhydrides: Access to Partially Renewable Aliphatic Polyesters with High Glass Transition Temperatures. *Macromolecules* **2016**, 49, 6394–6400.
20. Monica, D. F. Kleij, A. W. Synthesis and Characterization of Biobased Polyesters with Tunable  $T_g$  by ROCOP of Beta-Elementene Oxides and Phthalic Anhydride *ACS Sustainable Chem. Eng.* **2021** 9, 2619–2625
21. De Leo, V.; Casiello, M.; Deluca, G.; Cotugno, P.; Catucci, L.; Nacci, A.; Fusco, C.; D'Accolti, L. Concerning Synthesis of New Biobased Polycarbonates with Curcumin in Replacement of Bisphenol A and Recycled Diphenyl Carbonate as Example of Circular Economy. *Polymers* **2021**, 13, 361.
22. Kim, E.C.; Kim, M. J.; Ho, L. N. T.; Lee, W.; Ka, J. W.; Kim, D. G.; Shin, T. J.; Huh, K. M.; Park, S.; Kim, Y. S. Synthesis of Vinyl-Addition Polynorbornene Copolymers Bearing Pendant n-Alkyl Chains and Systematic Investigation of Their Properties *Macromolecules* **2021** 54 (14), 6762–6771
23. Xu, Z.; Croft, Z. L.; Guo, D.; Cao, K.; Liu, G. Recent development of polyimides: Synthesis, processing, and application in gas separation. *J Polym Sci* **2021**, 59, 943.
24. Yu, X.; Jia, J.; Xu, S.; Lao, K. U.; Sanford, M. J.; Ramakrishnan, R. K.; Nazarenko, S. I.; Hoyer, T. R.; Coates, G. W.; DiStasio Jr., R. A. Unraveling substituent effects on the glass transition temperatures of biorenewable polyesters. *Nature Comm.* **2018**, 9, 2880–2888.

## CHAPTER IV

### MACROCYCLIC POLYESTERS FROM RING OPENING POLYMERIZATION OF LACTONES USING ZINC AMIDO-OXAZOLINATE CATALYSTS

#### IV .1 INTRODUCTION

Polymer topology may have substantial and intricate effects on the physical characteristics of the materials.<sup>1,2</sup> In addition to linear polymers, a vast array of non-linear polymer structures, including as star, graft, crosslinked, and hyperbranched polymers, have been synthesized from a vast array of building blocks and thoroughly studied to address the different material characteristics and uses.<sup>3,4,5,6</sup> Cyclic polymers (CPs) are among the most researched polymers by both physicists and theoretical chemists. Compared to their linear counterparts, CPs impose topological limitations owing to the lack of an end group in CPs.<sup>7,8,9</sup> The absence of an end group leads in features such as a small hydrodynamic volume, low melting viscosity, fast crystallization, and non-chemical processing emission.<sup>10,11,12,13,14</sup> These qualities may be helpful in packaging, microelectronics, biomedical, and pharmaceutical industries as absorbable implant material and drug delivery vehicles.<sup>15-23</sup>

Yet, while having a unique set of physical characteristics, cyclic polymers are one of the least studied classes of polymer topologies due to the challenges associated with their synthesis and purification.<sup>24</sup> Two general approaches have been used to generate CPs: ring closure of linear polymer precursors using techniques such as polymeric supports, interfacial strategies, and electrostatic self-assembly;<sup>25,26,27,28,29</sup> and ring-expansion

polymerization.<sup>30,31,32,33,34,35,36</sup> Recent examples of CPs using carbosiloxanes,<sup>37</sup> lactones,<sup>38,39,40,41,42</sup> phosphates,<sup>43</sup> peptoids,<sup>44,45</sup> and isosorbide-based poly(ethers)<sup>46</sup> have been published. Nonetheless, the topological distinction between cyclic and linear macromolecules and their effect on physical characteristics are poorly understood. Waymouth and colleagues have paved the way for synthesizing pure, well-tailored, and high molecular weight CPs under moderate circumstances by means of zwitterionic polymerization,<sup>47,48,49,50,51</sup> which offers the possibility to compare the features of cyclic architecture to those of its counterpart. Crystallization kinetics of large molecular weights cyclic polycaprolactones (PCLs) showed that the cyclic PCLs crystallize quicker than their linear counterparts for molecular weight more than 75,000 g/mol.<sup>50</sup> Earlier, we have documented the activity of zinc complexes carrying amido-oxazolinatate ligand frameworks<sup>52</sup> as catalysts for the ROCOP<sup>53,54,55,56</sup> and ROP.<sup>33,57</sup> In the absence of alcohol initiators, we have recently developed a synthetic approach for the ROP of *rac*-butyrolactone ( $\beta$ -BL), yielding solely CPs.<sup>33</sup> To create high molecular weight cyclic polyesters, we expand this efficient method to additional lactones such as  $\epsilon$ -caprolactone ( $\epsilon$ -CL) and  $\delta$ -valerolactone ( $\delta$ -VL). Block cyclic copolymers through two-step and gradient polymerization and statistical cyclic copolymers via batch polymerization have been produced by using the reactivity difference of monomers. Using NMR, ESI, GPC, DSC, and TGA methods, the structural and thermal characteristics are studied.<sup>58,59</sup>

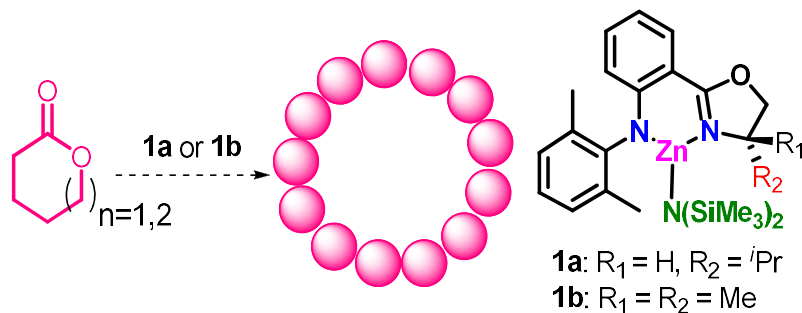


## IV.2 RESULTS AND DISCUSSION

### IV.2.1 ROP of Lactones

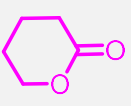
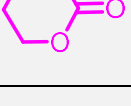
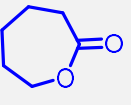
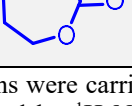
We first investigated the ROP of lactones of various ring sizes with the readily accessible zinc catalyst **1a** (Scheme 1). The progress of the reaction was monitored by  $^1\text{H}$  NMR spectroscopy. As shown in Table 1, the zinc-catalyzed ROP in toluene at room temperature with  $[\delta\text{-VL}]/[\text{cat}] = 200/1$  and  $[\epsilon\text{-CL}]/[\text{cat}] = 200/1$  achieved >98% conversion after 30 min (Table 1, entries 1 & 3). The resultant polymers PVL and PCL had a high number-average molecular weight ( $M_n = 61$  &  $85 \text{ kg mol}^{-1}$  by GPC) with a relatively narrow dispersity of  $\bar{D} = 1.4\text{--}1.7$ . On the other hand, when the ROP of  $\epsilon\text{-CL}$  and  $\delta\text{-VL}$  was examined at room temperature with BnOH as co-initiator at the ratio of  $[\epsilon\text{-CL}]/[\text{cat}]/[\text{BnOH}] = 200/1/1$  and  $[\delta\text{-VL}]/[\text{cat}]/[\text{BnOH}] = 200/1/1$ , >95% conversion was achieved after 4 h (Table 1, entries 2 & 4), which is slower than the reaction without the BnOH initiator. As observed before, the polymerization reaction without the BnOH initiator shows high molecular weight when compared to calculated molecular weight, which is different from the results with the initiator (entries 2 & 4). It should also be noted the ROP of the four-membered  $\beta\text{-BL}$  requires heating at relatively high temperatures ( $100^\circ\text{C}$ ) while the ROP of  $\epsilon\text{-CL}$  and  $\delta\text{-VL}$  proceeds smoothly at room temperature. The activity of the achiral catalyst **1b** was also investigated in the polymerization of  $\epsilon\text{-CL}$  and  $\delta\text{-VL}$ . High molecular weights and narrow dispersity ( $\bar{D}$ ) values were obtained under similar conditions (Table A.III-1, entries 3 & 5). Both catalysts **1a** and **1b** exhibited comparable

activities, with a turnover frequency of 400 h<sup>-1</sup> without initiator and 50 h<sup>-1</sup> in the presence of an alcohol initiator.



**Scheme 1.** ROP of  $\epsilon$ -CL and  $\delta$ -VL with Zn catalysts

**Table 1:** ROP of  $\delta$ -Valerolactone and  $\epsilon$ -Caprolactone with Zn Catalyst (**1a**)<sup>a</sup>

Entry	Monomer	[Zn] <sub>0</sub> : [I] <sub>0</sub> : [M] <sub>0</sub>	<i>t</i> (h)	TOF (h <sup>-1</sup> ) <sup>b</sup>	<i>M</i> <sub>n</sub> (GPC) <sup>c</sup>	<i>M</i> <sub>w</sub> (GPC) <sup>c</sup>	<i>M</i> <sub>w</sub> (DOSY) <sup>d</sup>	<i>D</i> <sub>(GPC)</sub> <sup>c</sup>
1		1:0:200	0.5	400	61.3	89.1	97.7	1.45
2		1:1:200	4	50	7.9	10.3	11.8	1.3
3		1:0:200	0.5	400	85.0	147.5	139.5	1.73
4		1:1:200	4	50	13.5	14.8	21.7	1.09

<sup>a</sup>Reactions were carried out with [ $\delta$ -VL]<sub>0</sub> or [ $\epsilon$ -CL]<sub>0</sub> = 0.95 M at RT in toluene. <sup>b</sup>Monomer conversion was determined by <sup>1</sup>H NMR. <sup>c</sup>Determined by GPC with THF as eluent. <sup>d</sup>*M*<sub>w</sub>(DOSY) was calculated using the experimental value of *D* from the calibration curve,  $y = -0.5362x - 7.4985$  ( $R^2 = 0.9969$ ), obtained with the polystyrene standard at 25 °C in CDCl<sub>3</sub>.

#### IV.2.2 Microstructure of Cyclic and Linear PVL and PCL

The microstructure of the obtained PCL and PVL was carefully studied by the NMR spectroscopy. The  $^1\text{H}$  NMR spectrum of the cyclic PCL (**Fig. 1A**) shows four main peaks at 4.06 ppm, assignable to the methylene protons adjacent to an ester oxygen, 2.31 ppm, representing the methylene proton adjacent to a carbonyl group, 1.65 and 1.39 ppm, assignable to the remaining three methylene protons. Consistent with this, only six signals corresponding to the main chain carbons are present in the  $^{13}\text{C}$  NMR spectrum (Appendix III, Fig. A.III-5). Similarly, PVL exhibits four methylene peaks in the  $^1\text{H}$  NMR and five peaks in the  $^{13}\text{C}$  NMR spectrum, corresponding to the main chain of the PVL (Appendix III, Fig. A.III-2 & A.III-3), while no other peaks are observed. These observations suggest the absence of end groups, i.e., a cyclic structure of the polymers.

In comparison, small signals attributable to the end groups can be consistently observed in the PCL sample obtained in the presence of BnOH (**Fig. 1B**). The peaks at 7.35 and 5.1 ppm can be assigned to the aromatic and benzylic protons, respectively, of the benzyloxyl group, while the 3.6 ppm peak is attributed to the hydroxy proton and methylene protons of the PCL attached to the hydroxyl oxygen.<sup>26</sup> The integration of this peak (3.6 ppm) vs. benzylic (5.1 ppm) protons is 3:2, in agreement with them being the two ends of the polymer chain.<sup>60</sup> The  $^1\text{H}$ - $^1\text{H}$  COSY NMR spectrum (Appendix III, Fig. A.III-8) shows strong cross contour with methylene protons (3.6 ppm) with methylene protons (2.3 ppm) and a weak contour with methylene proton (1.3 ppm). In the  $^{13}\text{C}$  NMR spectrum (Appendix III, Fig. A.III-7), the peak at 63.1 ppm was allotted to methylene carbon adjacent to

hydroxyl oxygen, and the peak at 66.1 ppm was assigned to benzyl carbon based on the CH-correlation (Appendix III, Fig. A.III-9). Together, these observations support the linear structure of the polymer with hydroxyl at one end and benzyloxyl at the other end.

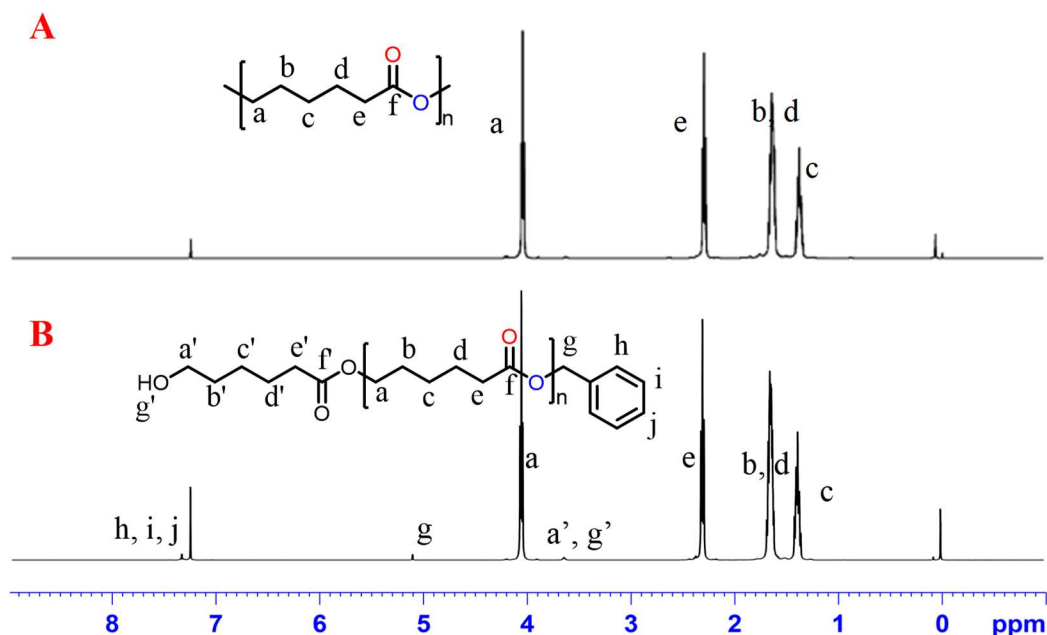


**Figure 1:**  $^1\text{H}$  NMR of polycaprolactones (A) Cyclic PCL produced by catalyst **1a** ( $[\epsilon\text{-CL}]/[\text{cat}] = 200/1$ ); (B) Linear PCL produced by catalyst **1a** with benzyl alcohol as initiator ( $[\epsilon\text{-CL}]/[\text{cat}]/[\text{BnOH}] = 200/1/1$ ).

#### IV.2.3 Differentiation between Linear and Cyclic Polyesters by Crystallization

##### Kinetics

For further differentiation between cyclic and linear polyesters, crystallization kinetics of cyclic and linear polymers of PVL and PCL<sup>61</sup> samples were studied by DSC according to procedures used by the Waymouth group.<sup>50</sup> Cyclic and linear PCL samples with high molecular weights ( $\sim 100$  kDa) were used to determine the crystallization behavior. At a

series of annealing times  $t$ , the samples were isothermally crystallized at 45 °C and the melting enthalpy or the heat of fusion  $\Delta H_m$  was calculated by integrating the melting endotherm curves when the samples were heated above their melting temperature  $T_m$ . The relative crystallinity ( $\chi_c$ ) was monitored from  $\Delta H_m$  relative to the maximum  $\Delta H_m$  achieved under experimental conditions for a given annealing time  $t$ . As shown in Fig. 2a, the cyclic PCL samples crystallized more rapidly than the linear PCL samples. From the linear form of the Avrami equation (Fig. 2b), the Avrami coefficient  $k$  and Avrami exponent  $n$  of the primary crystallization process could be estimated, from which the half-life of crystallization  $t_{1/2}$  was calculated by using the equation  $k = \ln(2) / t_{1/2}^n$ . This gave  $t_{1/2(\text{linear})} = 75$  min and  $t_{1/2(\text{cyclic})} = 31$  min, confirming that the cyclic PCL samples crystallize faster than linear PCL samples. Similarly, the half-life of crystallization of PVL were determined from the Avrami plot (Appendix III, Fig. A.III-42 & 43) to be  $t_{1/2(\text{linear})} = 72$  min and  $t_{1/2(\text{cyclic})} = 23$  min, again indicating the cyclic PVL crystallizes faster than linear PVL.

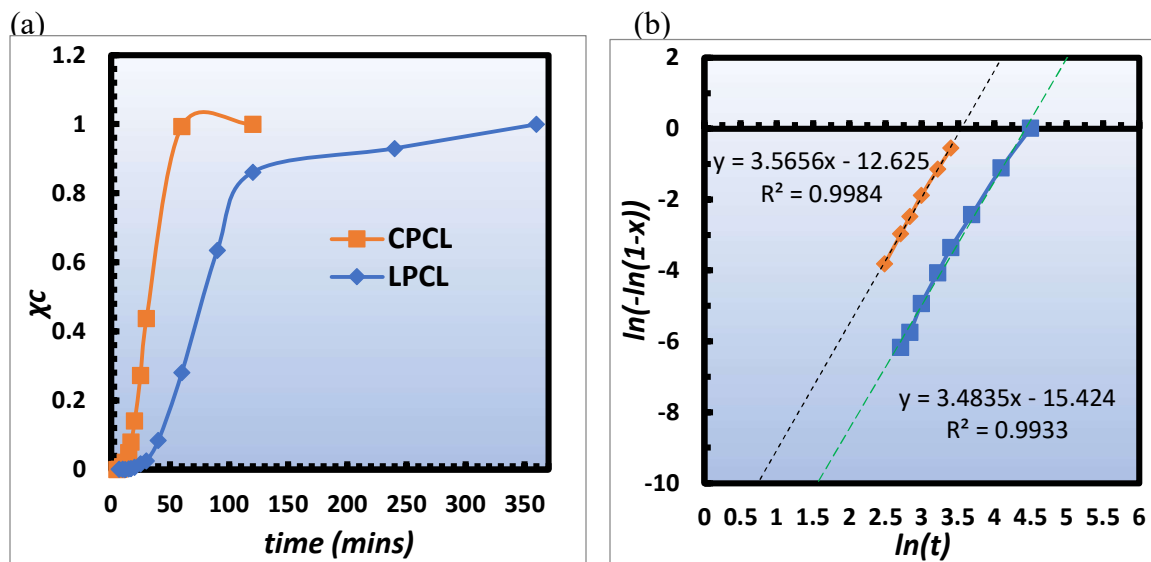


**Figure 2.** Relative crystallinity ( $\chi_c$ ) as a function of time (left) and a linear fit of Avrami equation  $\ln(-\ln(1 - \chi_t)) = n \ln(t) + \ln(k)$  for cyclic and linear PCL.

The Hoffman-Weeks plot was further constructed to compare the equilibrium melting point of linear and cyclic polymers by extrapolating  $T_m$  versus  $T_c$  through DSC studies. The results (Fig. 3) suggested that the equilibrium melting point of the cyclic PCL is  $\sim 5$  °C higher than that of linear PCL (86.4 vs 81.8 °C), in agreement with the literature report.<sup>50</sup> It should be mentioned here that the equilibrium melting point for linear PCL was reported to be 98 °C in the literature,<sup>62</sup> which is 16 °C higher than observed here. Similarly, the high molecular weight PVL ( $M_n = \sim 90$  kDa) showed the equilibrium melting point of 75 (cyclic) & 73 °C (linear) (see Appendix III, Fig. A.III-42&43), lower than PCL and with a narrow difference between their equilibrium melting points.

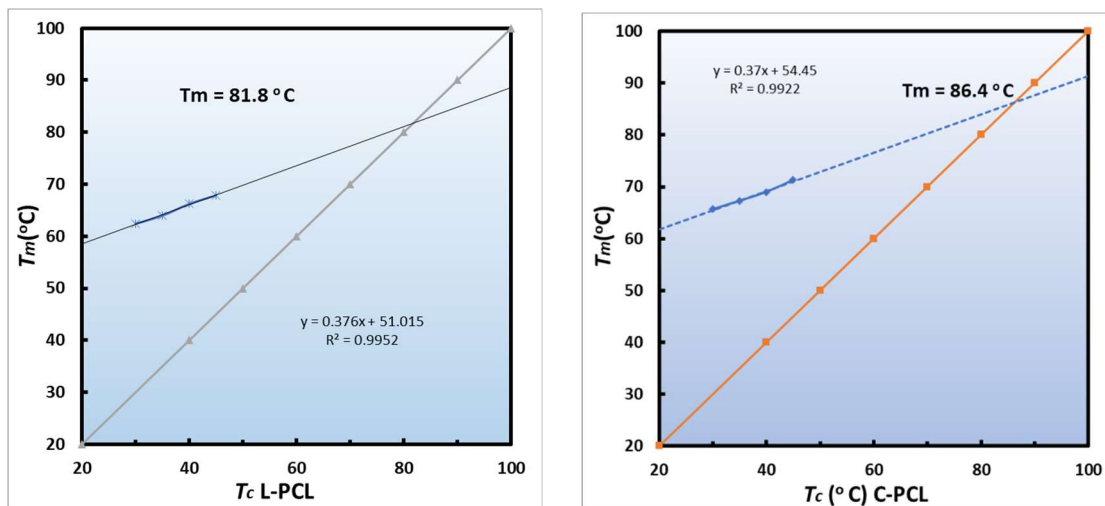


**Figure 3.** Hoffman-Weeks plots of (a) Linear PCL and (b) Cyclic PCL

#### IV.2.4 Synthesis of Statistical or Random Copolymers

Encouraged by the reactivity of the 4, 6, and 7-membered lactones under zinc catalysis, we further explored the preparation of cyclic copolyesters by using two lactone monomers. Depending on the combination of monomers and the reaction conditions, statistical, gradient, and block copolyesters could be obtained.<sup>63</sup> The achiral zinc complex **1b** was used in these reactions and the results are summarized in Table 2.

In a one-pot reaction, a mixture of 1:1 molar ratio of  $\epsilon$ -CL and  $\delta$ -VL was copolymerized at RT in toluene (Table 2, Entry 1). The GPC traces revealed that a unimodal distribution peak with  $M_n=17.4$  kDa with dispersity of  $D=2.19$  (Appendix III, Fig. A.III-44). Because the pair's reactivity was quite similar, the formation of random polymers was expected. The  $^{13}\text{C}$  NMR spectrum of the PCL-*s*-PVL reveal two distinct broad signals at 173.5 and 173.7 ppm (Fig. 4), assignable to the C=O carbons of PCL and

PVL, respectively. In addition, four signals were observed at around 64 ppm for the methylene carbons ( $\alpha$ -position) to the ester oxygen. Two of them were assigned to the CL-CL diads (64.3 ppm) and VL-VL diads (64.5 ppm). The other two at 64.2 and 64.6 ppm were assigned to  $\epsilon$ -CL in CL-VL diads (CL-VL) and  $\delta$ -VL in VL-CL diads (VL-CL), respectively. The predominance of CL-CL and VL-VL diads evidenced the monomer units' random arrangement (Appendix III, Fig. A.III-34(d)).<sup>64,65</sup> Further analysis of the DOSY-NMR showed only single diffusion coefficient which indicated the resultant copolymer is homogenous (Fig. 4).<sup>66</sup>

**Table 2:** Copolyesters with Achiral Zn Catalyst (**1b**)

<i>Entry</i>	<i>Polymer</i>	<i>[M<sub>1</sub>]:[M<sub>2</sub>]</i>	<i>M<sub>n</sub>(theo)<sup>k</sup></i>	<i>M<sub>n</sub>(GPC)<sup>f</sup></i>	<i>Đ<sup>f</sup></i>	<i>M<sub>w</sub>(GPC)<sup>f</sup></i>	<i>M<sub>w</sub>(DOSY)<sup>g</sup></i>
1	PCL- <i>s</i> -PVL	1:1	42.8	17.4	2.19	38.2	39.4
2	PBL- <i>g</i> -PCL	1:1	40.0	46.0	1.07	49.3	56.8
3	PBL- <i>g</i> -PVL	1:1	37.2	32.6	1.37	44.6	44.2
4	PCL- <i>b</i> -PVL	1:1	42.8	55.6	1.14	63.5	69.7
5	PBL- <i>b</i> -PVL	1:1	37.2	27.4	2.38	65.4	40.1
6	PBL- <i>b</i> -PCL	1:1	40.0	35.4	1.27	44.8	23.0

<sup>k</sup>Calculated using  $M_{n(\text{theo})} = [\text{no. equiv. of } M_1 \times \text{Mol.wt of } M_1 + \text{no. Equiv. of } M_2 \times \text{Mol.wt of } M_2]$ . <sup>f</sup>Number average molecular weight, weight average molecular weights, and molecular weight distribution determined by GPC in THF. <sup>g</sup><sup>1</sup>H-DOSY measurement was performed at 25 °C in CDCl<sub>3</sub>, using the equation of the PS standard calibration curve is  $y = -0.5362x - 7.4985$  ( $R^2 = 0.9969$ ).  $M_w$  (DOSY) was calculated from the calibration curve using the experimental value of D.



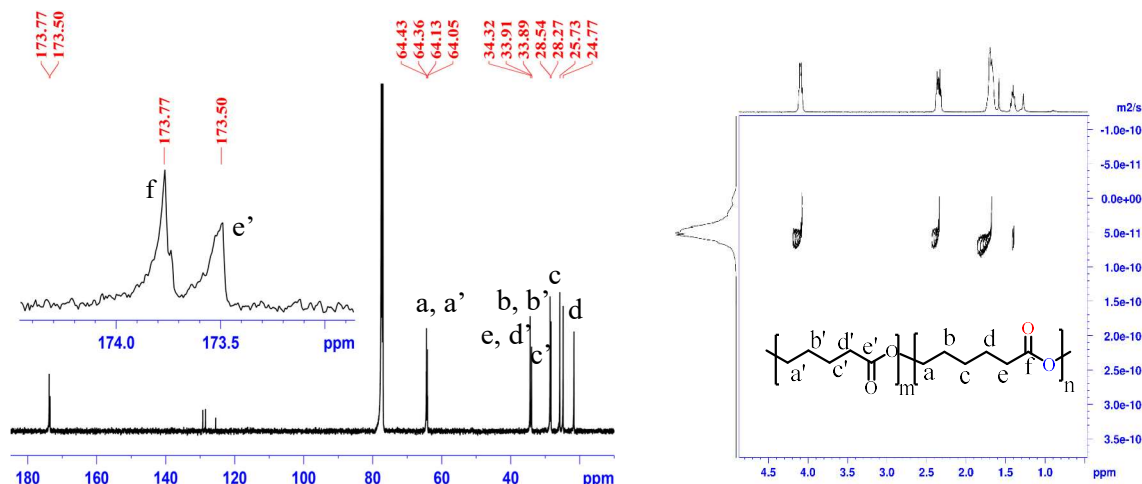


**Figure 4:**  $^{13}\text{C}$  and DOSY- NMR of PCL-*s*-PVL from  $\delta$ -VL and  $\epsilon$ -CL (Entry 1, Table 3)

#### IV.2.5 Synthesis of Gradient Copolymers

Ring opening copolymerization of  $\epsilon$ -CL and  $\beta$ -BL was carried out under identical circumstances as PCL-*s*-PVL, with a 1:1 molar feed of monomers in a one-pot process. While homopolymerization of  $\beta$ -BL alone with catalyst **1b** needed elevated temperatures and could not occur at ambient temperature,  $\beta$ -BL could be copolymerized at room temperature in the presence of another lactone  $\epsilon$ -CL. The copolymer's GPC trace revealed a unimodal distribution with  $M_n = 46 \text{ kDa}$  and dispersity of = 1.07 (Appendix III, Fig. A.III-44), and the  $M_{n(\text{GPC})}$  agreed well with  $M_{n(\text{theo})}$  (Table 2, Entry 2). The  $^{13}\text{C}$  NMR spectrum (Fig. 5) of the purified copolymer showed two unique signals for the C=O group at 173.5 ppm (PCL) and 169.4 ppm (PBL) and two additional signals at 172.8 and 170.4 ppm from the CL-BL junctions, confirming the chain microstructure. The microstructure showed methylene-carbon signals at 64.3 and 67.8 ppm in  $\epsilon$ -CL and  $\beta$ -BL, respectively. The identical methylene-C atoms were detected at 64.6 and 67.3 ppm for  $\epsilon$ -CL and  $\beta$ -BL

in CL-BL diads. In the expanded  $^{13}\text{C}$ -NMR spectra at 64 and 67 ppm of cyclic copolyesters, CL-CL and BL-BL diads predominated, indicating the monomer unit's gradient arrangement (Fig. 5, Appendix III, Fig. A.III-34(b)).<sup>50,67</sup> A DOSY spectrum diffusion coefficient proved the copolymer's homogeneity (Fig. 5)

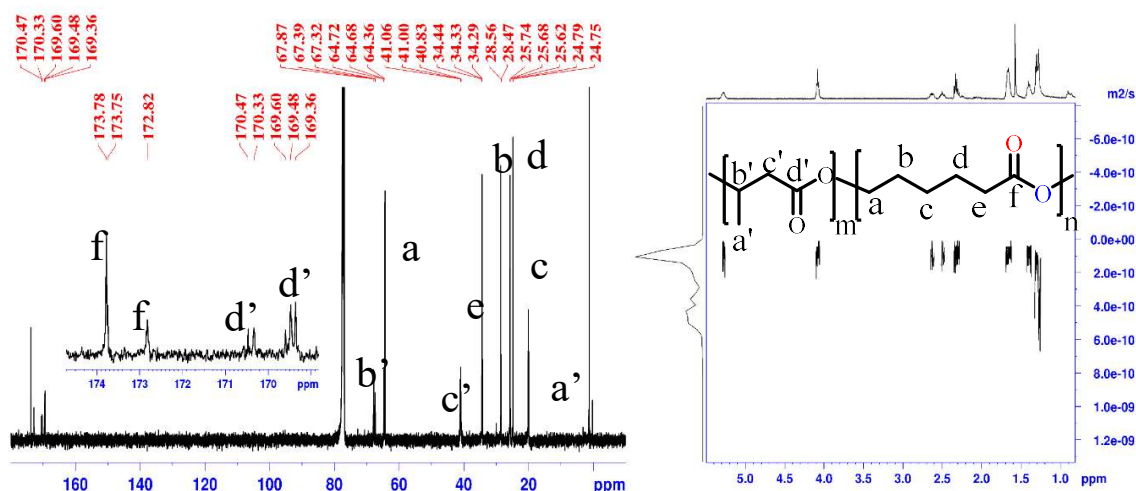


**Figure 5:**  $^{13}\text{C}$ - NMR and DOSY-NMR spectra of PCL-*g*-PBL.

To further shed light on the nature of the copolymers, the time profile of the monomer conversion was followed by  $^1\text{H}$  NMR spectroscopy (Appendix III, Fig. A.III-35(b)). The monomer consumption seemed to be slower than  $\epsilon$ -CL alone. After 12 h, about 73% of  $\epsilon$ -CL reacted while just 3% of  $\beta$ -BL reacted. Then the consumption of  $\beta$ -BL picked up and at 72 h, quantitative conversions for both  $\epsilon$ -CL and  $\beta$ -BL were observed. Thus, a gradient PCL-*g*-PBL copolymer was produced by this one-pot technique.<sup>51</sup>

Similarly, the ROP of  $\beta$ -BL and  $\delta$ -VL was carried out under the identical circumstances as the synthesis of the  $\beta$ -BL/ $\epsilon$ -CL gradient copolymer (Entry 3). The process

achieved high conversions as well, and the product exhibited a unimodal distribution in GPC and a single diffusion coefficient in DOSY NMR. The carbonyl signals in the  $^{13}\text{C}$ -NMR spectra (Appendix III, Fig. A.III-18 & 34(a)) followed a similar pattern as the PCL-*g*-PBL carbonyl signals (Appendix III, Fig. A.III-23 & 34(b)). The copolymerization kinetics of the  $\delta$ -VL/  $\beta$ -BL system likewise demonstrated that  $\delta$ -VL reacted quicker than  $\beta$ -BL (Appendix III, Fig. A.III-35a). Because of the variations in the reactivity of the monomers, these findings indicated the creation of a gradient cyclic copolyester PVL-*g*-PBL.

#### IV.2.6 Synthesis of Block Copolymers

Following the studies on the statistical and gradient polymerization of  $\epsilon$ -CL,  $\delta$ -VL, and  $\beta$ -BL, we next assessed the preparation of diblock copolymers. A diblock copolymer PCL-*b*-PVL was targeted in a one-pot, two-step process.  $\epsilon$ -CL was first polymerized with catalyst **1b** in toluene at room temperature. After  $\epsilon$ -CL was entirely consumed, as deduced from  $^1\text{H}$  NMR spectroscopy, an equimolar amount of  $\delta$ -VL was added to generate the second block. In the  $^{13}\text{C}$  NMR spectrum (Appendix III, Fig. A.III-26), two sharp signals for the carbonyl carbon at 173.5 ppm (PVL) and 173.8 ppm (PCL) were observed,<sup>54,55,68</sup> which were distinctly different from the broad signals observed in the statistical copolymers. This represented the formation of diblock copolymer as the cross junction of two monomer units was minimized in the polymer chain. GPC analysis of the PCL-*b*-PVL copolymer showed a unimodal distribution with  $M_n = 55$  kDa with dispersity

of  $\bar{D} = 1.14$ , (Appendix III, Fig. A.III-44) and the  $M_n$  (GPC) was in good agreement with  $M_n$  (theo).

Furthermore, diblock copolymers were synthesized with the combinations of  $\beta$ -BL/ $\epsilon$ -CL and  $\beta$ -BL/ $\delta$ -VL in a similar two-step procedure. In these reactions,  $\beta$ -BL was polymerized first at 100 °C with catalyst **1b** in toluene, and after its total consumption, an equimolar amount of the second monomer,  $\delta$ -VL or  $\epsilon$ -CL, was added to the reaction mixture and polymerized at room temperature (Table 2, Entries 4-6). The  $^{13}\text{C}$  NMR analysis of the carbonyl region indicated that clean block copolymers were obtained in these reactions. For example, two sets of sharp peaks were observed for the PBL-*b*-PVL: 169.4 and 169.3 ppm for the PBL segment, and 173.4 ppm for the PVL segment (Fig. 7a).<sup>56</sup> As expected, the DOSY-NMR showed only single diffusion coefficient (Fig. 7b).

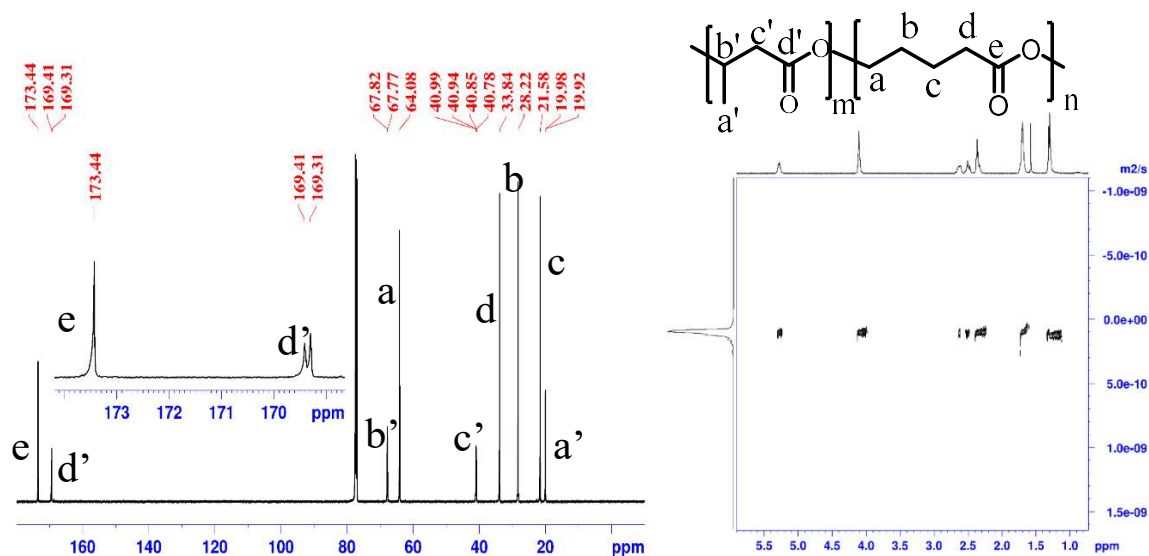


**Figure 7:**  $^{13}\text{C}$ - NMR and DOSY-NMR of PBL-*b*-PVL (Two-step reaction)

#### IV.2.7 Thermal Properties of Homopolymer and Copolymers

Differential scanning calorimetry (DSC) and TGA experiments were conducted on all homo and copolymers to evaluate their thermal properties and the influence of comonomer components on the copolymer material properties. The DSC and TGA results are compiled in Tables 3 & 4.

The thermal properties of cyclic and linear polymers of PVL and PCL were analyzed and compared. The obtained polyesters display melting temperatures ( $T_m$ ) ranging from 55-59 °C and crystallization temperatures ( $T_c$ ) between 25-35 °C, as determined by DSC (Appendix III, Fig. A.III-39). As shown in Table 3, the cyclic polymers tend to show higher  $T_m$  and  $T_c$  than their linear counterparts, but the differences are small (1-4 °C). The onset degradation temperatures ( $T_{d,5}$ ) for cyclic PVL and PCL measured at a 5% loss of the initial weight were 164 °C and 227 °C, respectively, comparable with their linear counterparts (Fig. S38). According to Grayson et al.,<sup>69</sup> the cyclic topology polymers do not have a significant effect on their thermal degradation compared to the linear polymers, and the results in Table 3 are in agreement with their observation.

**Table 3:** Thermal Studies of PCL and PVL with achiral catalyst **1b**

<i>Entry</i>	<i>Polymer</i>	$T_{d,5}^j$	$T_{50\%}^j$	$T_{99\%}^j$	$T_{max}^j$	$T_m^i$	$T_c^i$
<b>1</b>	Cyclic PVL	164	236	476	261	57	29
<b>2</b>	Linear PVL	165	230	328	254	55	25
<b>3</b>	Cyclic PCL	227	313	499	329	59	31

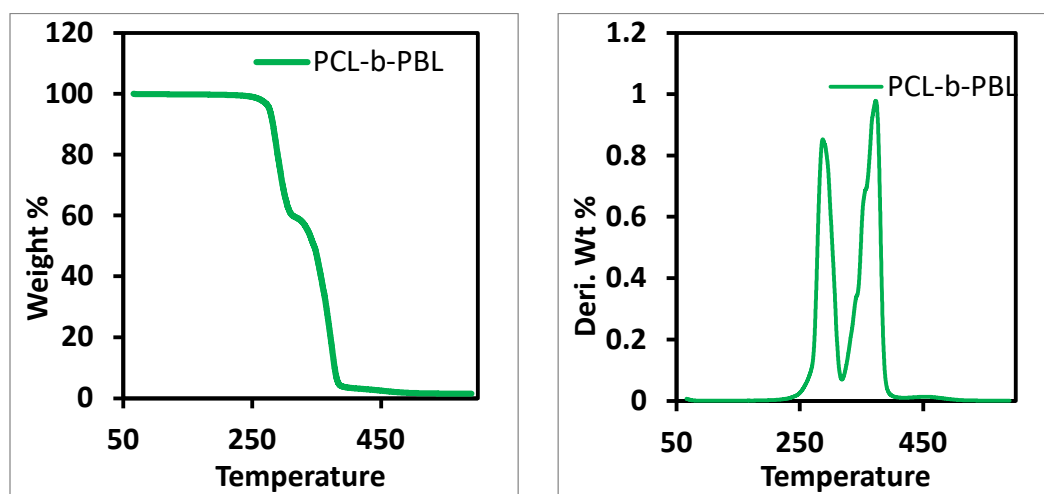
4	Linear PCL	236	312	477	333	55	30
---	------------	-----	-----	-----	-----	----	----

<sup>h</sup>T<sub>m</sub> and T<sub>c</sub> values were determined from the second heating cycle in DSC. <sup>j</sup>T<sub>d,5</sub>, T<sub>50%</sub>, T<sub>99%</sub>, and T<sub>max</sub> refer to the temperature at which 5%, 50%, 99%, and maximum weight losses were observed.

In general, statistical copolymers exhibited combined thermal properties, block copolymers with immiscible parent chains exhibited their respective thermal properties, while gradient copolymers' thermal properties were determined by both component proportions and chain segment lengths.<sup>50,51</sup> As shown in Table 4, cyclic PCL-*s*-PVL polymer thermally degraded in one-step (Appendix III, Fig. A.III-39), and the onset degradation temperature T<sub>d,5</sub> of 281 °C (entry 1) was higher than that of individual homopolymers. It also showed two distinct melting transitions (43 °C and 54 °C) and a single crystallization temperature at 2.1 °C (Fig. S41). The decrease of the T<sub>m</sub> of PCL-*s*-PVL was due to the random distribution of monomers in the polymer chain. In comparison, the block copolymer PCL-*b*-PVL showed two melting transitions (45 °C and 56 °C) which is due to the ordered arrangement of two monomers in the block copolymer (Table 4, Entry 2).

The gradient copolymer PBL-*g*-PVL started degradation at 317 °C with a two-stage degradation process, and the DSC showed a single melting point of 40 °C and a broad crystallization temperature T<sub>c</sub> of 7.1 °C (Table 4, Entry 4). In comparison, the gradient copolymer PBL-*g*-PCL started degradation at 324 °C with a two-stage degradation process, but it did not show a melting or crystalline transition by DSC. The two-stage degradation for these two gradient polymers may result from the presence of significant block

segments, as the reactivity difference between the two monomers were large. On the other hand, the diblock polymer PBL-*b*-PCL exhibited one melting transition of 61 °C, which was close to the PCL homopolymer, and  $T_g$  of 20 °C (Table 4, Entry 6). The glass transition occurred at 11 °C, which was close to the PBL homopolymer. The TGA profile showed two distinct degradation peaks (Fig. 8), indicating the presence of two blocks in the polymer.



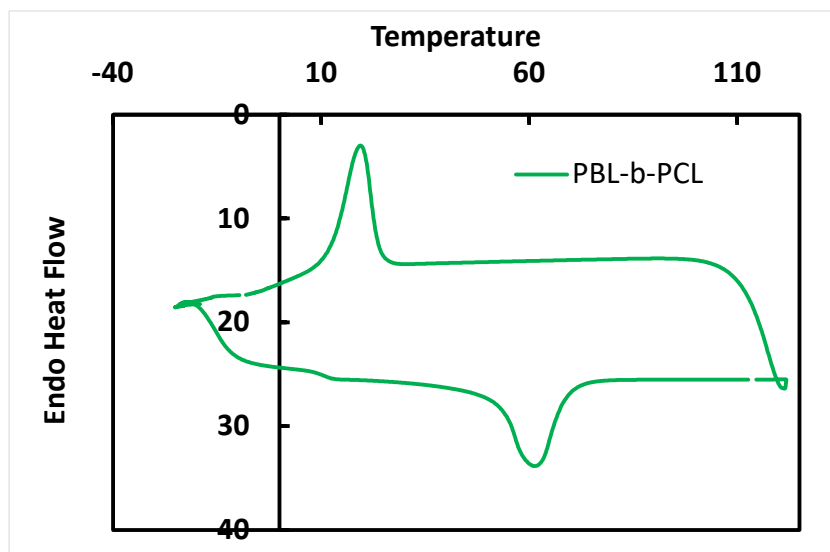


**Figure 8:** TGA and DSC profiles of a block polyester PCL-*b*-PBL

**Table 4:** Thermal properties of cyclic copolymers

Entry	Polymer	$T_d,5^j$	$T_{50\%}^j$	$T_{99\%}^j$	$T_{max}^j$	$T_m^i$	$T_c^i$	$T_g^i$
1	PVL-s-PCL	281	340	454	320, 395	43, 54	2.1	n.o.
2	PVL-b-PCL	263	330	425	332	45, 56	2.6	n.o.
3	Cyclic PBL	285	296	316	-	-	-	7.6
4	PBL-g-PVL	317	361	409	333, 398	40	7.1	n.o.
5	PBL-g-PCL	324	403	465	338, 443	--	--	n.o.
6	PBL-b-PVL	266	311	464	306, 338	59	19	4.9



7	PBL-b-PCL	250	345	475	288,373	61.4	20.1	10.6
---	-----------	-----	-----	-----	---------	------	------	------

<sup>h</sup>Temperature in °C. <sup>i</sup>T<sub>m</sub> and T<sub>c</sub> values were determined from the second heating cycle in DSC. <sup>j</sup>T<sub>d,5</sub>, T<sub>50%</sub>, T<sub>99%</sub>, and T<sub>max</sub> refer to the temperature at which 5%, 50% 99%, and maximum weight losses were observed in TGA, respectively.

### IV.3 CONCLUSION

In summary, we have demonstrated an effective method for cyclic polyesters by zinc catalyzed ROP of lactones such as  $\epsilon$ -CL and  $\delta$ -VL. Cyclic PVL and PCL with high molecular weight were obtained in the absence of an alcohol initiator. In contrast, the addition of an alcohol co-catalyst resulted in linear PVLs and PCLs with well-defined end groups. The topology and high molecular weight of the cyclic polymers were confirmed from the <sup>1</sup>H-DOSY experiment. The crystallization kinetics by DSC showed that the macrocyclic PCL and PVL samples crystallize faster and have higher equilibrium melting temperatures than their linear counterparts. Based on the reactivity difference of two monomers, cyclic random, gradient, and block copolymers of  $\epsilon$ -CL,  $\delta$ -VL and  $\beta$ -BL were synthesized by varying the feeding modes. TGA analysis showed decomposition temperature increases in the order of gradient > random > block > homopolymers. DSC analysis showed that the block copolymer shows the melting point increases in block > gradient > random, which can be explained from the randomness of the repeating units in the polymer chain.

## IV.4 EXPERIMENTAL SECTION

### Materials.

All reactions with air- and/or moisture-sensitive compounds were performed under dry nitrogen using standard glovebox (VAC atmosphere controller) and/or Schlenk line techniques. Analytical grade THF was purchased from Fisher Scientific and used as received. Deuterated solvents were purchased from Cambridge Isotope Laboratories. Other chemicals were purchased from Sigma-Aldrich.  $\beta$ -Butyrolactone was distilled over  $\text{CaH}_2$  following three freeze-pump-thaw cycles and stored over 4Å molecular sieves.  $\delta$ -Valerolactone and  $\epsilon$ -caprolactone were distilled over Na-metal and stored over 4Å molecular sieves.  $\text{CDCl}_3$  was distilled over  $\text{CaH}_2$  and degassed before use. Toluene was distilled under nitrogen from Na/benzophenone. The synthesis of zinc complexes **1a** & **1b** was conducted according to the literature methods.<sup>52,53,54,55,56,57</sup>

### Methods and Instrumentation.

NMR experiments (1D, 2D, and DOSY) were recorded on a Bruker AVANCE 500 or a AVANCE NEO 400 NMR spectrometer, and the spectra were referenced to the residual peaks in  $\text{CDCl}_3$ . The microstructures of homopolymers and copolymers were characterized by the  $^{13}\text{C}$  NMR spectra recorded at room temperature in  $\text{CDCl}_3$  with sample concentrations in the range 1 to 1.5 mg/mL. Gel permeation chromatography (GPC) analyses were carried out using an Agilent 1260 Infinity GPC system equipped with an autosampler and a refractive index detector. The Agilent PolyPore columns (5-micron, 4.6 mm ID) were eluted with THF at 30 °C at 1 mL/min and calibrated using

monodisperse polystyrene standards. Flash column chromatography was performed using silica gel (particle size 40–64  $\mu\text{m}$ , 230–400 mesh). Differential scanning calorimetry (DSC) was recorded with Perkin Elmer Jade DSC with a ramping rate of 20  $^{\circ}\text{C}/\text{min}$  under nitrogen protection. Heat flow was recorded from both the second heating and cooling curve. Thermogravimetric analysis (TGA) was carried out with a Hi-Res TGA Q500 (TA Instruments) using alumina pans at a heating rate of 20  $^{\circ}\text{C}/\text{min}$  under nitrogen with a sample weight of about 10 mg.

#### Crystallization Kinetics.

To remove their thermal history, polymer samples were heated to 120  $^{\circ}\text{C}$  at 30  $^{\circ}\text{C}/\text{min}$  for 10 minutes, then cooled to 45  $^{\circ}\text{C}$  at 30  $^{\circ}\text{C}/\text{min}$  while being maintained there for the annealing period,  $t$ . To examine the melting curve, the sample was then heated to 80 $^{\circ}\text{C}$  at a rate of 10 $^{\circ}\text{C}/\text{min}$ . By linearly integrating the melting curve, it was possible to calculate the heat of fusion,  $\Delta H_{\text{m}}$ . The ratio of  $\Delta H_{\text{m}}$  at annealing time  $t$  to the highest  $\Delta H_{\text{m}}$  achievable under experimental circumstances was used to calculate the relative degree of crystallinity, or  $\chi_{\text{c}}$ . The Avrami exponent  $n$ , and coefficient,  $k$ , were calculated using plots of the linear form of the Avrami equation from crystallinities ranging from 5% to 95%. Using the determined  $k$  and  $n$ , the  $t_{1/2}$  of crystallization was computed, and it was found to be in excellent accord with plots of relative crystallinity as a function of time.<sup>50</sup>

#### Hoffman-Weeks Plot.

Differential scanning calorimetry (DSC) was used to determine the melting temperatures of linear and cyclic PCL samples. The sample was first heated to 120 °C at 30 °C/min and maintained there for 10 minutes. Next, it was cooled to  $T_c$  (30, 35, 40, and 45 °C) at 30 °C/min and maintained there for the same annealing time  $\Delta t_c$  used by Warmouth. To examine the melting curve, the sample was then heated to 80 °C at a rate of 40 °C/min.  $T_m$  was calculated using the melting curve's peak.<sup>50</sup>

Diffusion Ordered Spectroscopy (DOSY).

Using Li et al. methods, a diffusion ordered NMR spectroscopy (DOSY) experiment linearly relates the chemical shift of  $^1\text{H}$  NMR resonances to the translational diffusion coefficient of a particular molecular species, which can be applied to determine  $M_w$  of polymers in dilute solutions. In diluted conditions, viscosity and density remain consistent throughout the solution, hence the linear relation between  $\text{Log } D_a$  and  $\text{Log } M_w$  using the Stokes-Einstein equation. We created a  $D$ - $M_w$  linear calibration curve from the  $^1\text{H}$ DOSY experiment,<sup>60</sup> using narrowly dispersed polystyrenes as standards for the GPC calibration (Figure S1). Chloroform was used as a solvent for all polymers because most of the polymers are soluble in  $\text{CDCl}_3$ . Next, we analyzed the purified samples of PCL and PVL at similar experimental  $^1\text{H}$ DOSY conditions used for standard samples. The molecular weights obtained from the GPC and DOSY were within 0.5-15% deviation (Table S1). The high molecular weight polymer shows a better agreement between DOSY and GPC values than the lower molecular weights.

### Synthesis of Catalyst 1b

#### Synthesis of the ligand.

In the first step, a mixture of 2-bromobenzonitrile (3.90 g, 21.4 mmol), ( $\pm$ )-2-amino-2-methyl-1-propanol (2.00 g, 22.5 mmol) and anhydrous  $\text{ZnCl}_2$  (0.106 g, 0.77 mmol) in chlorobenzene (15 mL) was refluxed for 26 h to give a yellow solution. The progress of the reaction was monitored by analyzing small aliquots using TLC and  $^1\text{H}$  NMR spectroscopy. After removal of the solvent in vacuo, the residue was purified by column chromatography on silica gel with hexane/EtOAc (5:1) to afford a yellow oil. Yield: 3.08 g (56%).  $^1\text{H}$  NMR (500.1 MHz;  $\text{CDCl}_3$ ; 298 K):  $\delta$  1.35 (6H,  $\text{NC}(\text{CH}_3)_2\text{CH}_2\text{O}$ ), 4.08 (2H,  $\text{NC}(\text{CH}_3)_2\text{CH}_2\text{O}$ ), 7.24 (2H, *ArH*), 7.38 (1H, *ArH*), 7.62 (1H, *ArH*). In the second step, an oven dried Schlenk flask was charged with  $\text{Pd}(\text{OAc})_2$  (5 mol%), *rac*-BINAP (5 mol%), achiral aryl bromide (oxazoline obtained above) (304 mg, 1.2 mmol, 1.0 equiv.), 2,6-dimethyl aniline (173  $\mu\text{l}$ , 1.4 mmol, 1.2 equiv.), *t*-BuONa (1.7 mmol, 1.4 equiv.), and anhydrous degassed toluene (5 mL), and the mixture was refluxed under  $\text{N}_2$  until an appropriate amount of the ligand was formed as judged by TLC (hexane–EtOAc, 10:0.5) and  $^1\text{H}$  NMR spectroscopy. The crude product was then purified by column chromatography on silica gel eluting with a mixture of 20:1 hexane and EtOAc. Yield 0.314 g (89%).  $^1\text{H}$  NMR (500.1 MHz;  $\text{CDCl}_3$ ; 298 K):  $\delta$  1.50 (6H,  $\text{NC}(\text{CH}_3)_2\text{CH}_2\text{O}$ ), 2.35 (6H, *ArCH}\_3*), 4.17 (2H,  $\text{NC}(\text{CH}_3)_2\text{CH}_2\text{O}$ ), 6.36 (1H, *ArH*), 6.76 (1H, *ArH*), 7.27 (4H, *ArH*), 7.39 (1H, *ArH*), 7.91 (1H, *ArH*), 10.12 (1H, *NH*).

#### Synthesis of Zinc-amidooxazolinato Complex 1b.

An oven dried Schlenk flask was charged with the ligand above (0.314 g, 1.07 mmol, 1.0 equiv.) and  $\text{Zn}(\text{N}(\text{SiMe}_3)_2)$  (0.411 g, 1.06 mmol, 1.0 equiv.) in 3 ml of toluene, and the mixture was stirred under  $\text{N}_2$  until all the ligand was converted as judged by  $^1\text{H}$  NMR spectroscopy. After removal of the solvent, the crude product was washed with dry hexanes and dried carefully under vacuum. Yield: 0.519 g (94%).  $^1\text{H}$  NMR (500.1 MHz;  $\text{CDCl}_3$ ; 298 K):  $\delta$  0.20 (18H,  $\text{N}(\text{SiMe}_3)_2$ ), 1.70 (6H,  $\text{NC}(\text{CH}_3)_2\text{CH}_2\text{O}$ ), 2.23 (6H,  $\text{ArCH}_3$ ), 4.36 (1H,  $\text{NC}(\text{CH}_3)_2\text{CH}_2\text{O}$ ), 6.31 (1H,  $\text{ArH}$ ), 6.34 (1H,  $\text{ArH}$ ), 7.27 (2H,  $\text{ArH}$ ), 7.38 (1H,  $\text{ArH}$ ), 7.49 (1H,  $\text{ArH}$ ), 7.96 (1H,  $\text{ArH}$ ).  $^{13}\text{C}$  NMR ( $\text{CDCl}_3$ , 298K):  $\delta$  169 ( $\text{C}=\text{N}$ ), 157.2 ( $\text{ArC}-\text{N}$ ), 147.3 ( $\text{ArC}-\text{N}$ ), 134.4 ( $\text{ArC}$ ), 134.2 ( $\text{ArC}$ ), 131.4 ( $\text{ArC}$ ), 128.4 ( $\text{ArC}$ ), 14.4 ( $\text{ArC}$ ), 116.4 ( $\text{ArC}$ ), 104.1 ( $\text{ArC}$ ), 78.6 ( $\text{N}=\text{COCH}_2$ ), 67.3 ( $\text{NC}(\text{CH}_3)_2$ ), 29.25 ( $\text{NC}(\text{CH}_3)_2$ ), 19.0 ( $\text{Ar}-\text{CH}_3$ ), 5.20 (9C,  $\text{N}(\text{SiMe}_3)_2$ ).

### Polymerization of Cyclic esters

#### Representative procedure for preparation of cyclic polymers of $\delta$ -VL and $\epsilon$ -CL

In a glove box, an oven-dried 10 mL Schlenk flask equipped with a stir bar was charged with **1a** or **1b** catalyst (0.0187 mmol, 1 equiv.) and toluene (4.0 mL). The mixture was stirred at rt for 5 min, and  $\delta$ -VL (348  $\mu\text{L}$ , 3.75 mmol, 200 equiv.) was added to the pale yellowish green solution. The flask was capped, and the reaction mixture was stirred at room temperature for 30 min. After removing the solvent in a vacuum, the residue was dissolved in DCM (1–3 mL), followed by the addition of hexane (4–5 mL). The precipitation of the polymeric products was facilitated by immersing the flask in liquid nitrogen. The supernatant was decanted, and the residues were washed and dried under a

vacuum. The same steps were followed for the homopolymerization of  $\epsilon$ -CL (416  $\mu$ L, 3.75 mmol, 200 equiv.).

**Cyclic Poly(valerolactone)**, Conversion: >99%. Yield: 96%.  $^1\text{H}$  NMR ( $\text{CDCl}_3$ , 298K):  $\delta$  4.09 (m,  $\text{CH}_2\text{CH}_2\text{O}$ , 2H), 2.35 (m,  $\text{CH}_2\text{CH}_2\text{C}=\text{O}$ , 2H), 1.69 (m,  $\text{CH}_2(\text{CH}_2)_2\text{CH}_2$ , 4H).  $^{13}\text{C}$  NMR ( $\text{CDCl}_3$ , 298K):  $\delta$  173.51 ( $\text{C}=\text{O}$ ), 64.18 ( $\text{CH}_2\text{CH}_2\text{O}$ ), 33.96 ( $\text{CH}_2\text{CH}_2\text{C}=\text{O}$ ), 28.36 ( $\text{CH}_2\text{CH}_2\text{CH}_2\text{O}$ ), 20.17 ( $\text{CH}_2\text{CH}_2\text{C}=\text{O}$ ).

**Cyclic Poly(caprolactone)**, Conversion: >99%. Yield: 95%.  $^1\text{H}$  NMR ( $\text{CDCl}_3$ , 298K):  $\delta$  4.06 (m,  $\text{CH}_2\text{CH}_2\text{O}$ , 2H), 2.31 (m,  $\text{CH}_2\text{CH}_2\text{C}=\text{O}$ , 2H), 1.65 (m,  $\text{CH}_2\text{CH}_2\text{CH}_2\text{CH}_2$ , 4H), 1.38 (m,  $\text{CH}_2\text{CH}_2\text{CH}_2$ , 2H).  $^{13}\text{C}$  NMR ( $\text{CDCl}_3$ , 298K):  $\delta$  173.76 ( $\text{C}=\text{O}$ ), 64.37 ( $\text{CH}_2\text{CH}_2\text{O}$ ), 34.35 ( $\text{CH}_2\text{CH}_2\text{C}=\text{O}$ ), 28.59 ( $\text{CH}_2\text{CH}_2\text{CH}_2\text{O}$ ), 25.76 ( $\text{CH}_2\text{CH}_2\text{C}=\text{O}$ ), 24.82 ( $\text{CH}_2\text{CH}_2\text{CH}_2$ ).

Representative procedure for preparation of linear polymers of  $\delta$ -VL and  $\epsilon$ -CL

An oven-dried 10 mL Schlenk flask equipped with a stir bar was charged with **1a**, or **1b** catalyst (0.0187 mmol, 1 equiv.) and toluene (4.0 mL). The initiator benzyl alcohol (2.0  $\mu$ L, 0.0187 mmol, 1 equiv.), were successively added. The mixture was stirred at rt for 5 min. After that,  $\delta$ -VL (348  $\mu$ L, 3.75 mmol, 200 equiv.) was added to the pale yellow is H green solution. The flask was capped, and the reaction mixture was stirred at room temperature for 4 h. After removing the solvent in a vacuum, the residue was dissolved in DCM (1–3 mL), followed by the addition of hexane (4–5 mL). The precipitation of the polymeric products was facilitated by immersing the flask in liquid nitrogen. The

supernatant was decanted, and the residues were washed and dried under a vacuum. The same steps were followed for the linear PCL (416  $\mu$ L, 3.75 mmol, 200 equiv.).

**Poly(valerolactone) in the presence of Benzyl Alcohol.** Conversion: 91%. Yield: 85%,  $^1\text{H}$  NMR ( $\text{CDCl}_3$ , 298K):  $\delta$  7.35 (s, ArH, 5H), 5.12 (s, ArCH<sub>2</sub>, 2H), 4.09 (m, CH<sub>2</sub>CH<sub>2</sub>O, 2H), 3.66 (m, CH<sub>2</sub>OH, 1H and CH<sub>2</sub>OH, 2H), 2.35 (m, CH<sub>2</sub>CH<sub>2</sub>C=O, 2H), 1.69 (m, CH<sub>2</sub>(CH<sub>2</sub>)<sub>2</sub>CH<sub>2</sub>, 4H).  $^{13}\text{C}$  NMR ( $\text{CDCl}_3$ , 298K):  $\delta$  173.51 (C=O), 173.51 (C=O), 128.46 (ArC), 64.18 (CH<sub>2</sub>CH<sub>2</sub>O), 64.18 (CH<sub>2</sub>CH<sub>2</sub>O), 33.96 (CH<sub>2</sub>CH<sub>2</sub>C=O), 33.96 (CH<sub>2</sub>CH<sub>2</sub>C=O), 28.36 (CH<sub>2</sub>CH<sub>2</sub>CH<sub>2</sub>O), 28.36 (CH<sub>2</sub>CH<sub>2</sub>CH<sub>2</sub>O), 20.17 (CH<sub>2</sub>CH<sub>2</sub>C=O), 20.17 (CH<sub>2</sub>CH<sub>2</sub>C=O).

**Poly(caprolactone) in the presence of Benzyl Alcohol.** Conversion: 94%. Yield: 90%,  $^1\text{H}$  NMR ( $\text{CDCl}_3$ , 298K):  $\delta$  7.35 (s, ArH, 5H), 5.12 (s, ArCH<sub>2</sub>, 2H), 4.07 m, CH<sub>2</sub>CH<sub>2</sub>O, 2H), 3.66 (m, CH<sub>2</sub>OH, 1H and CH<sub>2</sub>OH, 2H), 2.31 (m, CH<sub>2</sub>CH<sub>2</sub>C=O, 2H), 1.65 (m, CH<sub>2</sub>CH<sub>2</sub>CH<sub>2</sub>CH<sub>2</sub>, 4H), 1.38 (m, CH<sub>2</sub>CH<sub>2</sub>CH<sub>2</sub>, 2H).  $^{13}\text{C}$  NMR ( $\text{CDCl}_3$ , 298K):  $\delta$  173.73 (C=O), 173.73 (C=O), 128.46 (ArC), 64.37 (CH<sub>2</sub>CH<sub>2</sub>O), 63.08 (CH<sub>2</sub>CH<sub>2</sub>O), 34.45 (CH<sub>2</sub>CH<sub>2</sub>C=O), 32.69 (CH<sub>2</sub>CH<sub>2</sub>C=O), 28.61 (CH<sub>2</sub>CH<sub>2</sub>CH<sub>2</sub>O), 28.59 (CH<sub>2</sub>CH<sub>2</sub>CH<sub>2</sub>O), 25.76 (CH<sub>2</sub>CH<sub>2</sub>C=O), 25.53 (CH<sub>2</sub>CH<sub>2</sub>C=O), 24.91 (CH<sub>2</sub>CH<sub>2</sub>CH<sub>2</sub>).

Representative procedure for preparation of statistical and gradient copolymers

An oven-dried 25 mL Schlenk flask equipped with a stir bar was charged with catalyst **1b** (0.0187 mmol, 1 equiv.) and toluene (8.0 mL), and stirred at rt for 5 min. To the mixture, monomers  $\delta$ -VL (348  $\mu$ L, 3.75 mmol, 200 equiv.), and  $\epsilon$ -CL (416  $\mu$ L, 3.75



mmol, 200 equiv.) were added. All the addition took place in the glovebox. The flask was capped, and the reaction mixture was stirred at room temperature for 40 min in the glove box.  $^1\text{H}$  NMR spectroscopy was used to monitor the reaction until the complete conversion of  $\delta$ -VL and  $\varepsilon$ -CL (>96%). After removing the solvent in a vacuum, the residue was dissolved in DCM (4–6 mL), followed by the addition of hexane (8–10 mL). The precipitation of the polymeric products was facilitated by immersing the flask in liquid nitrogen. The supernatant was decanted, and the residues were washed and dried under a vacuum. The same steps were followed for the synthesis of PBL-*g*-PCL and PBL-*g*-PVL.

**Cyclic PVL-*s*-PCL**, Yield: 96%,  $^1\text{H}$  NMR ( $\text{CDCl}_3$ , 298K):  $\delta$  4.15 (m,  $\text{CH}_2\text{CH}_2\text{O}$ , 2H), (m,  $\text{CH}_2\text{CH}_2\text{O}$ , 2H), 2.43 (m,  $\text{CH}_2\text{CH}_2\text{C}=\text{O}$ , 2H), (m,  $\text{CH}_2\text{CH}_2\text{C}=\text{O}$ , 2H), 1.76 (m,  $\text{CH}_2(\text{CH}_2)_2\text{CH}_2$ , 4H), (m,  $\text{CH}_2\text{CH}_2\text{CH}_2\text{CH}_2$ , 4H), 1.46 (m,  $\text{CH}_2\text{CH}_2\text{CH}_2$ , 2H).  $^{13}\text{C}$  NMR ( $\text{CDCl}_3$ , 298K):  $\delta$  173.50 ( $\text{C}=\text{O}$ ), 64.13 ( $\text{CH}_2\text{CH}_2\text{O}$ ), 33.91 ( $\text{CH}_2\text{CH}_2\text{C}=\text{O}$ ), 28.27 ( $\text{CH}_2\text{CH}_2\text{CH}_2\text{O}$ ), 20.17 ( $\text{CH}_2\text{CH}_2\text{C}=\text{O}$ ), 173.77 ( $\text{C}=\text{O}$ ), 64.37 ( $\text{CH}_2\text{CH}_2\text{O}$ ), 34.32 ( $\text{CH}_2\text{CH}_2\text{C}=\text{O}$ ), 28.54 ( $\text{CH}_2\text{CH}_2\text{CH}_2\text{O}$ ), 25.73 ( $\text{CH}_2\text{CH}_2\text{C}=\text{O}$ ), 24.77 ( $\text{CH}_2\text{CH}_2\text{CH}_2$ ).

**Cyclic PBL-*g*-PVL**, Yield: 96%,  $^1\text{H}$  NMR ( $\text{CDCl}_3$ , 298K):  $\delta$  5.24 (m,  $\text{CH}_3\text{CHCH}_2$ , 1H), 2.58 (m,  $\text{CH}_3\text{CHCH}_2$ , 1H), 2.47 (m,  $\text{CH}_3\text{CHCH}_2$ , 1H), 1.26 (t,  $\text{CH}_3\text{CHCH}_2$ , 3H), 4.06 (m,  $\text{CH}_2\text{CH}_2\text{O}$ , 2H), 2.33 (m,  $\text{CH}_2\text{CH}_2\text{C}=\text{O}$ , 2H), 1.65 (m,  $\text{CH}_2(\text{CH}_2)_2\text{CH}_2$ , 4H).  $^{13}\text{C}$  NMR ( $\text{CDCl}_3$ , 298K): 170.37 ( $\text{C}=\text{O}$ ), 170.25 ( $\text{C}=\text{O}$ ), 169.52 ( $\text{C}=\text{O}$ ), 169.40 ( $\text{C}=\text{O}$ ), 169.29 ( $\text{C}=\text{O}$ ), 67.76 ( $\text{CH}_3\text{CHCH}_2$ ), 40.90 ( $\text{CH}_3\text{CHCH}_2$ ), 40.77 ( $\text{CH}_3\text{CHCH}_2$ ), 20.01

(CH<sub>3</sub>CHCH<sub>2</sub>), 173.44 (C=O), 173.38 (C=O), 172.52 (C=O), 64.35 (CH<sub>2</sub>CH<sub>2</sub>O), 33.97 (CH<sub>2</sub>CH<sub>2</sub>C=O), 28.20 (CH<sub>2</sub>CH<sub>2</sub>CH<sub>2</sub>O), 21.55 (CH<sub>2</sub>CH<sub>2</sub>C=O).

**Cyclic PBL-*g*-PCL**, Yield: 96%, <sup>1</sup>H NMR (CDCl<sub>3</sub>, 298K): δ 5.27 (m, CH<sub>3</sub>CHCH<sub>2</sub>, 1H), 2.62 (m, CH<sub>3</sub>CHCH<sub>2</sub>, 1H), 2.48 (m, CH<sub>3</sub>CHCH<sub>2</sub>, 1H), 1.28 (t, CH<sub>3</sub>CHCH<sub>2</sub>, 3H), 4.06 (m, CH<sub>2</sub>CH<sub>2</sub>O, 2H), 2.31 (m, CH<sub>2</sub>CH<sub>2</sub>C=O, 2H), 1.65 (m, CH<sub>2</sub>CH<sub>2</sub>CH<sub>2</sub>CH<sub>2</sub>, 4H), 1.39 (m, CH<sub>2</sub>CH<sub>2</sub>CH<sub>2</sub>, 2H). <sup>13</sup>C NMR (CDCl<sub>3</sub>, 298K): 170.33 (C=O), 169.60 (C=O), 169.48 (C=O), 169.36 (C=O), 67.87 (CH<sub>3</sub>CHCH<sub>2</sub>), 41.00 (CH<sub>3</sub>CHCH<sub>2</sub>), 40.83 (CH<sub>3</sub>CHCH<sub>2</sub>), 20.01 (CH<sub>3</sub>CHCH<sub>2</sub>), 173.78 (C=O), 173.75 (C=O), 172.82 (C=O), 170.47 (C=O), 170.33 (C=O), 169.60 (C=O), 169.48 (C=O), 169.36 (C=O), 64.37 (CH<sub>2</sub>CH<sub>2</sub>O), 34.35 (CH<sub>2</sub>CH<sub>2</sub>C=O), 28.59 (CH<sub>2</sub>CH<sub>2</sub>CH<sub>2</sub>O), 25.76 (CH<sub>2</sub>CH<sub>2</sub>C=O), 24.82 (CH<sub>2</sub>CH<sub>2</sub>CH<sub>2</sub>).

#### Representative procedure for preparation of diblock copolymers

An oven-dried 25 mL Schlenk flask equipped with a stir bar was charged with catalyst **1b** (0.0187 mmol, 1 equiv.) and toluene (8.0 mL) and stirred at rt for 5 min. To the mixture, monomers δ-VL (348 μL, 3.75 mmol, 200 equiv.) was added. The reaction mixture was stirred at room temperature in the glove box for 40 min. After the complete consumption of δ-VL, as monitored by <sup>1</sup>H NMR spectroscopy, ε-CL (416 μL, 3.75 mmol, 200 equiv.) was added. The reaction mixture was stirred at rt for 40 min in the glove box (until the complete consumption of ε-CL). All the addition took place in the glovebox. The reaction was monitored by <sup>1</sup>H NMR spectroscopy until the complete conversion of δ-VL (>96%). After removing the solvent in a vacuum, the residue was dissolved in DCM (1–3

mL), followed by the addition of hexane (4–5 mL). The precipitation of the polymeric products was facilitated by immersing the flask in liquid nitrogen. The supernatant was decanted, and the residues were washed and dried under a vacuum. The same steps were followed to synthesize block polymers of PBL-*b*-PVL (72 h) and PBL-*b*-PCL (72 h).

**Cyclic PVL-*b*-PCL**, Yield: 96%,  $^1\text{H}$  NMR ( $\text{CDCl}_3$ , 298K):  $\delta$  4.07 (m,  $\text{CH}_2\text{CH}_2\text{O}$ , 2H), (m,  $\text{CH}_2\text{CH}_2\text{O}$ , 2H), 2.32 (m,  $\text{CH}_2\text{CH}_2\text{C}=\text{O}$ , 2H), (m,  $\text{CH}_2\text{CH}_2\text{C}=\text{O}$ , 2H), 1.66 (m,  $\text{CH}_2(\text{CH}_2)_2\text{CH}_2$ , 4H), (m,  $\text{CH}_2\text{CH}_2\text{CH}_2\text{CH}_2$ , 4H), 1.38 (m,  $\text{CH}_2\text{CH}_2\text{CH}_2$ , 2H).  $^{13}\text{C}$  NMR ( $\text{CDCl}_3$ , 298K):  $\delta$  173.50 ( $\text{C}=\text{O}$ ), 64.13 ( $\text{CH}_2\text{CH}_2\text{O}$ ), 33.89 ( $\text{CH}_2\text{CH}_2\text{C}=\text{O}$ ), 28.27 ( $\text{CH}_2\text{CH}_2\text{CH}_2\text{O}$ ), 21.61 ( $\text{CH}_2\text{CH}_2\text{C}=\text{O}$ ), 173.77 ( $\text{C}=\text{O}$ ), 64.35 ( $\text{CH}_2\text{CH}_2\text{O}$ ), 34.32 ( $\text{CH}_2\text{CH}_2\text{C}=\text{O}$ ), 28.54 ( $\text{CH}_2\text{CH}_2\text{CH}_2\text{O}$ ), 25.72 ( $\text{CH}_2\text{CH}_2\text{C}=\text{O}$ ), 24.77 ( $\text{CH}_2\text{CH}_2\text{CH}_2$ ).

**Cyclic PBL-*b*-PVL**, Yield: 96%,  $^1\text{H}$  NMR ( $\text{CDCl}_3$ , 298K):  $\delta$  5.24 (m,  $\text{CH}_3\text{CHCH}_2$ , 1H), 2.60 (m,  $\text{CH}_3\text{CHCH}_2$ , 1H), 2.47 (m,  $\text{CH}_3\text{CHCH}_2$ , 1H), 1.26 (t,  $\text{CH}_3\text{CHCH}_2$ , 3H), 4.07 (m,  $\text{CH}_2\text{CH}_2\text{O}$ , 2H), 2.33 (m,  $\text{CH}_2\text{CH}_2\text{C}=\text{O}$ , 2H), 1.67 (m,  $\text{CH}_2(\text{CH}_2)_2\text{CH}_2$ , 4H).  $^{13}\text{C}$  NMR ( $\text{CDCl}_3$ , 298K): 173.44 ( $\text{C}=\text{O}$ ), 173.38 ( $\text{C}=\text{O}$ ), 172.52 ( $\text{C}=\text{O}$ ), 170.37 ( $\text{C}=\text{O}$ ), 170.25 ( $\text{C}=\text{O}$ ), 169.52 ( $\text{C}=\text{O}$ ), 169.40 ( $\text{C}=\text{O}$ ), 169.29 ( $\text{C}=\text{O}$ ), 67.76 ( $\text{CH}_3\text{CHCH}_2$ ), 40.90 ( $\text{CH}_3\text{CHCH}_2$ ), 40.77 ( $\text{CH}_3\text{CHCH}_2$ ), 20.01 ( $\text{CH}_3\text{CHCH}_2$ ), 173.44 ( $\text{C}=\text{O}$ ), 173.38 ( $\text{C}=\text{O}$ ), 172.52 ( $\text{C}=\text{O}$ ), 64.35 ( $\text{CH}_2\text{CH}_2\text{O}$ ), 33.97 ( $\text{CH}_2\text{CH}_2\text{C}=\text{O}$ ), 28.20 ( $\text{CH}_2\text{CH}_2\text{CH}_2\text{O}$ ), 21.55 ( $\text{CH}_2\text{CH}_2\text{C}=\text{O}$ ).

**Cyclic PBL-*b*-PCL**, Yield: 96%,  $^1\text{H}$  NMR ( $\text{CDCl}_3$ , 298K):  $\delta$  5.27 (m,  $\text{CH}_3\text{CHCH}_2$ , 1H), 2.62 (m,  $\text{CH}_3\text{CHCH}_2$ , 1H), 2.48 (m,  $\text{CH}_3\text{CHCH}_2$ , 1H), 1.28 (t,  $\text{CH}_3\text{CHCH}_2$ , 3H), 4.06

(m, CH<sub>2</sub>CH<sub>2</sub>O, 2H), 2.31 (m, CH<sub>2</sub>CH<sub>2</sub>C=O, 2H), 1.65 (m, CH<sub>2</sub>CH<sub>2</sub>CH<sub>2</sub>CH<sub>2</sub>, 4H), 1.39 (m, CH<sub>2</sub>CH<sub>2</sub>CH<sub>2</sub>, 2H). <sup>13</sup>C NMR (CDCl<sub>3</sub>, 298K): 169.41 (C=O), 169.301 (C=O), 67.87 (CH<sub>3</sub>CHCH<sub>2</sub>), 41.00 (CH<sub>3</sub>CHCH<sub>2</sub>), 40.83 (CH<sub>3</sub>CHCH<sub>2</sub>), 20.01 (CH<sub>3</sub>CHCH<sub>2</sub>), 173.44 (C=O), 64.35 (CH<sub>2</sub>CH<sub>2</sub>O), 34.32 (CH<sub>2</sub>CH<sub>2</sub>C=O), 28.54 (CH<sub>2</sub>CH<sub>2</sub>CH<sub>2</sub>O), 25.72 (CH<sub>2</sub>CH<sub>2</sub>C=O), 24.77 (CH<sub>2</sub>CH<sub>2</sub>CH<sub>2</sub>).

#### IV.5 REFERENCES

- 
1. Arrighi, V.; Higgins, J. S. Local Effects of Ring Topology Observed in Polymer Conformation and Dynamics by Neutron Scattering-A Review. *Polymers (Basel)* **2020**, *12* (9), 1884. <https://doi.org/10.3390/POLYM12091884>.
  2. Romio, M.; Trachsel, L.; Morgese, G.; Ramakrishna, S. N.; Spencer, N. D.; Benetti, E. M. Topological Polymer Chemistry Enters Materials Science: Expanding the Applicability of Cyclic Polymers. *ACS Macro Lett.* **2020**, *9* (7), 1024–1033. <https://doi.org/10.1021/acsmacrolett.0c00358>.
  3. Cuneo, T.; Gao, H. Recent Advances on Synthesis and Biomaterials Applications of Hyperbranched Polymers. *Wiley Interdiscip. Rev.: Nanomed. Nanobiotechnol.* **2020**, *12*, No. e1640. <https://doi.org/10.1002/wnan.1640>.
  4. Li, H.; Sun, J.; Zhu, H.; Wu, H.; Zhang, H.; Gu, Z.; Luo, K. Recent Advances in Development of Dendriticpolymer-Based Nanomedicines for Cancer Diagnosis. *Wiley Interdiscip. Rev.: Nanomed. Nanobiotechnol.* **2020**, *13*, No. e1670.

---

<https://doi.org/10.1002/wnan.1670>.

5. Cook, A. B.; Perrier, S. Branched and Dendritic Polymer Architectures: Functional Nanomaterials for Therapeutic Delivery. *Adv. Funct. Mater.* **2020**, *30* (2), 1–24.

<https://doi.org/10.1002/adfm.201901001>.

6. Sims, M. B. Controlled Radical Copolymerization of Multivinyl Crosslinkers: A Robust Route to Functional Branched Macromolecules. *Polym. Int.* **2020**, *70*, 14–23.

<https://doi.org/10.1002/pi.6084>.

7. Semlyen, J. A. Cyclic Polymers. *Pure Appl. Chem.* **1981**, *53* (9), 1797–1804. <https://doi.org/10.1351/pac198153091797>.

8. Haque, F. M.; Grayson, S. M. The Synthesis, Properties and Potential Applications of Cyclic Polymers. *Nat. Chem.* **2020**, *12* (5), 433–444. <https://doi.org/10.1038/s41557-020-0440-5>.

9. Tezuka, Y. Cyclic and Topological Polymers: Ongoing Innovations and Upcoming Breakthroughs. *React. Funct. Polym.* **2020**, *148* (January), 104489.

<https://doi.org/10.1016/j.reactfunctpolym.2020.104489>.

10. Hoskins, J. N.; Grayson, S. M. Cyclic Polyesters: Synthetic Approaches and Potential Applications. *Polym. Chem.* **2011**, *2* (2), 289–299. <https://doi.org/10.1039/c0py00102c>.

11. Grayson, S. M.; Getzler, Y.; Zhang, D. Special Issue ‘Cyclic Polymers: New Developments’. *React. Funct. Polym.* **2014**, *80*, 1–108.

- 
12. Jia, Z.; Monteiro, M. J. Synthesis of cyclic polymers via ring closure. In: Percec V, editor. *Hierarchical Macromolecular Structures: 60 Years after the Staudinger Nobel Prize II*. Cham: Springer International Publishing; 2013. p. 295–327.
13. Deffieux A, Schappacher M. 6.02 - Synthesis and properties of macrocyclic polymers. In: Matyjaszewski K, Möller M, editors. *Polymer Science: A Comprehensive Reference*. Amsterdam: Elsevier; 2012. p. 5–28.
14. Tezuka, Y. Topological Polymer Chemistry: Concepts and Practices. *Springer Singapore XI*; **2022**. p. 436
15. Tu, X. Y.; Liu, M. Z.; Wei, H. Recent Progress on Cyclic Polymers: Synthesis, Bioproperties, and Biomedical Applications. *J. Polym. Sci. Part A Polym. Chem.* **2016**, *54* (11), 1447–1458. <https://doi.org/10.1002/pola.28051>.
16. Zhu, Y.; Hosmane, N. S. Advanced Developments in Cyclic Polymers: Synthesis, Applications, and Perspectives. *ChemistryOpen* **2015**, *4* (4), 408–417. <https://doi.org/10.1002/open.201402172>.
17. Liénard, R.; De Winter, J.; Coulembier, O. Cyclic Polymers: Advances in Their Synthesis, Properties, and Biomedical Applications. *J. Polym. Sci.* **2020**, *58* (11), 1481–1502. <https://doi.org/10.1002/pol.20200236>.
18. Golba, B.; Benetti, E. M.; De Geest, B. G. Biomaterials Applications of Cyclic Polymers. *Biomaterials* **2021**, *267*, 120468.

---

<https://doi.org/10.1016/j.biomaterials.2020.120468>.

19. Laurent, B. A.; Grayson S. M. Synthetic approaches for the preparation of cyclic polymers. *Chem. Soc. Rev.* **2009**, 38, 2202–2213.
20. Chen, C.; Weil, T. Cyclic polymers: synthesis, characteristics, and emerging applications. *Nanoscale Horiz.* **2022**, 7, 1121–1135. DOI: 10.1039/d2nh00242f
21. Carlo, O. J.; Fabienne, P. A.; Bujans, B. Macrocyclic polymers: Synthesis, purification, properties and applications. *Prog. Polym. Sci.* **2022**, 134 (2022) 101606
22. Curole, B.J., Miles, A.V., Grayson, S.M. (2022). Recent Progress on the Synthesis of Cyclic Polymers. In: Tezuka, Y., Deguchi, T. (eds) Topological Polymer Chemistry. Springer, Singapore. [https://doi.org/10.1007/978-981-16-6807-4\\_14](https://doi.org/10.1007/978-981-16-6807-4_14)
23. Tang, Q., Zhang, K. (2022). Recent Progress on the Synthesis of Cyclic Polymers via Ring-Closure Methods. In: Tezuka, Y., Deguchi, T. (eds) Topological Polymer Chemistry. Springer, Singapore. [https://doi.org/10.1007/978-981-16-6807-4\\_15](https://doi.org/10.1007/978-981-16-6807-4_15)
- <sup>24</sup> Edwards, J. P.; Wolf, W. J.; Grubbs, R. H. The synthesis of cyclic polymers by olefin metathesis: achievements and challenges. *J. Polym. Sci. A: Polym. Chem.* **2019**, 57, 228–242.
25. Chisholm, M. H.; Gallucci, J. C.; Yin, H. Cyclic Esters and Cyclodepsipeptides Derived from Lactide and 2,5-Morpholinediones. *Proc. Natl. Acad. Sci. U. S. A.* **2006**, 103 (42), 15315–15320. <https://doi.org/10.1073/pnas.0602662103>.

- 
26. Tezuka, Y.; Mori, K. & Oike, H. Efficient synthesis of cyclic poly(oxyethylene) by electrostatic self-assembly and covalent fixation with telechelic precursor having cyclic ammonium salt groups. *Macromolecules* **2002**, *35*, 5707–5711.
27. Jia, Z.; Monteiro, M. J. Cyclic polymers: methods and strategies. *J. Polym. Sci. A: Polym. Chem.* **2012**, *50*, 2085–2097.
28. Yang, P. B.; Davidson, M. G.; Edler, K.J.; Brown, S. Synthesis, properties, and applications of bio-based cyclic aliphatic polyesters. *Biomacromolecules*. **2021**, *22*, 3649–3667.
29. Josse, T.; Winter, J. D.; Gerbaux, P.; Coulembier, O. Cyclic Polymers by Ring-Closure Strategies. *Angew. Chem. Int. Eng.* **2016**, *55*, 13944–13958
30. Bielawski, C. W.; Benitez, D.; Grubbs, R. H. An “Endless” Route to Cyclic Polymers. *Science* **2002**, *297*, 2041–2044. <https://doi.org/10.1126/science.1075401>.
31. Xia, Y.; Boydston, A. J.; Yao, Y.; Kornfield, J. A.; Gorodetskaya, I. A.; Spiess, H. W.; Grubbs, R. H. Ring-Expansion Metathesis Polymerization: Catalyst-Dependent Polymerization Profiles. *J. Am. Chem. Soc.* **2009**, *131* (7), 2670–2677. <https://doi.org/10.1021/ja808296a>.
32. Boydston, A. J.; Holcombe, T. W.; Unruh, D. A.; Fréchet, J. M. J.; Grubbs, R. H. A Direct Route to Cyclic Organic Nanostructures via Ring-Expansion Metathesis Polymerization of a Dendronized Macromonomer. *J. Am. Chem. Soc.* **2009**, *131* (15),



---

5388–5389. <https://doi.org/10.1021/ja901658c>.

33. Boydston, A. J.; Xia, Y.; Kornfield, J. A.; Gorodetskaya, I. A.; Grubbs, R. H. Cyclic Ruthenium-Alkylidene Catalysts for Ring-Expansion Metathesis Polymerization. *J. Am. Chem. Soc.* **2008**, *130* (38), 12775–12782. <https://doi.org/10.1021/ja8037849>.

34. Wang, T. W.; Golder, M. R. Advancing macromolecular hoop construction: recent developments in synthetic cyclic polymer chemistry. *Polym. Chem.* **2021**, *12*, 958–969.

35. Chang, Y. A.; Waymouth R. M. Recent progress on the synthesis of cyclic polymers via ring-expansion strategies. *J. Polym. Sci. A: Polym. Chem.* **2017**, *55*, 2892–2902.

36. Ouchi, M.; Kammiyada, H.; Sawamoto, M. Ring-expansion cationic polymerization of vinyl ethers. *Polym. Chem.* **2017**, *8*, 4970–4977.

37. Brown, H. A.; Chang, Y. A.; Waymouth, R. M. Zwitterionic Polymerization to Generate High Molecular Weight Cyclic Poly(Carbosiloxane)s. *J. Am. Chem. Soc.* **2013**, *135*, 18738–18741. <https://doi.org/10.1021/ja409843v>.

38. Yang, R.; Xu, G.; Lv, C.; Dong, B.; Zhou, L.; Wang, Q. Zn(HMDS)<sub>2</sub> as a Versatile Transesterification Catalyst for Polyesters Synthesis and Degradation toward a Circular Materials Economy Approach. *ACS Sustain. Chem. Eng.* **2020**, *50*, 18347–18353 <https://doi.org/10.1021/acssuschemeng.0c07595>.

39. Wang, Y.; Xu, T. Q. Topology-Controlled Ring-Opening Polymerization of O-carboxyanhydride. *Macromolecules* **2020**, *20*, 8829–8836.

---

<https://doi.org/10.1021/acs.macromol.0c01541>.

40. Shaik, M.; Peterson, J.; Du, G. Cyclic and Linear Polyhydroxylbutyrates from Ring-Opening Polymerization of  $\beta$ -Butyrolactone with Amido-Oxazolate Zinc Catalysts. *Macromolecules* **2019**, 52 (1), 157–166. <https://doi.org/10.1021/acs.macromol.8b02096>.
41. Gruszka, W.; Walker, L. C.; Shaver, M. P.; Garden, J. A. In Situ Versus Isolated Zinc Catalysts in the Selective Synthesis of Homo and Multi-Block Polyesters. *Macromolecules* **2020**, 53 (11), 4294–4302. <https://doi.org/10.1021/acs.macromol.0c00277>.
42. Ungpittagul, T.; Wongmahasirikun, P.; Phomphrai, K. Synthesis and Characterization of Guanidinate Tin (II) Complexes for Ring-Opening Polymerization of Cyclic Esters. *Dalt. Trans.* **2020**, 49 (25), 8460–8471. <https://doi.org/10.1039/d0dt01115k>.
43. Stukenbroeker, T. S.; Solis-Ibarra, D.; Waymouth, R. M. Synthesis and Topological Trapping of Cyclic Poly(alkylene phosphates). *Macromolecules*. **2014**, 47, 8224–8230. <https://doi.org/10.1021/ma501764c>
44. Guo, L.; Lahasky, S. H.; Ghale, K.; Zhang, D. N-Heterocyclic Carbene-Mediated Zwitterionic Polymerization of N-Substituted N-Carboxyanhydrides toward Poly( $\alpha$ -peptoid)s: Kinetic, Mechanism, and Architectural Control. *J. Am. Chem. Soc.* **2012**, 134, 9163–9171. <https://doi.org/10.1021/ja210842b>
45. Shi, C. X.; Guo, Y. T.; Wu, Y. H.; Li, Z. Y.; Wang, Y. Z.; Du, F. S.; Li, Z. C. Synthesis and Controlled Organobase-Catalyzed Ring-Opening Polymerization of Morpholine-2,5-

---

Dione Derivatives and Monomer Recovery by Acid-Catalyzed Degradation of the Polymers. *Macromolecules* **2019**, *52*, 4260–4269.

<https://doi.org/10.1021/acs.macromol.8b02498>.

46. Saxon, D. J.; Nasiri, M.; Mandal, M.; Maduskar, S.; Dauenhauer, P. J.; Cramer, C. J.; Lapointe, A. M.; Reineke, T. M. Architectural Control of Isosorbide-Based Polyethers via Ring-Opening Polymerization. *J. Am. Chem. Soc.* **2019**, *141*, 5107–5111. <https://doi.org/10.1021/jacs.9b00083>.

47. Zhang, X.; Waymouth, R. M. Zwitterionic Ring Opening Polymerization with Isothioureas. *ACS Macro Lett.* **2014**, *3* (10), 1024–1028. <https://doi.org/10.1021/mz500525n>.

48. Jeong, W.; Shin, E. J.; Culkin, D. A.; Hedrick, J. L.; Waymouth, R. M. Zwitterionic Polymerization: A Kinetic Strategy for the Controlled Synthesis of Cyclic Polylactide. *J. Am. Chem. Soc.* **2009**, *131* (13), 4884–4891. <https://doi.org/10.1021/ja809617v>.

49. Ali, E. A. 'N-Heterocyclic Carbenes: A Powerful Catalyst for Polymerization', in S. Saha, A. Manna (eds.), *Carbene*, **2022**, IntechOpen, London. doi: 10.5772/intechopen.102466.

50. Shin, E. J.; Jeong, W.; Brown, H. A.; Koo, B. J.; Hedrick, J. L.; Waymouth, R. M. Crystallization of Cyclic Polymers: Synthesis and Crystallization Behavior of High Molecular Weight Cyclic Poly( $\epsilon$ -Caprolactone)S. *Macromolecules* **2011**, *44* (8), 2773–

---

2779. <https://doi.org/10.1021/ma102970m>.

51. Brown, H. A.; Waymouth R. M. Zwitterionic ring-opening polymerization for the synthesis of high molecular weight cyclic polymers. *Acc. Chem. Res.* **2013**, *46*, 2585–2596.

52. Binda, P. I.; Abbina, S.; Du, G. Modular Synthesis of Chiral  $\beta$ -Diketiminato-Type Ligands Containing 2-Oxazoline Moiety via Palladium-Catalyzed Amination. *Synthesis (Stuttg)*. **2011**, No. 16, 2609–2618. <https://doi.org/10.1055/s-0030-1260124>.

53. Abbina, S.; Du, G. Chiral Amido-Oxazolate Zinc Complexes for Asymmetric Alternating Copolymerization of CO<sub>2</sub> and Cyclohexene Oxide. *Organometallics* **2012**, *31* (21), 7394–7403. <https://doi.org/10.1021/om3006992>.

54. Abbina, S.; Chidara, V. K.; Du, G. Ring-Opening Copolymerization of Styrene Oxide and Cyclic Anhydrides by Using Highly Effective Zinc Amido–Oxazolate Catalysts. *ChemCatChem* **2017**, *9* (7), 1343–1348. <https://doi.org/10.1002/cctc.201601679>.

55. Abbina, S.; Chidara, V. K.; Bian, S.; Ugrinov, A.; Du, G. Synthesis of Chiral C<sub>2</sub>-Symmetric Bimetallic Zinc Complexes of Amido-Oxazolines and Their Application in Copolymerization of CO<sub>2</sub> and Cyclohexene Oxide. *ChemistrySelect* **2016**, *1* (12), 3175–3183. <https://doi.org/10.1002/slct.201600581>.

56. Shaik, M.; Chidara, V. K.; Abbina, S.; Du, G. Zinc Amido-Oxazolate Catalyzed Ring Opening Copolymerization and Terpolymerization of Maleic Anhydride and Epoxides. *Molecules* **2020**, *25* (18). <https://doi.org/10.3390/molecules25184044>.

- 
57. Abbina, S.; Du, G. Zinc-Catalyzed Highly Isoselective Ring Opening Polymerization of Rac-Lactide. *ACS Macro Lett.* **2014**, *3* (7), 689–692. <https://doi.org/10.1021/mz5002959>.
58. Lin, L.; Xu, Y.; Wang, S.; Xiao, M.; Meng, Y. Ring-opening polymerization of l-lactide and  $\epsilon$ -caprolactone catalyzed by versatile tri-zinc complex: Synthesis of biodegradable polyester with gradient sequence structure. *Eur. Polym. J.* **2016**, *74*, 109–119 DOI: <https://doi.org/10.1016/j.eurpolymj.2015.09.029>
59. Zhou, Y.; Gao, Z.; Hu, C.; Meng, S.; Duan, R.; Sun, Z.; Pang, X. Facile Synthesis of Gradient Polycarbonate–Polyester Terpolymers from Monomer Mixtures Mediated by an Asymmetric Chromium Complex. *Macromolecules* **2022**, *22*, 9951–9959 DOI: <https://doi.org/10.1021/acs.macromol.2c01680>.
60. Chen, Y.; Zhang, J.; Xiao, W.; Chen, A.; Dong, Z.; Xu, J.; Xu, W.; Lei, C. Reinvestigation of the ring-opening polymerization of  $\epsilon$ -caprolactone with 1,8-diazacyclo[5.4.0]undec-7-ene organocatalyst in bulk. *Eur. Polym. J.* **2021**, *161*, 110861. [doi.org/10.1016/j.eurpolymj.2021.110861](https://doi.org/10.1016/j.eurpolymj.2021.110861).
61. Zhu, L.; Li, J.; Li, H.; Liu, B.; Chen, J.; Jiang, S. The role of entanglement in crystallization and melting of cyclic poly( $\epsilon$ -caprolactone)s. *CrystEngComm* **2023**, *25*, 1383–1392. <https://doi.org/10.1039/D2CE01514E>
62. Heck, B.; Hugel, T.; Lijima, M.; Sadiku, E.; Strobl, G. Steps in the transition of an

---

entangled polymer melt to the partially crystalline state. *New J. Phys.* **1999**, *17*, 11–17.

63. Ishizu, K.; Ichimura, A. Synthesis of Cyclic Diblock Copolymers by Interfacial Condensation. *Polymer (Guildf)*. **1998**, *39* (25), 6555–6558. [https://doi.org/10.1016/S0032-3861\(98\)00037-8](https://doi.org/10.1016/S0032-3861(98)00037-8).

64. Feng, R.; Jie, S.; Braunstein, P.; Li, B. G. Gradient copolymers of  $\epsilon$ -caprolactone and  $\delta$ -valerolactone via solvent-free ring-opening copolymerization with a pyridyl-urea/MTBD system. *J Polym Sci*. **2020**, *58*, 2108–2115. <https://doi.org/10.1002/pol.20200174>

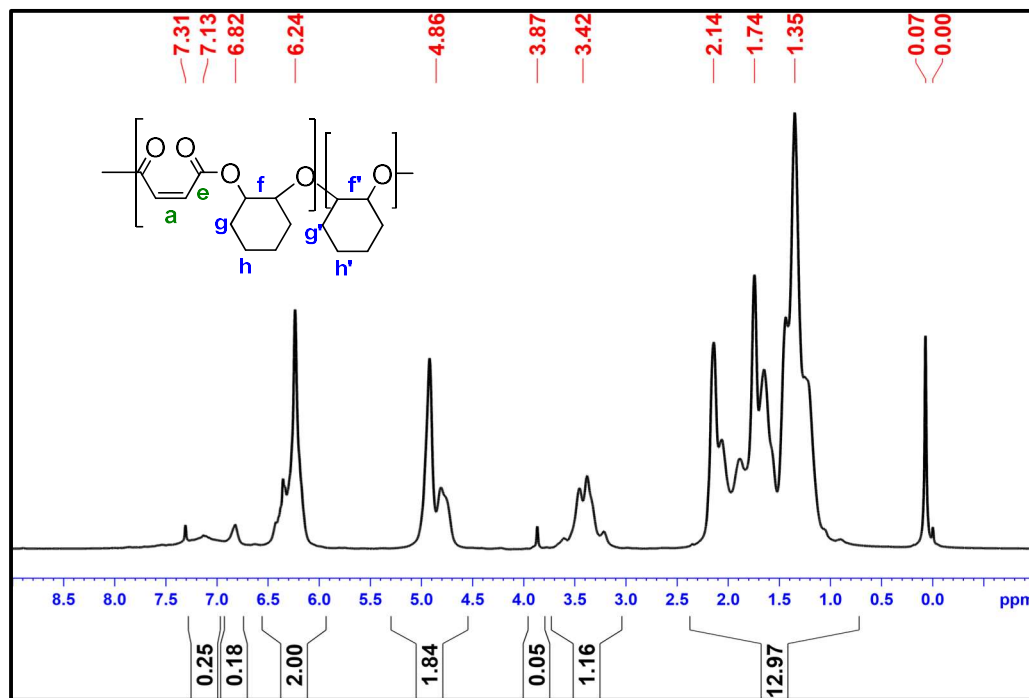
65. Abdur, M. R.; Mousavi, B.; Shahadat, H. M.; Akther, N.; Luo, Z.; Zhuiykov, S.; Verpoort, F. Ring-opening copolymerization of  $\epsilon$ -caprolactone and  $\delta$ -valerolactone by a titanium-based metal–organic framework. *New J. Chem.* **2021**, *45*, 11313–11316. <https://doi.org/10.1039/D1NJ01946E>.

66 Liu, M.; Wang, B.; Pan, L.; Liu, X. H.; Li, Y. S. Sequentially bridging anionic addition and ring-opening polymerization by cooperative organocatalysis: well-defined block copolymers from methacrylates and cyclic esters. *Polym. Chem.* **2022**, *13*, 3451–3459. <https://doi.org/10.1039/D2PY00339B>

67. Walther, P.; Naumann, S. *N*-Heterocyclic Olefin-Based (Co)polymerization of a Challenging Monomer: Homopolymerization of  $\omega$ -Pentadecalactone and Its Copolymers with  $\gamma$ -Butyrolactone,  $\delta$ -Valerolactone, and  $\epsilon$ -Caprolactone. *Macromolecules* **2017**, *50* (21), 8406–8416. DOI: 10.1021/acs.macromol.7b01678

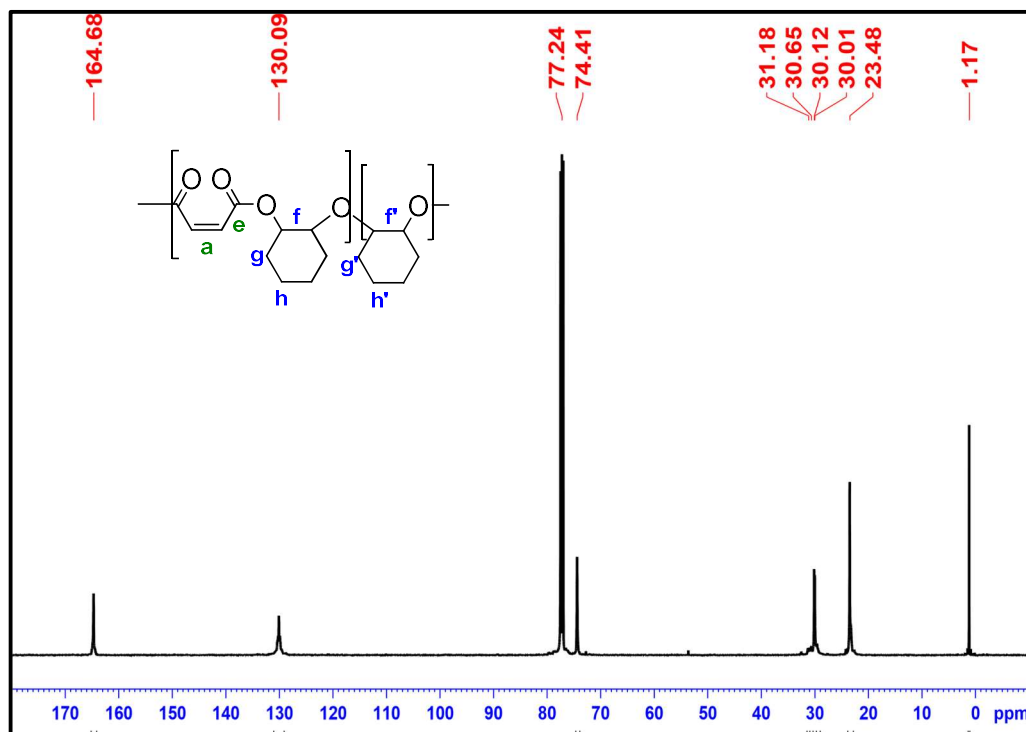
- 
68. Ge, Z.; Zhou, Y.; Xu, J.; Liu, H.; Chen, D.; Liu, S. High-Efficiency Preparation of Macrocyclic Diblock Copolymers via Selective Click Reaction in Micellar Media. *J. Am. Chem. Soc.* **2009**, *131* (5), 1628–1629. <https://doi.org/10.1021/ja808772z>.
- <sup>69</sup>69. Hoskins, N. J.; Grayson, M. S. Synthesis and Degradation Behavior of Cyclic Poly( $\epsilon$ -caprolactone). *Macromolecules* **2009**, *42*, 6406–6413. DOI: 10.1021/ma9011076.

# APPENDIX I

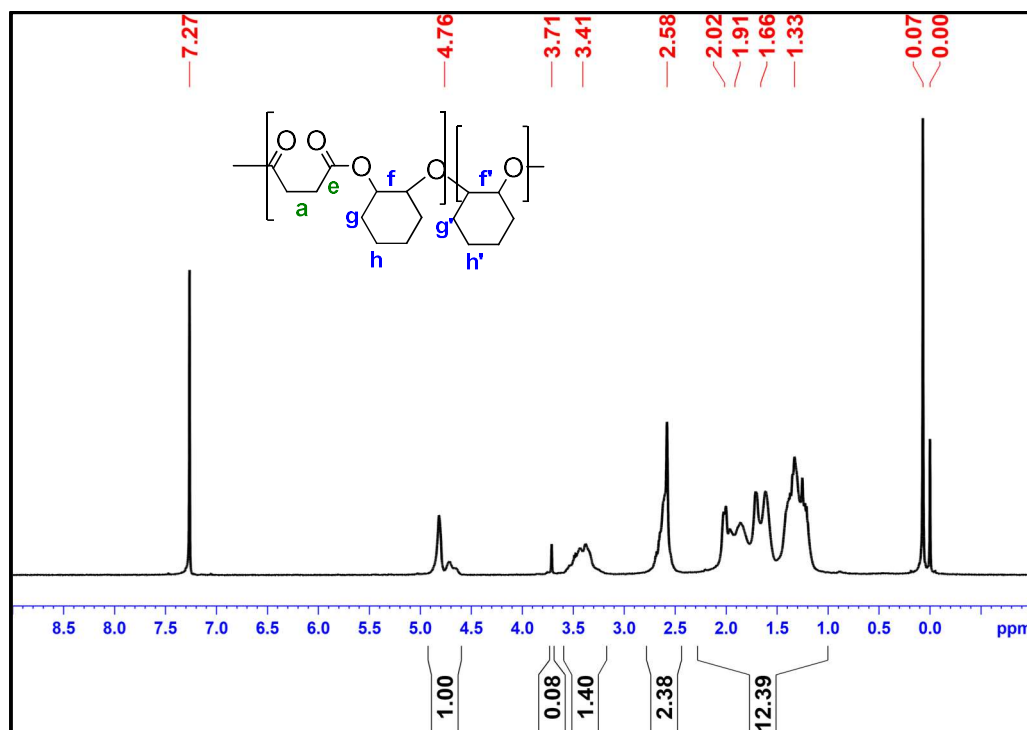


**Figure A.I-1.**  $^1\text{H}$  NMR of poly(CHO-MA) from ROCOP of CHO & MA with catalyst **1**

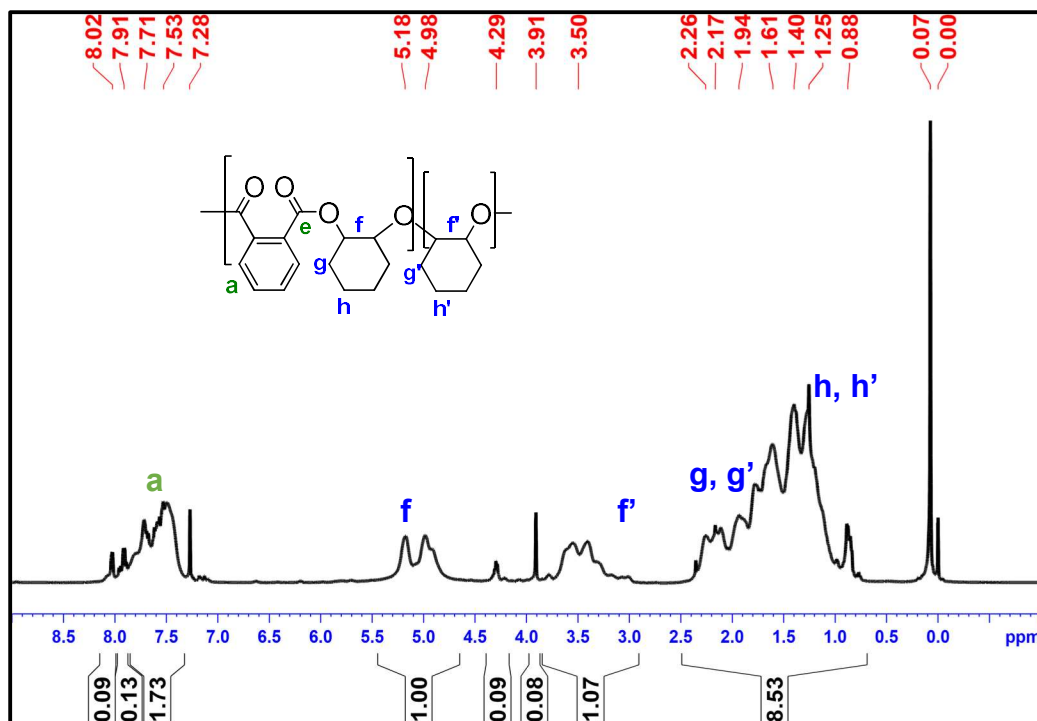




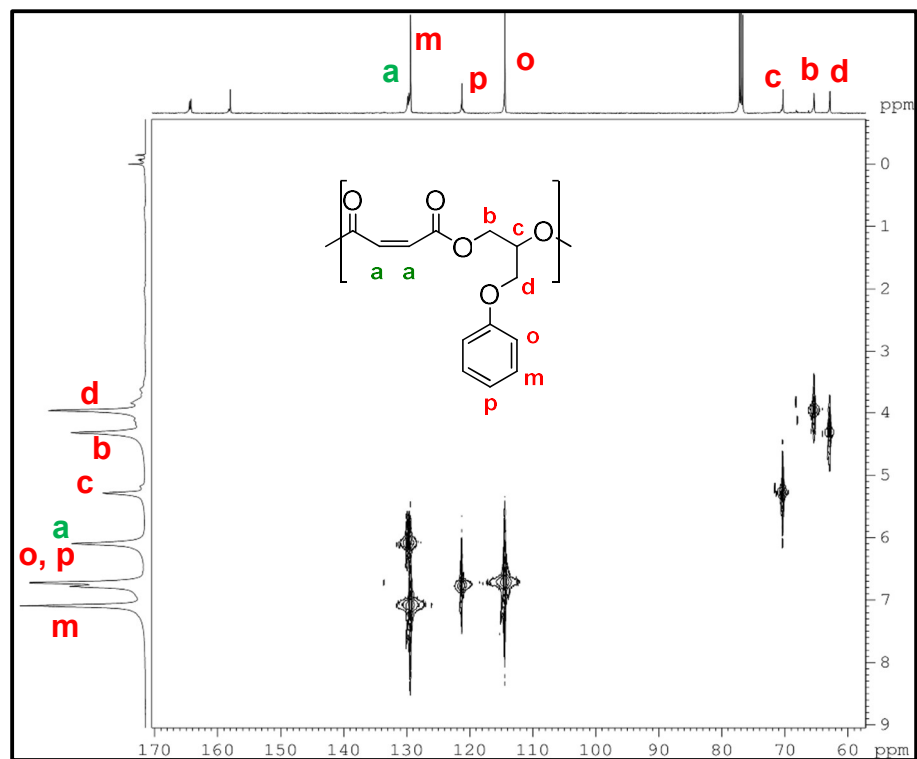
**Figure A.I-2.**  $^{13}\text{C}$  NMR of poly(CHO-MA) from ROCOP of CHO & MA with catalyst **1**



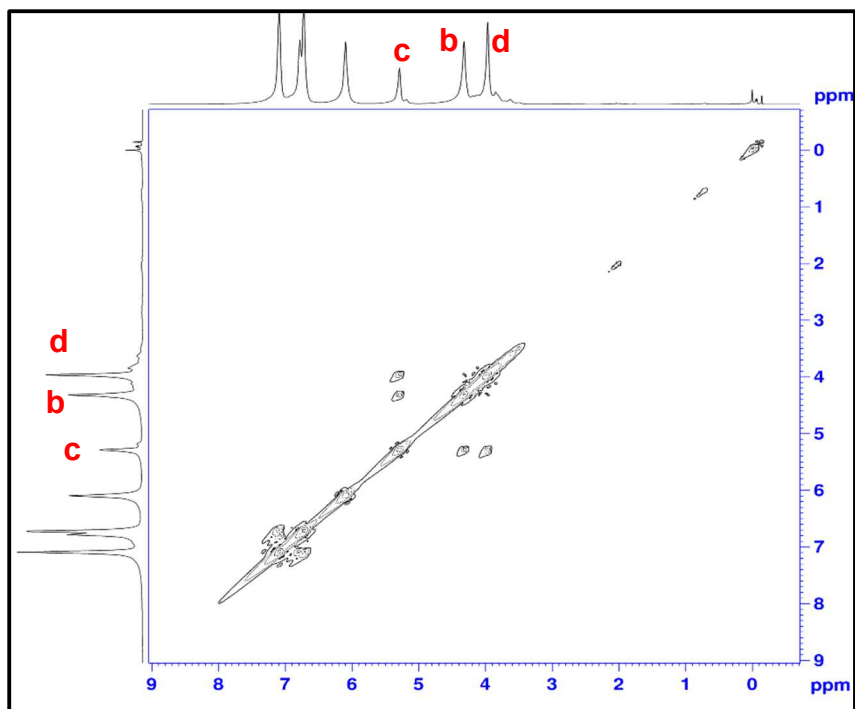
**Figure A.I-3.**  $^1\text{H}$  NMR of poly(CHO-SA) from ROCOP of CHO & SA with catalyst **1**



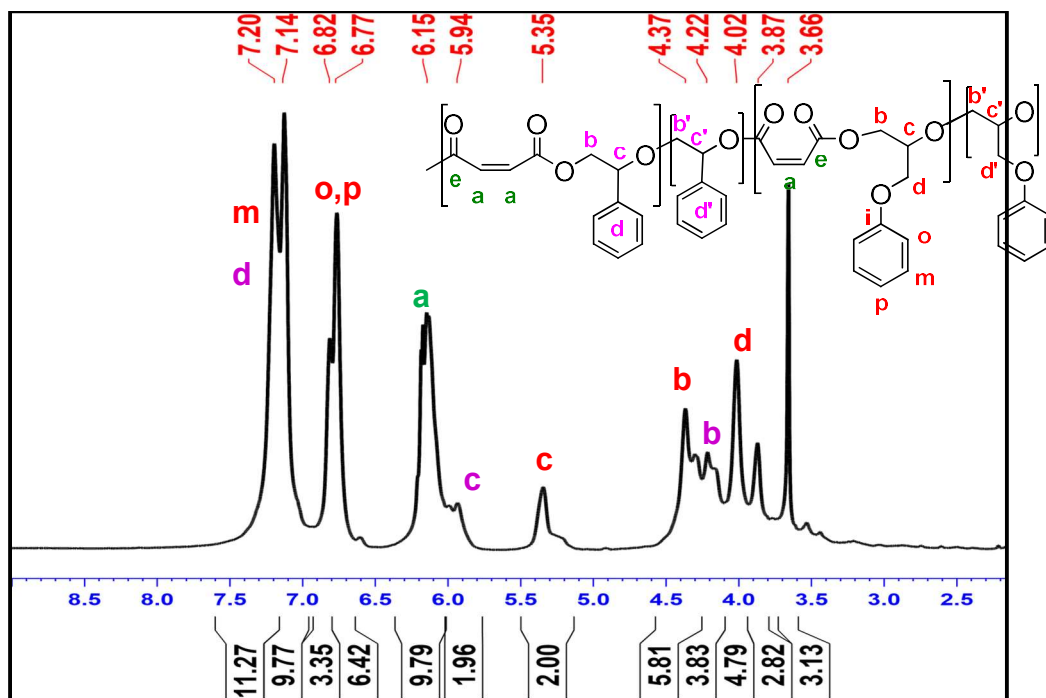
**Figure A.I-4.**  $^1\text{H}$  NMR of poly(CHO-PA) from ROCOP of CHO & PA with catalyst **1**



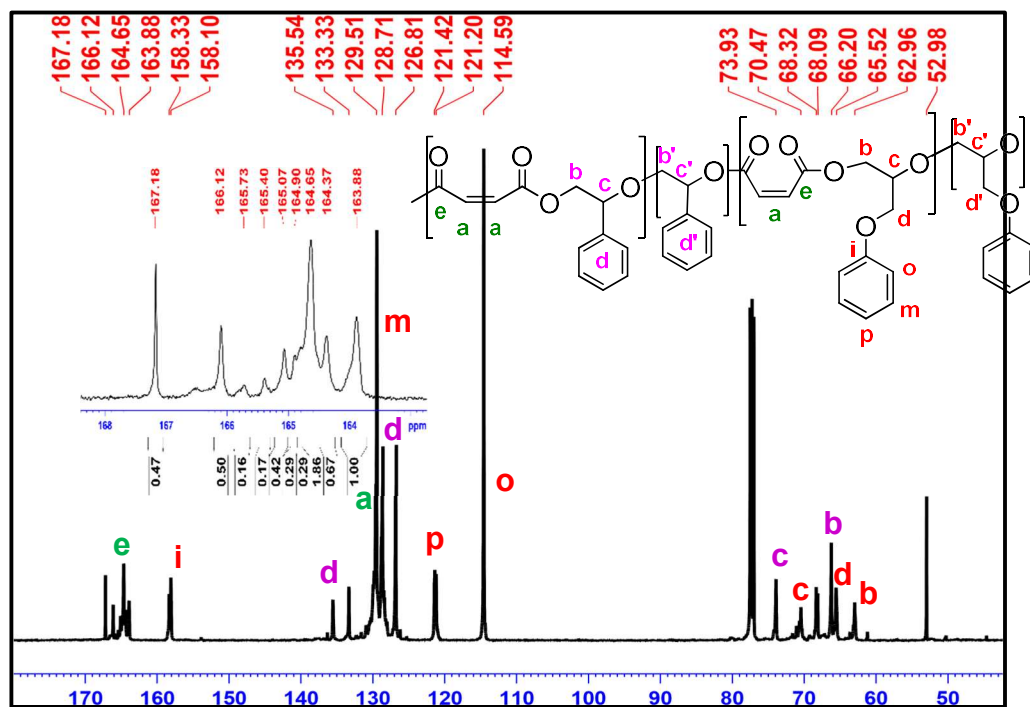
**Figure A.I-5.**  $^1\text{H}$ - $^{13}\text{C}$  HETCOR of poly(PGE-MA) from ROCOP of PGE, & MA with catalyst **1**



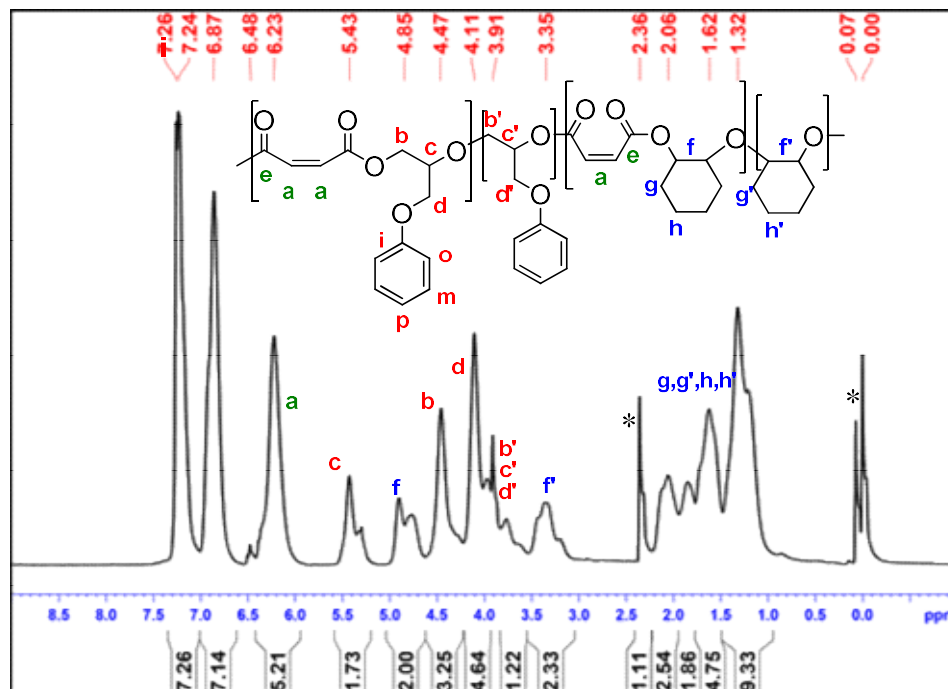
**Figure A.I-6.**  $^1\text{H}$ - $^1\text{H}$  COSY-NMR of poly(PGE-MA) from ROCOP of PGE, & MA with catalyst **1**



**Figure A.I-7.**  $^1\text{H}$  NMR of poly(PGE-SO-MA) from ROCOP of PGE, SO& MA with catalyst **1** Table 4, entry 6

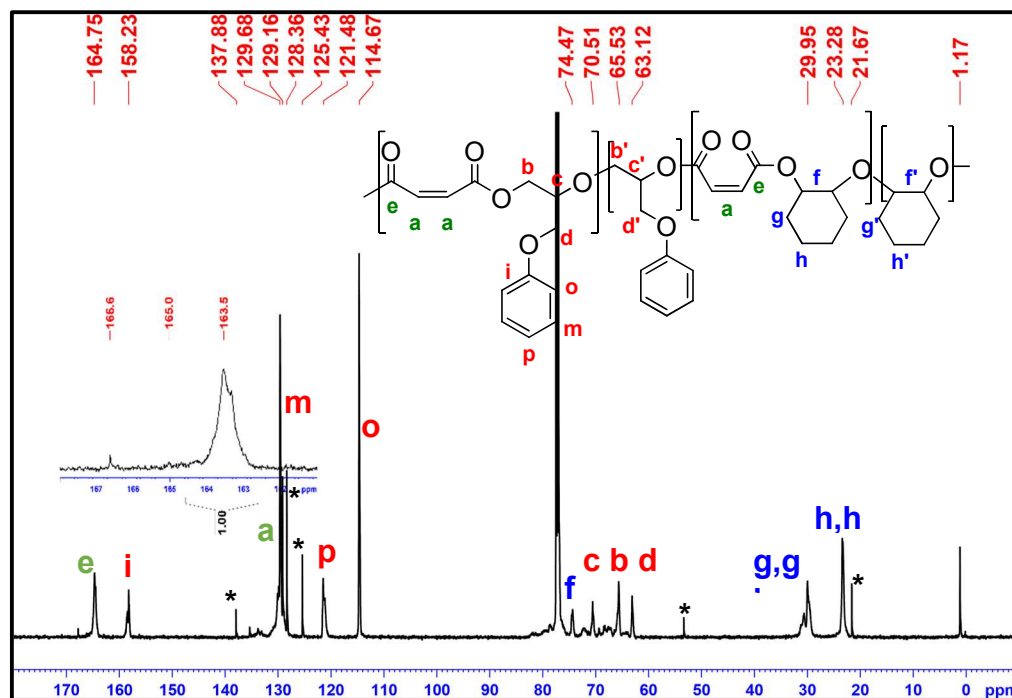


**Figure A.I-8.**  $^{13}\text{C}$  NMR of poly(PGE-SO-MA) from ROCOP of PGE, SO & MA with catalyst **1**

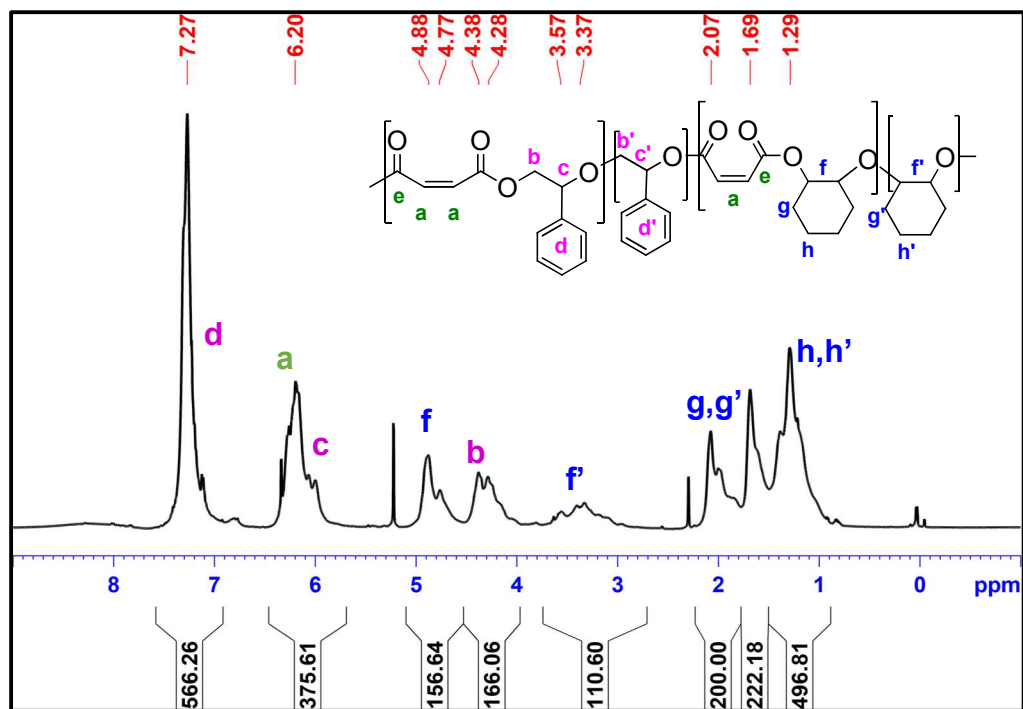


**Figure A.I-9.**  $^1\text{H}$  NMR of poly(PGE-CHO-MA) from ROCOP of PGE, CHO & MA with cat-1 Table 4, entry 4

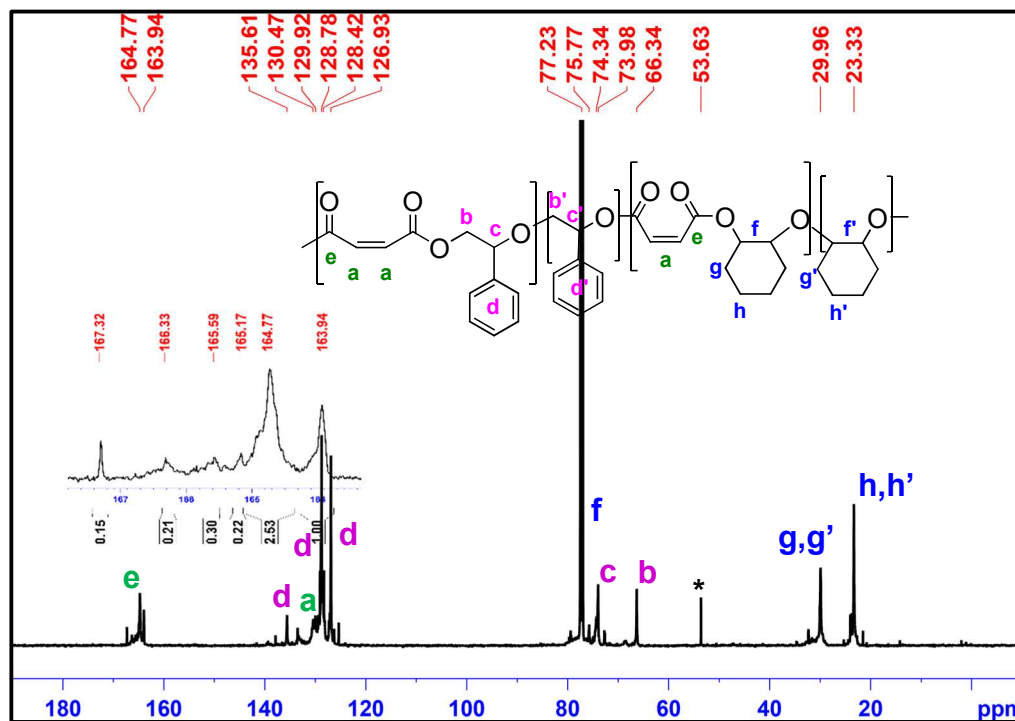




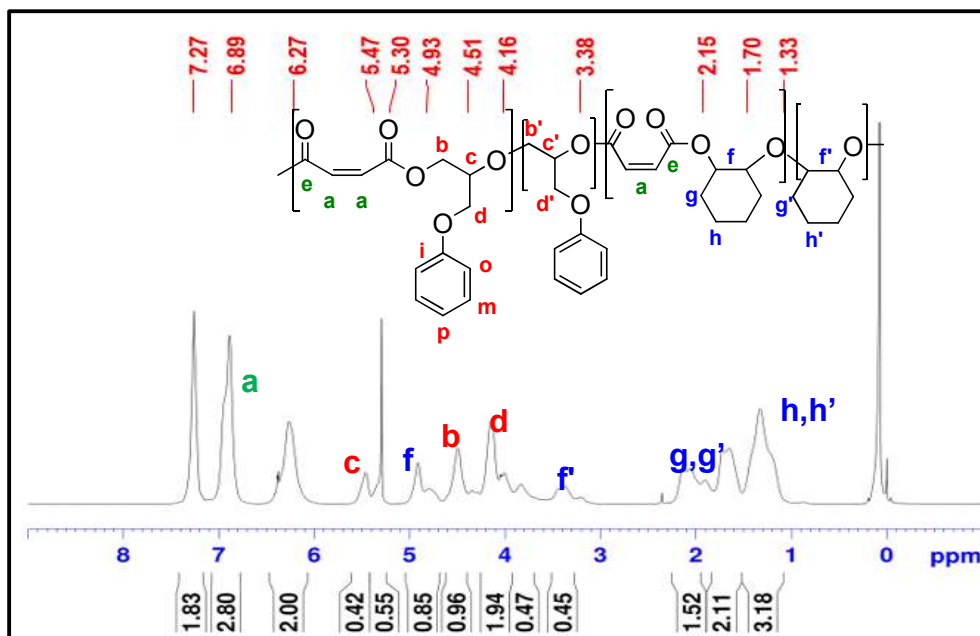
**Figure A.I-10.**  $^{13}\text{C}$  NMR of poly(PGE-CHO-MA) from ROCOP of PGE, CHO&MA with cat-1



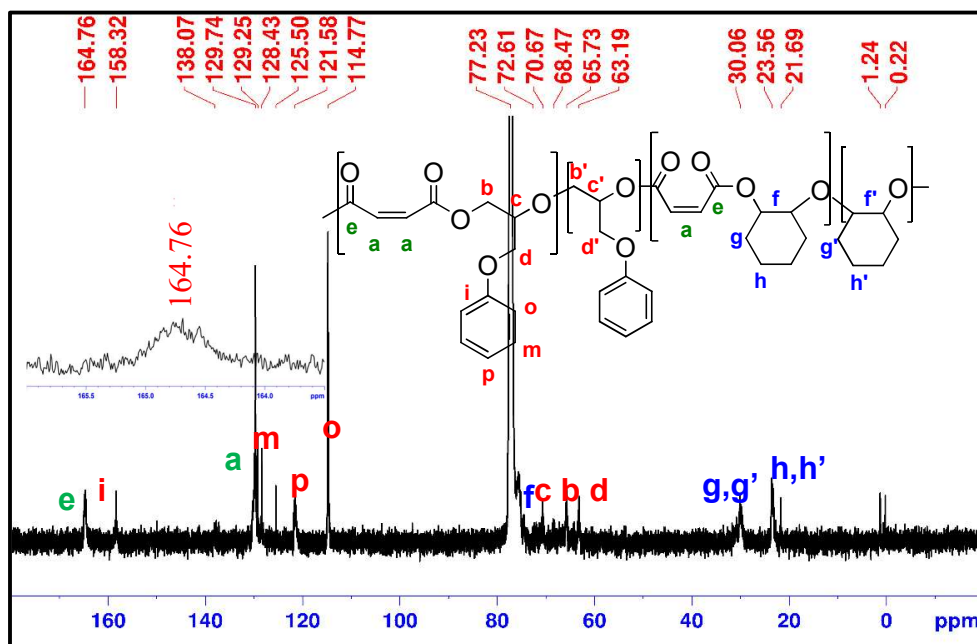
**Figure A.I-11.**  $^1\text{H}$  NMR of poly(SO-CHO-MA) from ROCOP of CHO, SO & MA with catalyst **1** (Table 4, entry 5)



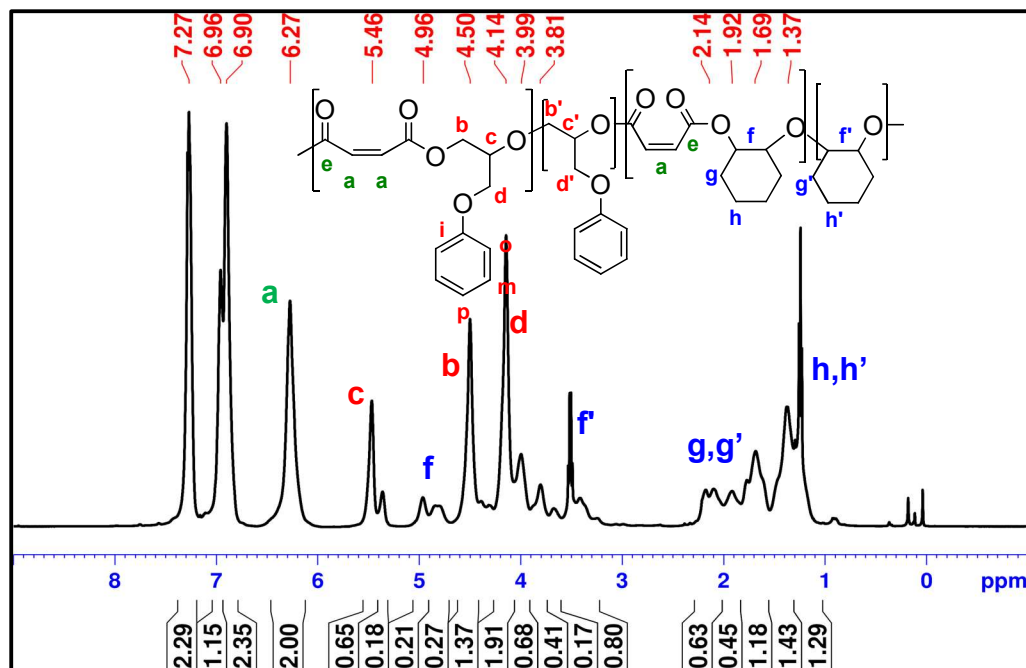
**Figure A.I-12.**  $^{13}\text{C}$  NMR of poly(SO-CHO-MA) from ROCOP of CHO, SO & MA with catalyst 1



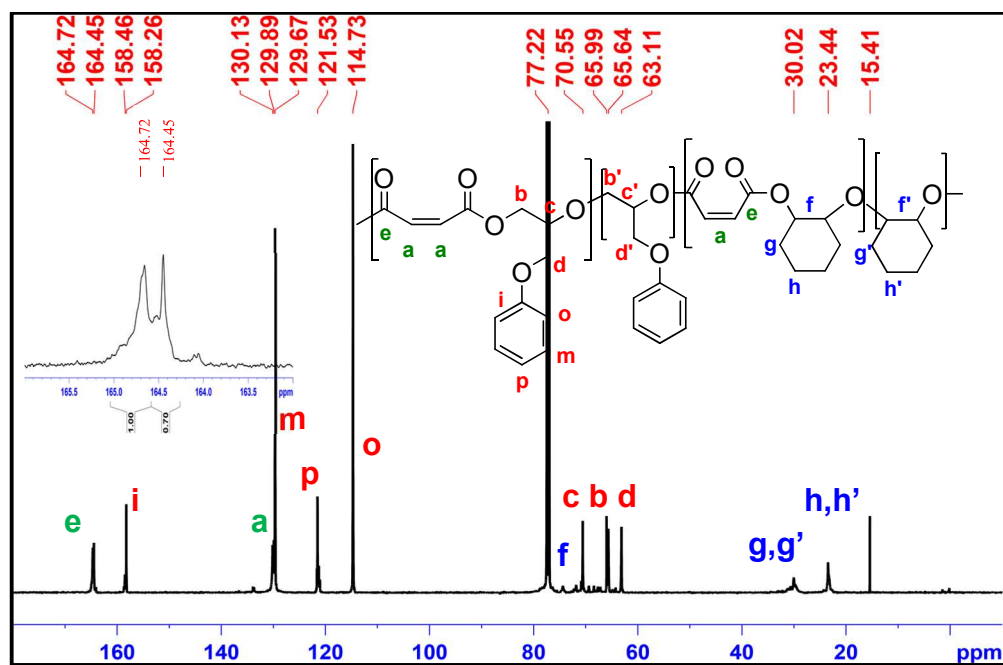
**Figure A.I-13.** <sup>1</sup>H NMR of poly(CHO-PGE-MA) from ROCOP of CHO, PGE & MA (Two step addition, Table 4, entry 1)



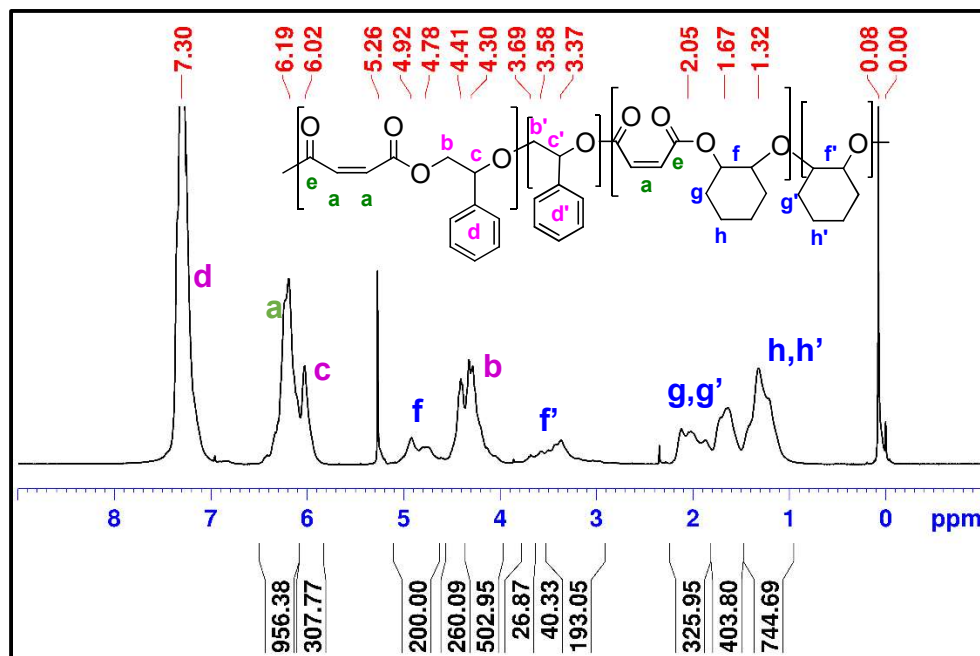
**Figure A.I-14.** <sup>13</sup>C NMR of poly(CHO-PGE-MA) from ROCOP of CHO, PGE & MA (Two step addition)



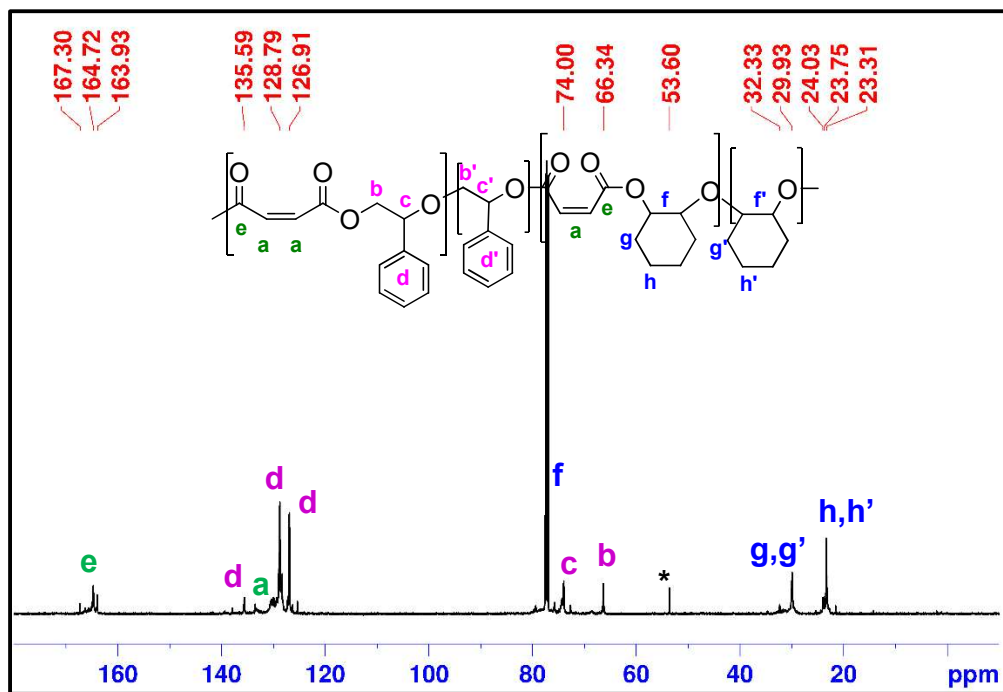
**Figure A.I-15.** <sup>1</sup>H NMR of poly(PGE-CHO-MA) from ROCOP of PGE, CHO & MA (Two step addition, Table 4, entry 2)



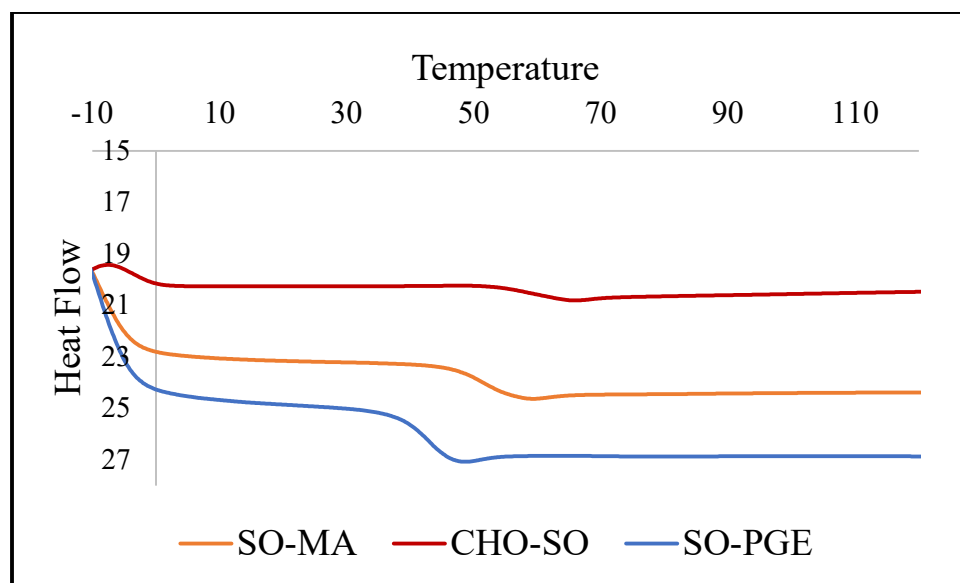
**Figure A.I-16.**  $^{13}\text{C}$  NMR of poly(PGE-CHO-MA) from ROCOP of PGE, CHO & MA (Two step addition, Table 4, entry 2)



**Figure A.I-17.**  $^1\text{H}$  NMR of poly(SO-CHO-MA) from ROCOP of CHO, SO & MA with catalyst **1** (Two step reaction Table 4, entry 3)

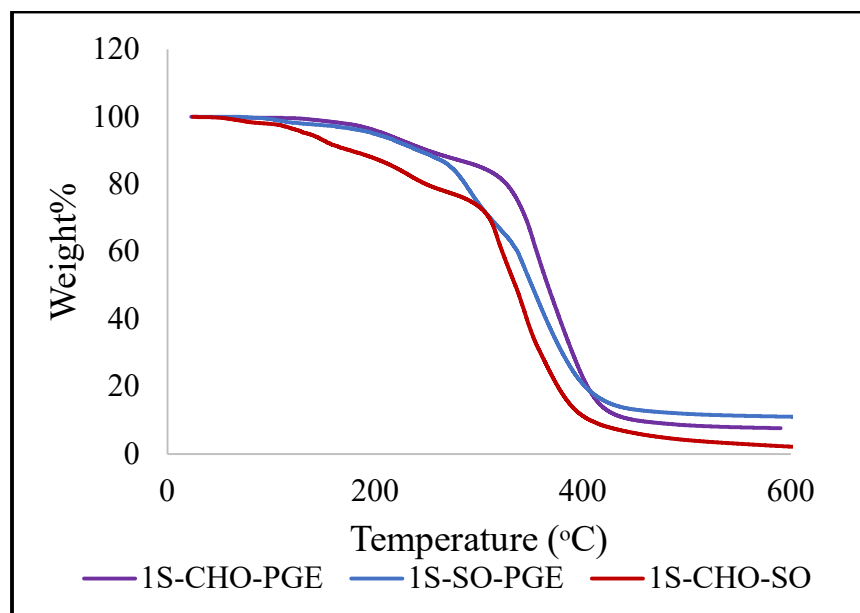
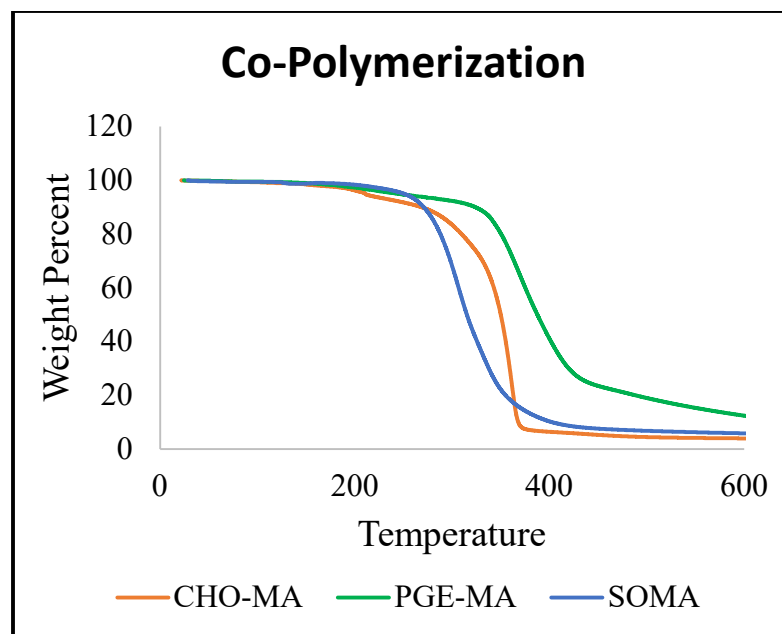


**Figure A.I-18.**  $^{13}\text{C}$  NMR of poly(SO-CHO-MA) from ROCOP of CHO, SO & MA with catalyst **1** (Two step reaction Table 4, entry 3)



**Figure A.I-19.** DSC profiles of the synthesized one pot terpolymers.





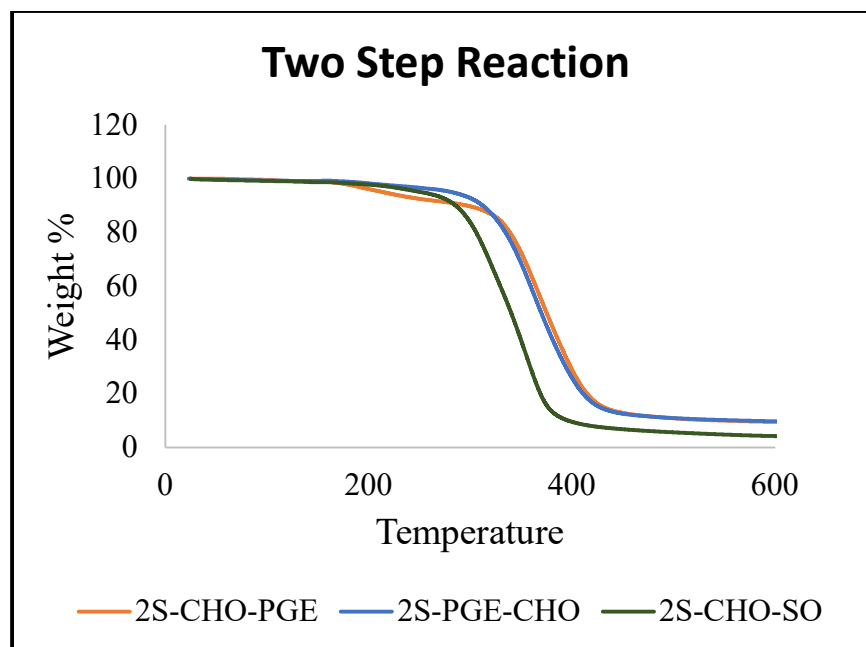


Figure A.I-20. TGA profiles of the synthesized copolymers and terpolymers

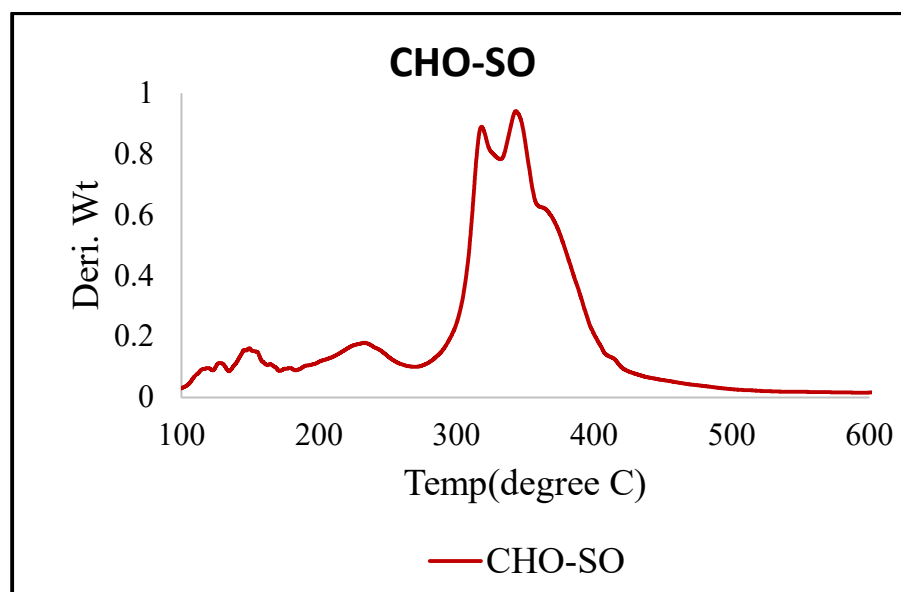


Figure A.I-21. TGA profiles of the synthesized copolymers and terpolymers

## APPENDIX II

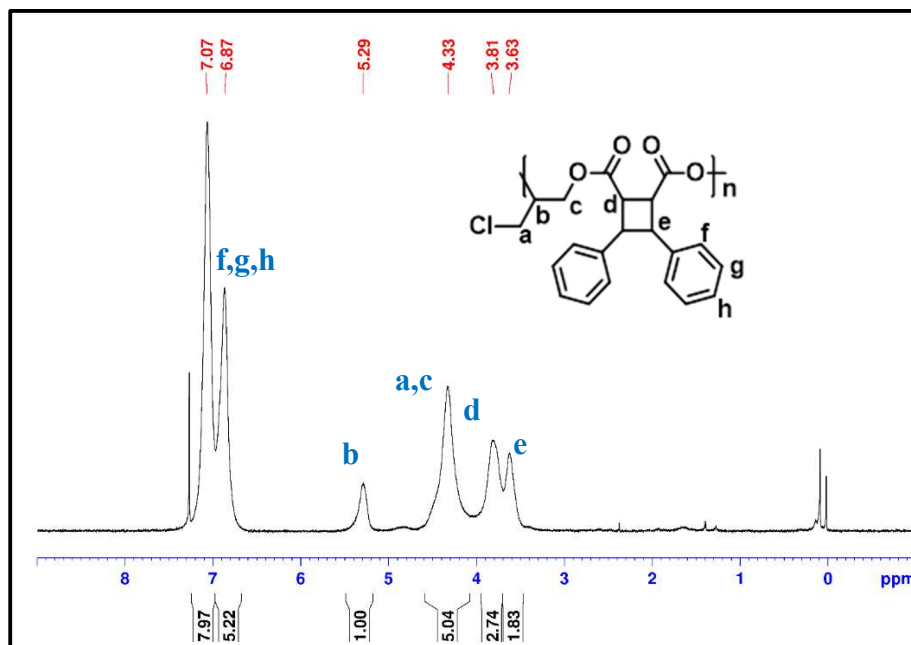


Figure A.II-1-. <sup>1</sup>H-NMR of Poly (ECH-alt-1a) in CDCl<sub>3</sub>

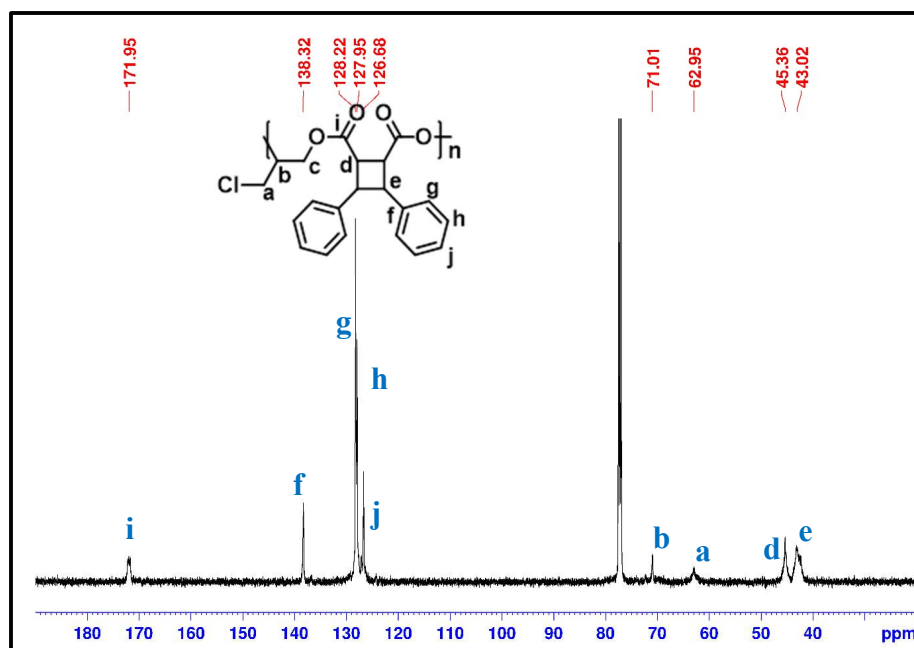


Figure A.II-2. <sup>13</sup>C-NMR of Poly (ECH-alt-1a) in CDCl<sub>3</sub>

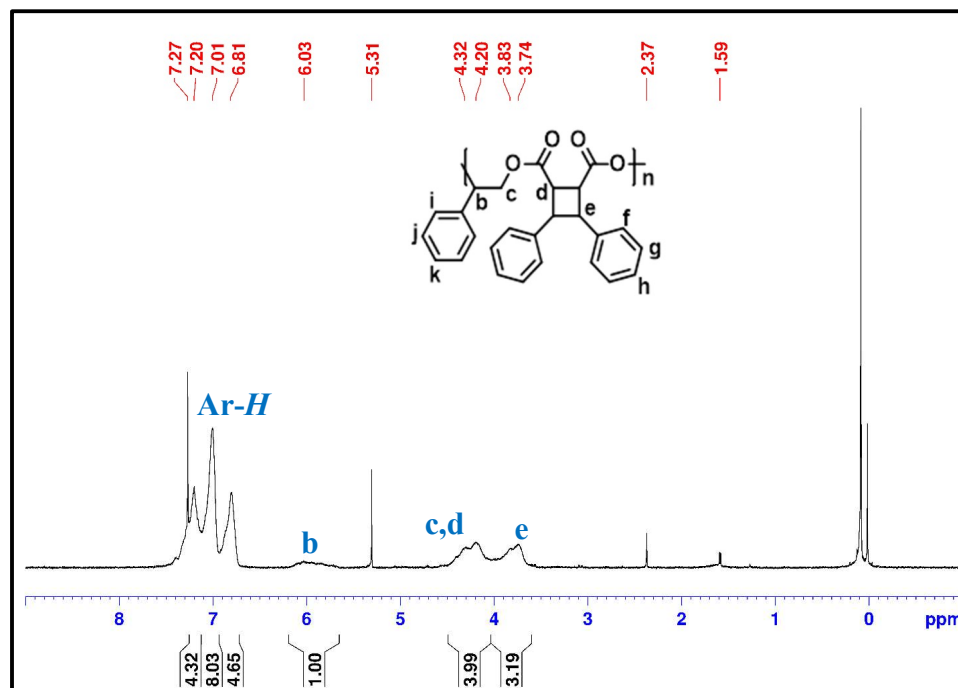


Figure A.II-3. <sup>1</sup>H-NMR of Poly (SO-alt-1a) in CDCl<sub>3</sub>

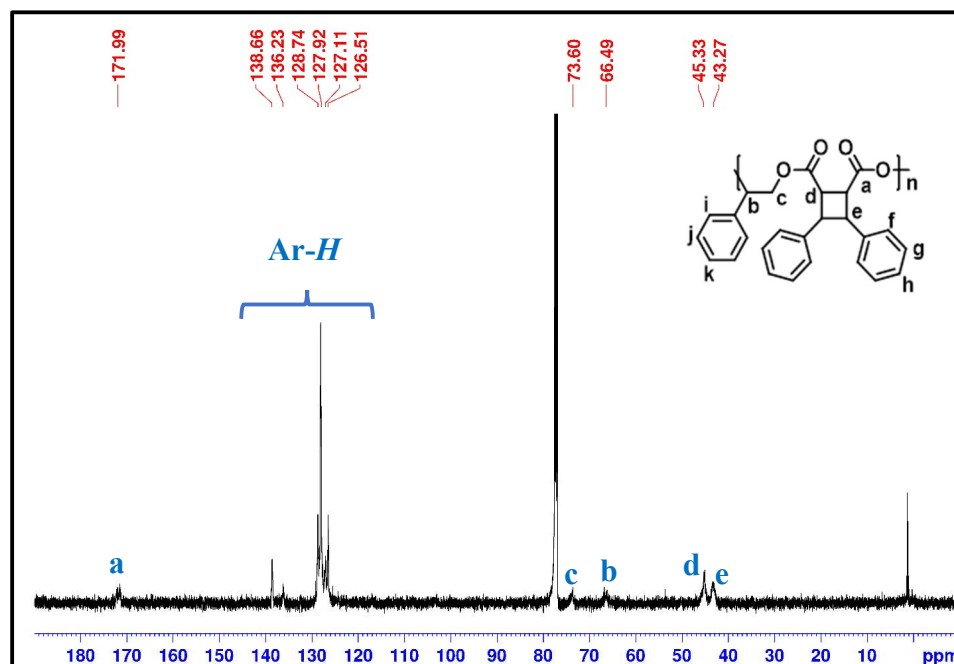


Figure A.II-4. <sup>13</sup>C-NMR of Poly (SO-alt-1a) in CDCl<sub>3</sub>

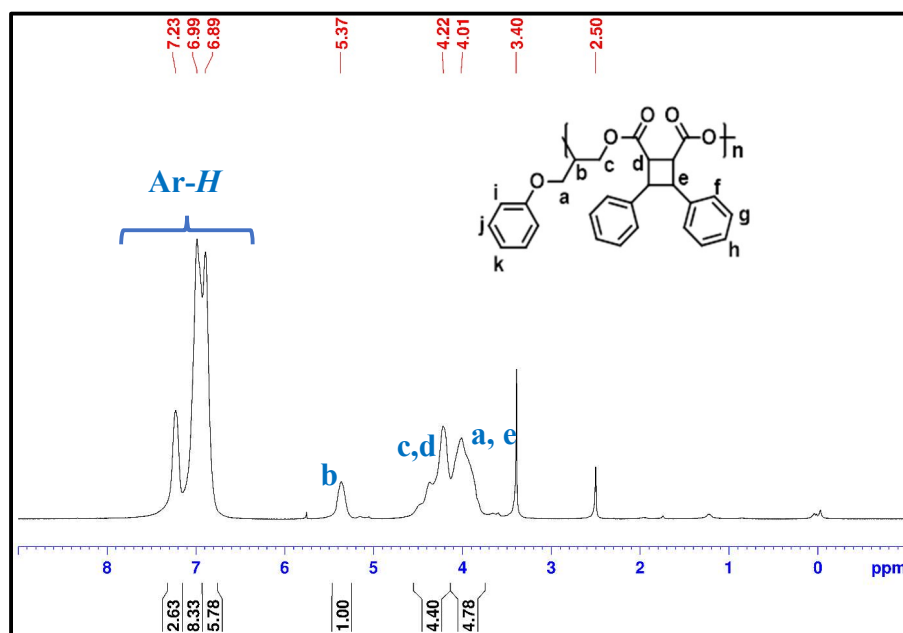


Figure A.II-5. <sup>1</sup>H-NMR of Poly (PGE-*alt*-1a) in DMSO

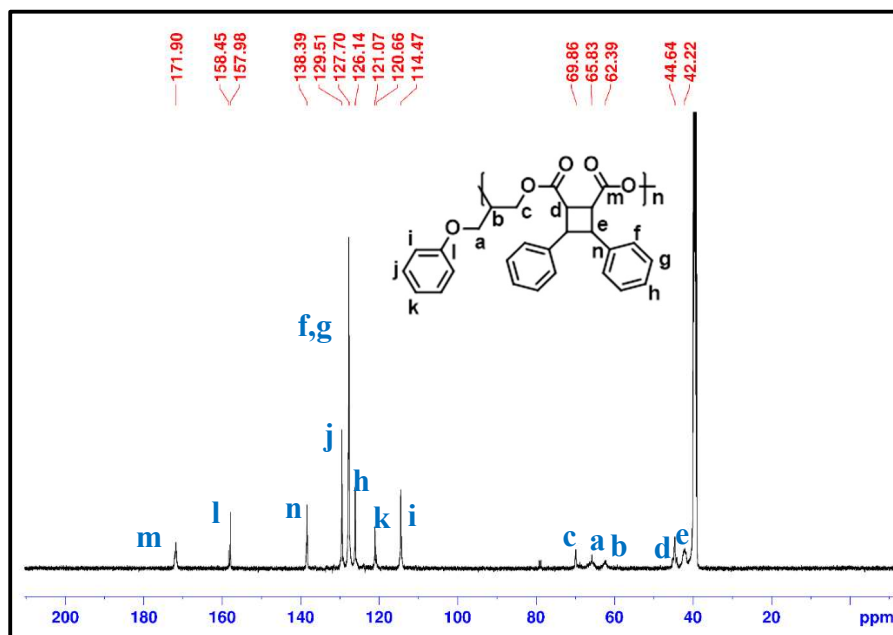


Figure A.II-6. <sup>13</sup>C-NMR of Poly (PGE-*alt*-1a) in DMSO

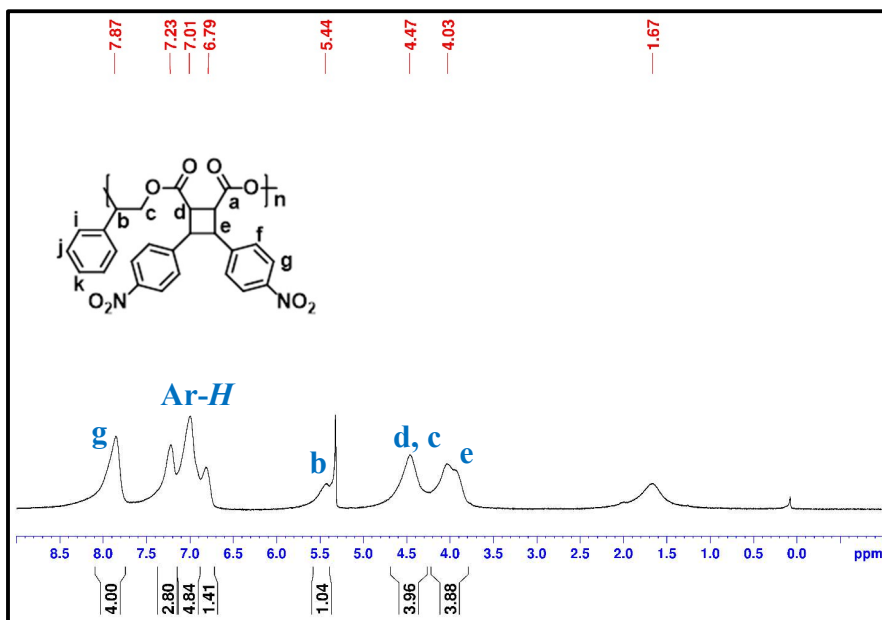


Figure A.II-7. <sup>1</sup>H-NMR of Poly (SO-*alt*-1c) in CD<sub>2</sub>Cl<sub>2</sub>

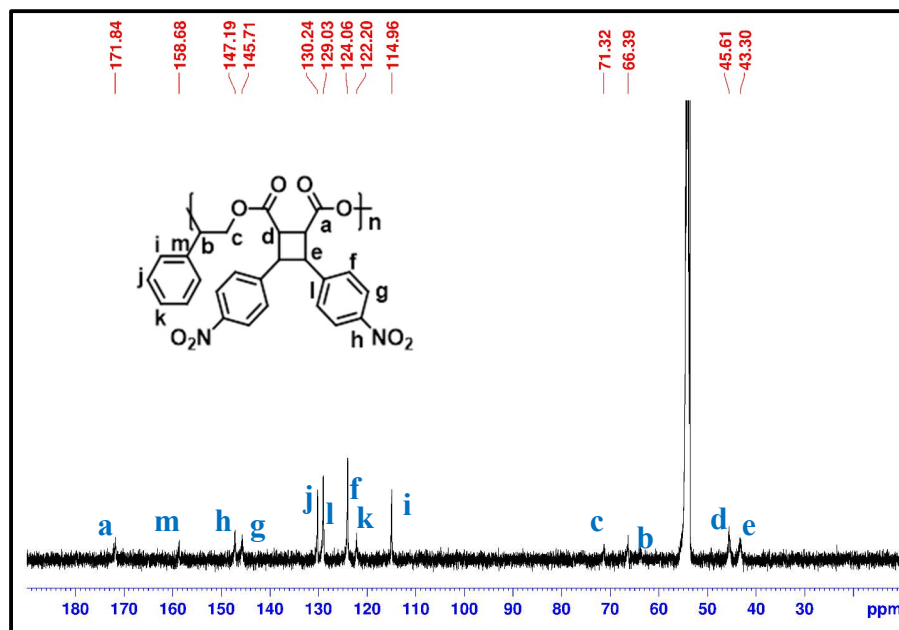


Figure A.II-8. <sup>13</sup>C-NMR of Poly (SO-*alt*-1c) in CD<sub>2</sub>Cl<sub>2</sub>

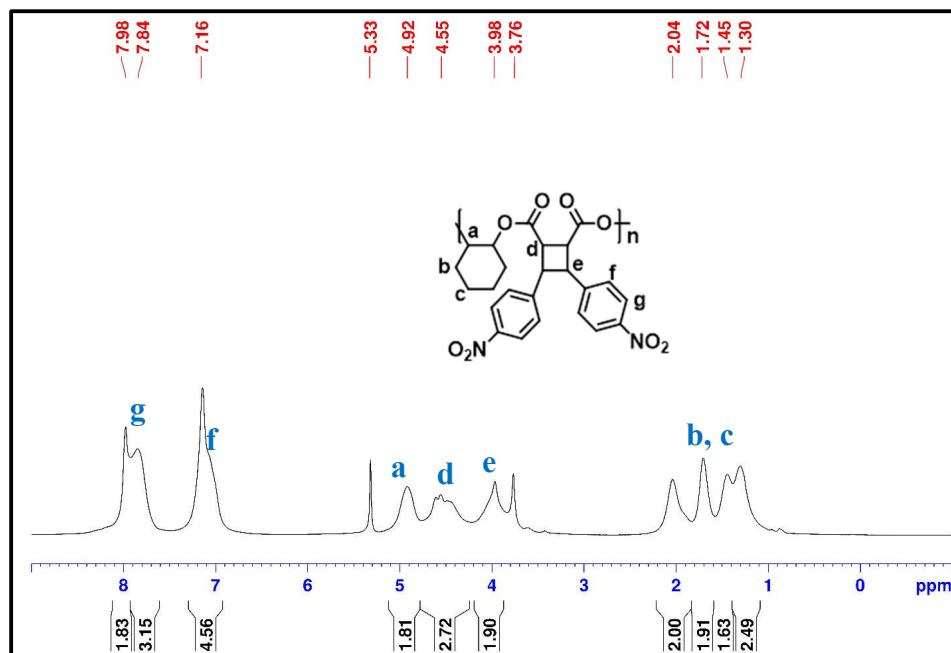


Figure A.II-9.  $^1\text{H}$ -NMR of Poly (CHO-*alt*-1c) in  $\text{CD}_2\text{Cl}_2$

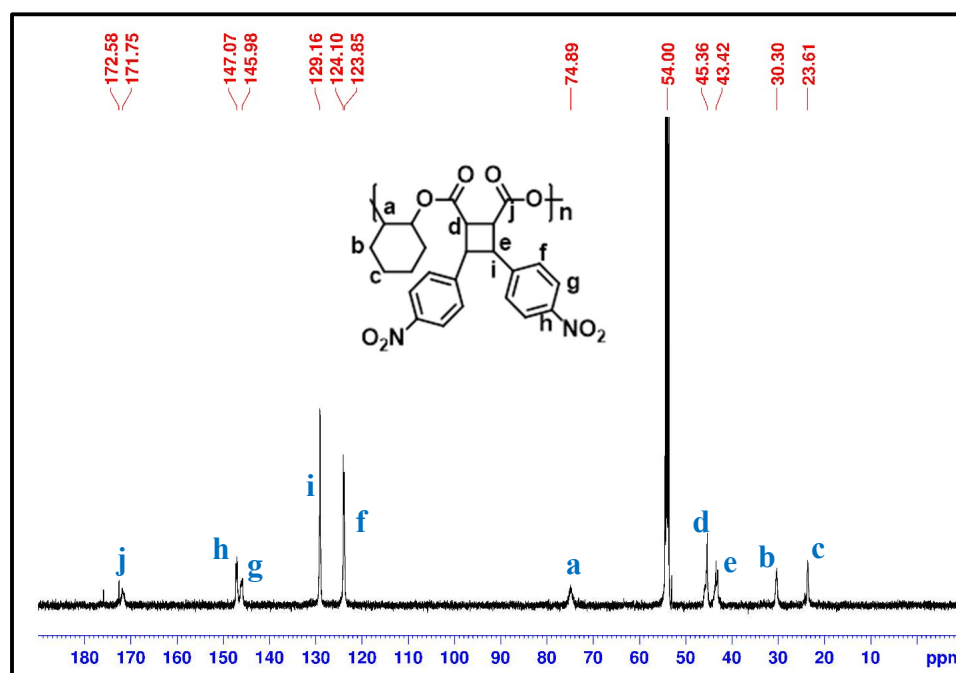


Figure A.II-10.  $^{13}\text{C}$ -NMR of Poly (CHO-*alt*-1c) in  $\text{CD}_2\text{Cl}_2$

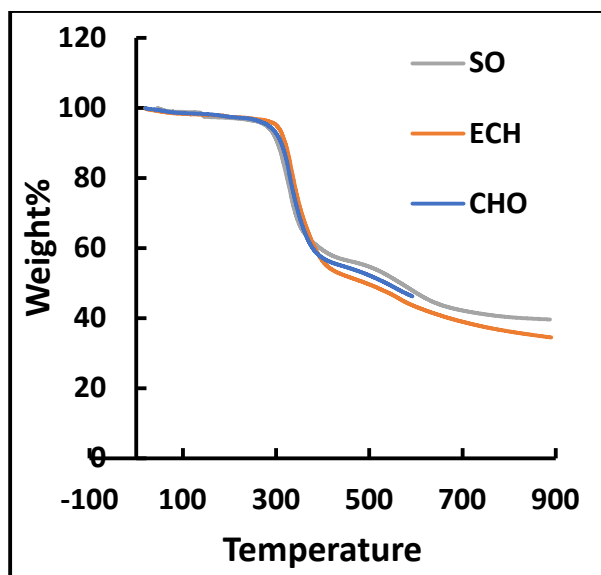


Figure A.II-11. TGA graph of polyesters with **1c** anhydride as comonomer

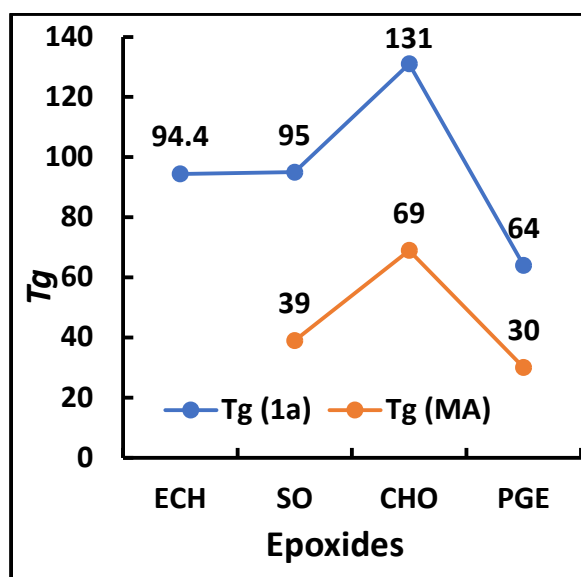
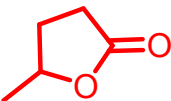
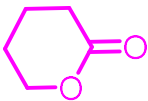
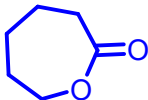


Figure A.II-12. Comparative studies— $T_g$ 's of polyester with **1a** and maleic anhydride



## APPENDIX III

Table 1 **A.III-1**:  $\delta$ -Valerolactone and  $\epsilon$ -Caprolactone ROP with Chiral Zn Catalyst (1b)<sup>a</sup>

Entry	Monomer	[Zn] <sub>0</sub> : [I] <sub>0</sub> : [M] <sub>0</sub>	T(h)	M <sub>n</sub> <sup>c</sup> (KDa)	M <sub>w</sub> <sup>c</sup> (KDa)	M <sub>w</sub> (DOSY) (KDa)	D <sup>c</sup>
1		1:0:200	48	0	0	--	0
2		1:1:200	--	--	--	--	--
3		1:0:200	0.5	43.0	84.2	88.4	1.96
4		1:1:200	4	7.9	9.3	9.0	1.18
5		1:0:200	0.5	74.5	139.9	139.1	1.88
6		1:1:200	4	10.9	13.0	14	1.19

<sup>a</sup>Unless otherwise stated, all reactions were carried out with [ $\delta$ -VL]<sub>0</sub> or [ $\epsilon$ -CL]<sub>0</sub> = 0.002 M at RT in Toluene.

<sup>b</sup>Monomer conversion was determined by <sup>1</sup>H NMR. <sup>c</sup>Absolute molecular weight and molecular weight distribution determined by GPC in THF. <sup>d</sup><sup>1</sup>H DOSY measurement was performed at 25 °C in CDCl<sub>3</sub>, using equation of the PS standard calibration curve is  $y = -0.5477x - 7.4766$  (R<sup>2</sup> = 0.9928). M<sub>w</sub>(DOSY) was calculated from the calibration curve using the experimental value of D.

### Diffusion Ordered Spectroscopy (DOSY)

Using Li et al. methods, a diffusion ordered NMR spectroscopy (DOSY) experiment linearly relates the chemical shift of <sup>1</sup>H NMR resonances to the translational diffusion coefficient of a particular molecular species, which can be applied to determine M<sub>w</sub> of polymers in dilute solutions. In diluted conditions, viscosity and density remain consistent throughout the solution, hence the linear relation between Log Da and Log M<sub>w</sub> using the Stokes-Einstein equation. We created a D-M<sub>w</sub> linear calibration curve from the <sup>1</sup>H-DOSY experiment,<sup>22,23</sup> using narrowly dispersed polystyrenes as standards for the GPC

calibration. (Figure S1) Chloroform was used as a solvent for all polymers because most of the polymers are soluble in  $\text{CDCl}_3$ . Next, we analyzed the purified samples of PCL and PVL at similar experimental  $^1\text{H}$ -DOSY conditions used for standard samples. The molecular weights obtained from the GPC and DOSY were within 0.5-15% deviation (Table S1). The high molecular weight polymer shows a better agreement between DOSY and GPC values than the lower molecular weights.

Table1 **A.III-2**: D-Fw results of PS calibration curve and predictions.

Entry	Samples	Mw(g/mol)	ave. D	STDEV	%error
1	PS	1480	6.50E-10	4.13252E-11	7.23
2	PS	2340	4.98E-10	6.56872E-11	14.92
3	PS	5030	3.29E-10	7.51798E-12	2.58
4	PS	8450	2.44E-10	1.89867E-11	8.66
5	PS	19760	1.53E-10	6.9419E-12	4.94
6	PS	38100	1.03E-10	3.67766E-12	3.96
7	PS	70950	8.73E-11	2.24761E-12	2.86
8	PS	132900	5.66E-11	2.70555E-13	0.5

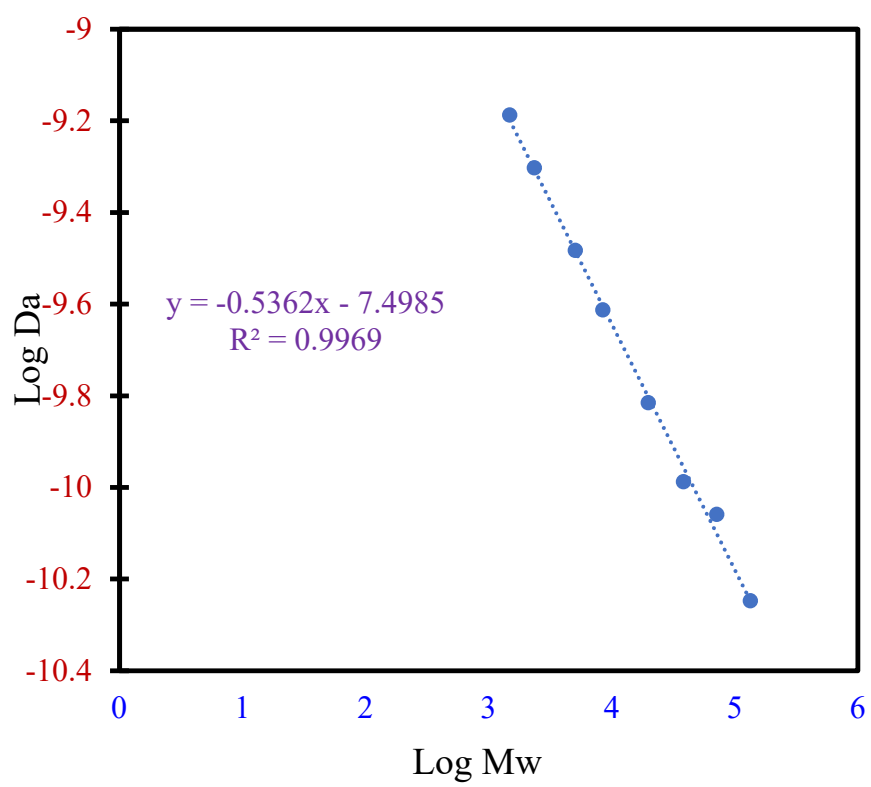


Figure A.III-1. PS calibration curve in  $\text{CDCl}_3$  for  $M_w$  prediction.

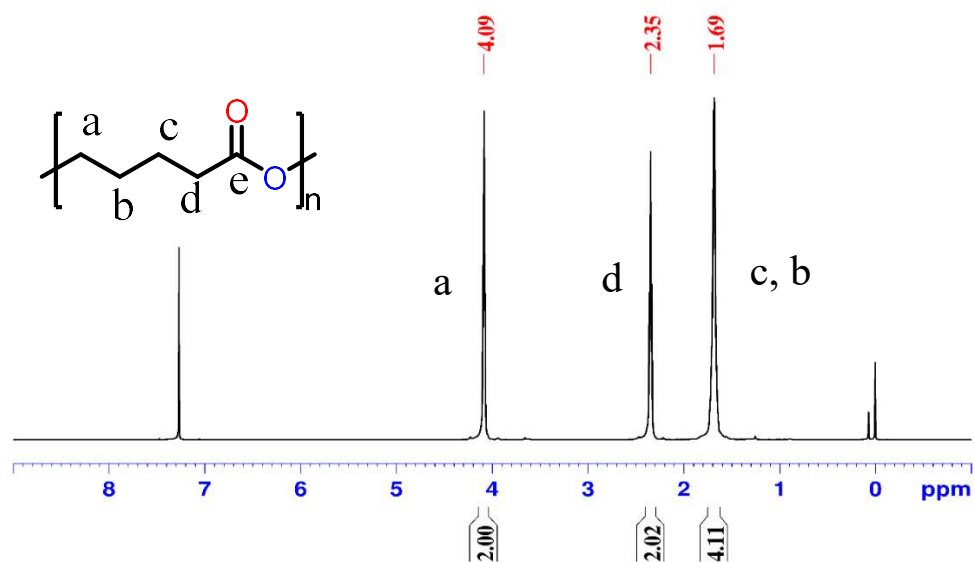


Figure A.III-2.  $^1\text{H}$ - NMR of Polyvalerolactone with 1a

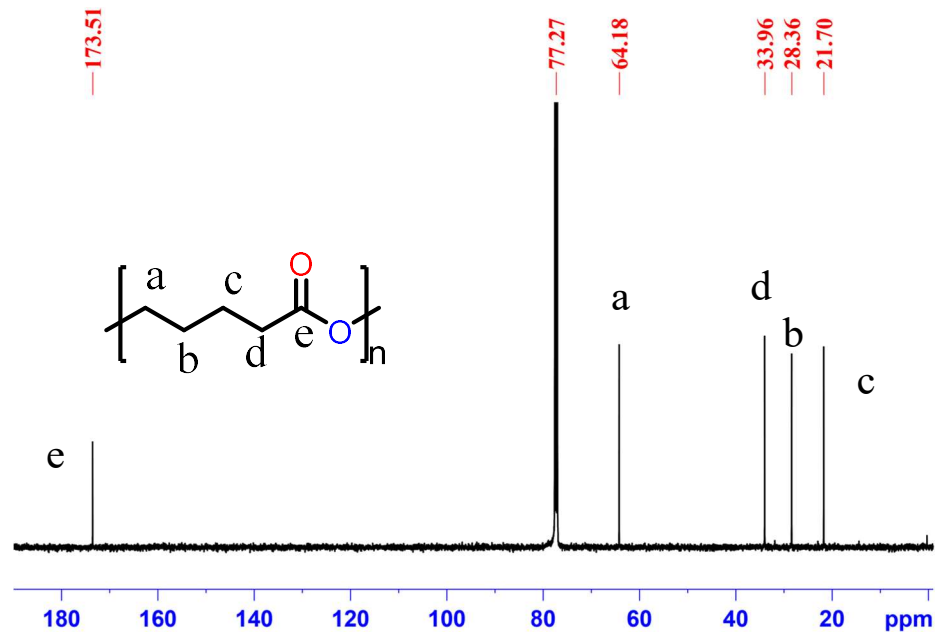


Figure A.III-3.  $^{13}\text{C}$ - NMR of Polyvalerolactone with 1a

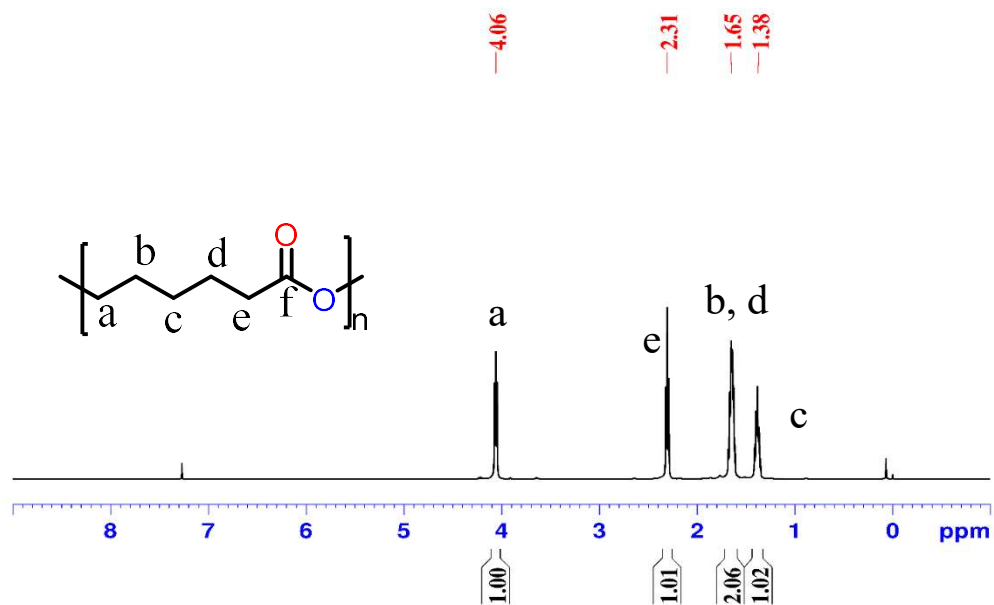


Figure A.III-4. <sup>1</sup>H- NMR of Polycaprolactone with 1a

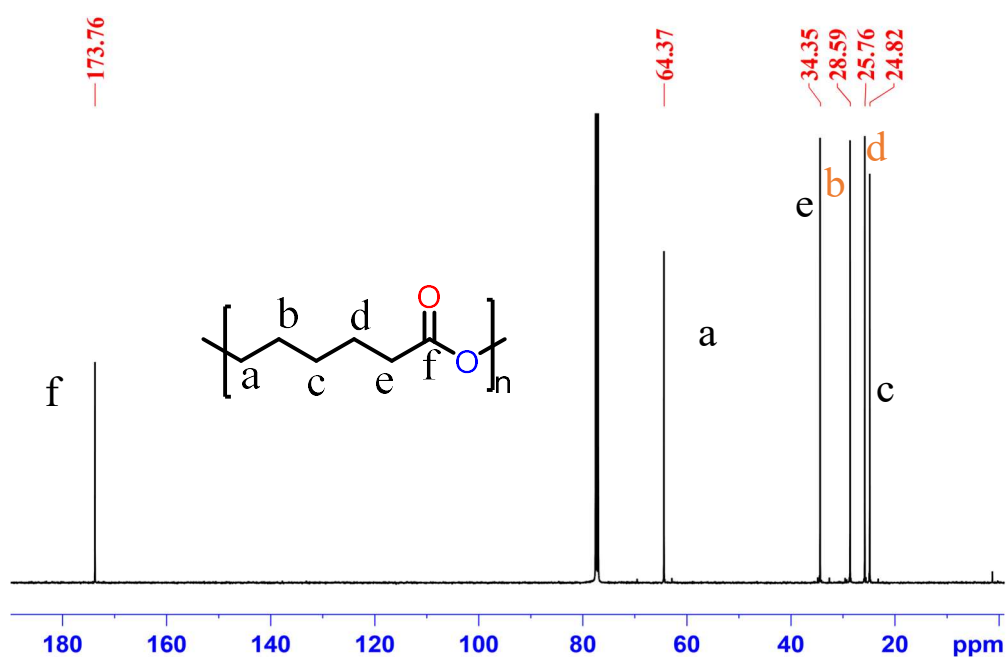


Figure A.III-5. <sup>13</sup>C- NMR of Polycaprolactone with 1a

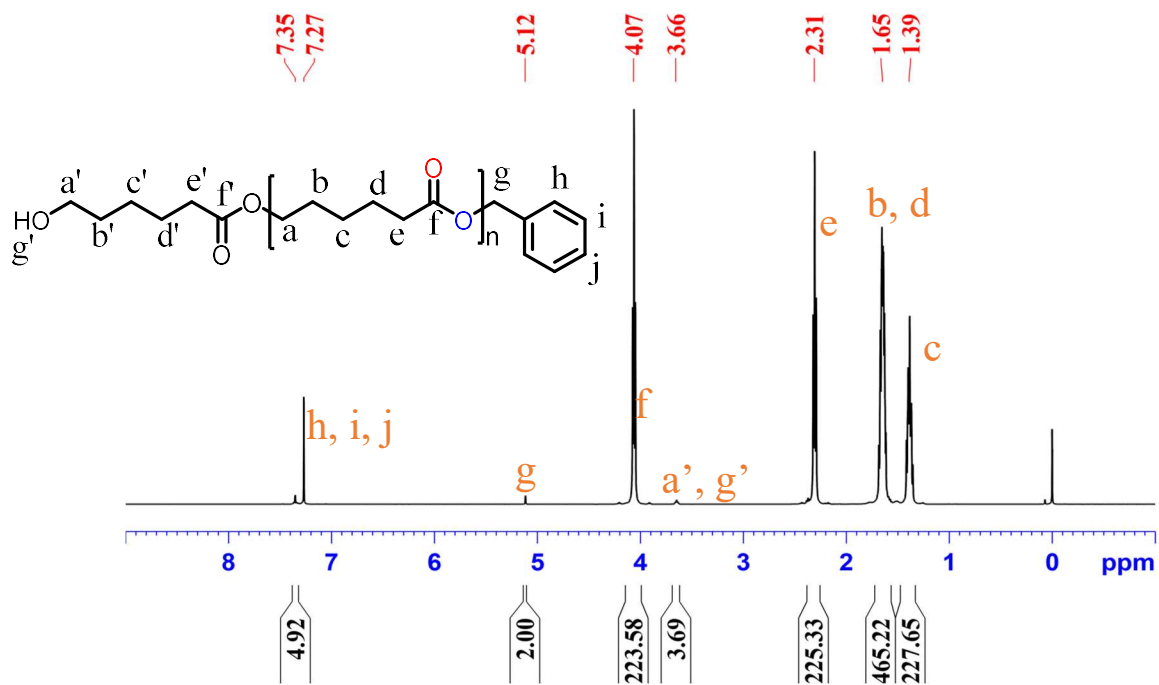


Figure A.III-6. <sup>1</sup>H- NMR of Polycaprolactone with benzyl alcohol as initiator

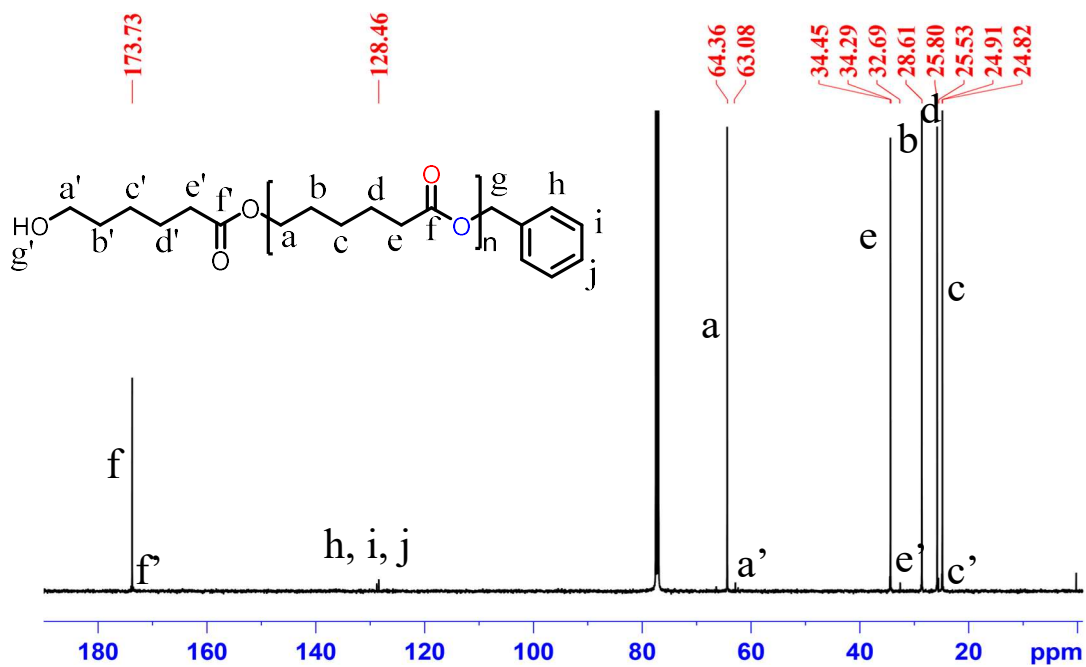


Figure A.III-7. <sup>13</sup>C- NMR of Polycaprolactone with benzyl alcohol as initiator

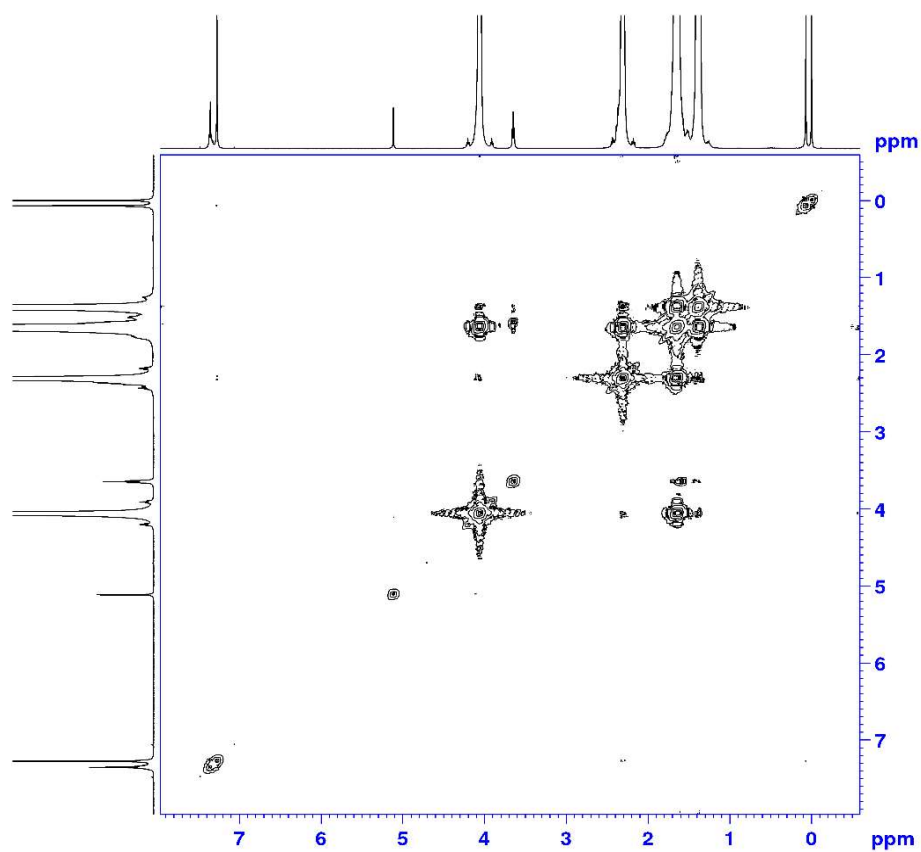


Figure A.III-8.  $^1\text{H}$ - $^1\text{H}$  COSY- NMR of Polycaprolactone with benzyl alcohol as initiator

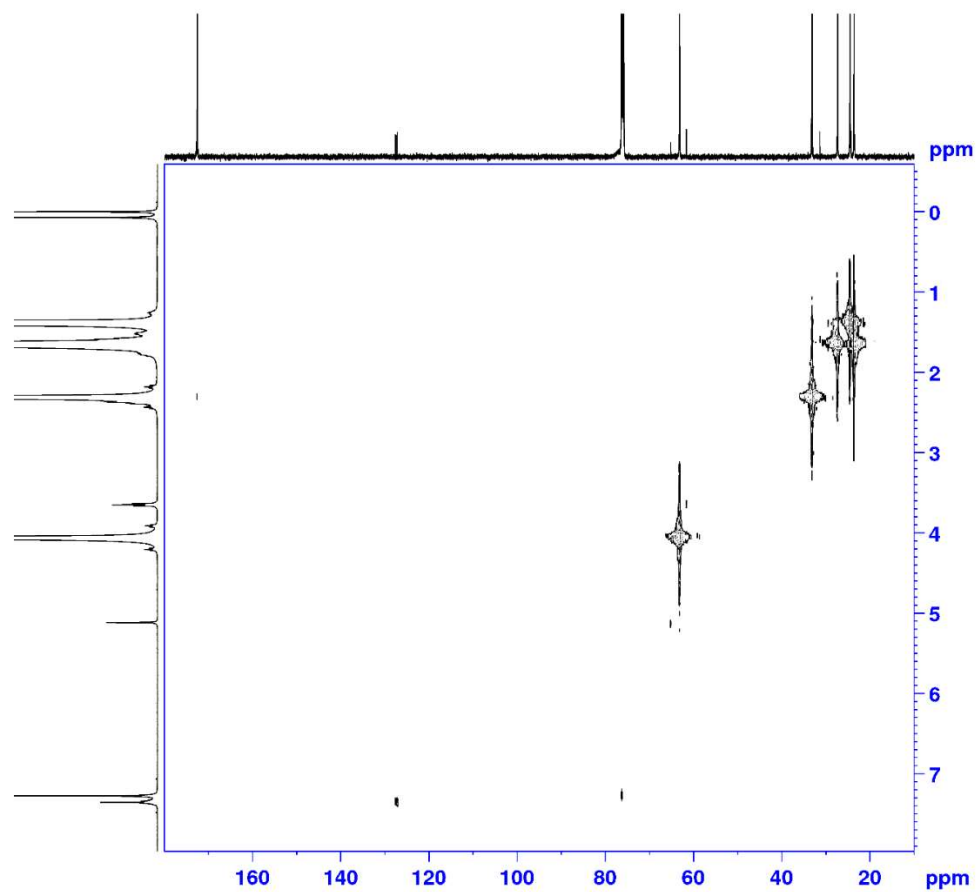


Figure A.III-9.  $^1\text{H}$ - $^{13}\text{C}$  COSY- NMR of Polycaprolactone with benzyl alcohol as initiator



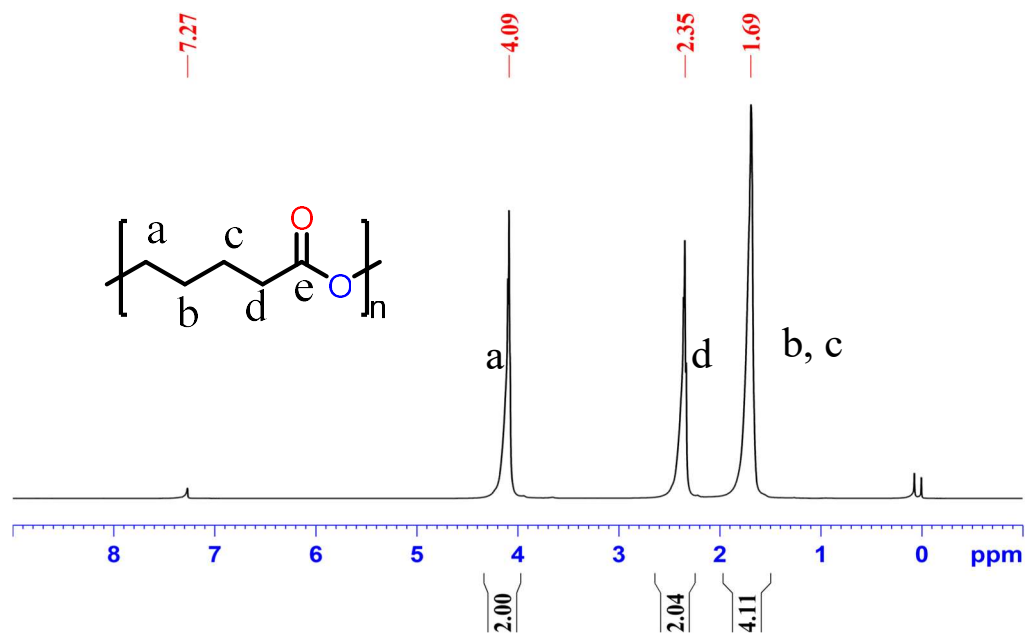


Figure A.III-10. <sup>1</sup>H- NMR of Polyvalerolactone with 1b

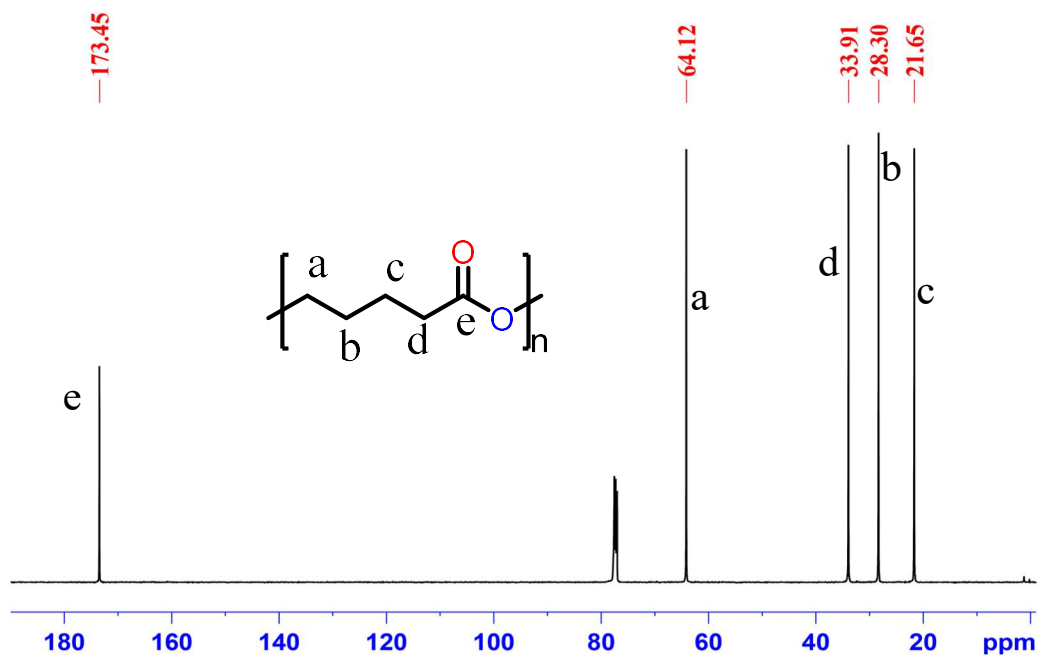


Figure A.III-11. <sup>13</sup>C- NMR of Polyvalerolactone with 1b

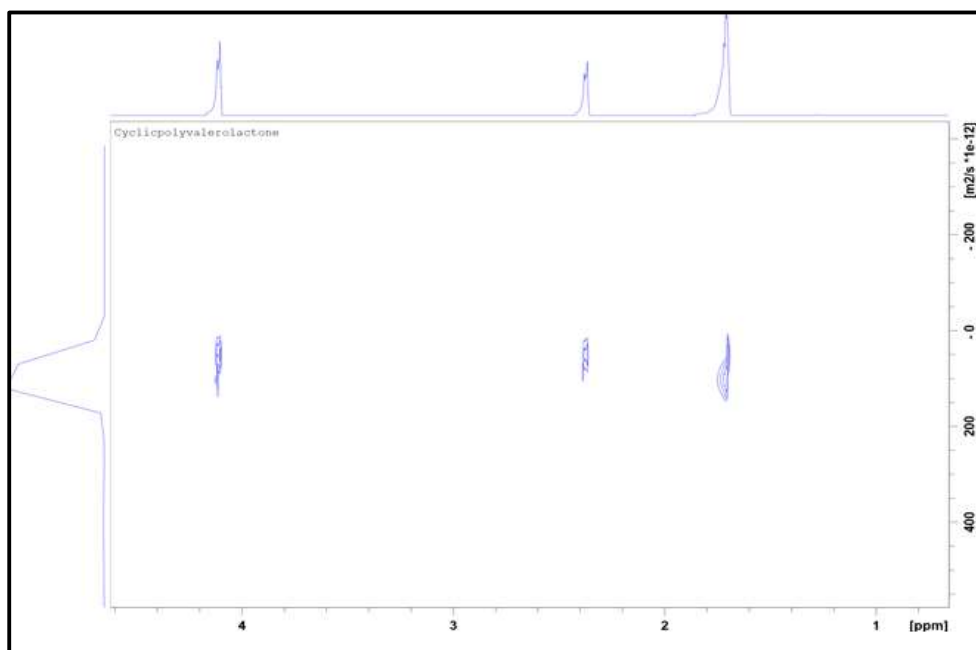


Figure A.III-12. DOSY-NMR of Cyclic Polyvalerolactone

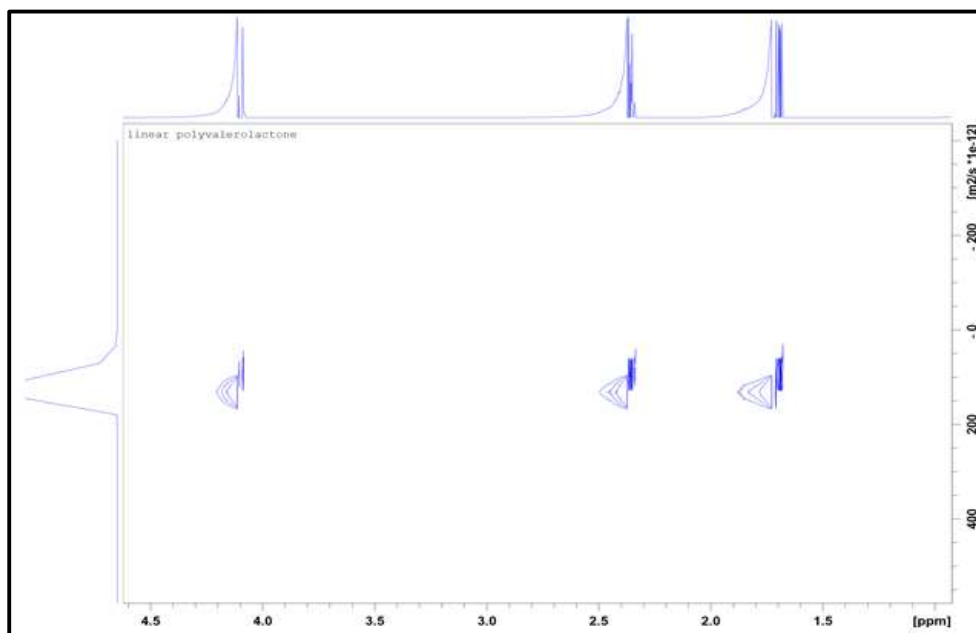


Figure A.III-13: DOSY-NMR of Linear polyvalerolactone

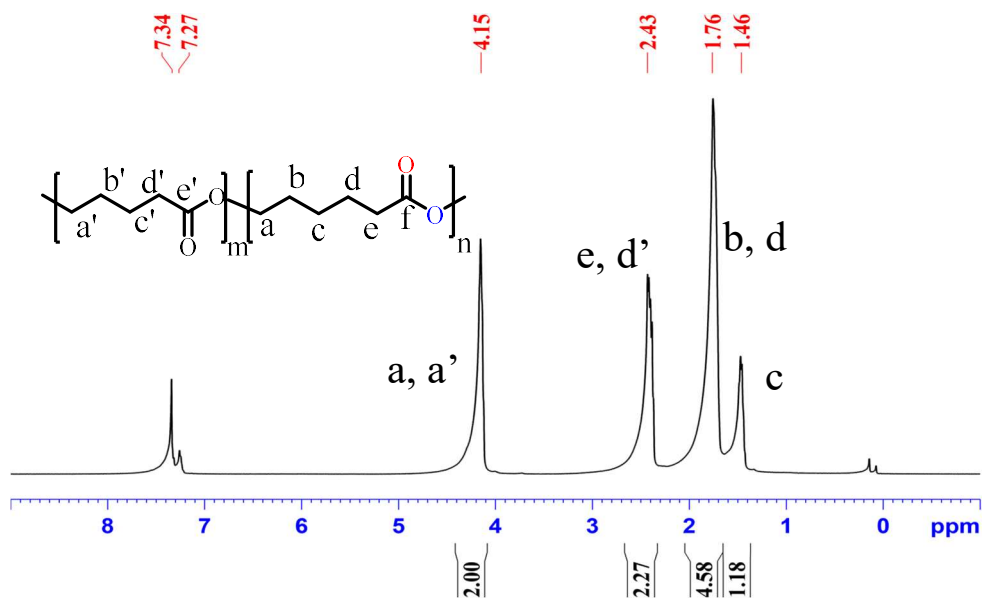


Figure A.III-14:  $^1\text{H}$ -NMR of block polymer for  $\delta$ -valerolactone and  $\epsilon$ -caprolactone with 1a (one pot reaction)

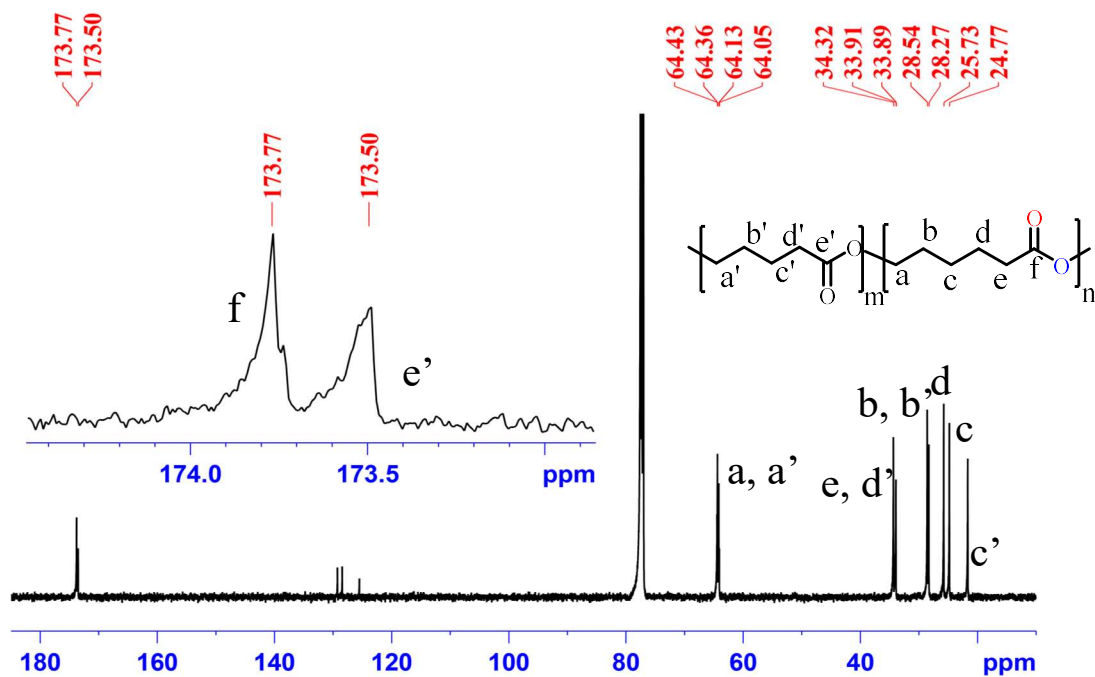


Figure A.III-15:  $^{13}\text{C}$ -NMR of block polymer for  $\delta$ -valerolactone and  $\epsilon$ -caprolactone with 1a (one pot reaction)

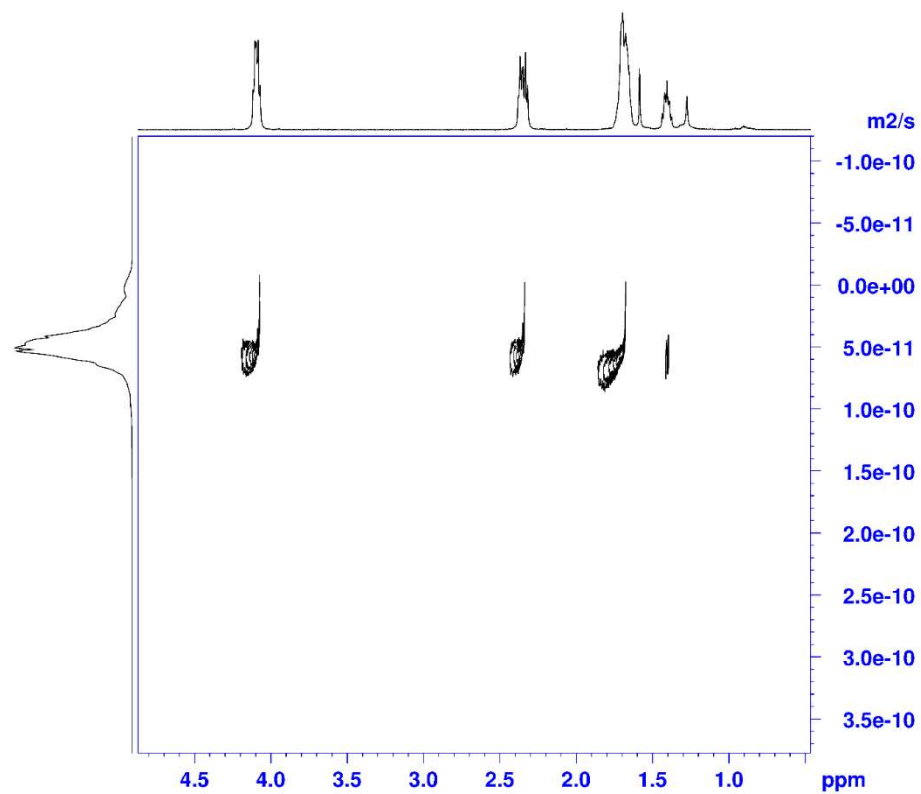


Figure A.III-16: DOSY- NMR of statistical polymer for  $\delta$ -valerolactone and  $\epsilon$ -caprolactone with 1a (one-pot reaction)

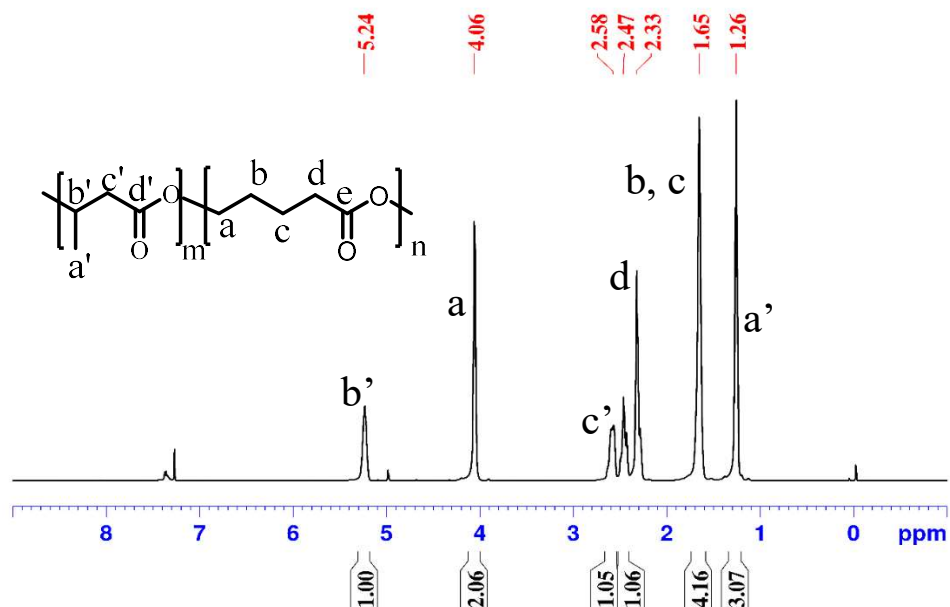


Figure A.III-17:  $^1\text{H}$ - NMR of gradient polymer for  $\beta$ -butyrolactone and  $\delta$ -valerolactone with 1a (one pot reaction)

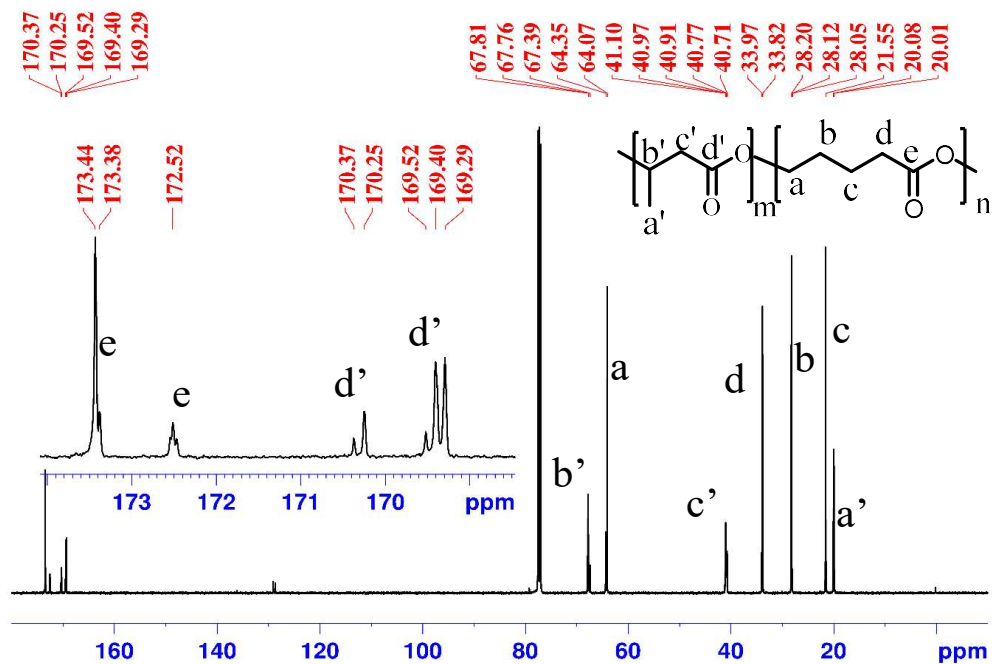


Figure A.III-18:  $^{13}\text{C}$ - NMR of gradient polymer for  $\beta$ -butyrolactone and  $\delta$ -valerolactone with 1a (one pot reaction)

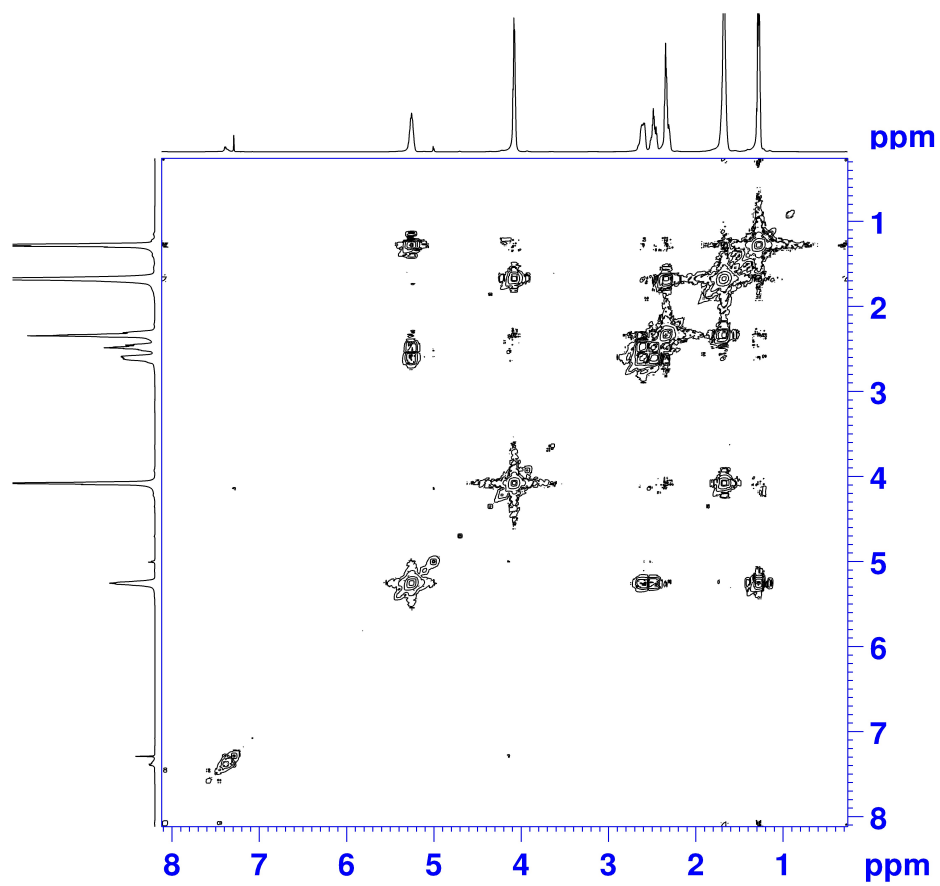


Figure A.III-19:  $^1\text{H}$ - $^1\text{H}$ - NMR of gradient polymer for  $\beta$ -butyrolactone and  $\delta$ -valerolactone with 1a (one pot reaction)

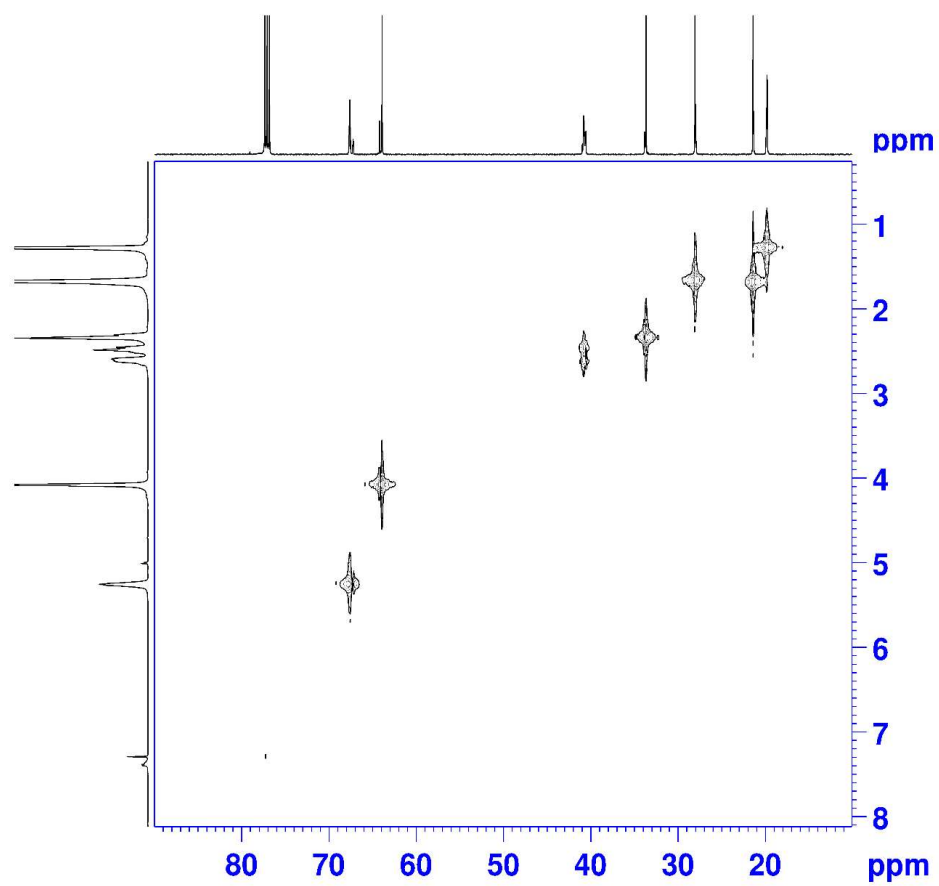


Figure A.III-20:  $^1\text{H}$ - $^{13}\text{C}$ - NMR of gradient polymer for  $\beta$ -butyrolactone and  $\delta$ -valerolactone with 1a (one pot reaction)

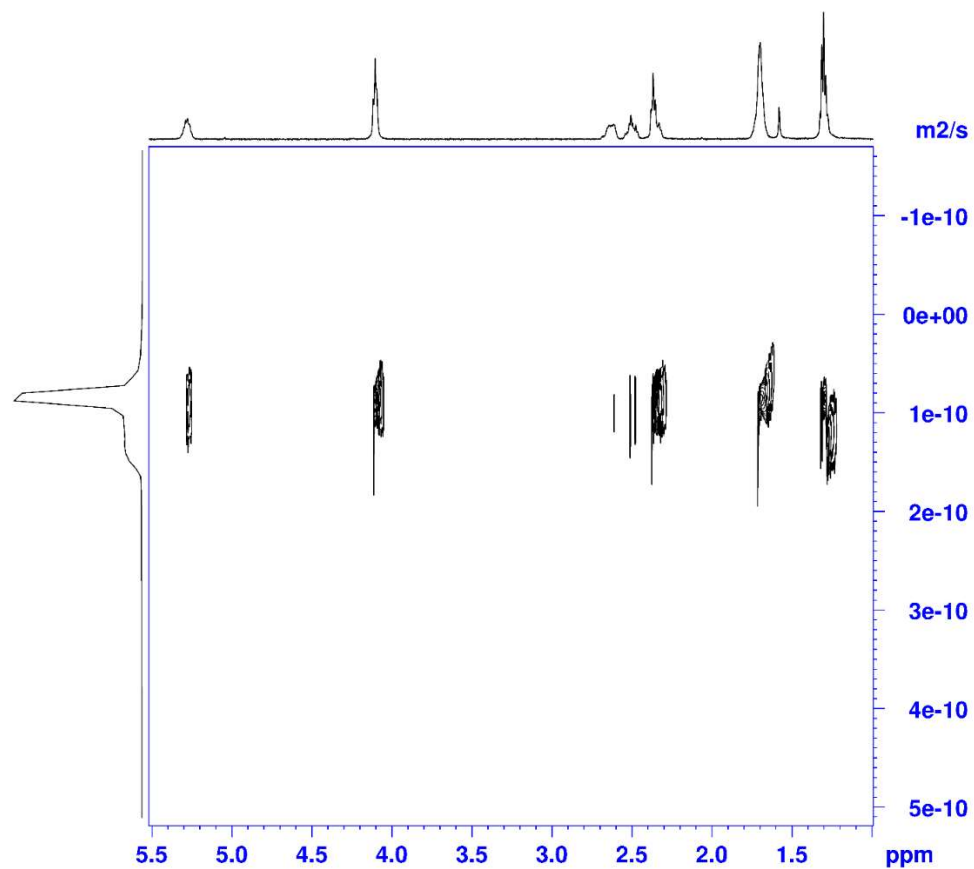


Figure A.III-21: DOSY- NMR of gradient polymer for  $\beta$ -butyrolactone and  $\delta$ -valerolactone with 1a (one pot reaction)



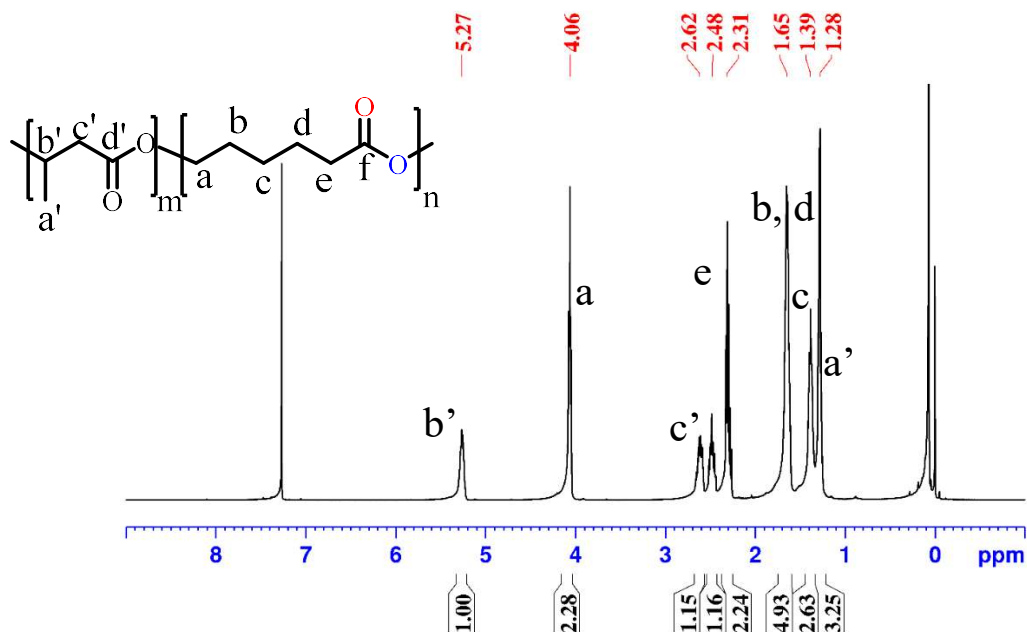


Figure A.III-22:  $^1\text{H}$ -NMR of gradient polymer for  $\beta$ -butyrolactone and  $\epsilon$ -caprolactone with 1a (one pot reaction)

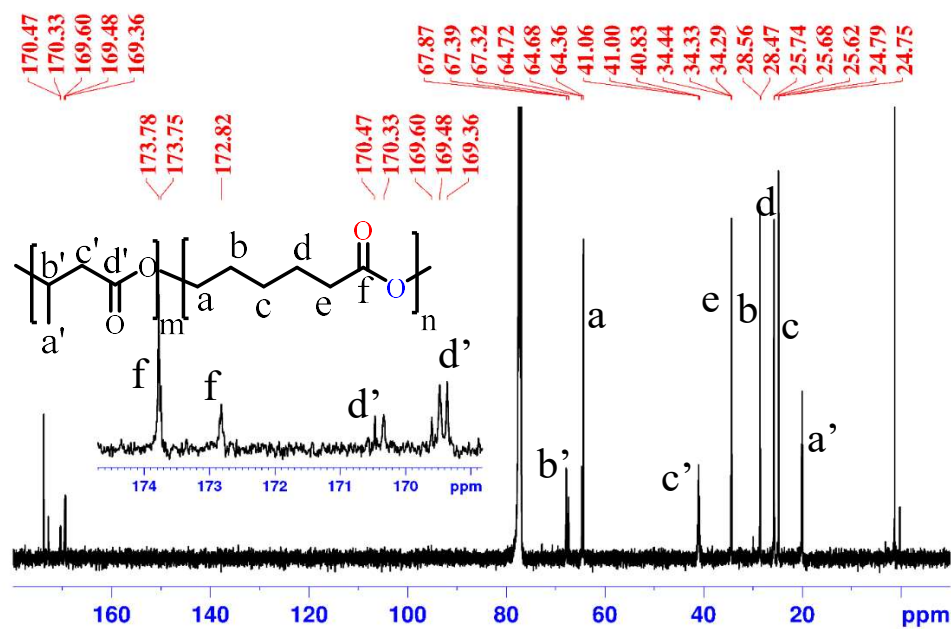


Figure A.III-23:  $^{13}\text{C}$ -NMR of gradient polymer for  $\beta$ -butyrolactone and  $\epsilon$ -caprolactone with 1a (one pot reaction)

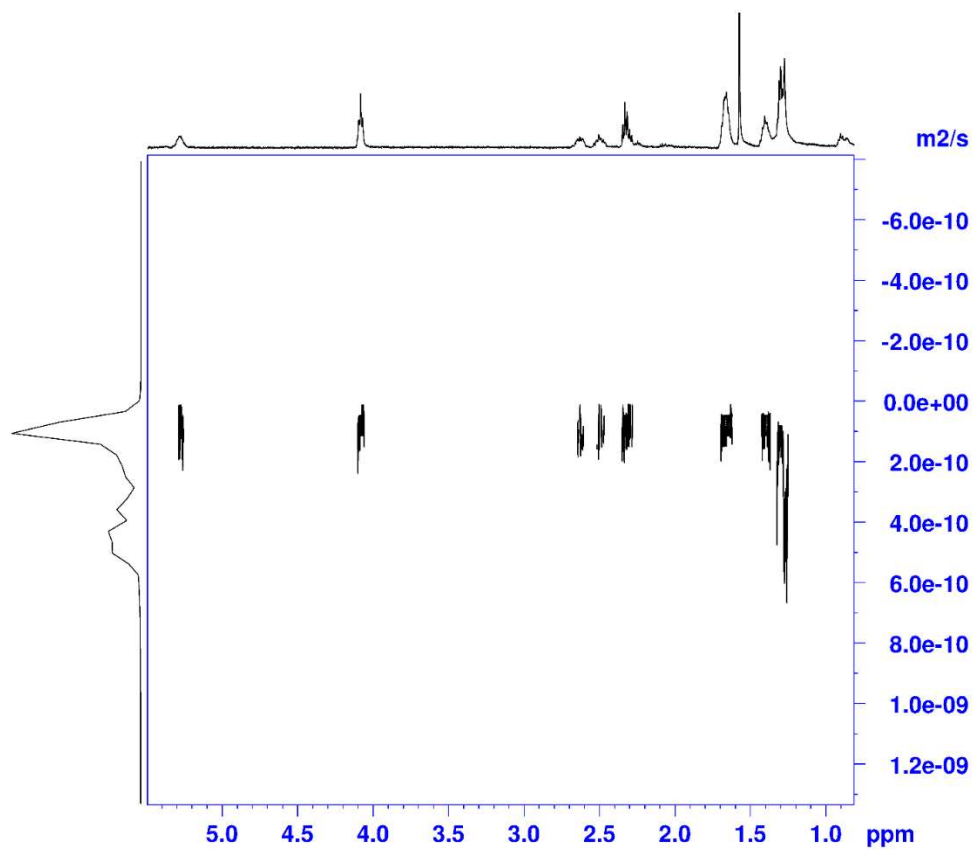


Figure A.III-24: DOSY- NMR of gradient polymer for  $\beta$ -butyrolactone and  $\epsilon$ -caprolactone with 1a (one pot reaction)

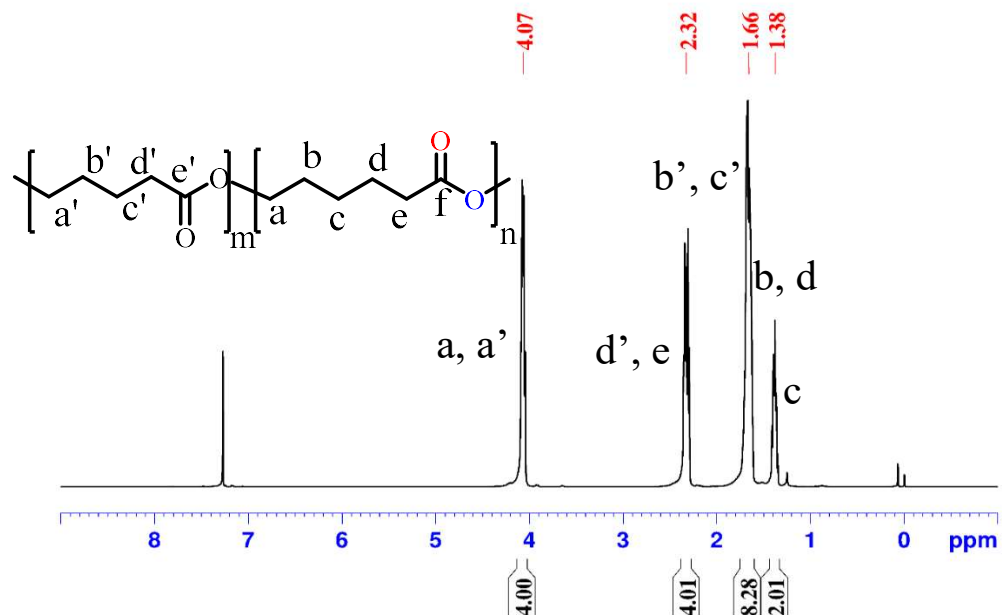


Figure A.III-25: <sup>1</sup>H- NMR of block polymer for δ-valerolactone and ε-caprolactone with 1a (Two step reaction)

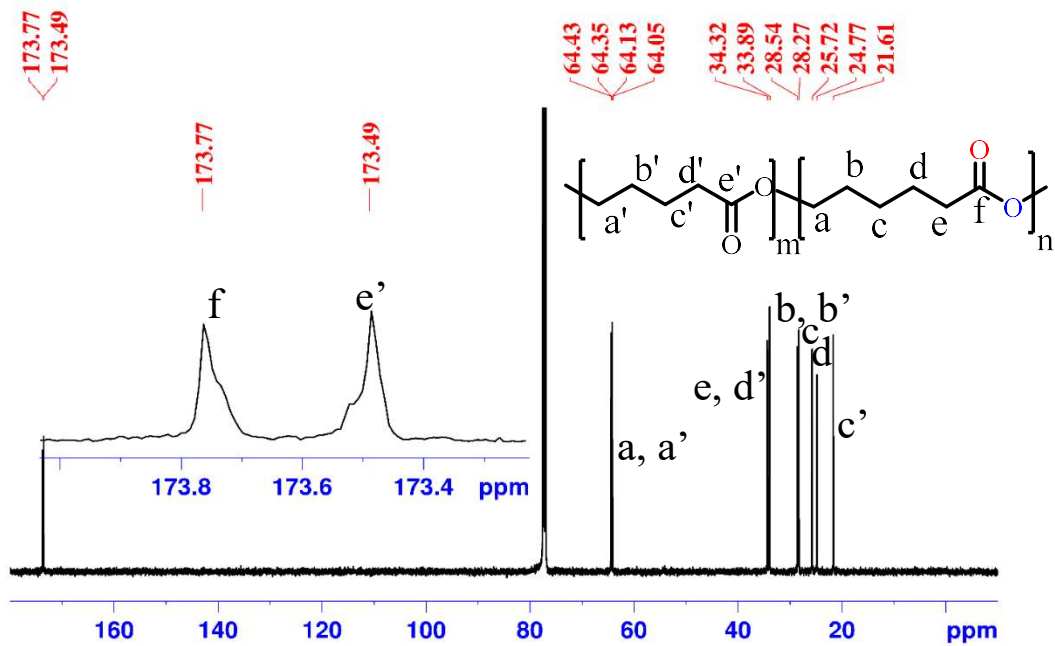


Figure A.III-26: <sup>13</sup>C- NMR of block polymer for δ-valerolactone and ε-caprolactone with 1a (Two step reaction)

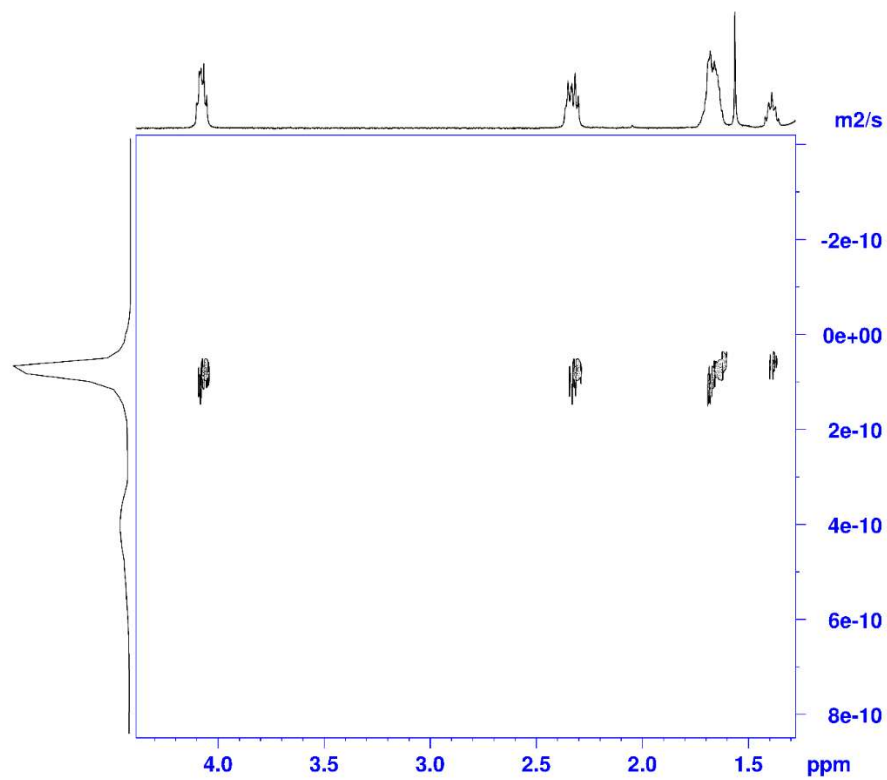


Figure A.III-27: DOSY- NMR of block polymer for  $\delta$ -valerolactone and  $\epsilon$ -caprolactone with 1a (Two step reaction)

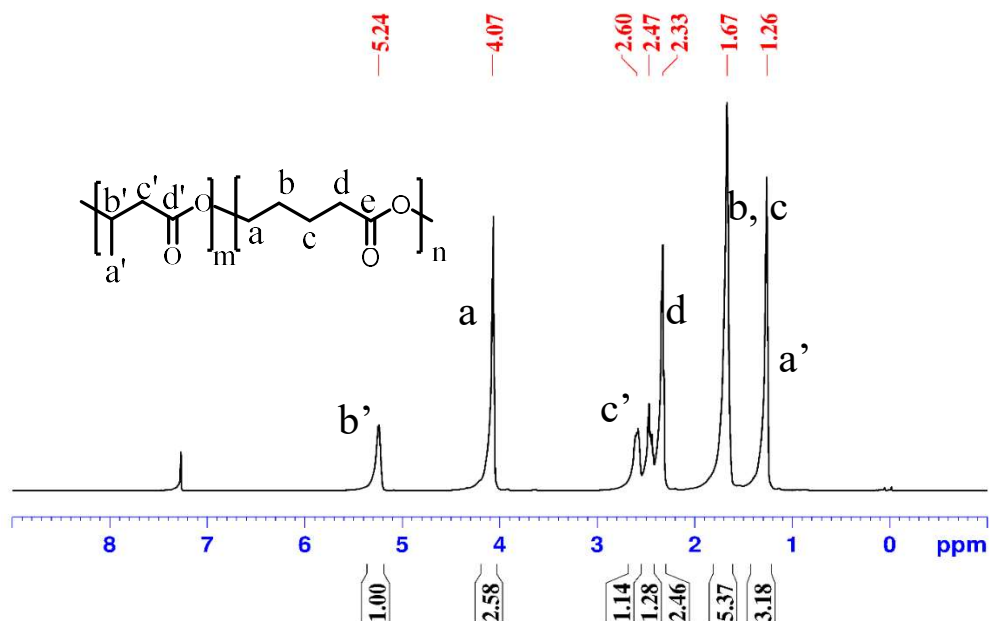


Figure A.III-28:  $^1\text{H}$ - NMR of block polymer for  $\beta$ -butyrolactone and  $\delta$ -valerolactone with 1a (Two step reaction)

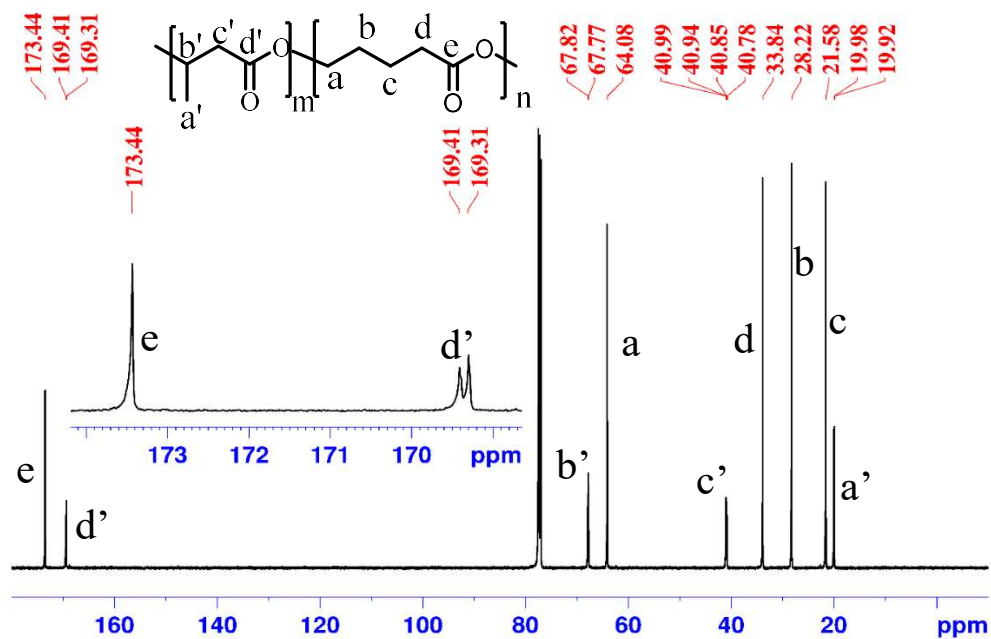


Figure A.III-29:  $^{13}\text{C}$ - NMR of block polymer for  $\beta$ -butyrolactone and  $\delta$ -valerolactone with 1a (Two step reaction)

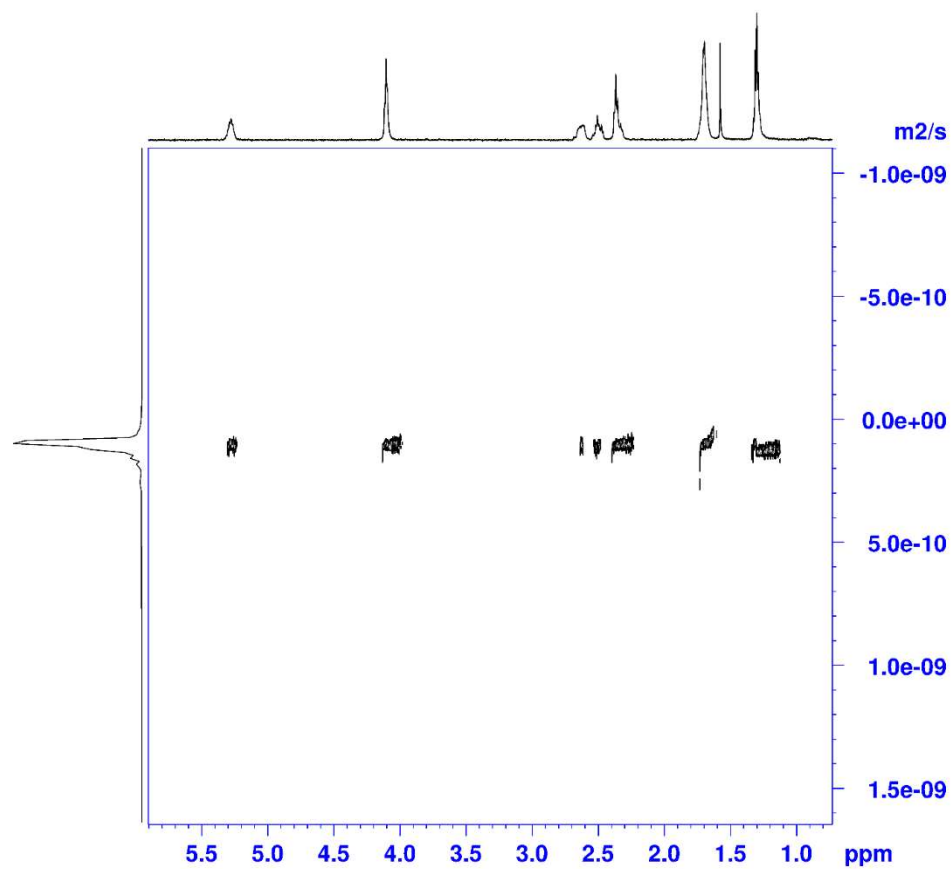


Figure A.III-30: DOSY- NMR of block polymer for  $\beta$ -butyrolactone and  $\delta$ -valerolactone with 1a (Two step reaction)

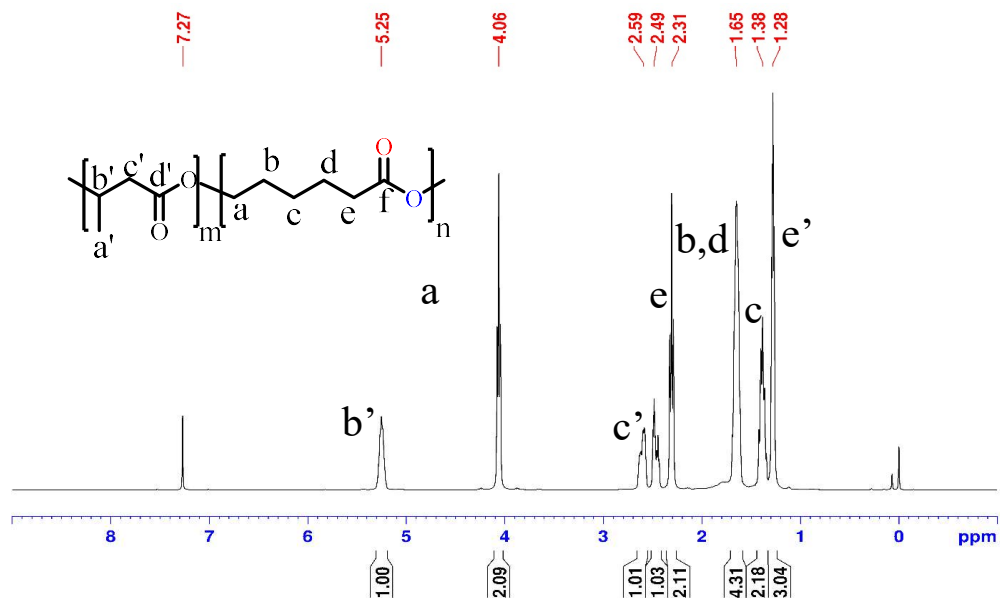


Figure A.III-31:  $^1\text{H}$ -NMR of block polymer for  $\beta$ -butyrolactone and  $\epsilon$ -caprolactone with 1a (Two-step reaction)

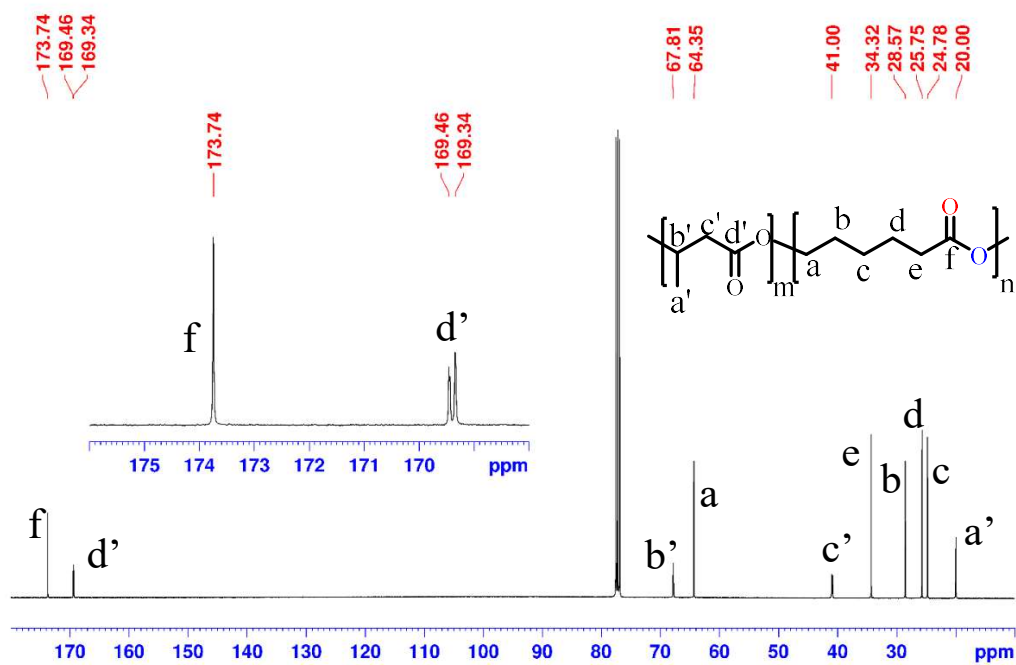


Figure A.III-32:  $^{13}\text{C}$ -NMR of block polymer for  $\beta$ -butyrolactone and  $\epsilon$ -caprolactone with 1a (Two-step reaction)

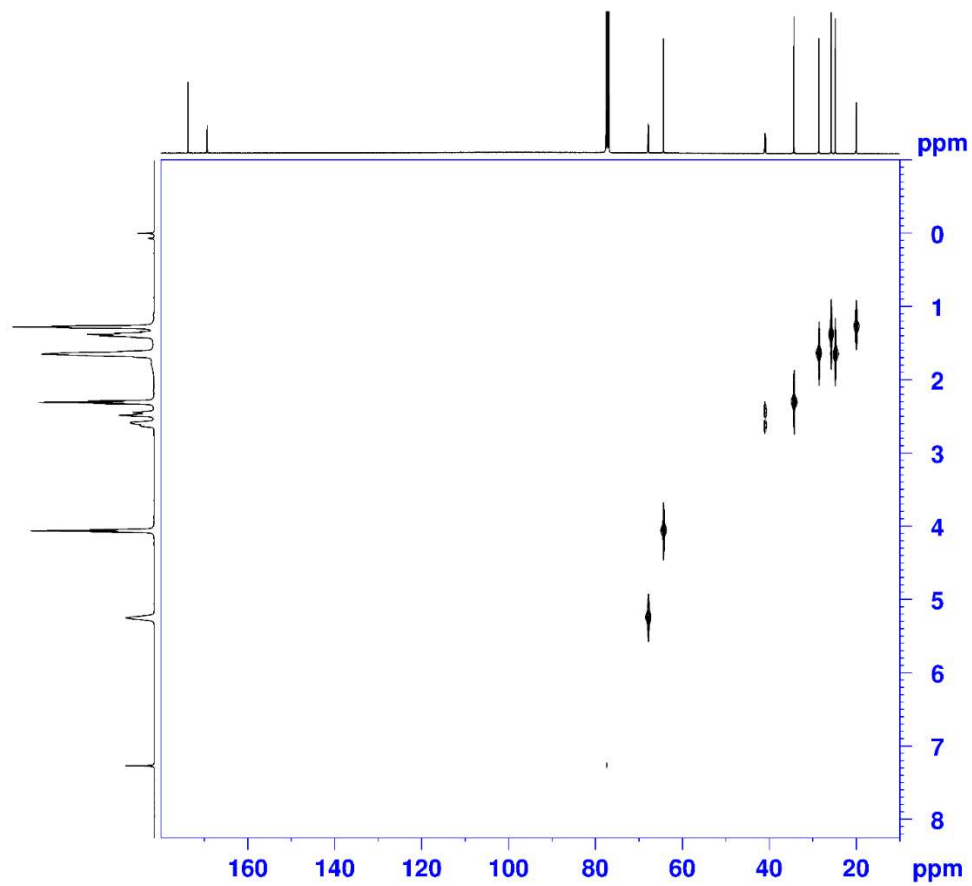
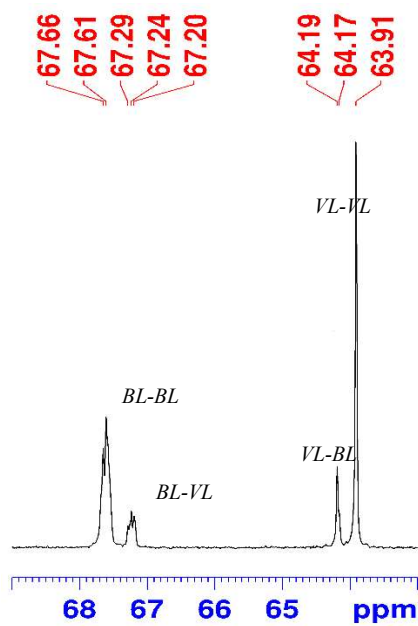


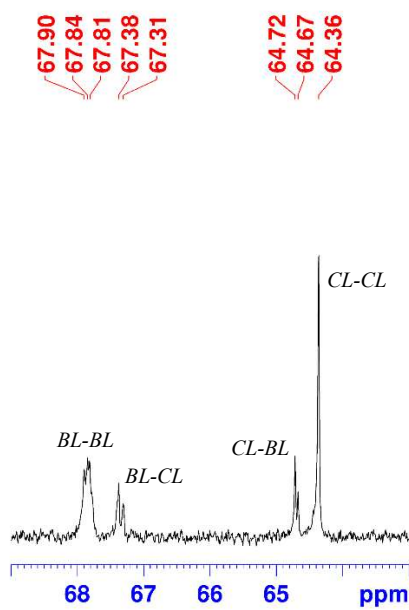
Figure A.III-33:  $^1\text{H}$ - $^{13}\text{C}$ - NMR of block polymer for  $\beta$ -butyrolactone and  $\epsilon$ -caprolactone with 1a (Two-step reaction)



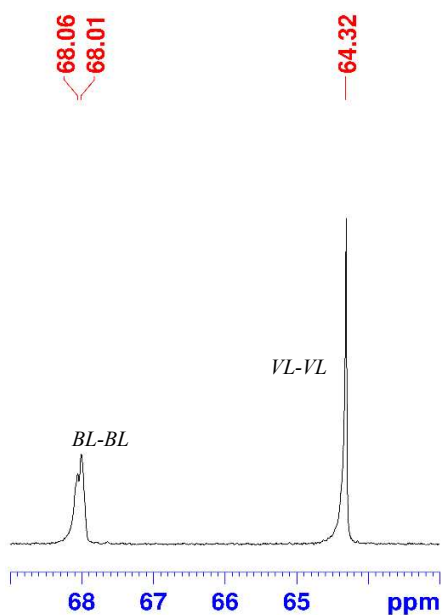
(a) Cyclic gradient BL-VL



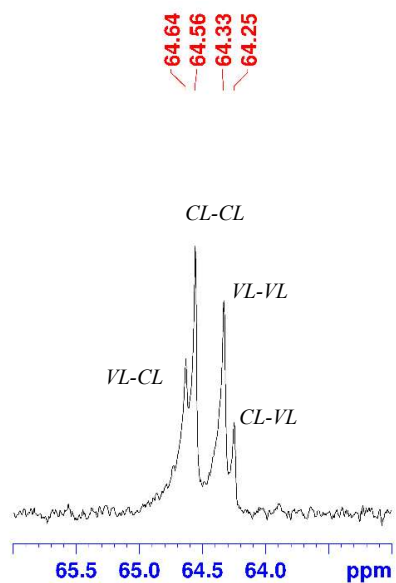
(b) Cyclic gradient BL-CL



(c) Cyclic block BL-VL



(d) Cyclic statistical CL-VL



(e) Cyclic block BL-CL

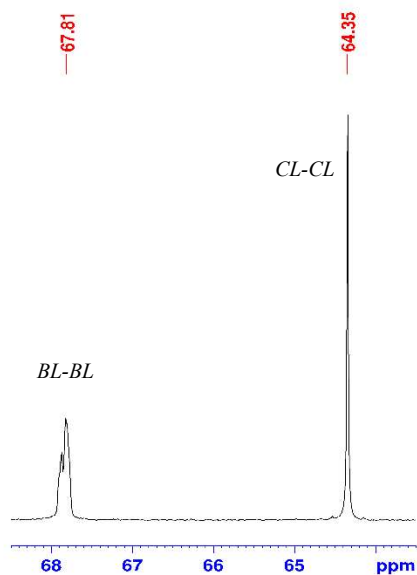
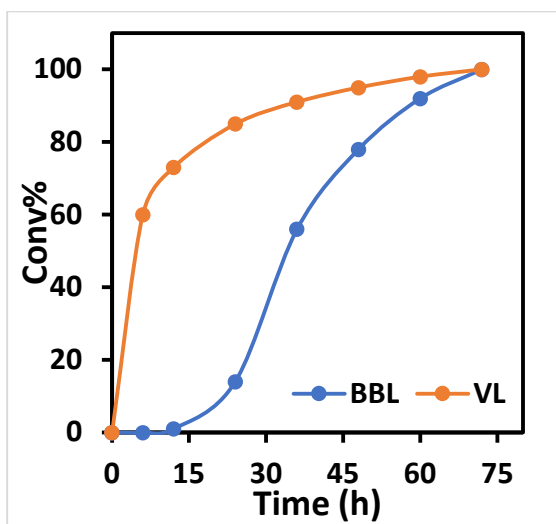


Figure A.III-34:  $^{13}\text{C}$ - NMR of samples of Table 3. For example., gradient polymer for  $\beta$ -butyrolactone and valerolactone with 1a (BL-VL means the methylene signal of the butyrolactone unit connected to a valerolactone, i.e. BL-O-CH<sub>2</sub>-CH<sub>2</sub>-CH<sub>2</sub>-CH<sub>2</sub>-CO-)

(a)



(b)

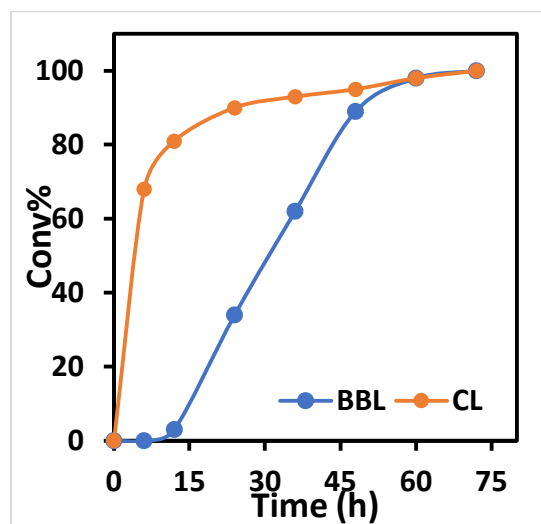


Figure A.III-35: Conversion of a) BBL and VL b) BBL and CL versus time

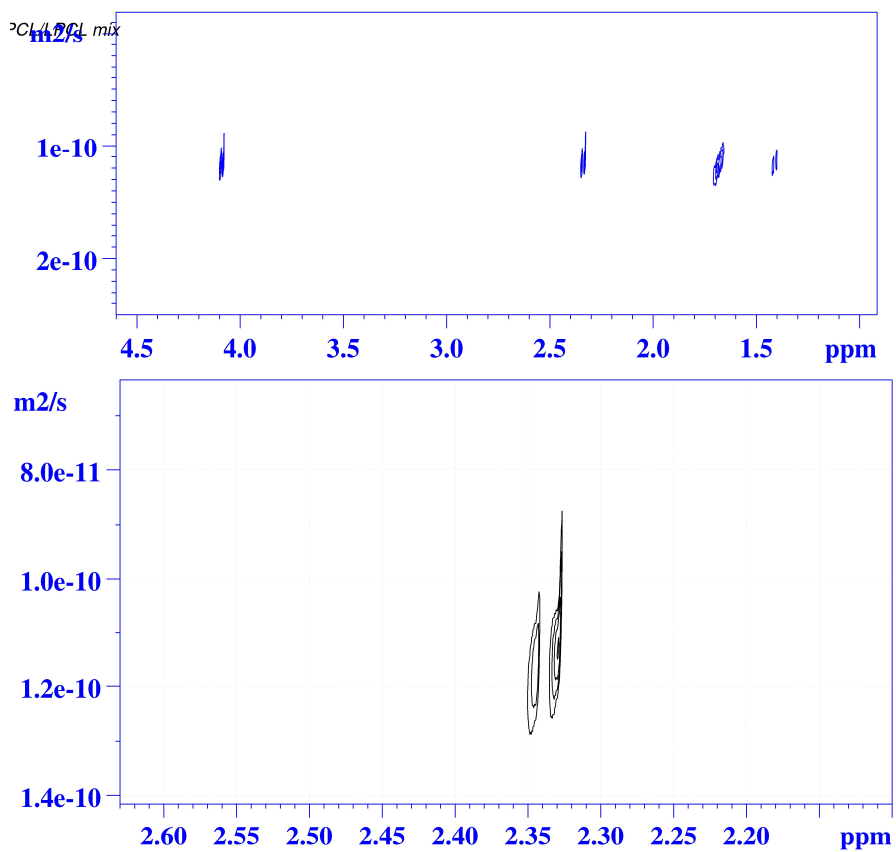


Figure A.III-36. DOSY-NMR of PCL mix of cyclic and linear polymers

Table A.III-3: Thermal Studies of PCL and PVL with chiral catalyst 1a

Entry	Monomer	T <sub>1%</sub>	T <sub>5%</sub>	T <sub>50%</sub>	T <sub>99%</sub>	T <sub>max</sub>	T <sub>m</sub>	T <sub>c</sub>
1	PVL	159	185	233	254	250	57	29
2	PVL-OH	135	177	237	260	258	55	25
3	PCL	218	284	346	369	353	59	31
4	PCL-OH	193	213	299	500	311	55	30

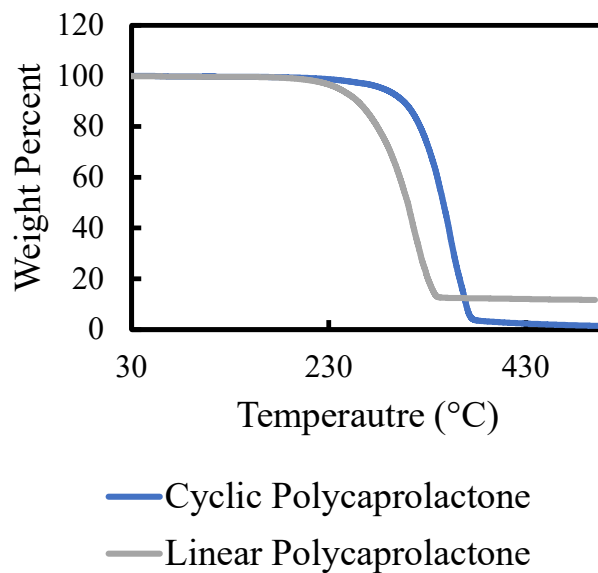


Figure A.III-37. TGA data for cyclic and linear polycaprolactone

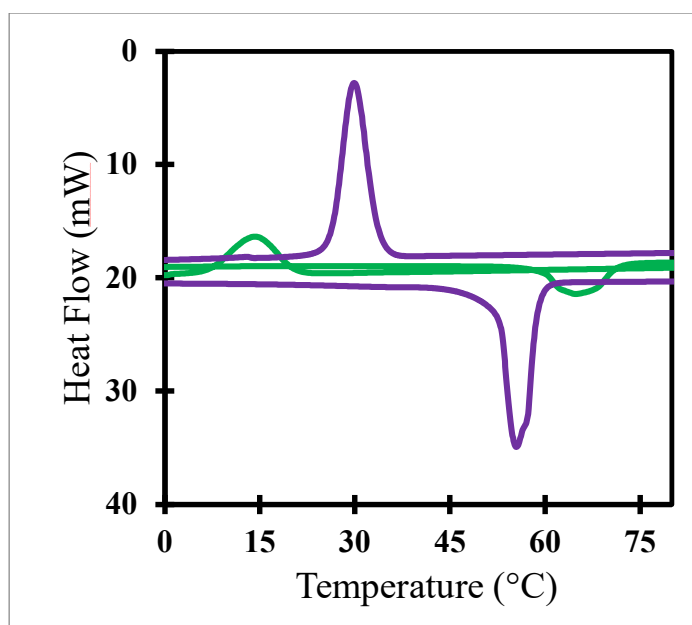


Figure A.III-38. DSC data for cyclic and linear polycaprolactone

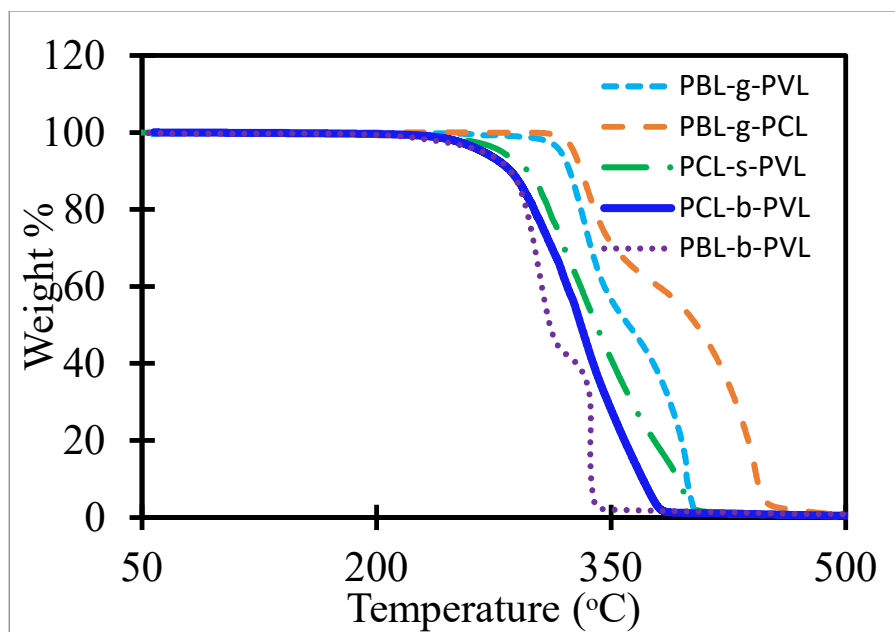


Figure A.III-39. TGA data for cyclic copolymers

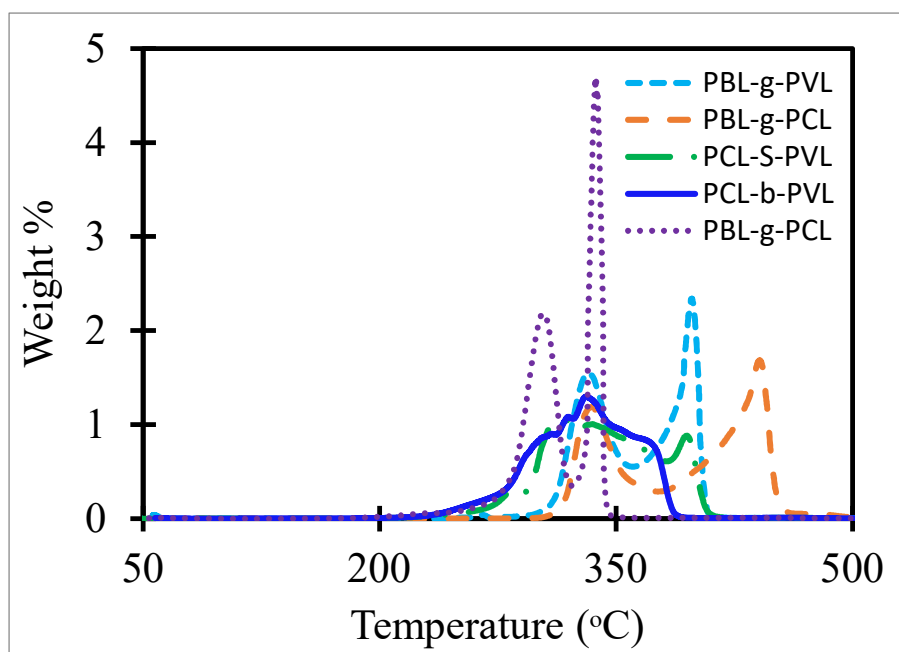


Figure A.III-40. TGA data (deri. Wt%) for cyclic copolymers

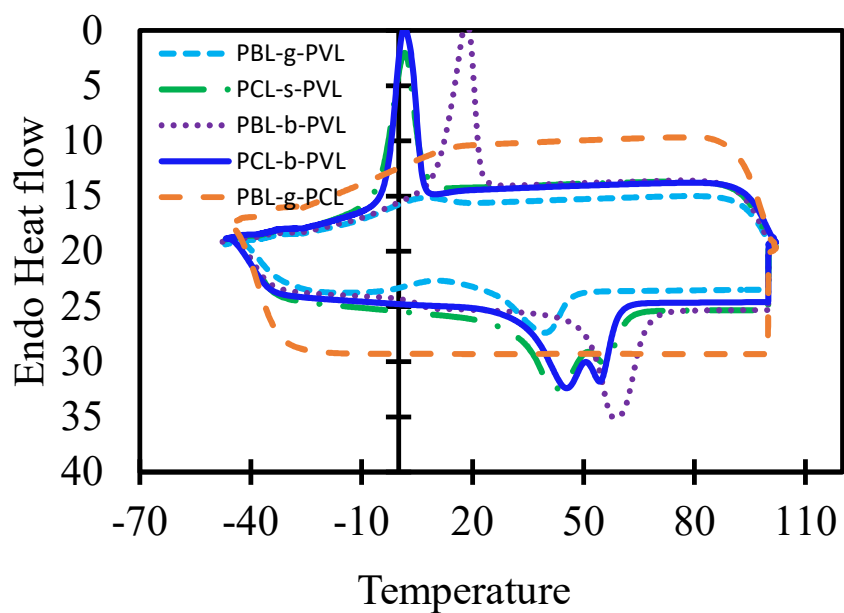


Figure A.III-41. DSC data for cyclic copolymers

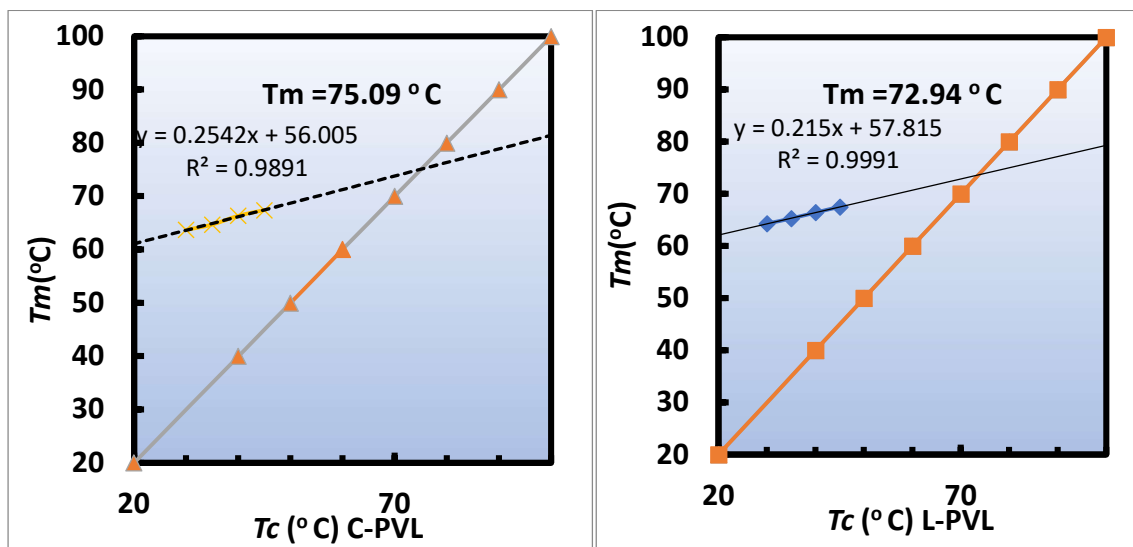


Figure A.III-42. Hoffmann-week plots for (a) Cyclic PVL (b) Linear PVL

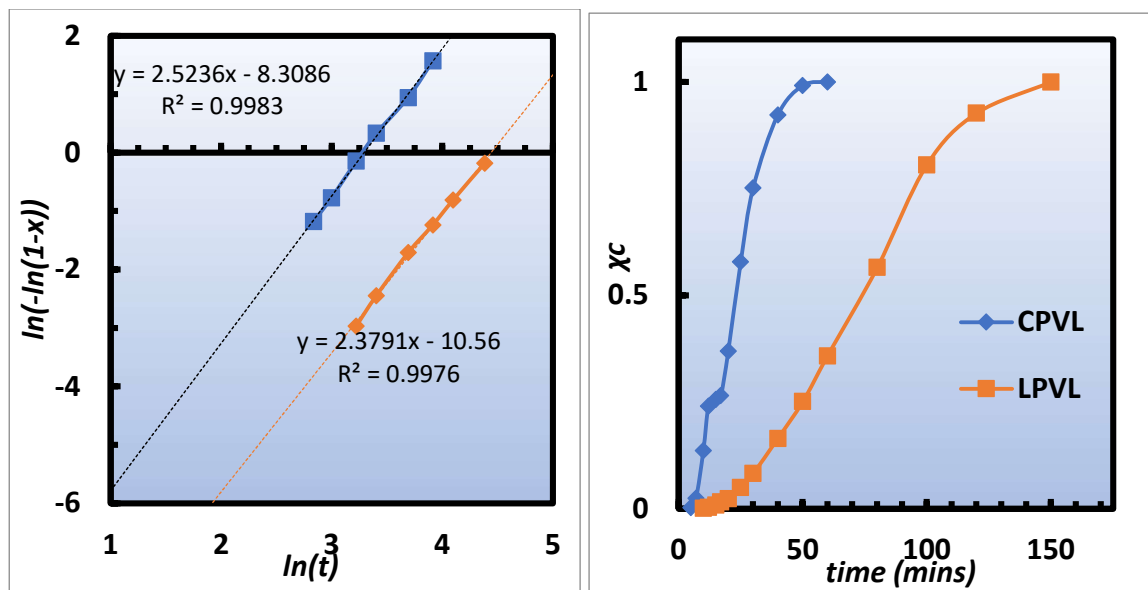


Figure A.III-43. Relative crystallinity ( $\chi_c$ ) as a function of time (left) and a linear fit of Avrami equation for cyclic and linear PCL plots

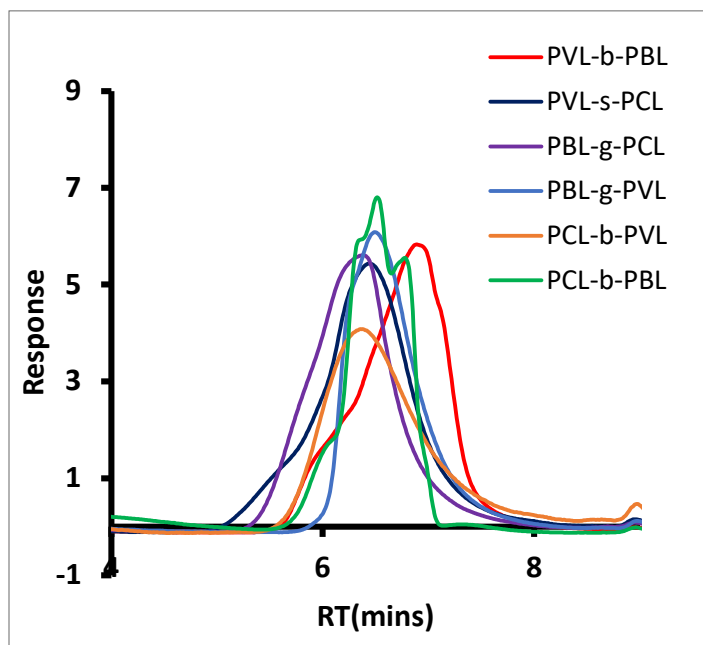


Figure A.III-44. GPC data of block polymers



Differential scanning calorimetry

$$\ln(-\ln(1 - \chi_t)) = n \ln(t) + \ln(k) \quad (1)$$

$$k = \ln(2) / t_{1/2}^n \quad (2)$$

### 5.1 Crystallization kinetics

Polymer	M <sub>n</sub>	M <sub>w</sub>	D	n	k	t <sub>1/2</sub> (mins)
<i>LPVL</i>	89	110	1.23	2.54	2.05*10 <sup>-5</sup>	60
<i>LPCL</i>	98	127	1.29	3.52	2.12*10 <sup>-7</sup>	71
<i>CPVL</i>	61	89	1.45	5.41	9.84*10 <sup>-7</sup>	12
<i>CPCL</i>	85	147.5	1.73	3.57	3.59*10 <sup>-6</sup>	30.1

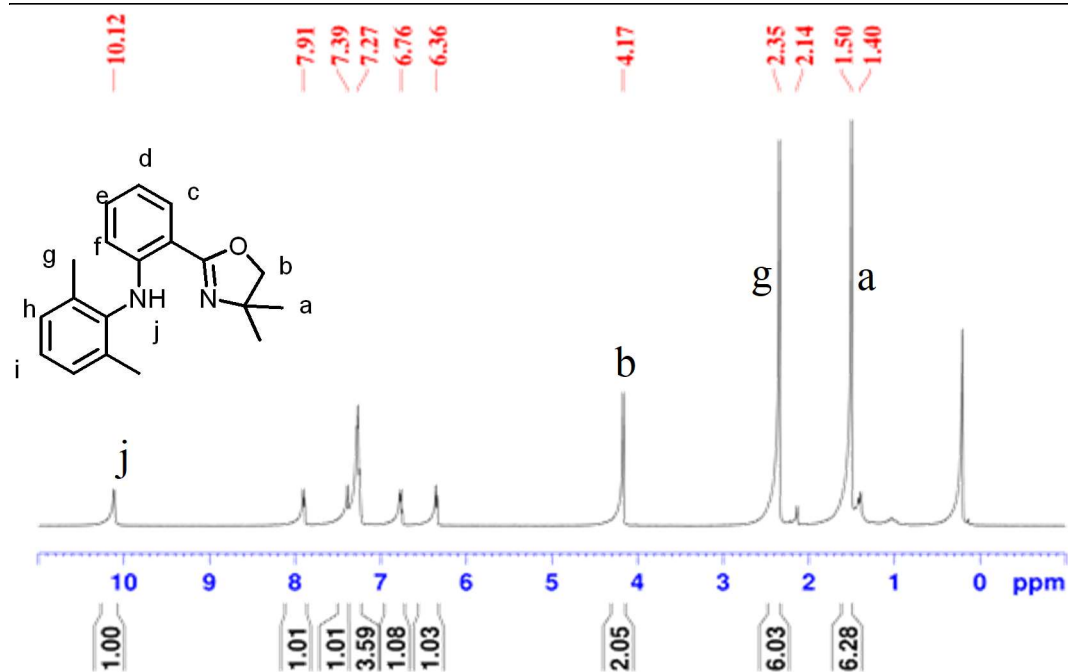


Fig A.III-45. <sup>1</sup>H-NMR of ligand 1b

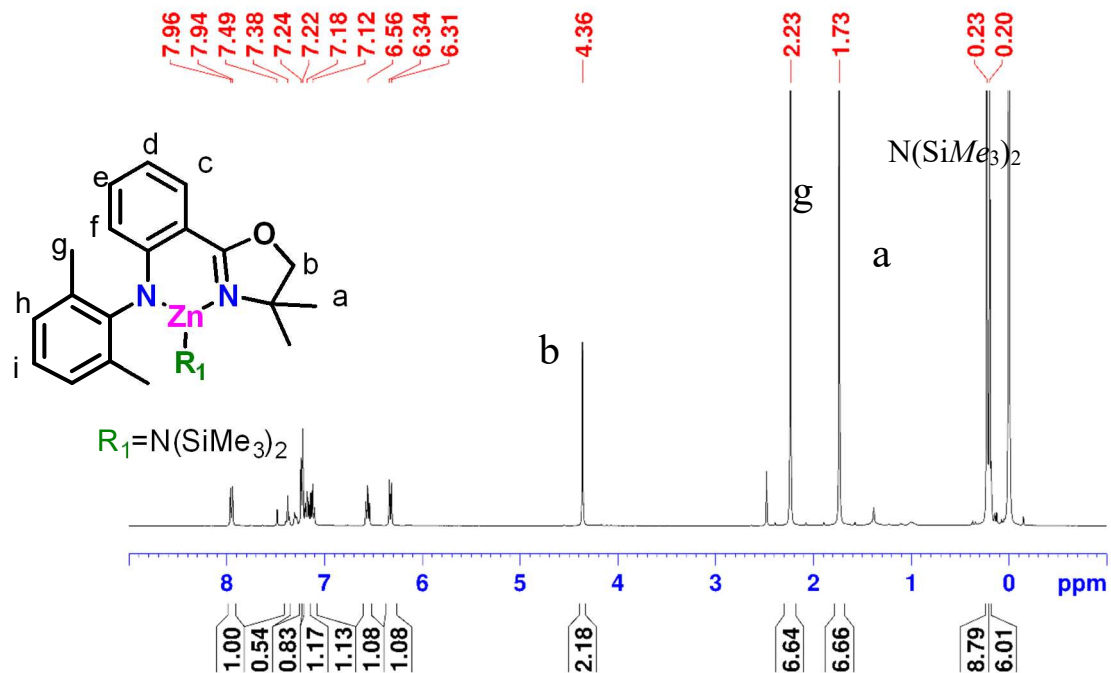


Fig A.III-46. <sup>1</sup>H-NMR of Zn-Catalyst 1b

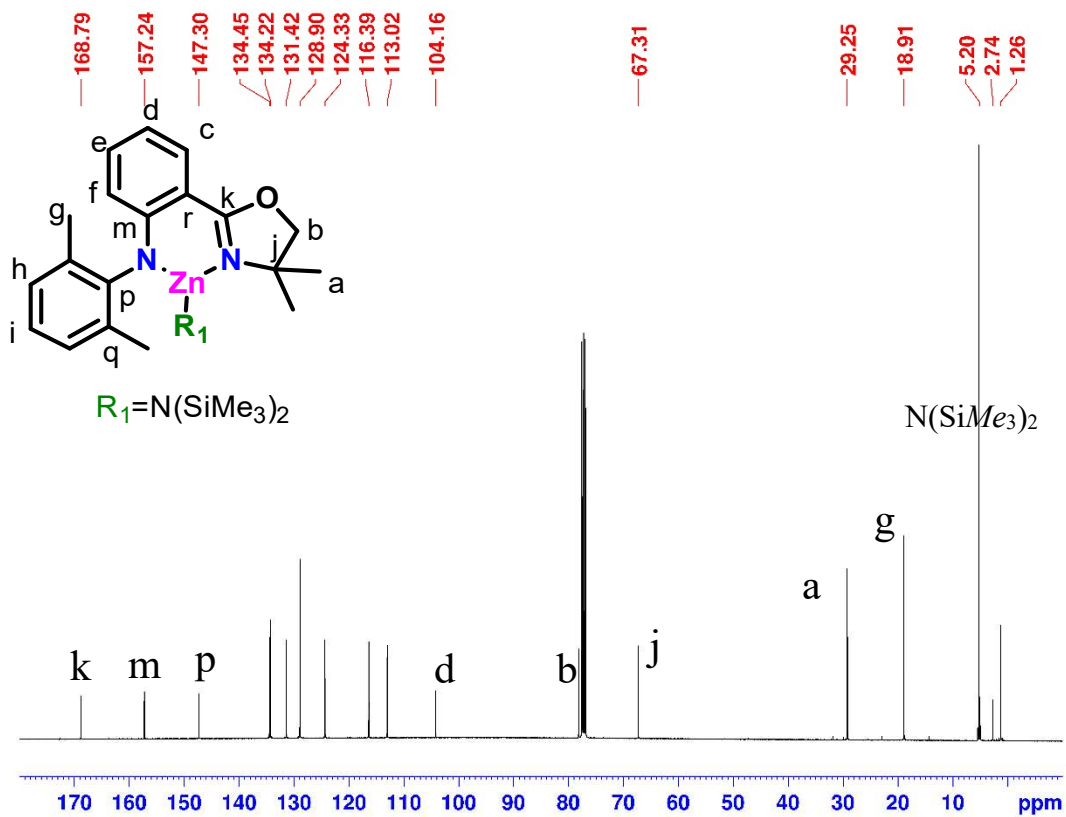


Fig A.III-47. <sup>13</sup>C-NMR of Zn-Catalyst 1b